NATIONAL ADVISORY COMMITTEE FOR AERONAUTICS

TECHNICAL NOTE 3529

THE TRANSONIC CHARACTERISTICS OF 36 SYMMETRICAL WINGS OF VARYING TAPER, ASPECT RATIO, AND THICKNESS AS DETERMINED BY THE TRANSONIC-BUMP TECHNIQUE

By Warren H. Nelson, Edwin C. Allen, and
Walter J. Krumm

Ames Aeronautical Laboratory
Moffett Field, Calif.

Washington
December 1955

NATIONAL ADVISORY COMMITTEE FOR AERONAUTICS

TECHNICAL NOTE 3529

THE TRANSONIC CHARACTERISTICS OF 36 SYMMETRICAL WINGS OF VARYING TAPER, ASPECT RATIO, AND THICKNESS AS DETERMINED BY THE TRANSONIC-BUMP TECHNIQUE[1]

By Warren H. Nelson, Edwin C. Allen, and Walter J. Krumm

SUMMARY

An investigation of the effects of plan-form taper on the aerodynamic characteristics of a series of wings having various tapers, aspect ratios, and thicknesses was conducted in the Ames 16-foot high-speed wind tunnel, utilizing the transonic-bump method. The Mach number range of the investigation was from 0.6 to 1.1, corresponding to a Reynolds number range of about 1.4 million to 2.0 million. The lift, drag, and pitching-moment data are presented for wings having aspect ratios of 4 (taper ratios of 0, 0.2, and 0.5), 3 (taper ratios of 0.14, 0.33, and 0.6), and 2 (taper ratios of 0.33, 0.5, and 0.72), and NACA 63A00X sections with thickness-to-chord ratios of 8, 6, 4, and 2 percent.

The results indicate that the greatest effect of taper on the lift-curve slope occurred for the wing having the highest aspect ratio and the thinnest section. This effect, which was to increase the lift-curve slope with increasing taper ratio, diminished as the aspect ratio was decreased and/or the thickness increased. Increasing taper ratio generally increased the over-all center-of-pressure travel for all the wings in going from subsonic to supersonic speeds.

INTRODUCTION

A comprehensive investigation has been initiated in the Ames 16-foot high-speed wind tunnel to determine the transonic aerodynamic characteristics of wings having various aspect ratios, thicknesses, cambers, and plan-form taper ratios. The experimental data on the effects of aspect ratio, thickness, and camber have been reported in references 1 and 2, and analyses of the data using the transonic similarity rules have been reported in reference 3.

[1]Supersedes recently declassified NACA RM A53I29 by Warren H. Nelson, Edwin C. Allen, and Walter J. Krumm, 1953.

The purpose of this report is to present that part of the general investigation involving the effect of plan-form taper.

Three basic plan-form taper ratios, 0, 0.2, and 0.5, were investigated for wings having an aspect ratio of 4 and NACA 63A-series symmetrical sections with thickness-to-chord ratios of 2, 4, 6, and 8 percent. These wings, in turn, were reduced in span by cutting off the tips to give aspect ratios of 3 and 2. The resulting plan-form taper ratios for the wings having an aspect ratio of 2 were 0.33, 0.50, and 0.72.

NOTATION

C_D drag coefficient, $\frac{\text{twice semispan drag}}{qS}$

$C_{D_{min}}$ minimum drag coefficient

C_{D_f} friction-drag coefficient, assumed equal to the minimum drag coefficient at 0.6 Mach number

$\left(C_{D_p}\right)_{min}$ minimum pressure-drag coefficient, assumed equal to $\left(C_{D_{min}} - C_{D_f}\right)$

C_L lift coefficient, $\frac{\text{twice semispan lift}}{qS}$

C_m pitching-moment coefficient, referred to 0.25 $\bar{c}$, $\frac{\text{twice semispan pitching moment}}{qS\bar{c}}$

A aspect ratio, $\frac{b^2}{S}$

M mean Mach number

M_L local Mach number

S total wing area, twice wing area of semispan model, sq ft

V velocity, ft/sec

b twice span of semispan model, ft

c local wing chord, ft

$\bar{c}$ mean aerodynamic chord, $\frac{\int_0^{b/2} c^2 dy}{\int_0^{b/2} c\, dy}$

q	dynamic pressure, $\frac{1}{2}\rho V^2$, lb/sq ft
$\frac{t}{c}$	thickness-to-chord ratio
y	spanwise distance from plane of symmetry, ft
α	angle of attack, deg
λ	taper ratio, $\frac{\text{tip chord}}{\text{root chord}}$
ρ	air density, slugs/cu ft
$\frac{dC_L}{d\alpha}$	slope of lift curve measured at zero lift, per deg
$\frac{dC_m}{dC_L}$	slope of pitching-moment curve measured at zero lift

APPARATUS AND MODELS

The tests were conducted in the Ames 16-foot high-speed wind tunnel, utilizing a transonic bump. A description of the bump may be found in reference 4. The aerodynamic forces and moments were measured by means of a strain-gage balance mounted inside the bump.

A photograph of one of the wings of aspect ratio 4 mounted on the bump is shown in figure 1. The principal plan-form dimensions of the wings are shown in figure 2. The profiles used were NACA 63A00X sections with thickness-to-chord ratios of 2, 4, 6, and 8 percent (ref. 5). Three basic wings of aspect ratio 4 having taper ratios of 0, 0.2, and 0.5 and equal areas were constructed of steel for each thickness-to-chord ratio. Aspect ratios of 3 and 2 were obtained by successively cutting off the tips of the wings. The following aspect-ratio and taper-ratio combinations were included in the tests:

Aspect ratio	Taper ratio		
4	0	0.20	0.50
3	.14	.33	.60
2	.33	.50	.72

The mean aerodynamic chord of the wings changed with the taper ratio; this change was such that at any one aspect ratio the mean aerodynamic chord of the wing with the highest taper ratio was about

80 percent that of the wing with the lowest taper ratio. The wing tips were faired by using one-half of the wing thickness at each chord station as a radius.

A fence 3/16 inch from the bump surface was used to prevent the flow through the gap between the wing and bump surface from affecting the flow over the wing.

TESTS AND PROCEDURE

The lift, drag, and pitching-moment characteristics were obtained over a Mach number range of 0.6 to 1.10. The corresponding Reynolds number range depended on the wing mean aerodynamic chord, the extreme range of Reynolds numbers being from about 1.4 million to 2.0 million. The angle-of-attack range, in general, was from -2° to the stall, or to where the root bending stress became critical.

A Mach number gradient existed in the flow over the bump where the wings were mounted. Typical contours of the local Mach number in the absence of the wings are shown in figure 3. Outlines of the two extreme taper ratios for the aspect-ratio-4 wings have been superimposed on these contours to indicate the Mach number gradients which existed across the wings during the tests. No attempt has been made to evaluate the effects of these gradients. The test Mach numbers presented are the mean values in the region of the wings.

The data have been reduced to standard NACA coefficient form. A tare correction was made to account for the drag of the fence and support. This drag was evaluated by cutting the wing off flush with the fence and measuring the forces on the fence and support. The interference effects of the fence on the wings and the effects of leakage around the fence are unknown.

RESULTS AND DISCUSSION

The basic lift, drag, and pitching-moment data are presented in figures 4 through 12.

The variation of lift-curve slope with Mach number is shown in figure 13. The effects of aspect ratio and of thickness on lift-curve slope through the transonic speed range were as would be expected; decreasing the aspect ratio and/or increasing the thickness ratio decreased the magnitude and the variation with Mach number of the lift-curve slope. These effects on rectangular wings have been correlated in reference 3 by use of the transonic similarity rules. The effects of

taper on lift-curve slope were not nearly so pronounced as were those of aspect ratio and thickness. The largest effects of taper occurred for the wings of aspect ratio 4 where the taper ratio varied from 0 to 0.5. (It should be pointed out that, in these tests, as the aspect ratio was reduced, the values of taper ratio increased and the range of taper ratio decreased.) Moreover, the effects of taper were greatest for the thinnest wings and decreased as the thickness was increased. For the wings of aspect ratio 4, increasing the taper ratio increased the lift-curve slope, this effect being greatest for taper ratios between 0 and 0.2. The 8-percent-thick wings, having taper ratios of 0.2 and 0.5 (aspect ratio 4), had the type of variation of lift-curve slope with Mach number associated with shock stall. In the case of the wings of aspect ratios 2 and 3, there was little effect of changes in taper ratio on the lift-curve slope, except for the wing of aspect ratio 3 having a thickness ratio of 2 percent. For this wing, there was an increase in lift-curve slope with increasing taper ratio throughout the Mach number range.

The variation of minimum pressure drag coefficient $\left(C_{D_{min}} - C_{D_f}\right)$ with Mach number for the wings is shown in figure 14. The effect of changes in thickness is quite apparent; decreasing the thickness ratio caused a reduction in pressure drag, as would be expected. However, the effects of taper and aspect ratio are not so apparent. In general, there were no large, significant, or consistent effects of taper ratio or aspect ratio on the minimum pressure drag, although some drag reduction was obtained at the higher Mach numbers by decreasing the aspect ratio from 3 to 2. In the case of the 8-percent-thick wings, the effects of taper appear large in light of a previous subsonic investigation reported in reference 6. In reference 6, the effect of taper on full-span wings having the same plan forms and sections was investigated up to a Mach number of 0.94. Data from reference 6 have been included in figure 14(a) for comparison. In general, the data of reference 6 indicate there is no effect of taper ratio on the Mach number of drag divergence except for the wings of aspect ratio 2 where the difference amounts to 0.01 Mach number. This is in contrast to the data for the present investigation where for the wings of aspect ratio 4 there is a difference of 0.025 in drag-divergence Mach number. The drag rise for the wings of reference 6 is also more abrupt than that for the present investigation. The reason for the lack of agreement between the data is not understood; however, to some extent it may be the result of the differences in the testing techniques.

The variation of pitching-moment-curve slope with Mach number is shown in figure 15. In general, increasing the taper ratio shifted the center of pressure toward the leading edge and increased the over-all center-of-pressure travel in going from subsonic to supersonic speeds.

CONCLUDING REMARKS

The greatest effect of taper ratio on the lift-curve slope occurred for the wing having the highest aspect ratio and the thinnest section; this effect, which was to increase the lift-curve slope with increasing taper ratio, was considerably reduced by decreasing aspect ratio and/or increasing thickness. In general, increasing taper ratio had an adverse effect on the pitching-moment coefficient, in that the over-all center-of-pressure travel was increased in going from subsonic to supersonic speeds. In the case of the drag coefficient, the effect of taper ratio was not consistent.

Ames Aeronautical Laboratory
National Advisory Committee for Aeronautics
Moffett Field, Calif., Sept. 29, 1953

1. Nelson, Warren H., and McDevitt, John B.: The Transonic Characteristics of 22 Rectangular, Symmetrical Wing Models of Varying Aspect Ratio and Thickness. NACA TN 3501, 1955.

2. Nelson, Warren H., and Krumm, Walter J.: The Transonic Characteristics of 38 Cambered Rectangular Wings of Varying Aspect Ratio and Thickness as Determined by the Transonic-Bump Technique. NACA TN 3502, 1955.

3. McDevitt, John B.: A Correlation by Means of the Transonic Similarity Rules of the Experimentally Determined Characteristics of a Series of Rectangular Wings. NACA Rep. 1253, 1955.

4. Axelson, John A., and Taylor, Robert A.: Preliminary Investigation of the Transonic Characteristic of an NACA Submerged Inlet. NACA RM A50C13, 1950.

5. Loftin, Laurence K., Jr.: Theoretical and Experimental Data for a Number of NACA 6A-Series Airfoil Sections. NACA Rep. 903, 1948.

6. Allen, Edwin C.: Experimental Investigation of the Effects of Plan-Form Taper on the Aerodynamic Characteristics of Symmetrical Unswept Wings of Varying Aspect Ratio. NACA RM A53C19, 1953.

7. Allen, Edwin C.: Experimental Investigation of the Effects of Plan-Form Taper on the Aerodynamic Characteristics of Symmetrical Unswept Wings of Varying Aspect Ratio. NACA RM A53C19, 1953.

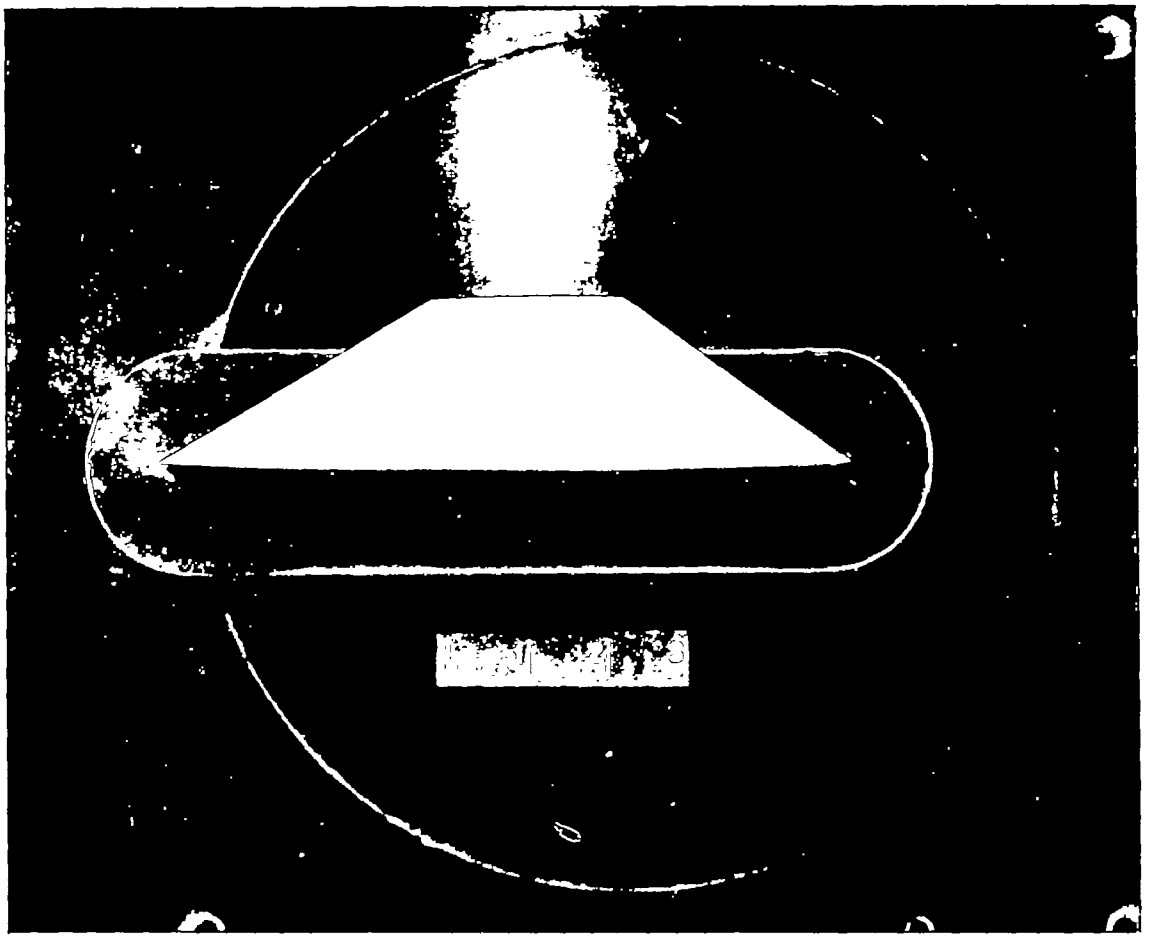

A-17628.1

Figure 1.- Photograph of the wing having an aspect ratio of 4 and a taper ratio of 0.2 mounted on the bump.

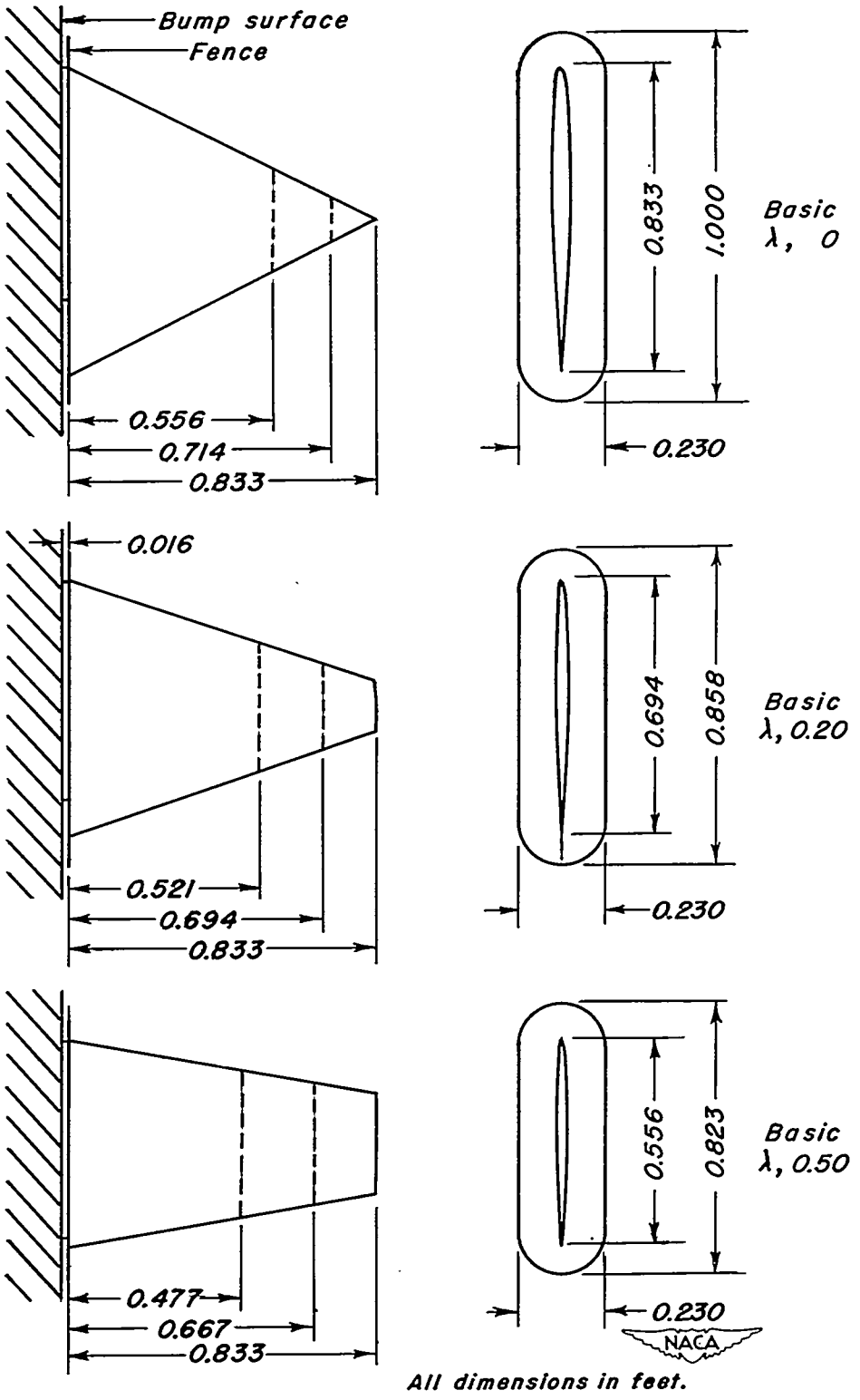

Figure 2.- Plan forms of the wings.

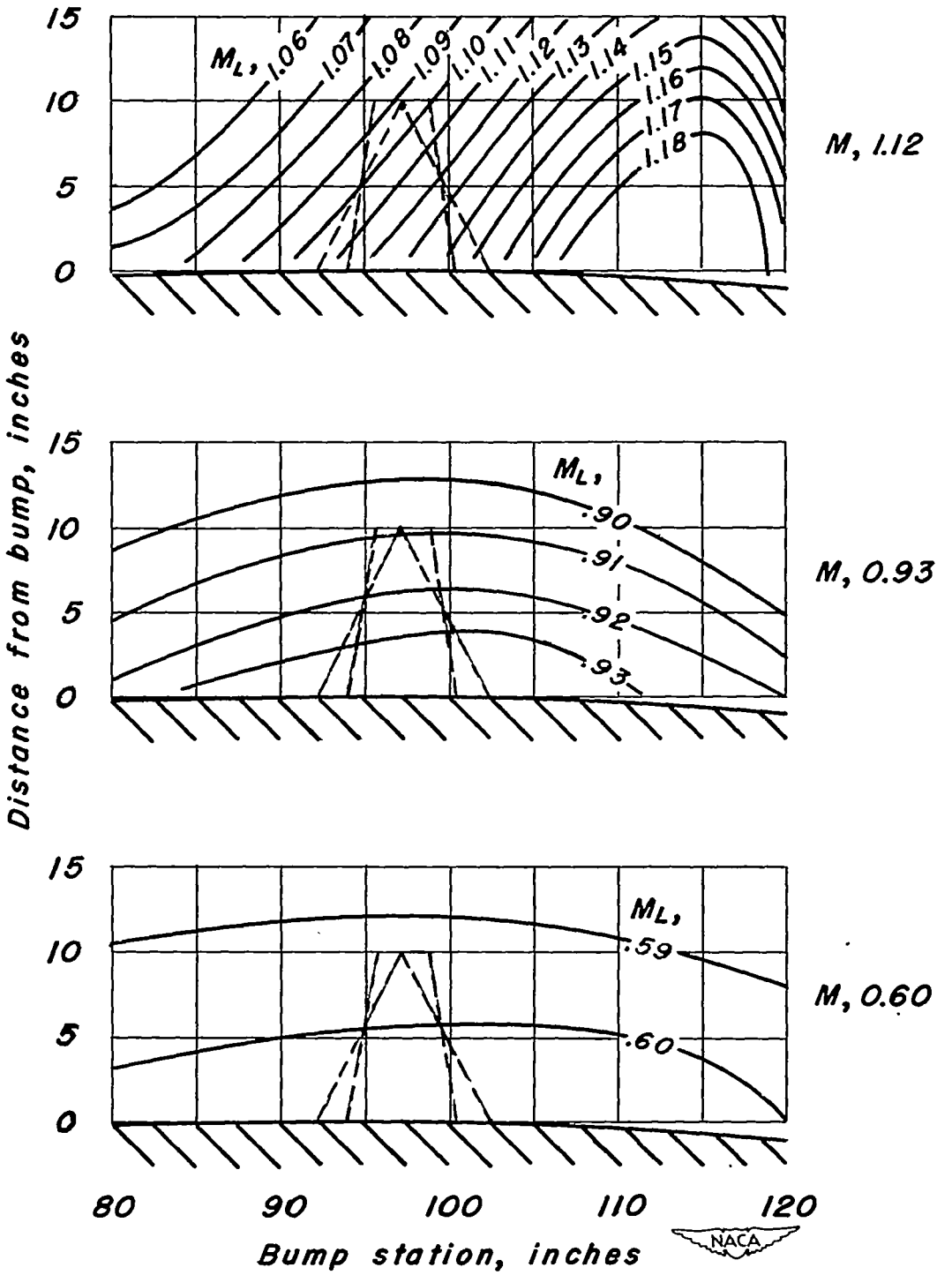

Figure 3.- Typical Mach number contours over the transonic bump in the Ames 16-foot high-speed wind tunnel.

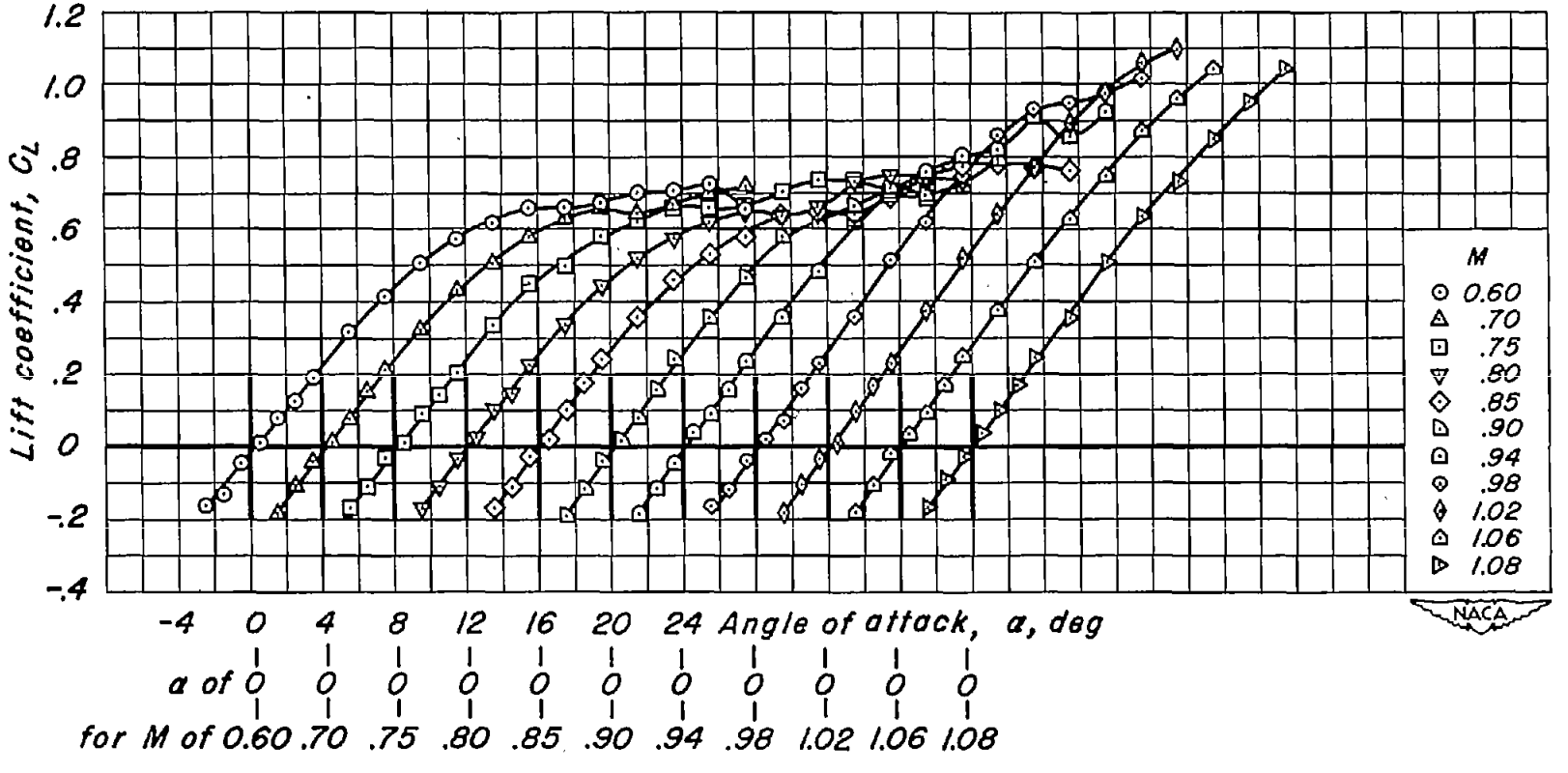

(a) t/c = 0.08; λ = 0

Figure 4.- The variation of lift coefficient with angle of attack for the aspect-ratio-4 wings.

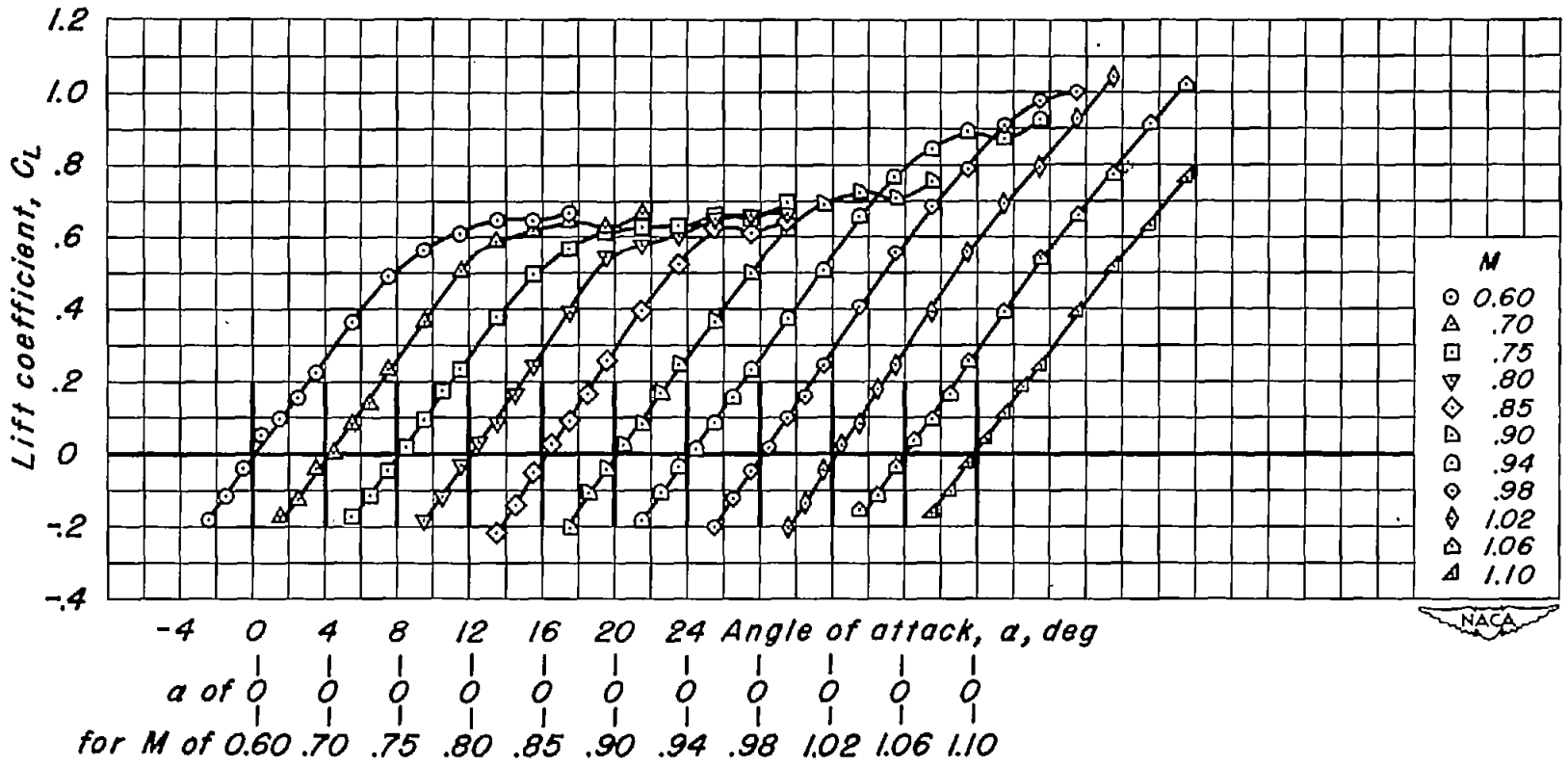

(b) t/c = 0.08; λ = 0.2

Figure 4.- Continued.

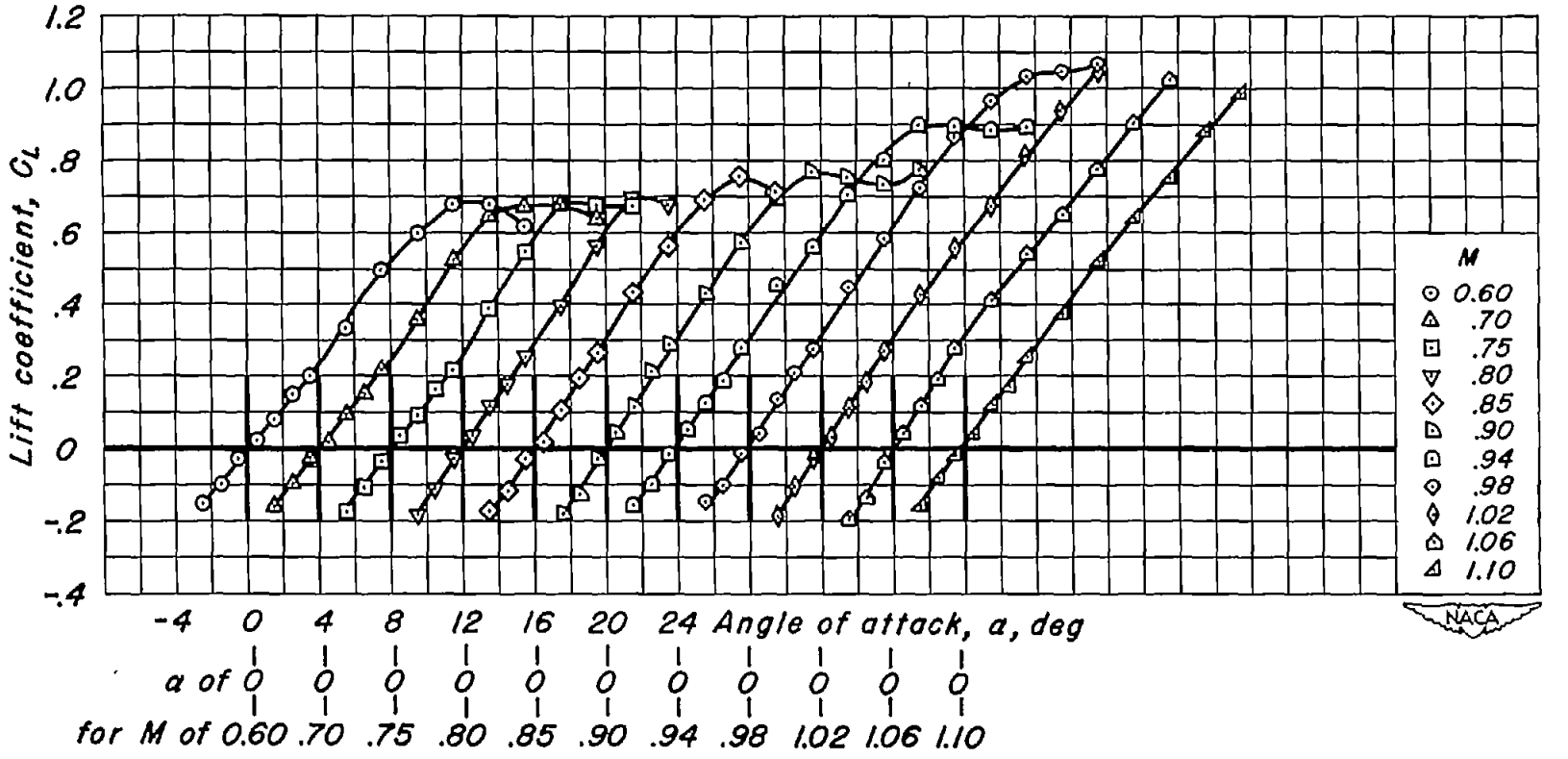

(c) t/c = 0.08; λ = 0.5

Figure 4.- Continued.

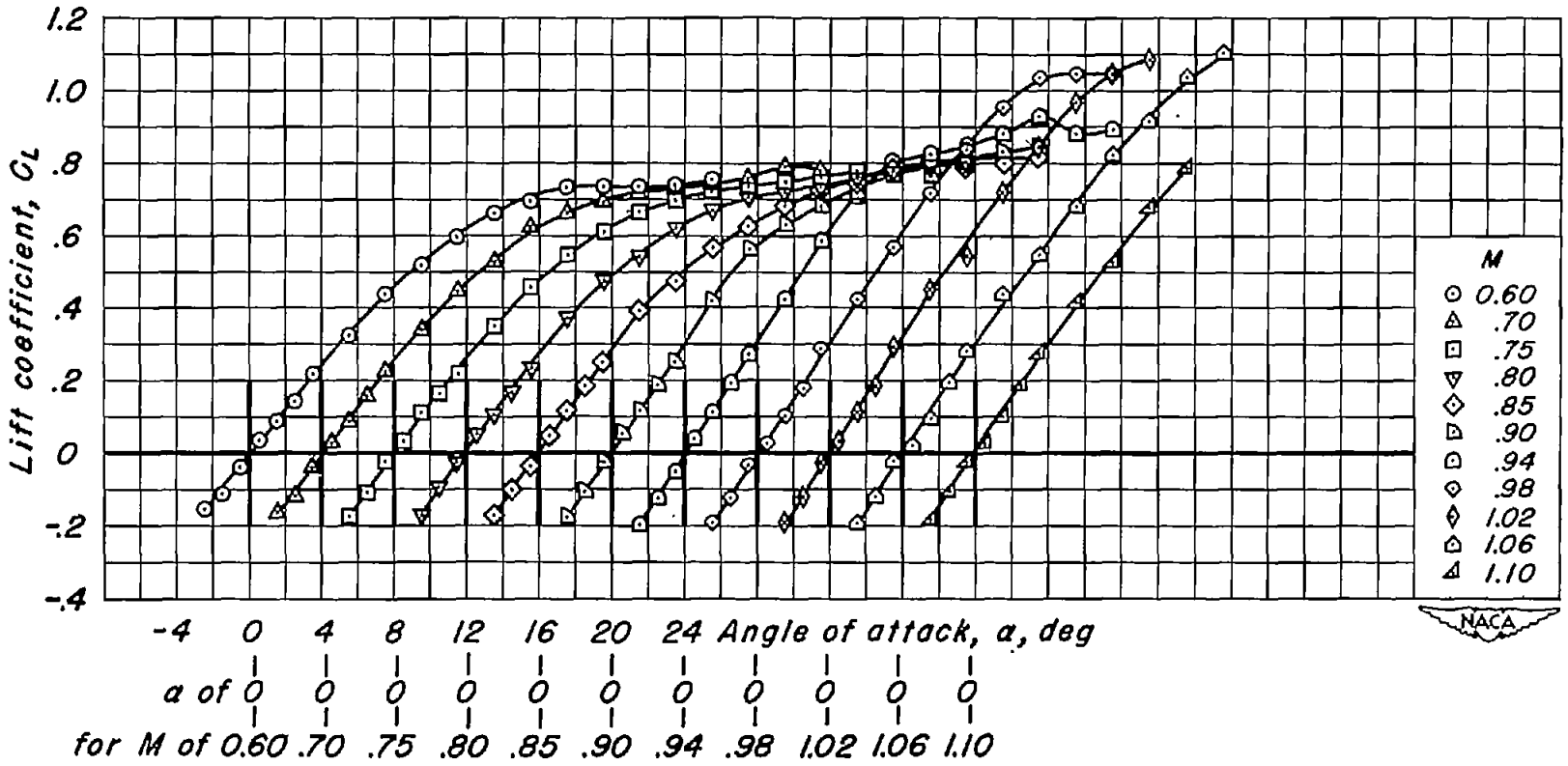

(d) t/c = 0.06; λ = 0

Figure 4.- Continued.

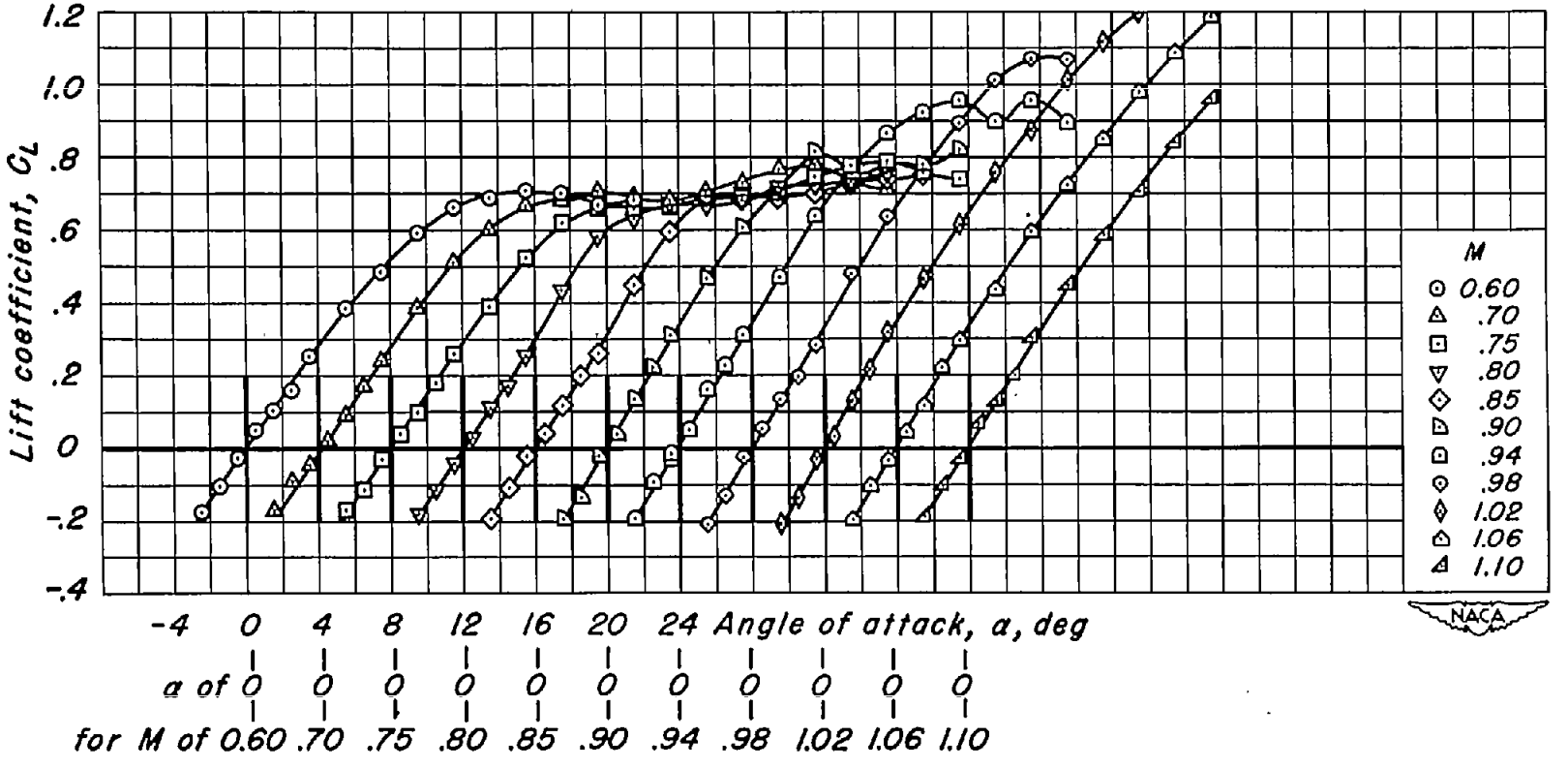

(e) t/c = 0.06; λ = 0.2

Figure 4.- Continued.

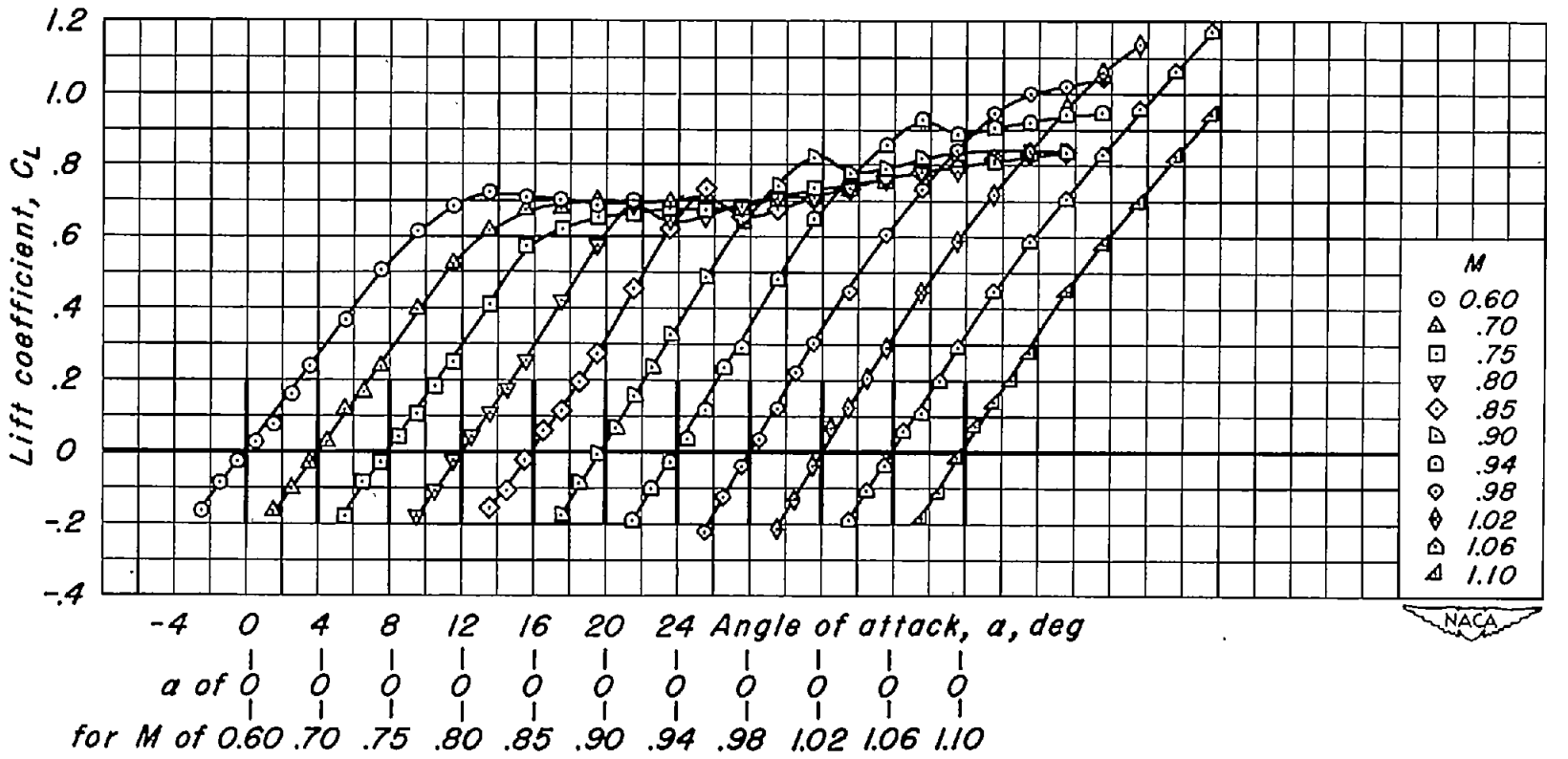

(f) t/c = 0.06; λ = 0.5

Figure 4.- Continued.

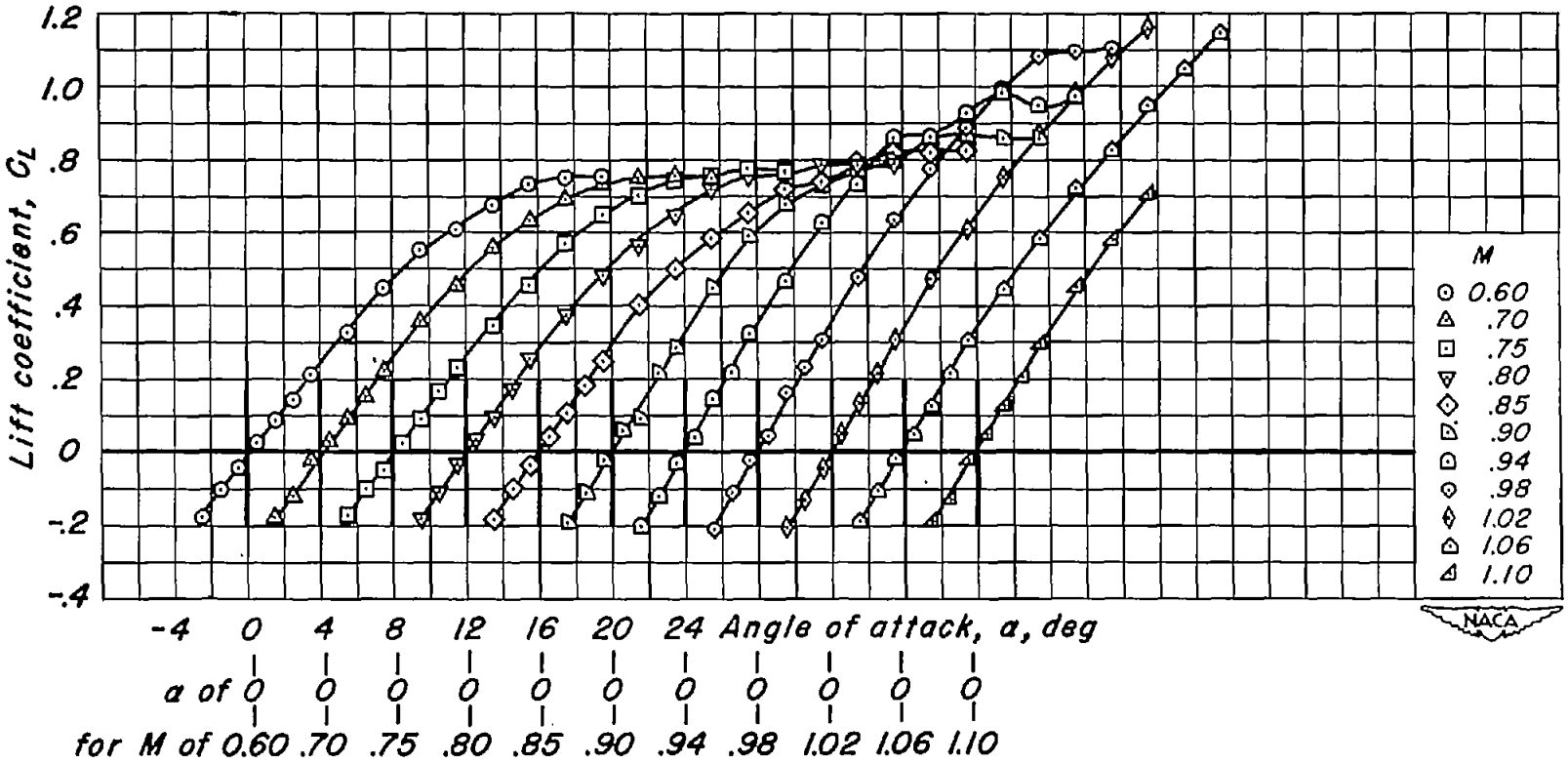

(g) t/c = 0.04; λ = 0

Figure 4.- Continued.

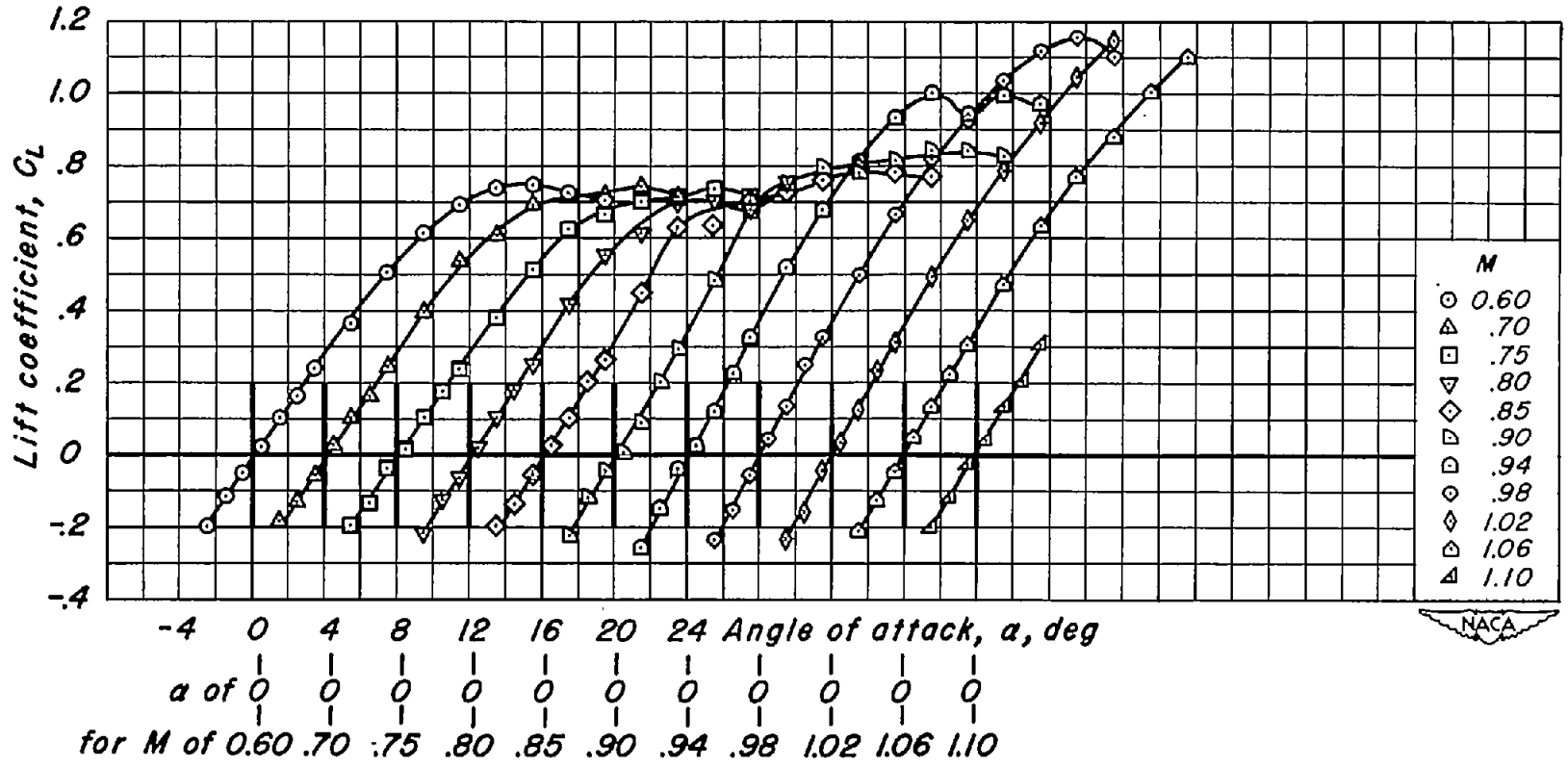

(h) t/c = 0.04; λ = 0.2

Figure 4.- Continued.

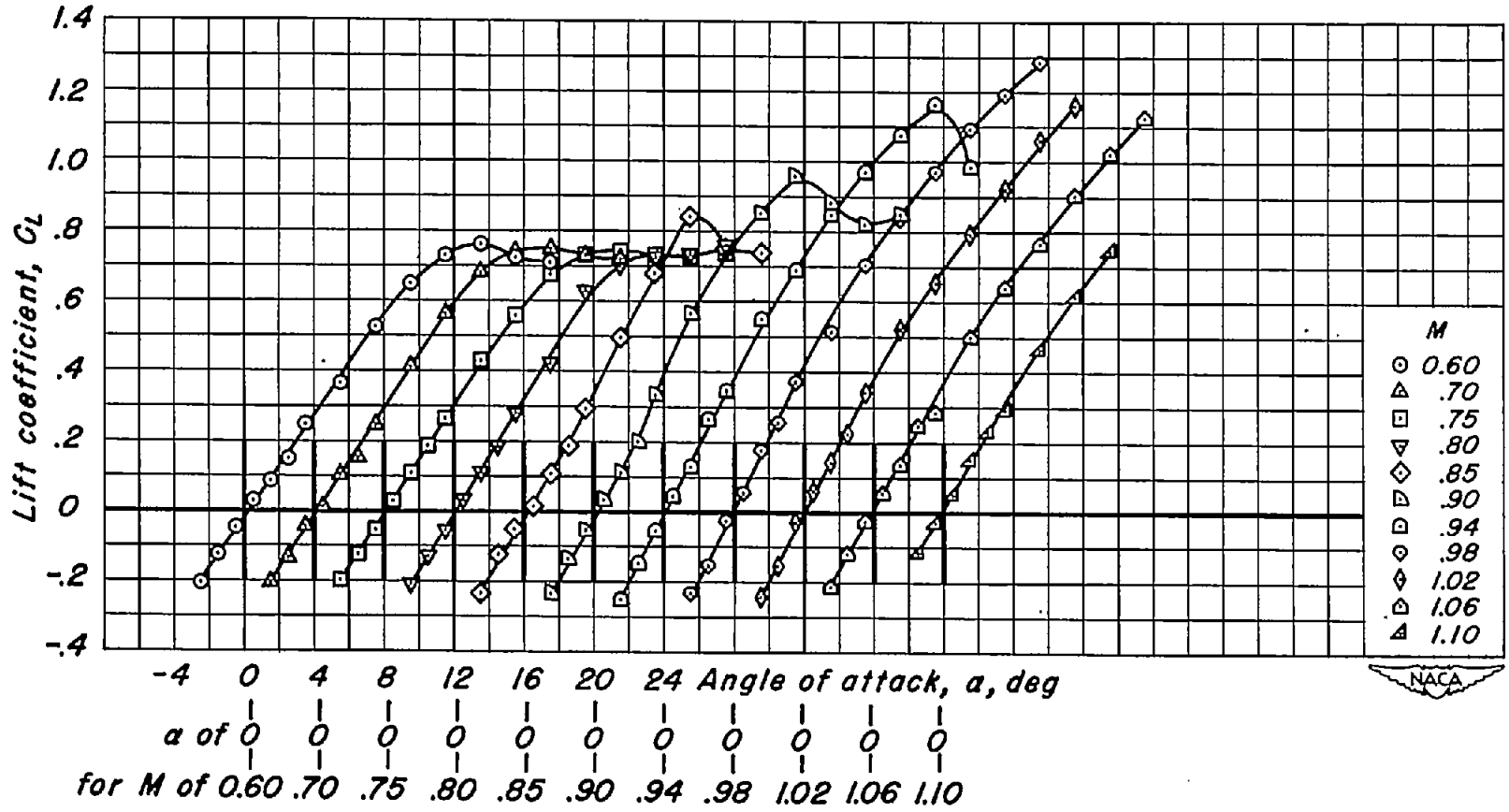

(i) t/c = 0.04; λ = 0.5

Figure 4.- Continued.

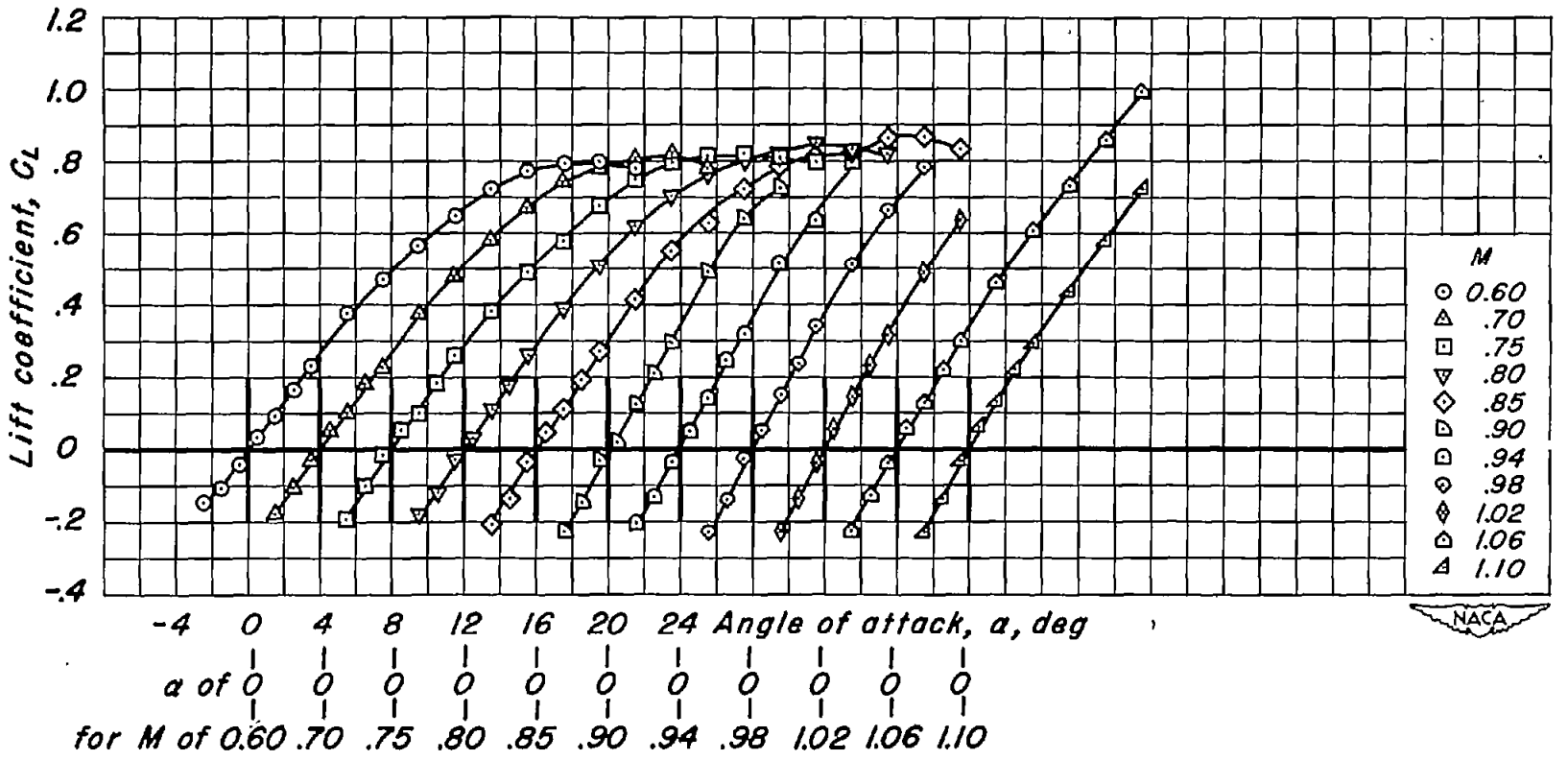

(j) t/c = 0.02; λ = 0

Figure 4.- Continued.

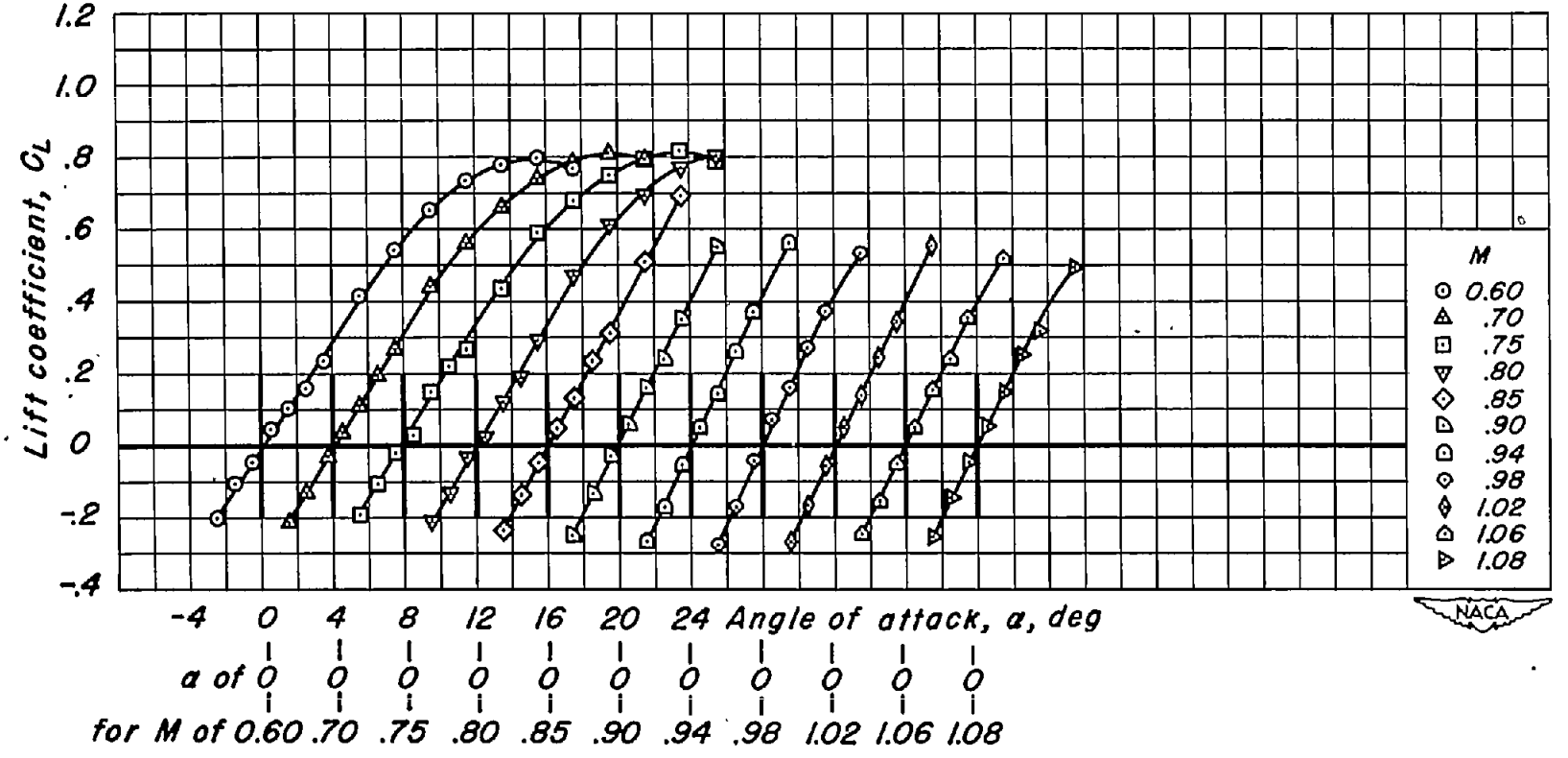

(k) t/c = 0.02; λ = 0.2

Figure 4.- Continued.

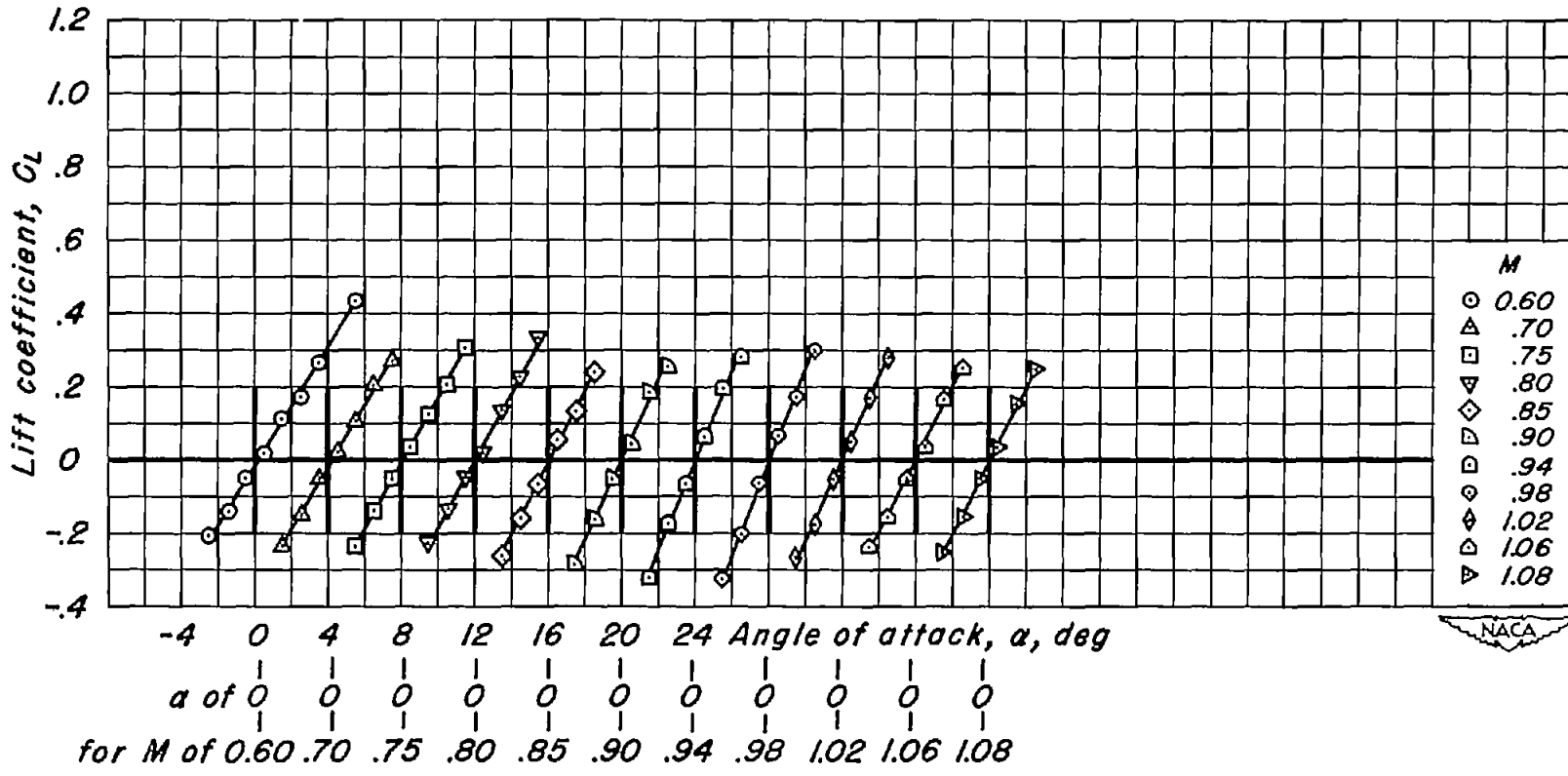

(l) t/c = 0.02; λ = 0.5

Figure 4.- Concluded.

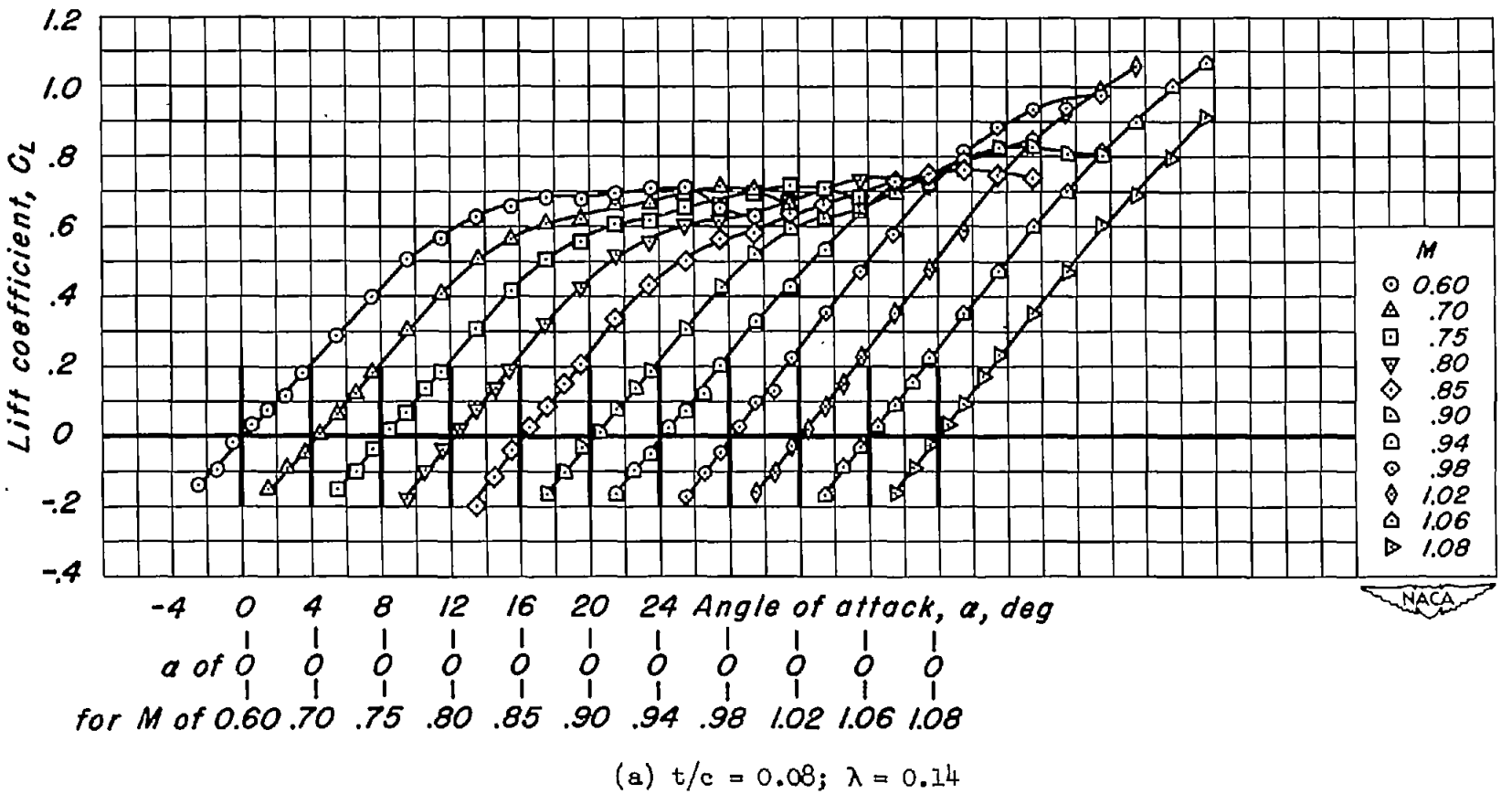

(a) t/c = 0.08; λ = 0.14

Figure 5.- The variation of lift coefficient with angle of attack for the aspect-ratio-3 wings.

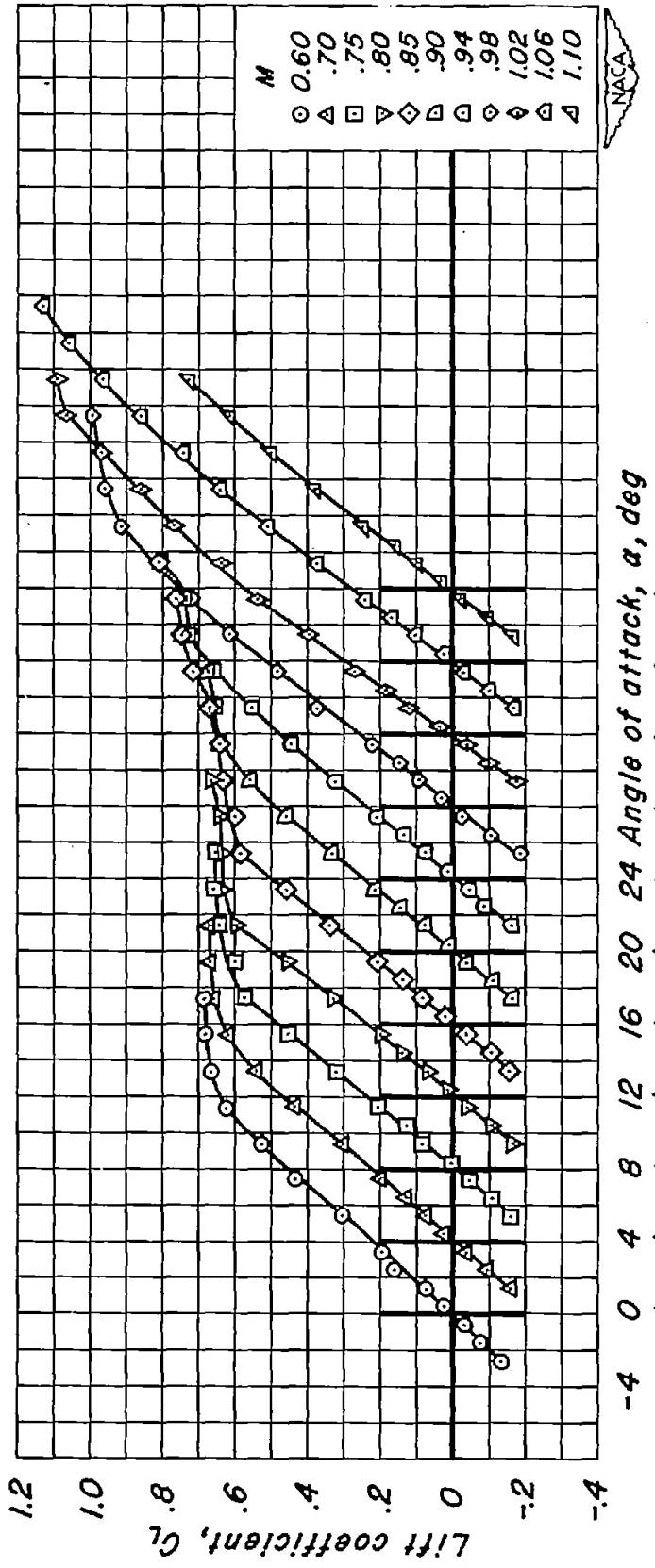

(b) t/c = 0.08; λ = 0.33

Figure 5.- Continued.

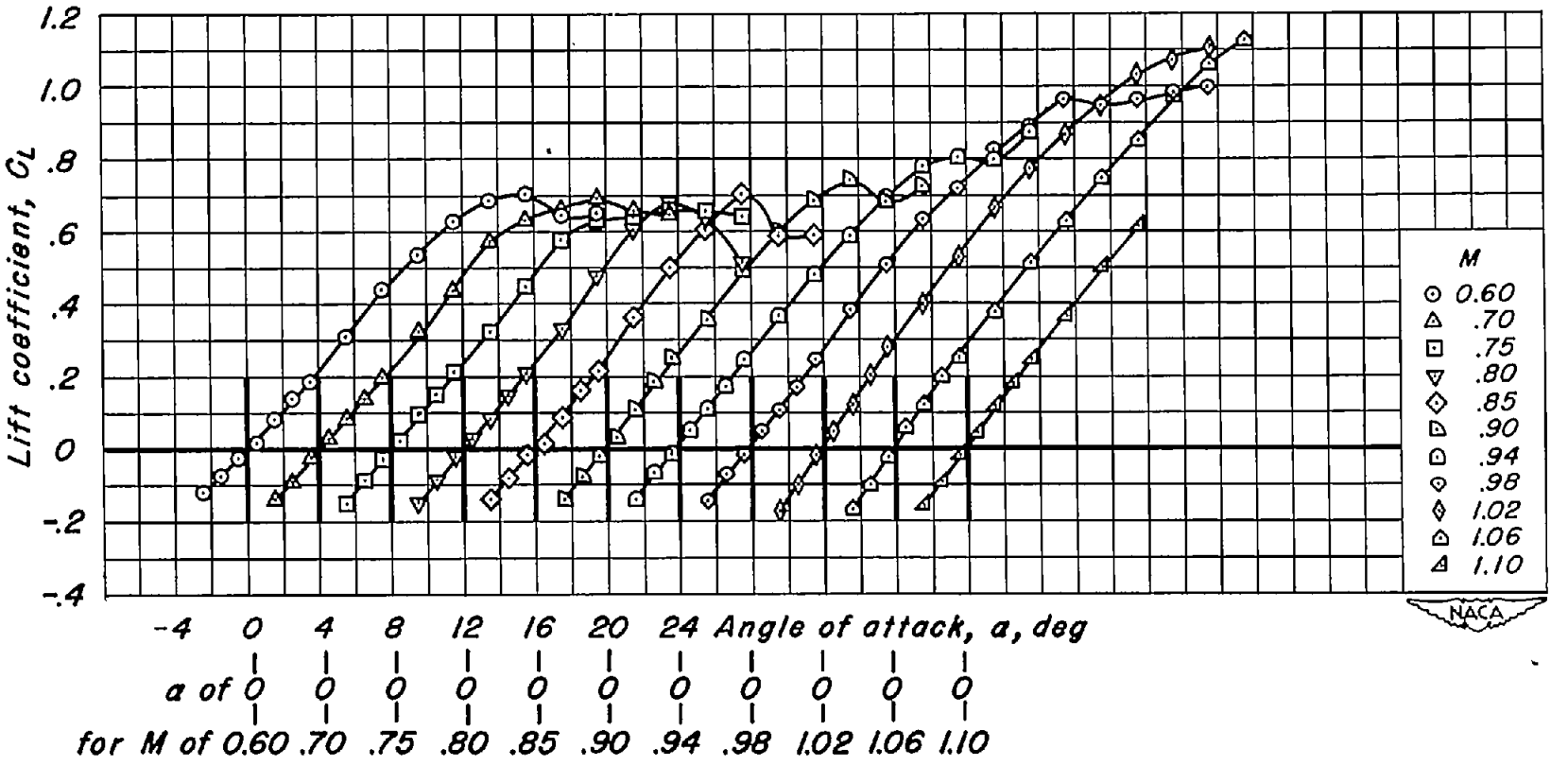

(c) t/c = 0.08; λ = 0.60

Figure 5.- Continued.

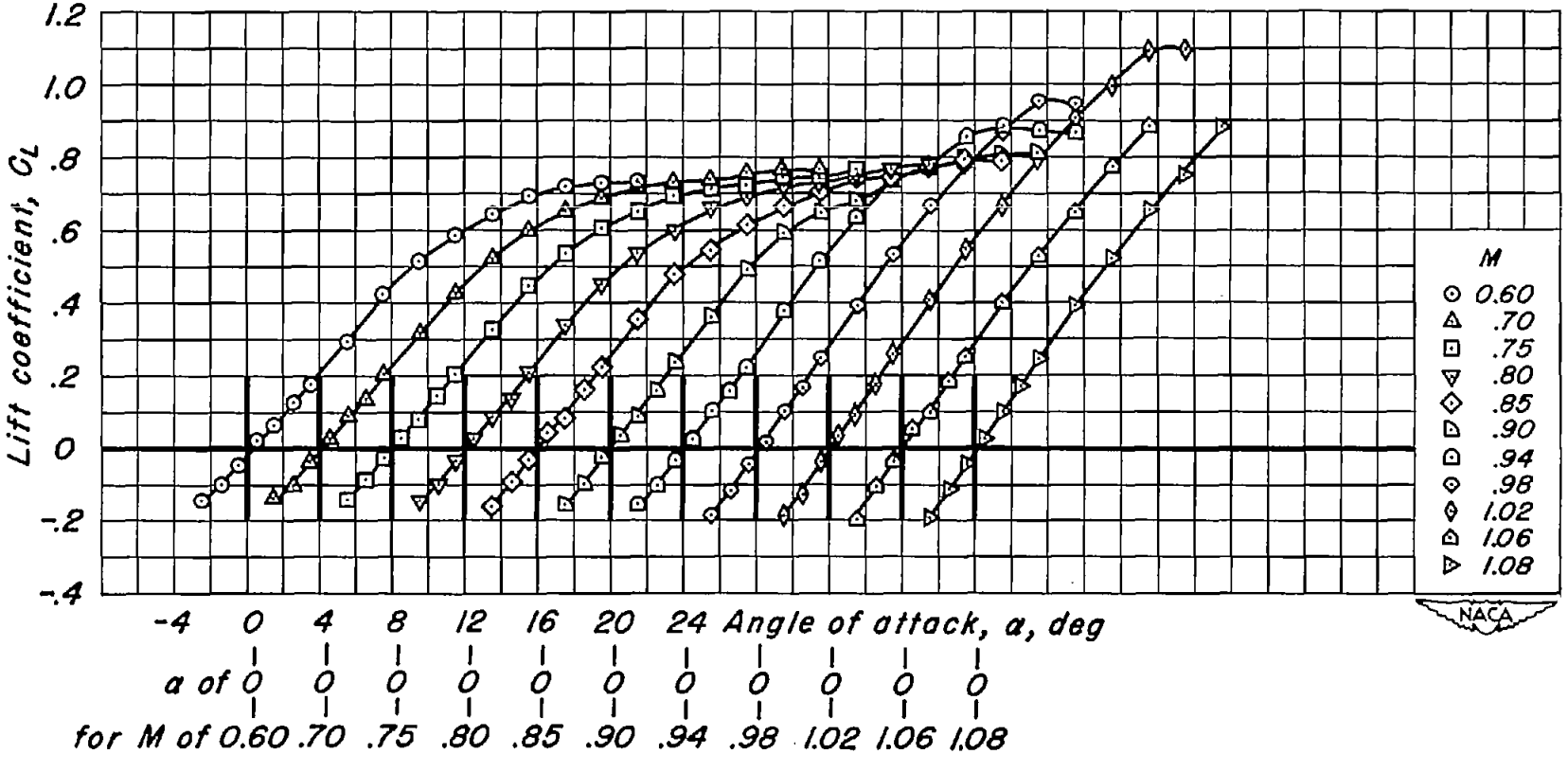

(d) t/c = 0.06; λ = 0.14

Figure 5.- Continued.

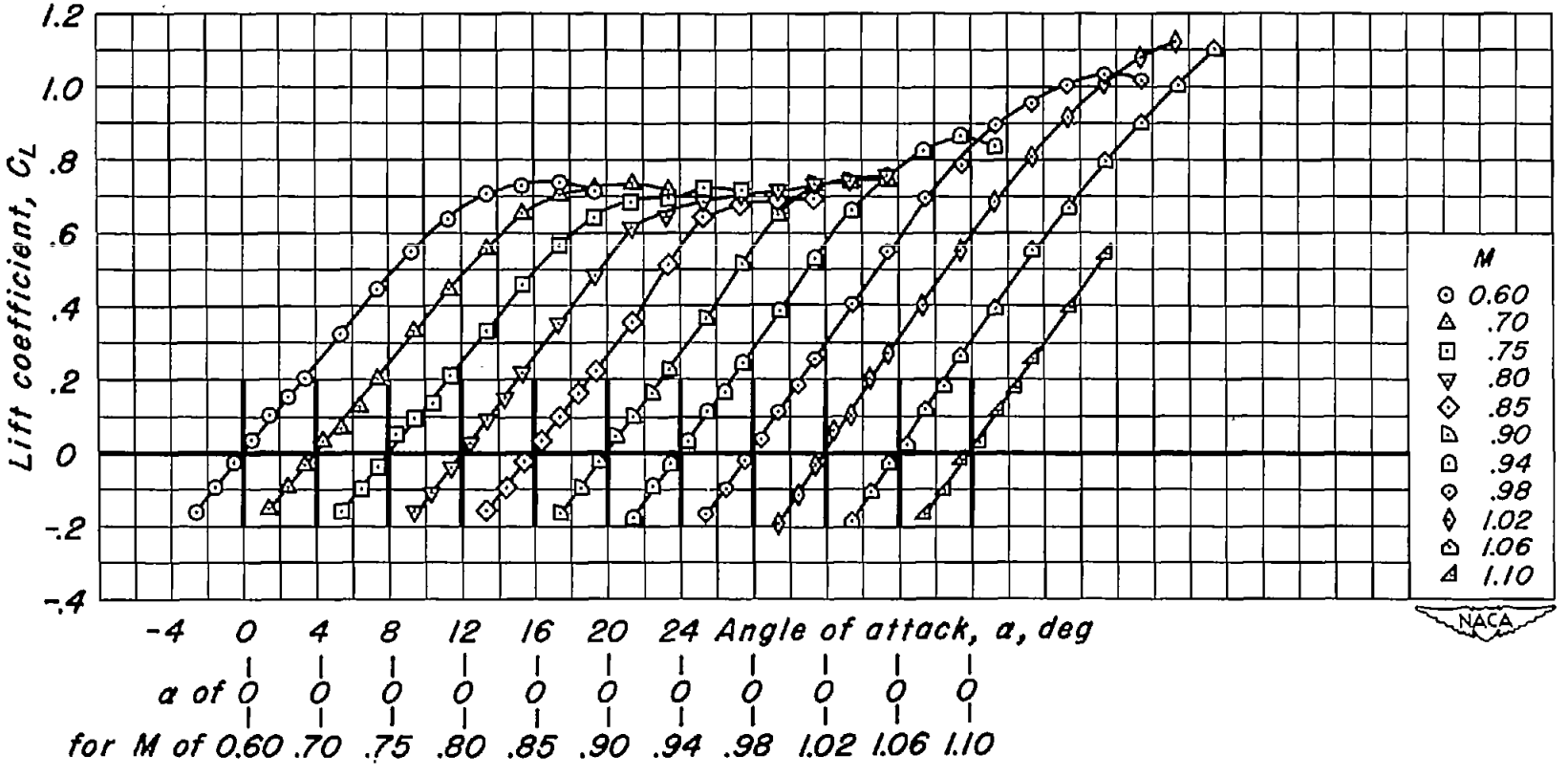

(e) t/c = 0.06; λ = 0.33

Figure 5.- Continued.

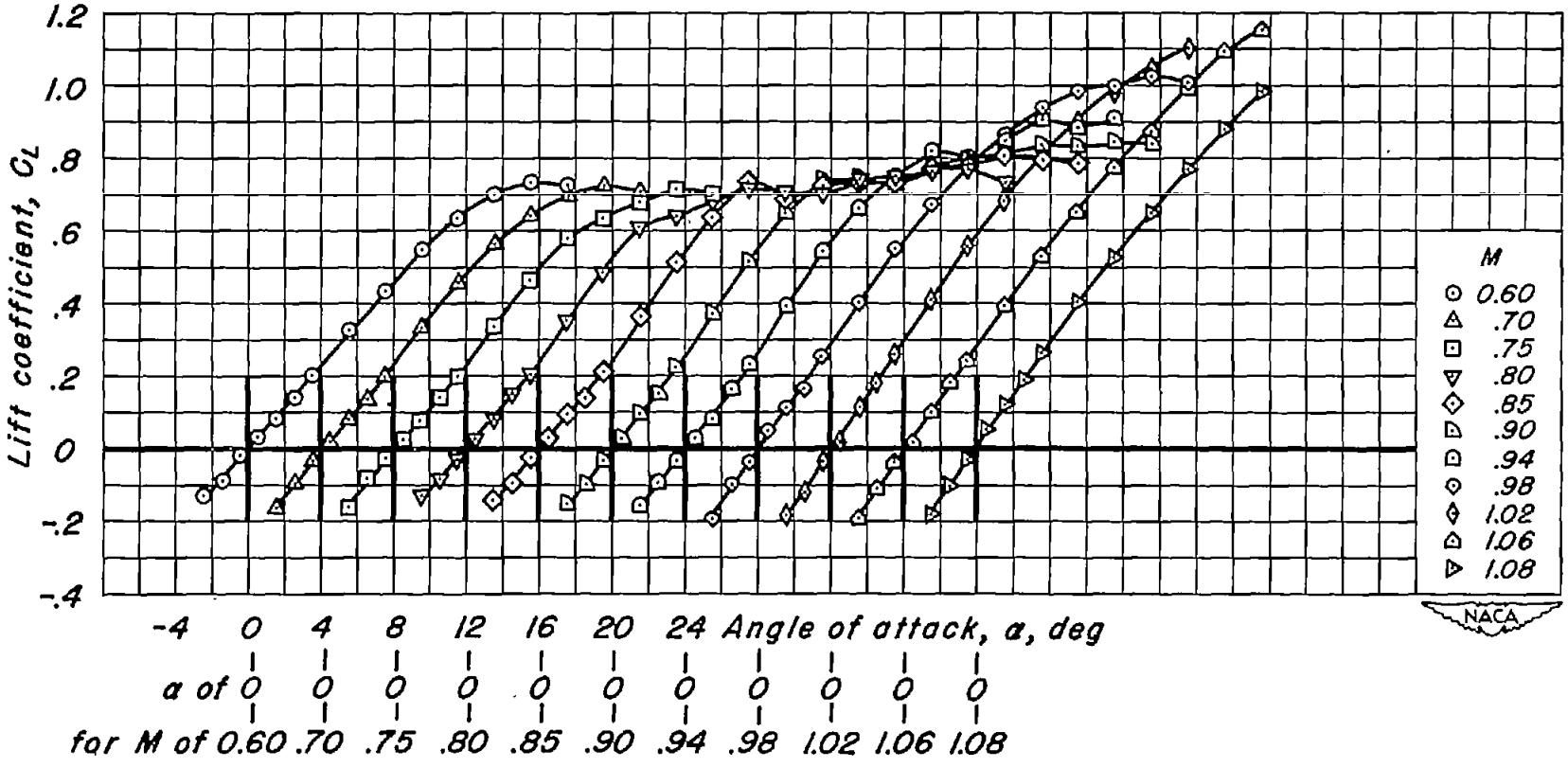

(f) t/c = 0.06; λ = 0.60

Figure 5.- Continued.

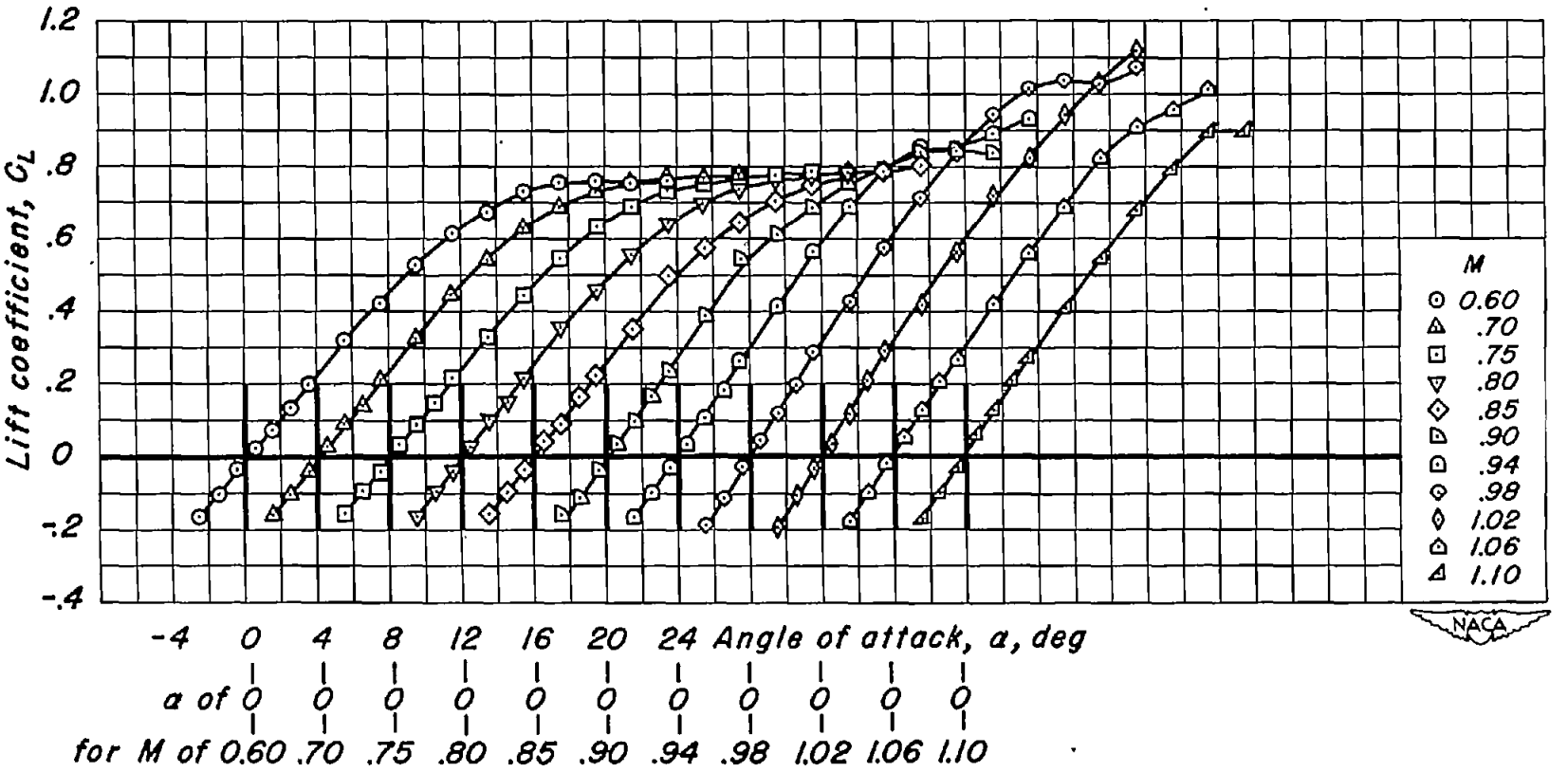

(g) t/c = 0.04; λ = 0.14

Figure 5.- Continued.

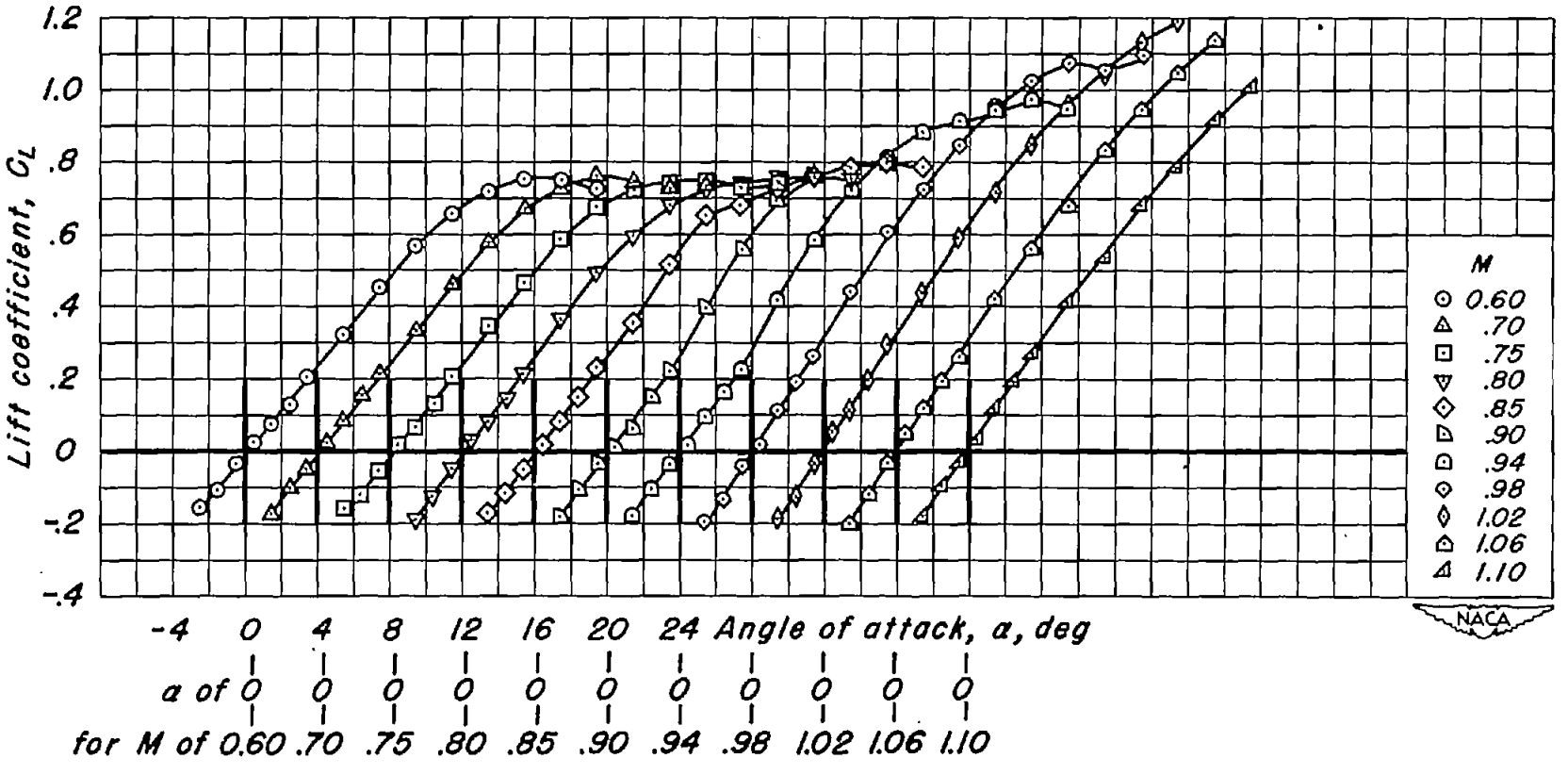

(h) t/c = 0.04; λ = 0.33

Figure 5.- Continued.

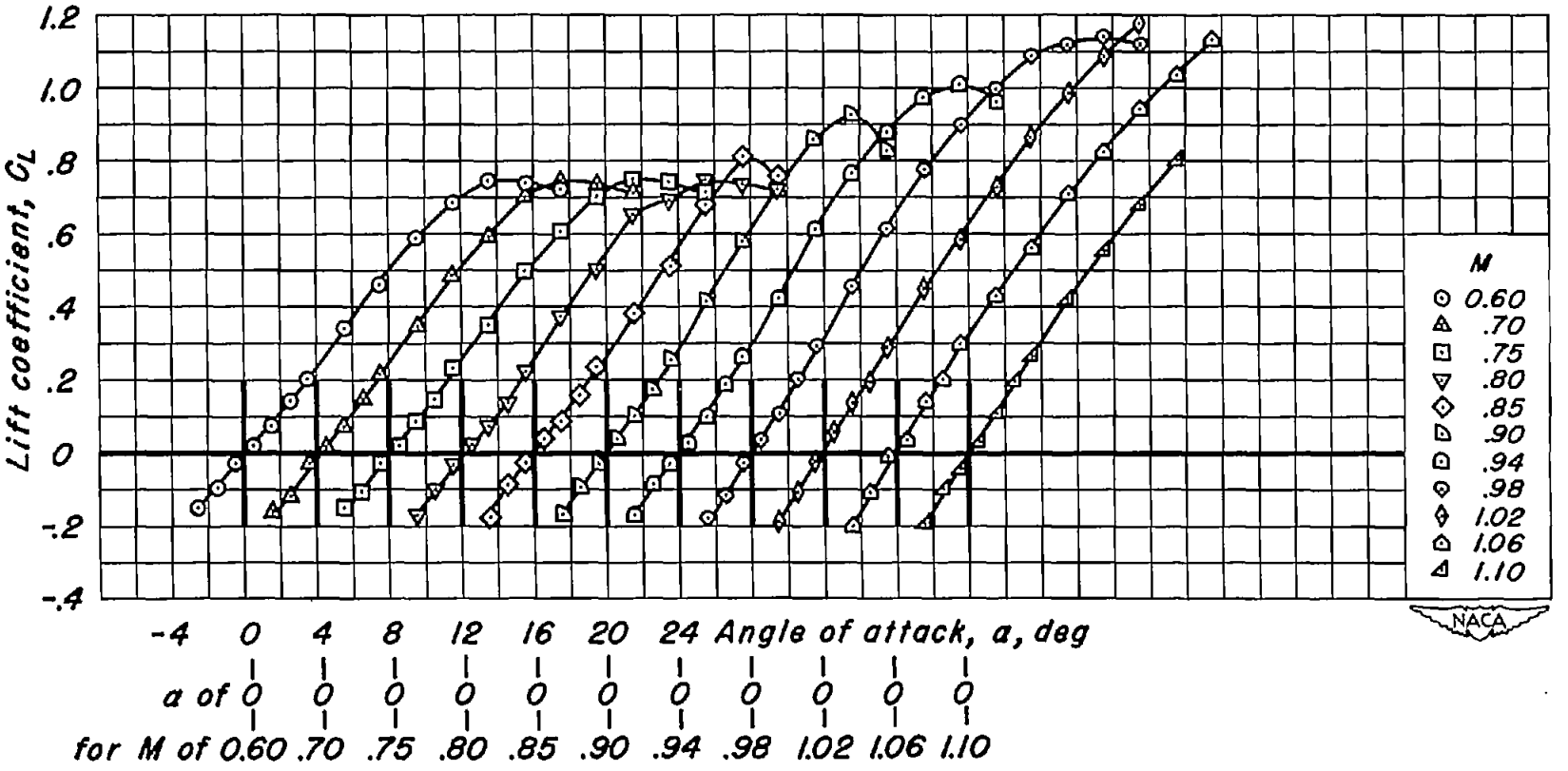

(i) t/c = 0.04; λ = 0.60

Figure 5.- Continued.

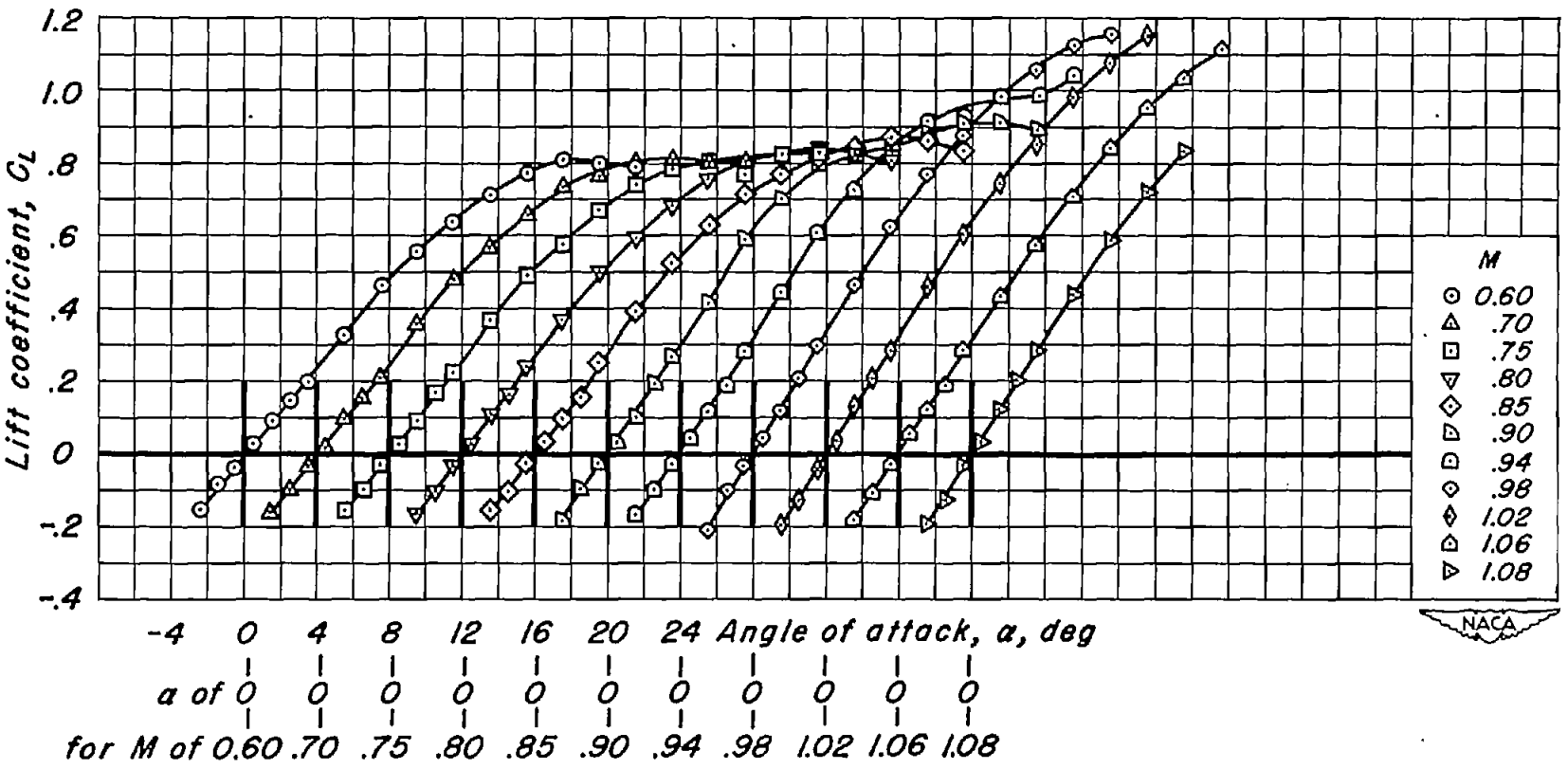

(j) t/c = 0.02; λ = 0.14

Figure 5.- Continued.

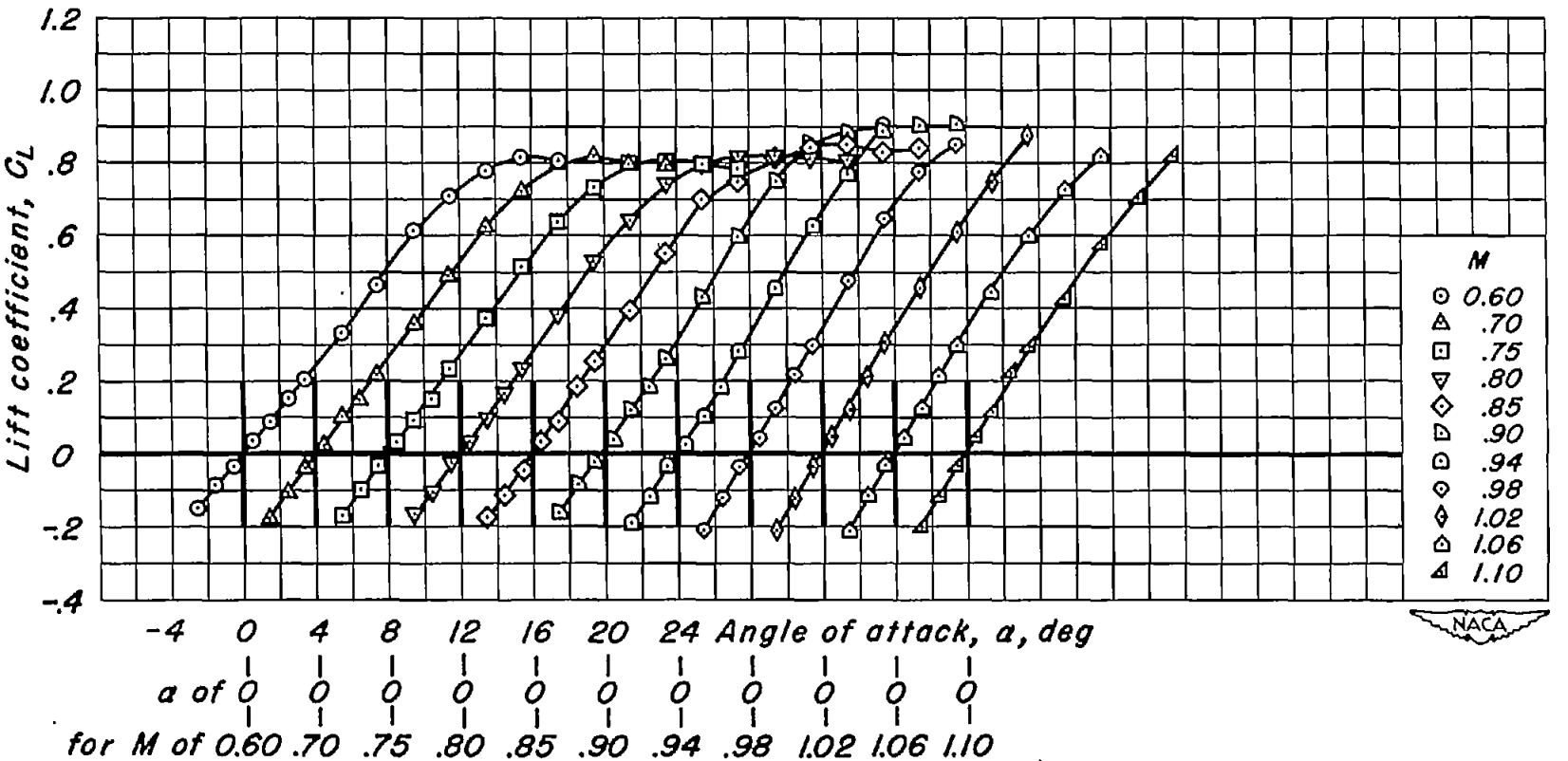

(k) t/c = 0.02; λ = 0.33

Figure 5.- Continued.

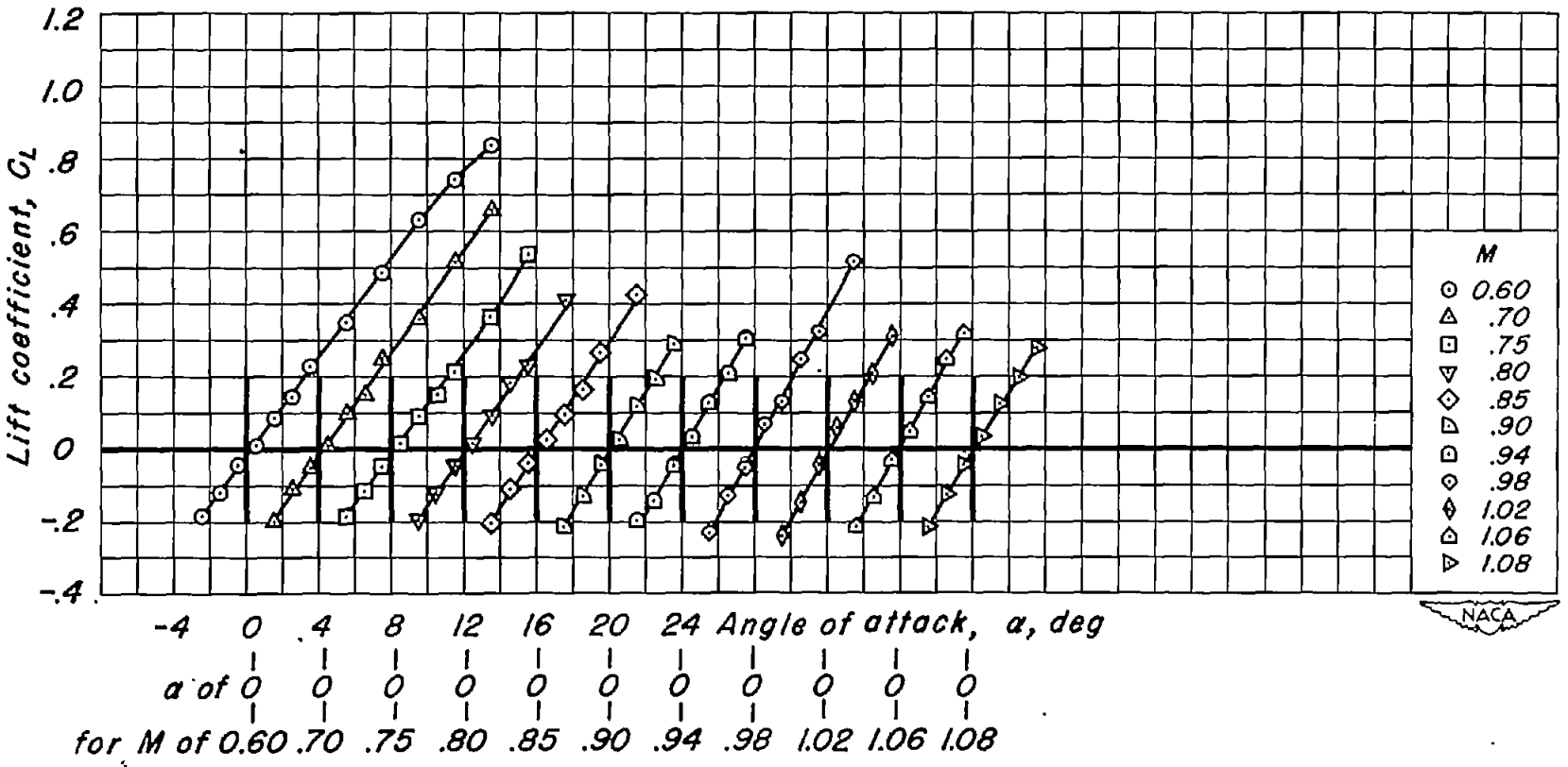

(l) t/c = 0.02; λ = 0.60

Figure 5.- Concluded.

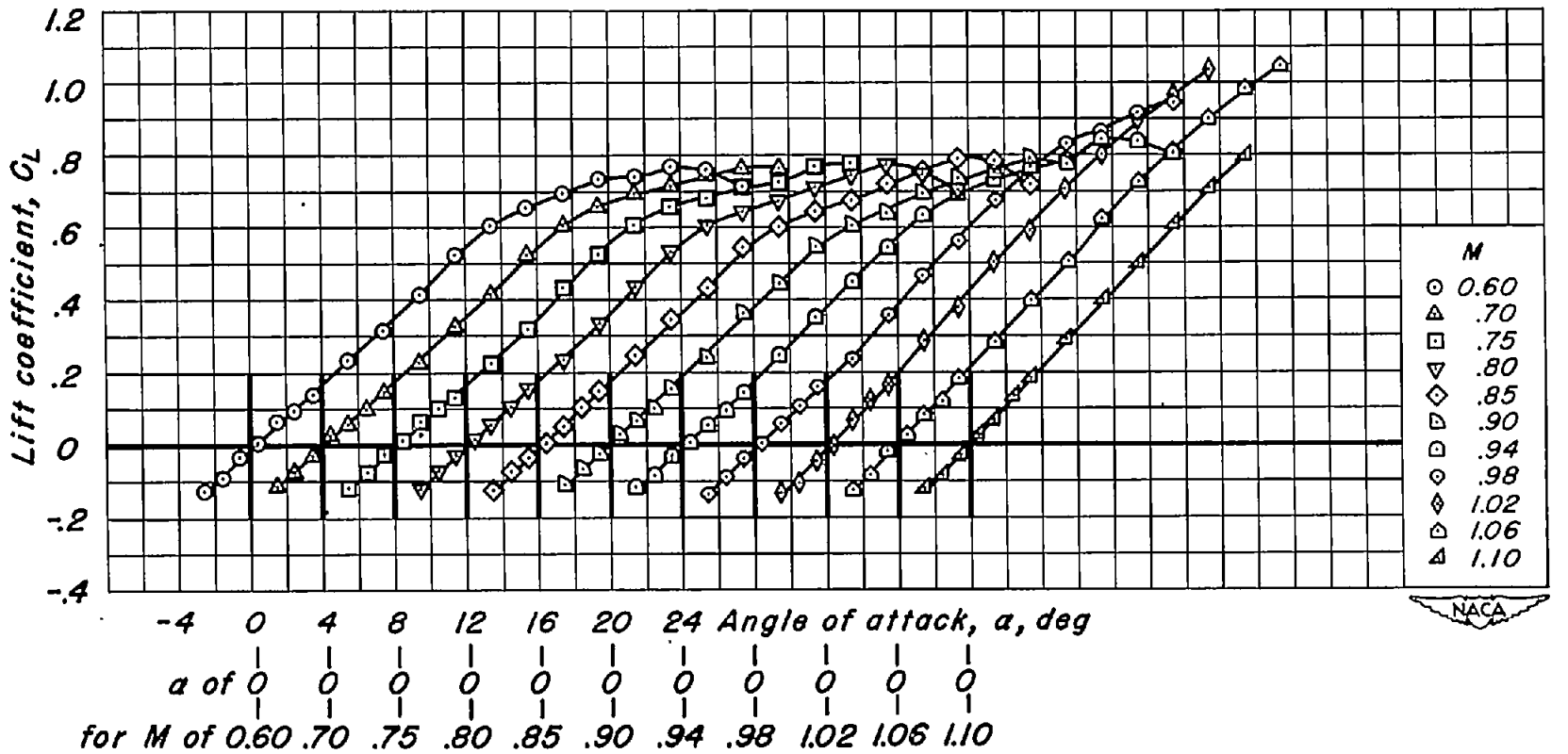

(a) t/c = 0.08; λ = 0.33

Figure 6.- The variation of lift coefficient with angle of attack for the aspect-ratio-2 wings.

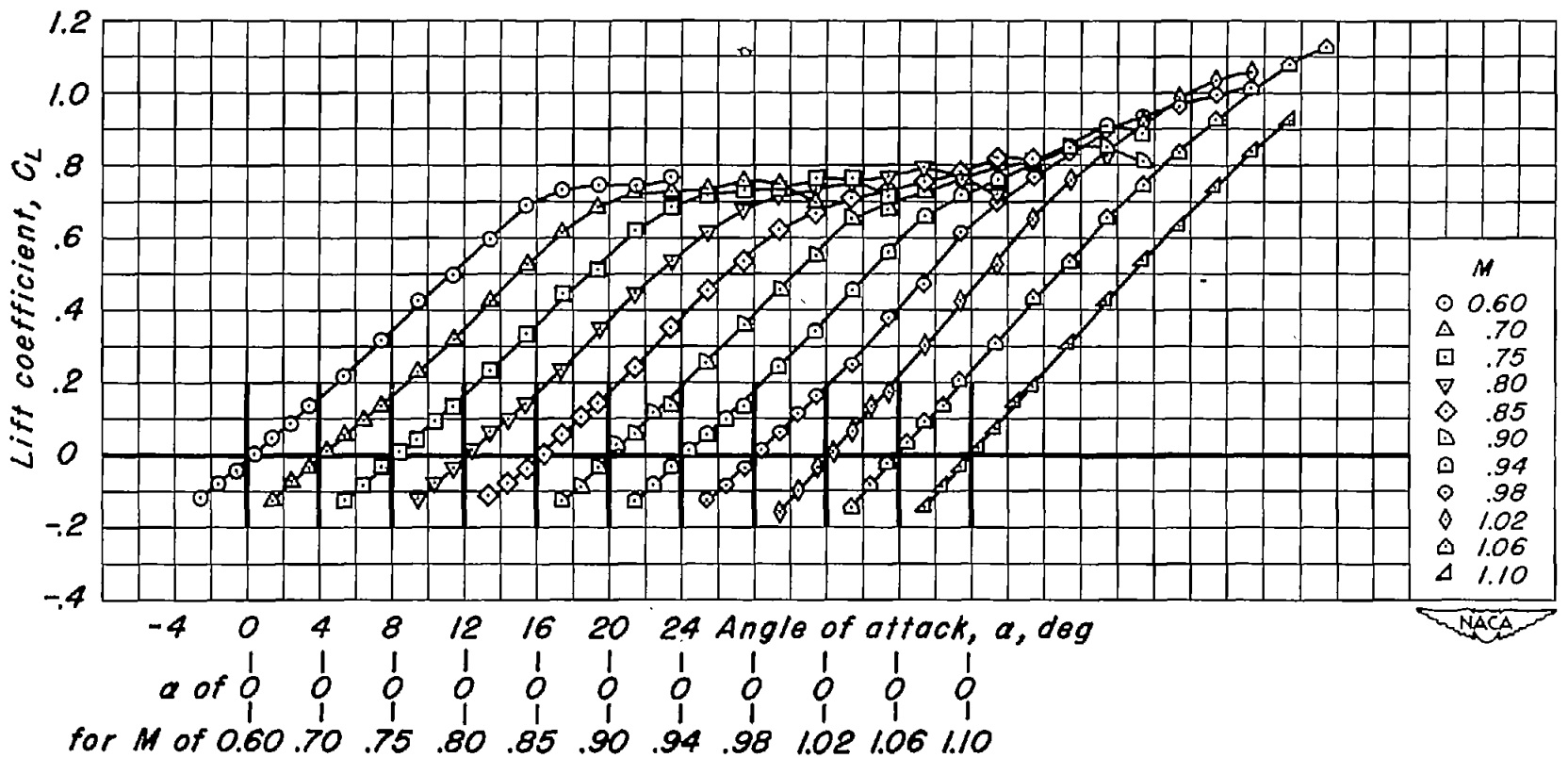

(b) t/c = 0.08; λ = 0.50

Figure 6.- Continued.

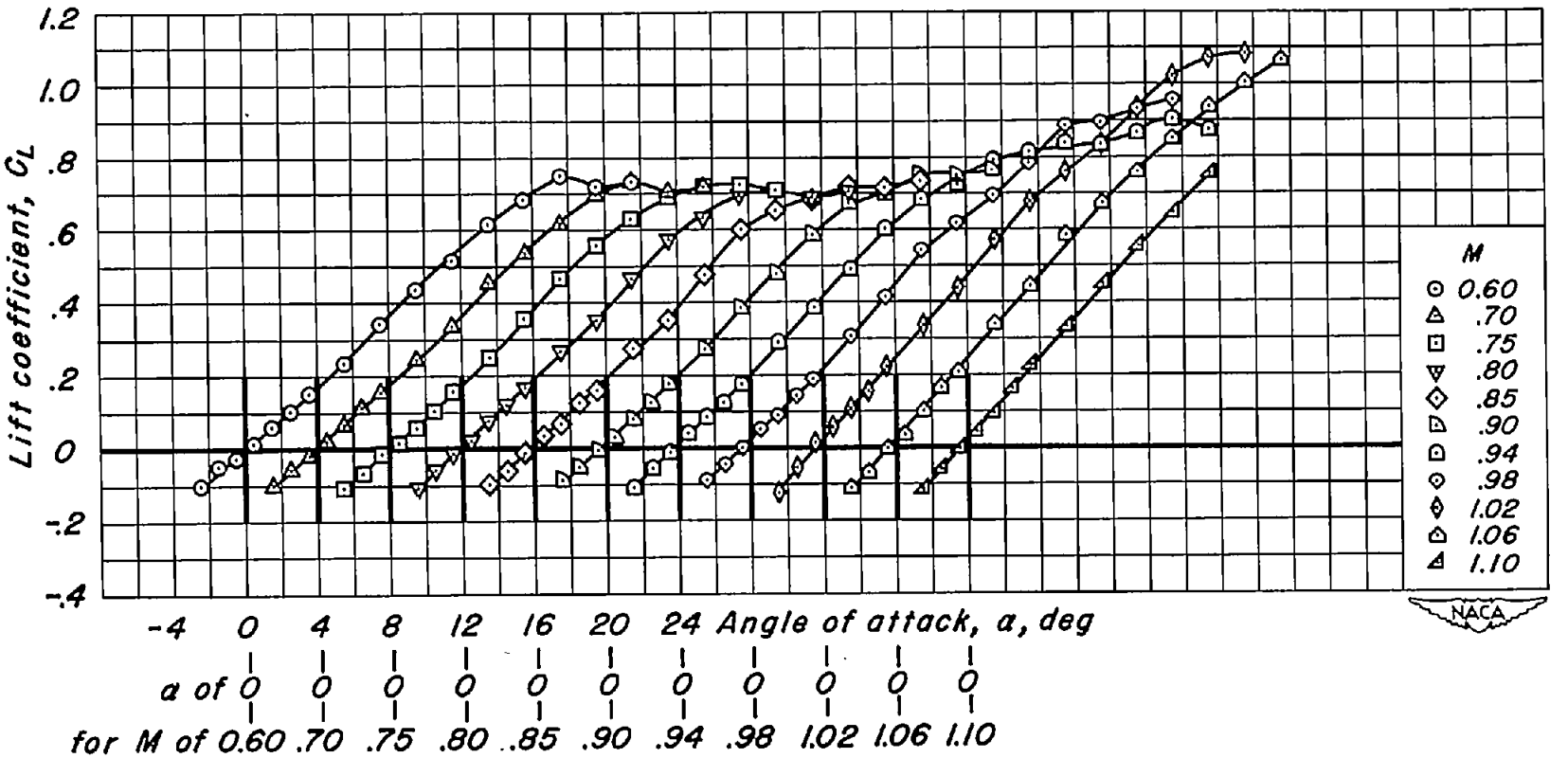

(c) $t/c = 0.08$; $\lambda = 0.72$

Figure 6.- Continued.

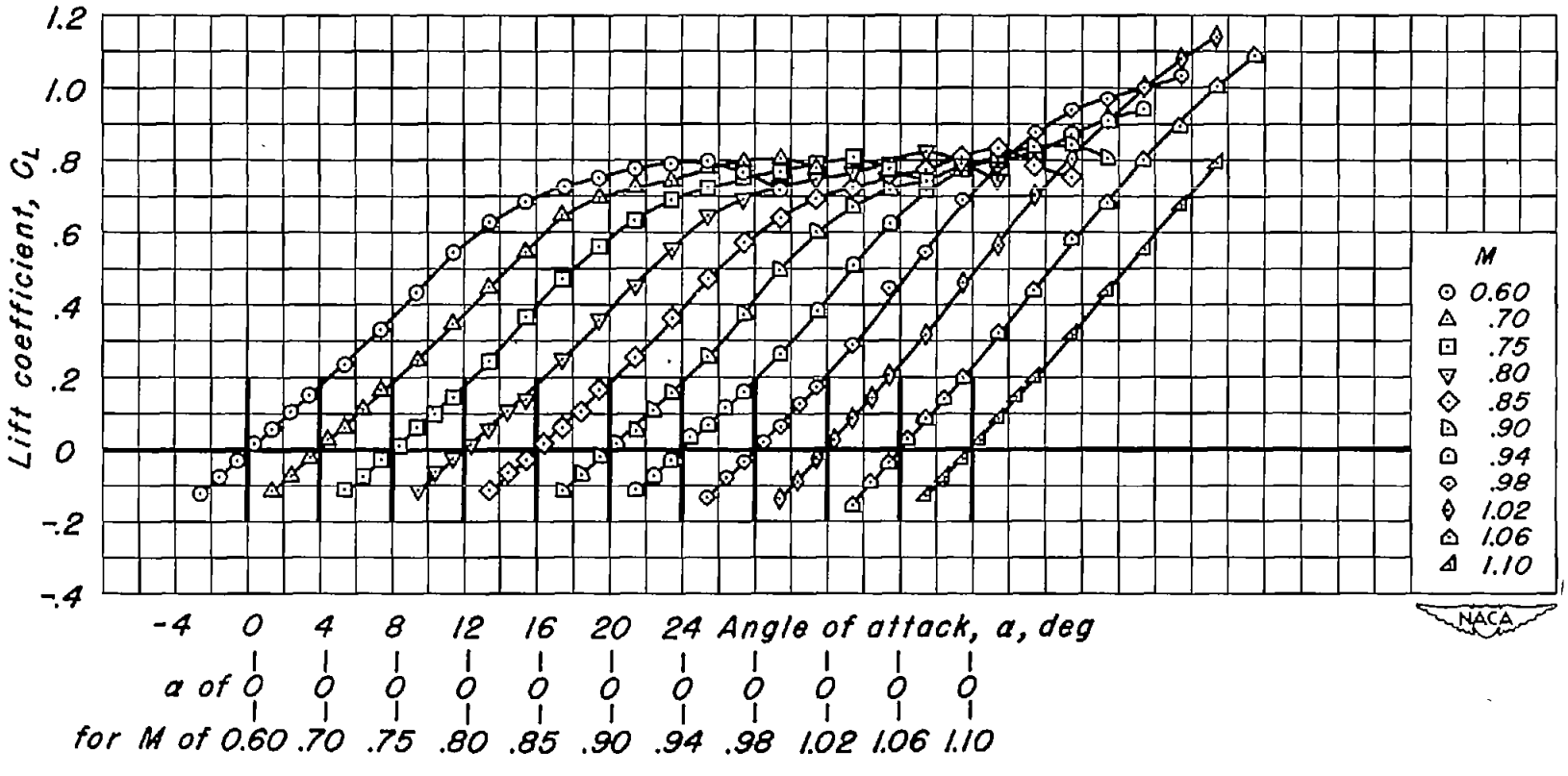

(d) t/c = 0.06; λ = 0.33

Figure 6.- Continued.

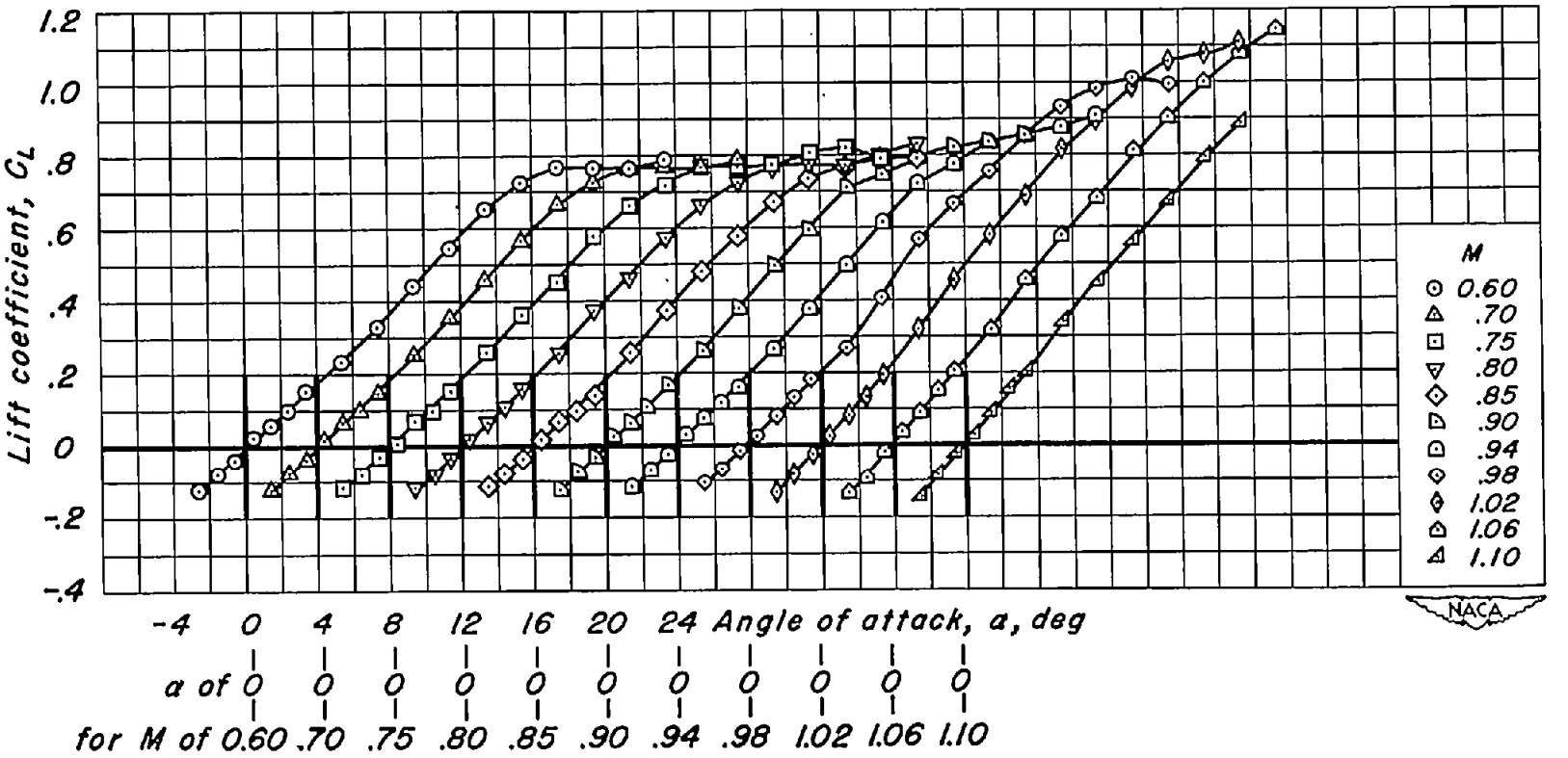

(e) t/c = 0.06; λ = 0.50

Figure 6.- Continued.

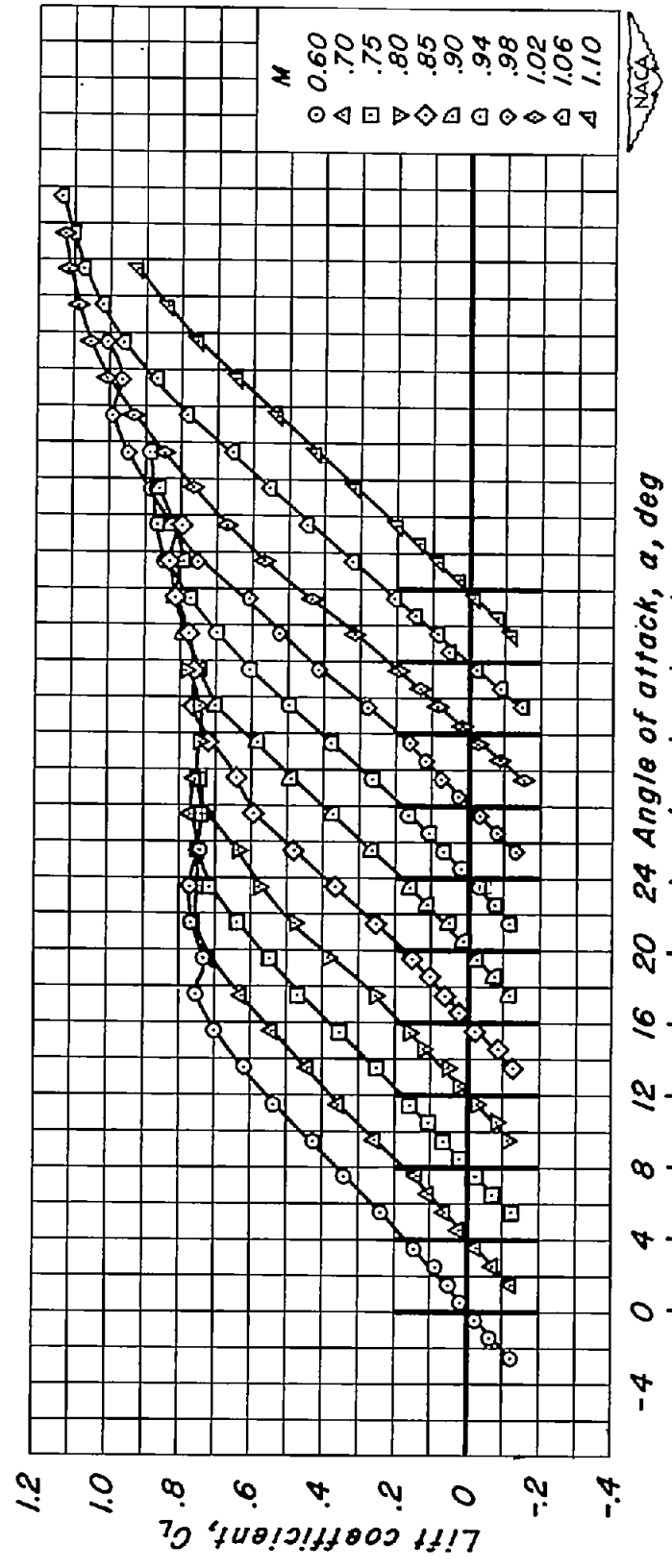

(f) $t/c = 0.06$; $\Lambda = 0.72$

Figure 6.- Continued.

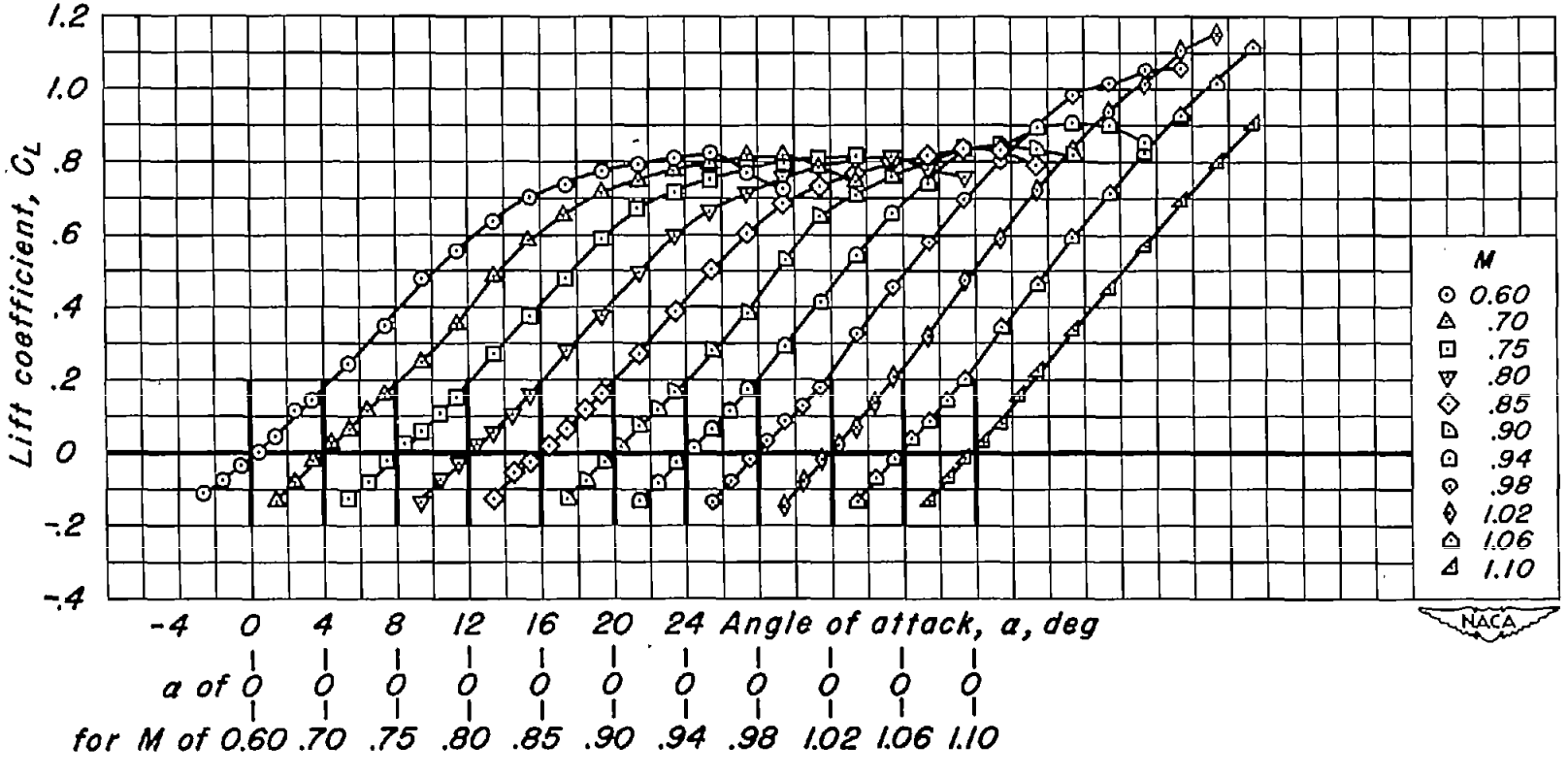

(g) t/c = 0.04; λ = 0.33

Figure 6.- Continued.

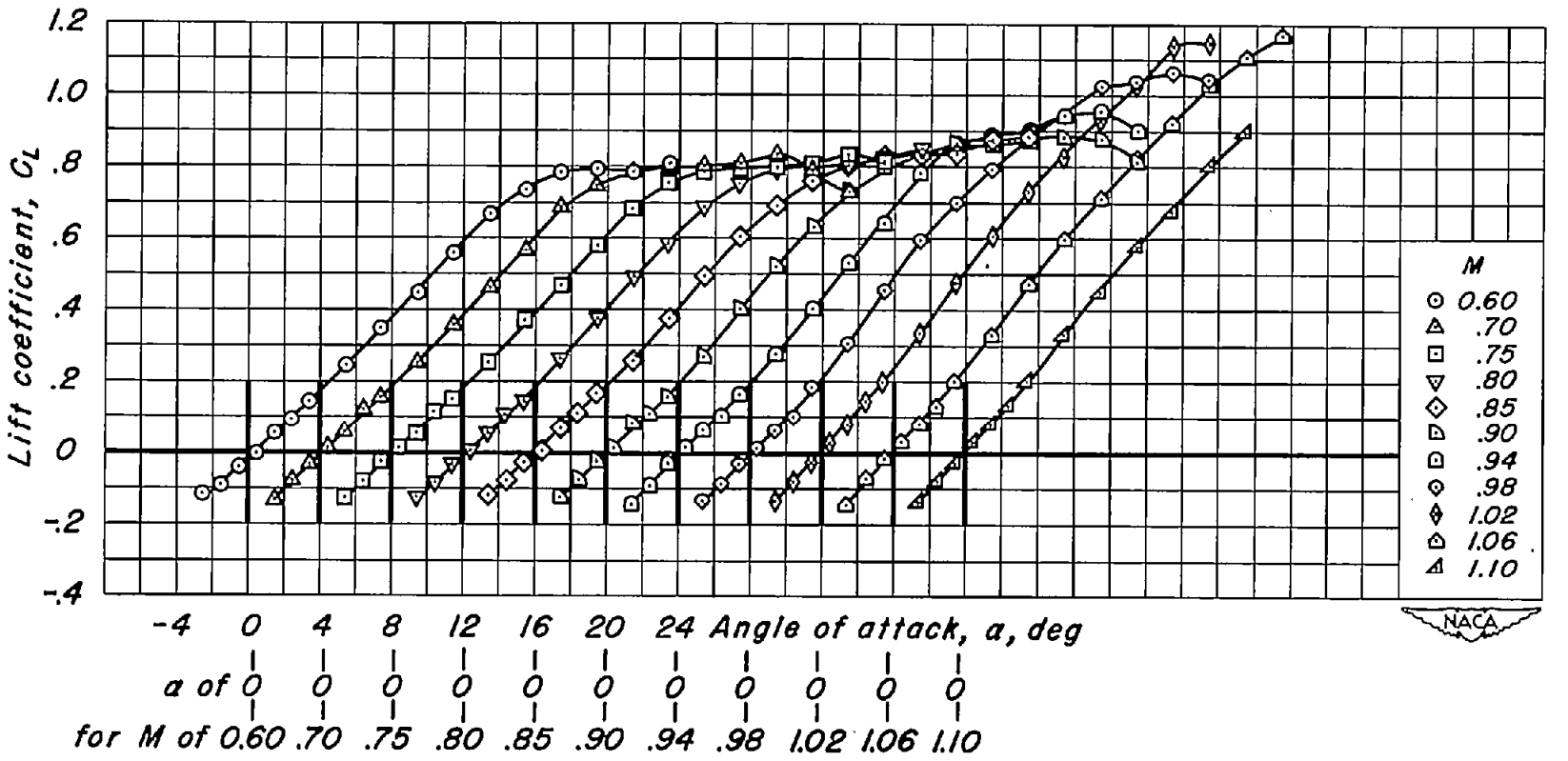

(h) t/c = 0.04; λ = 0.50

Figure 6.- Continued.

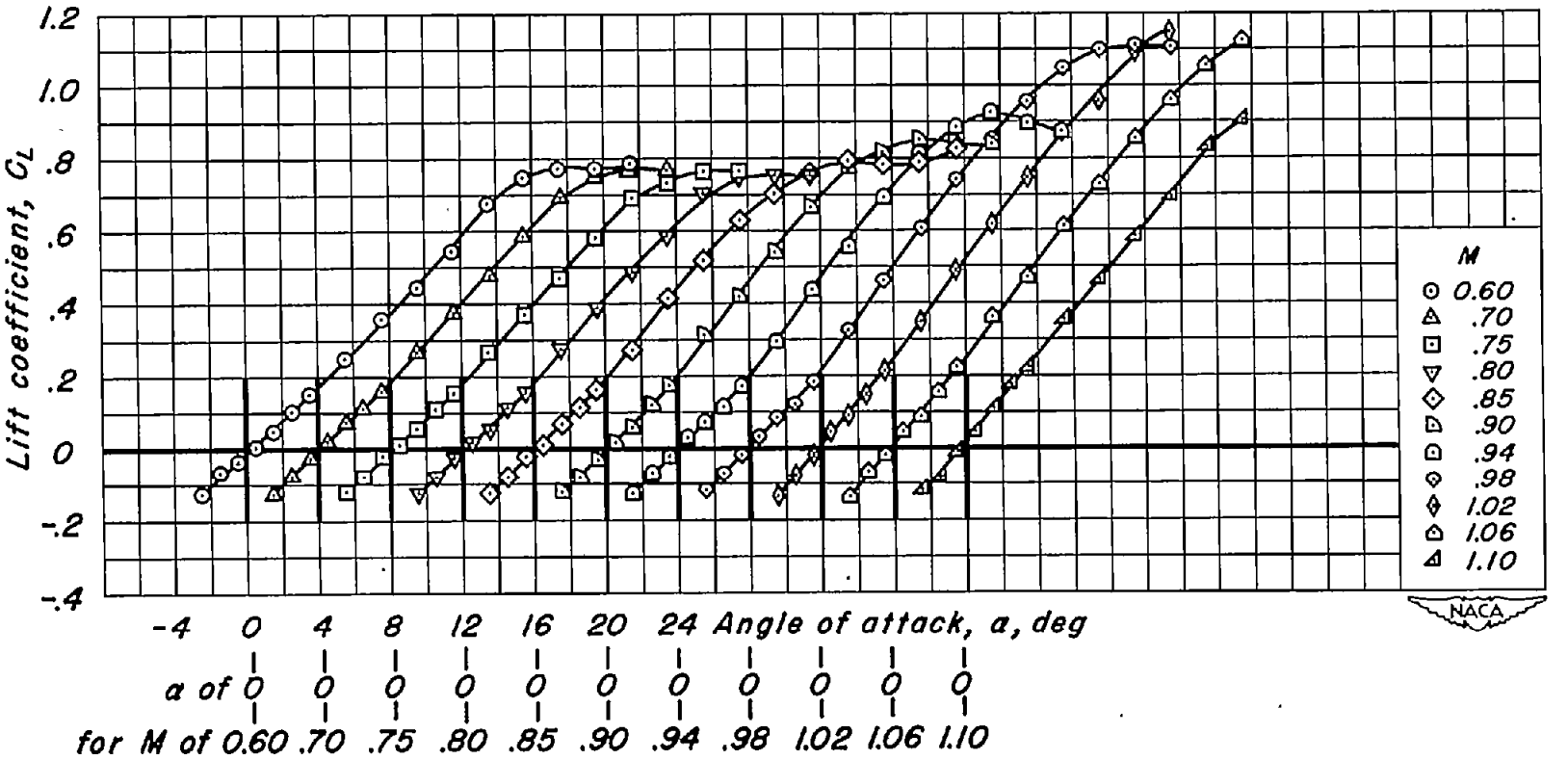

(i) t/c = 0.04; λ = 0.72

Figure 6.- Continued.

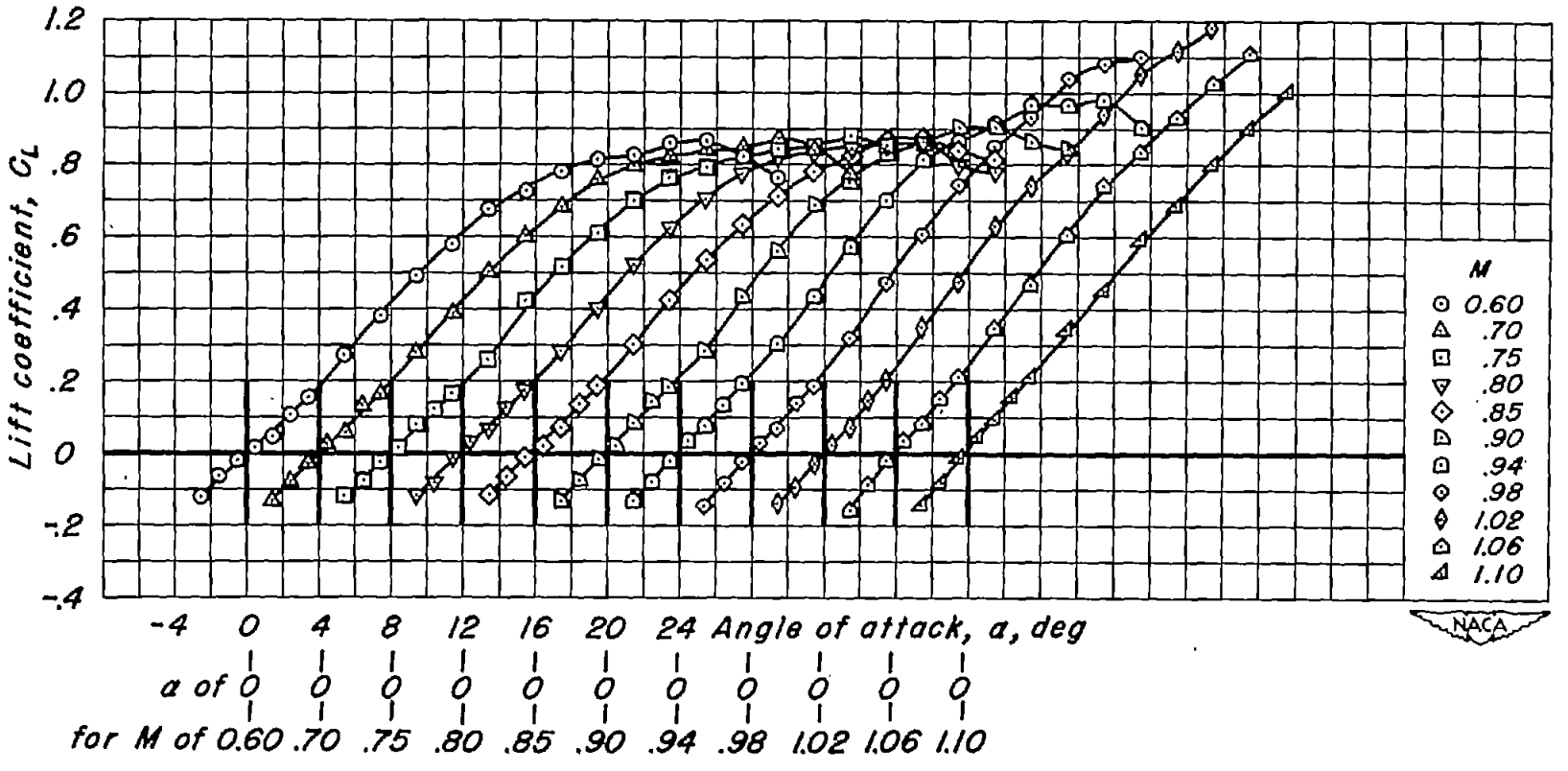

(j) t/c = 0.02; λ = 0.33

Figure 6.- Continued.

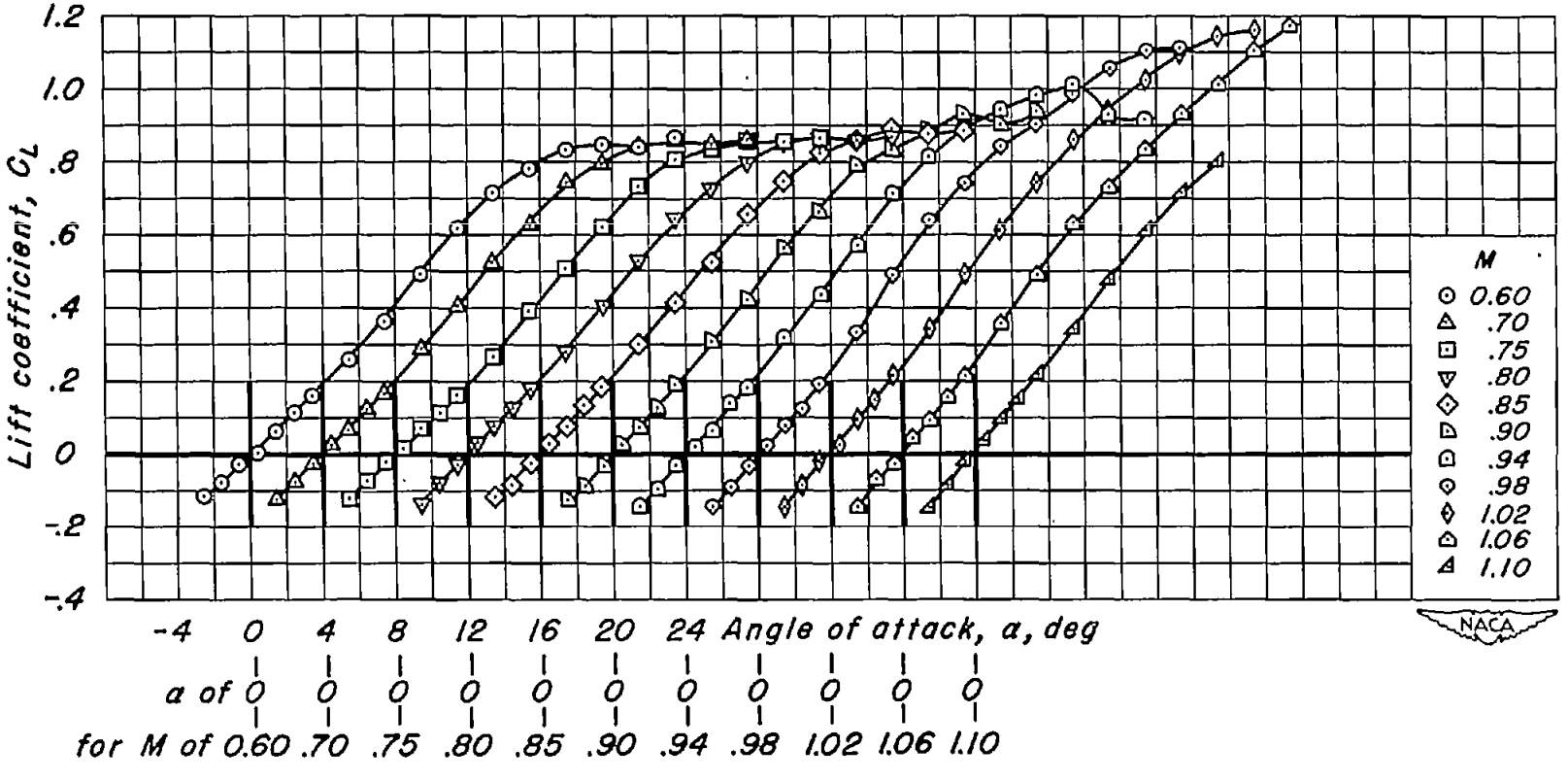

(k) t/c = 0.02; λ = 0.50

Figure 6.- Continued.

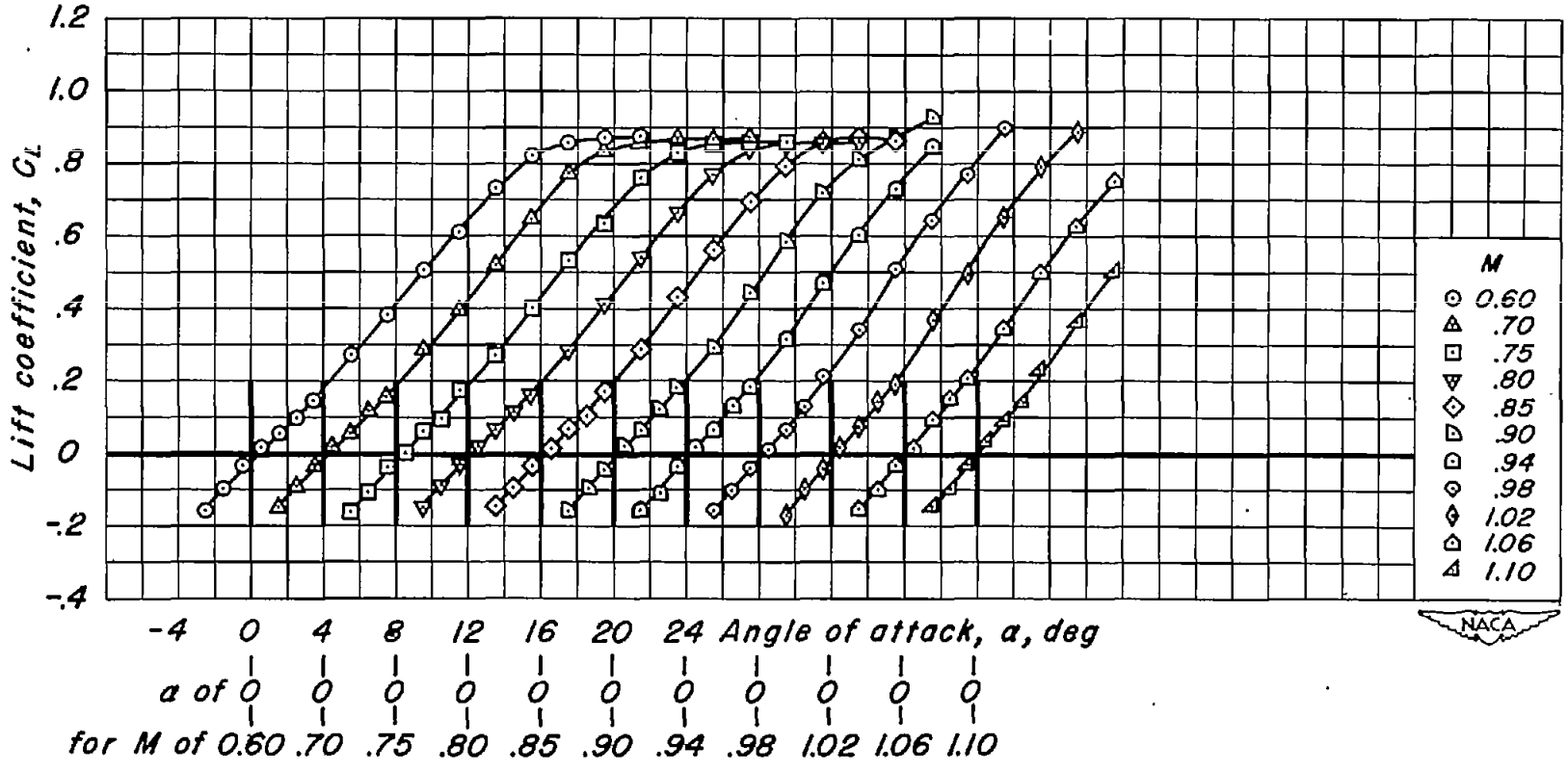

(l) t/c = 0.02; λ = 0.72

Figure 6.- Concluded.

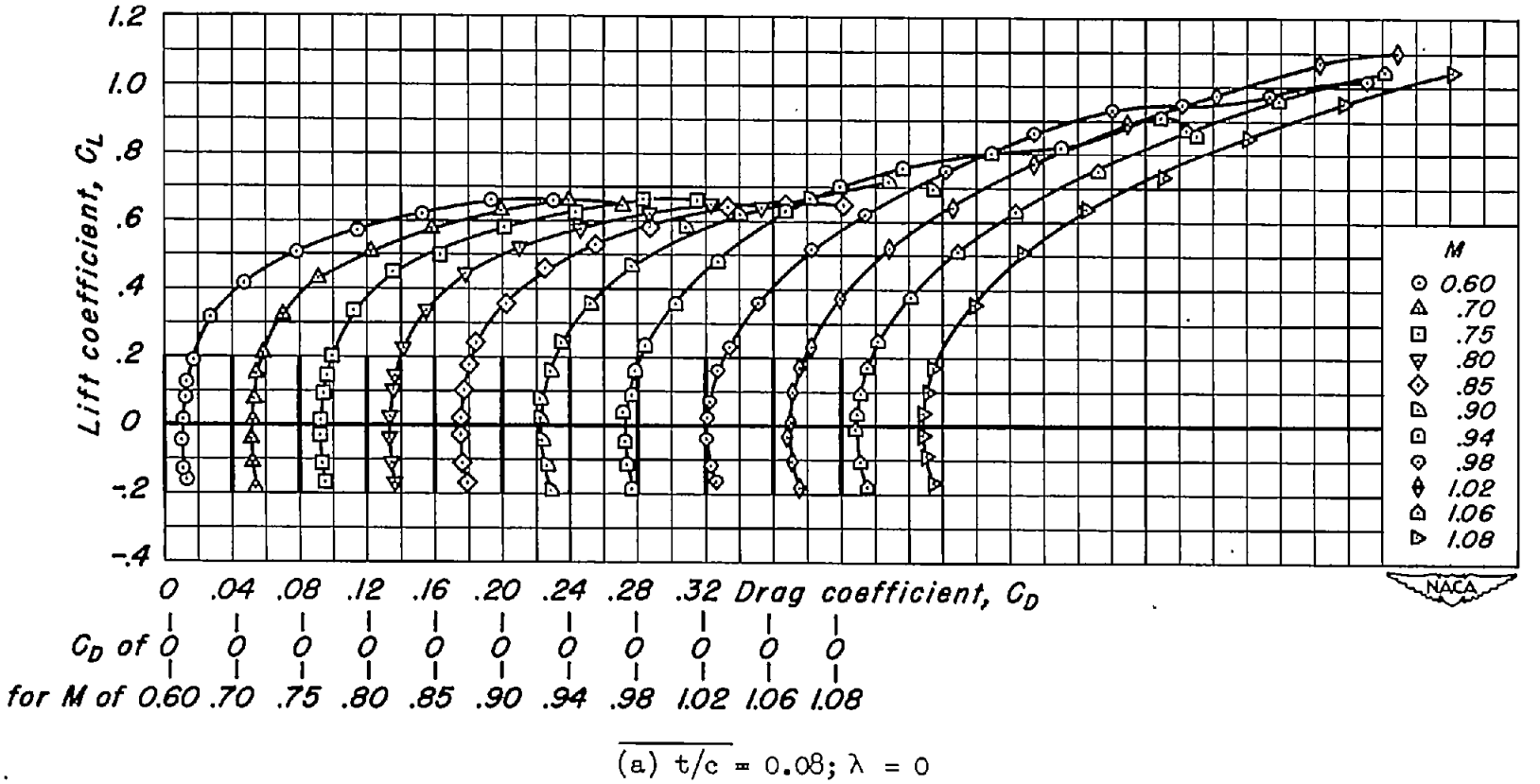

(a) $\overline{t/c} = 0.08$; $\lambda = 0$

Figure 7.- The variation of lift coefficient with drag coefficient for the aspect-ratio-4 wings.

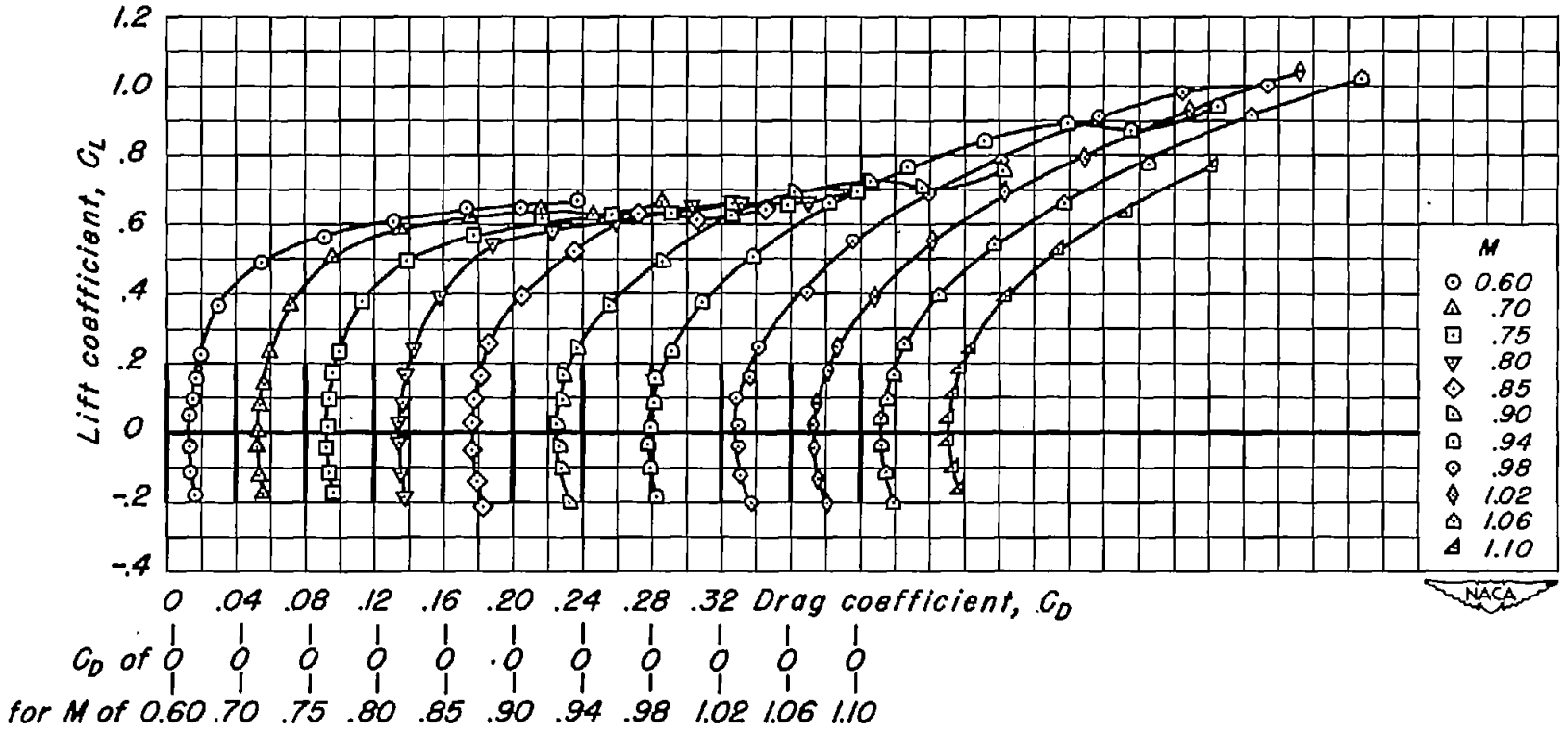

(b) t/c = 0.08; λ = 0.20

Figure 7.- Continued.

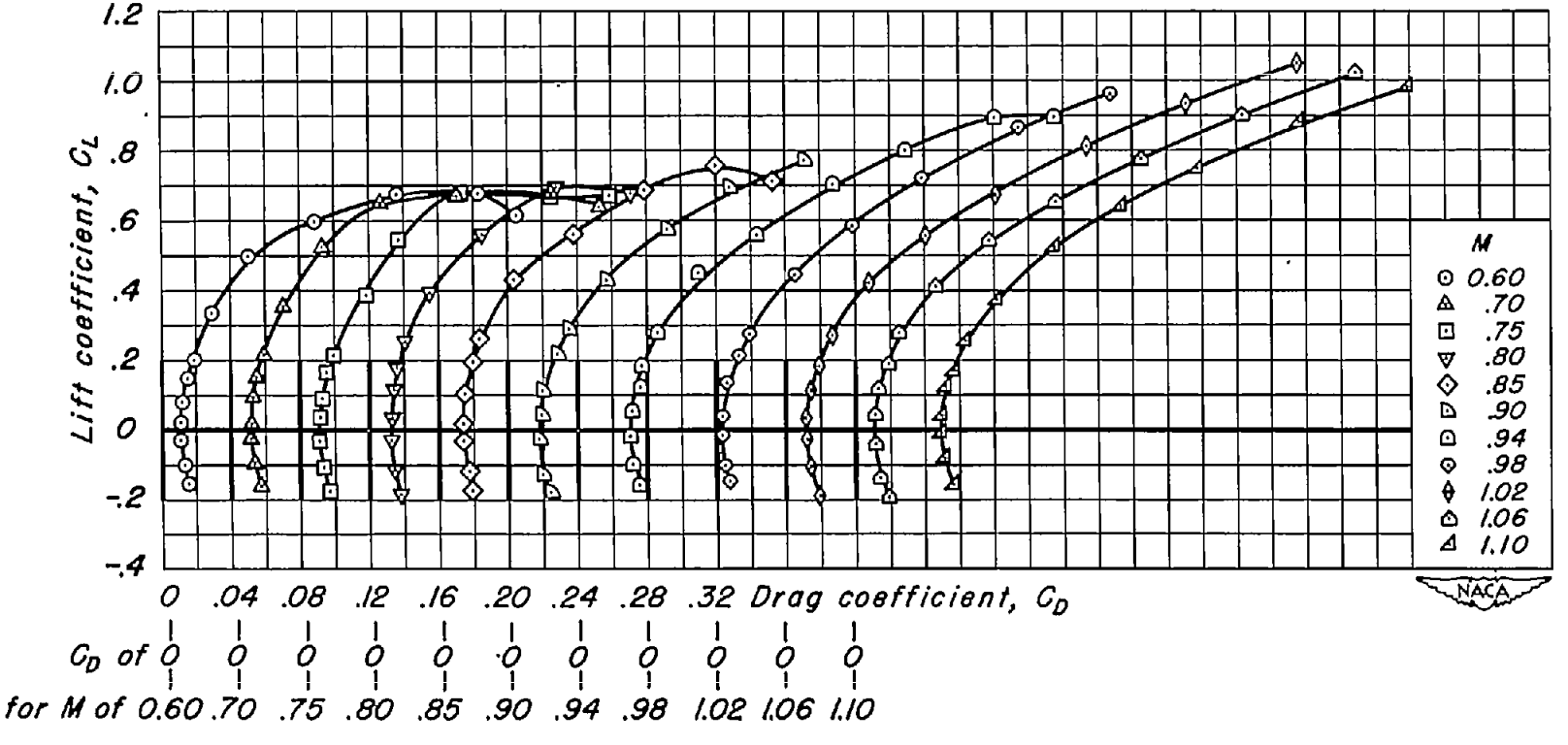

(c) t/c = 0.08; λ = 0.50

Figure 7.- Continued.

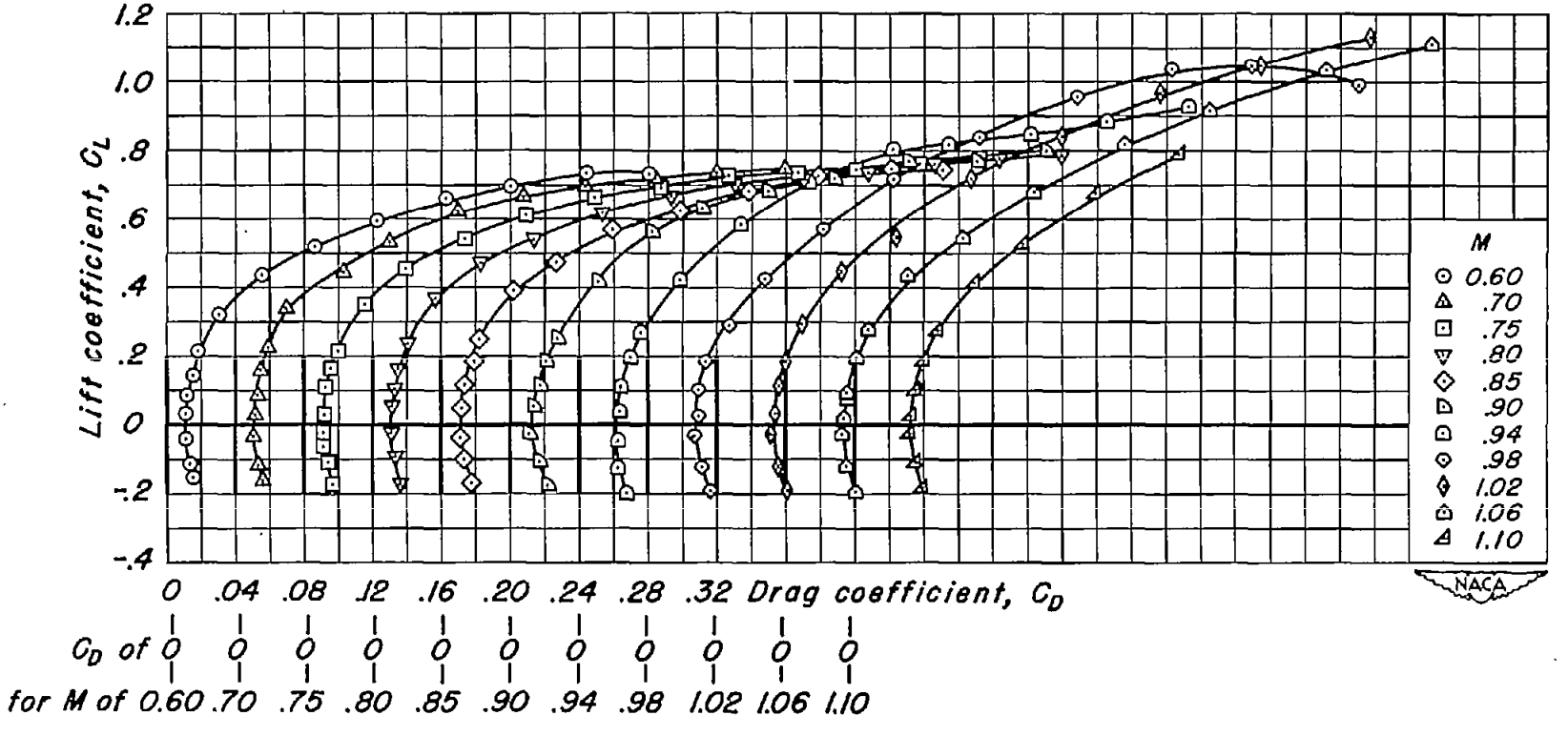

(d) t/c = 0.06; λ = 0

Figure 7.- Continued.

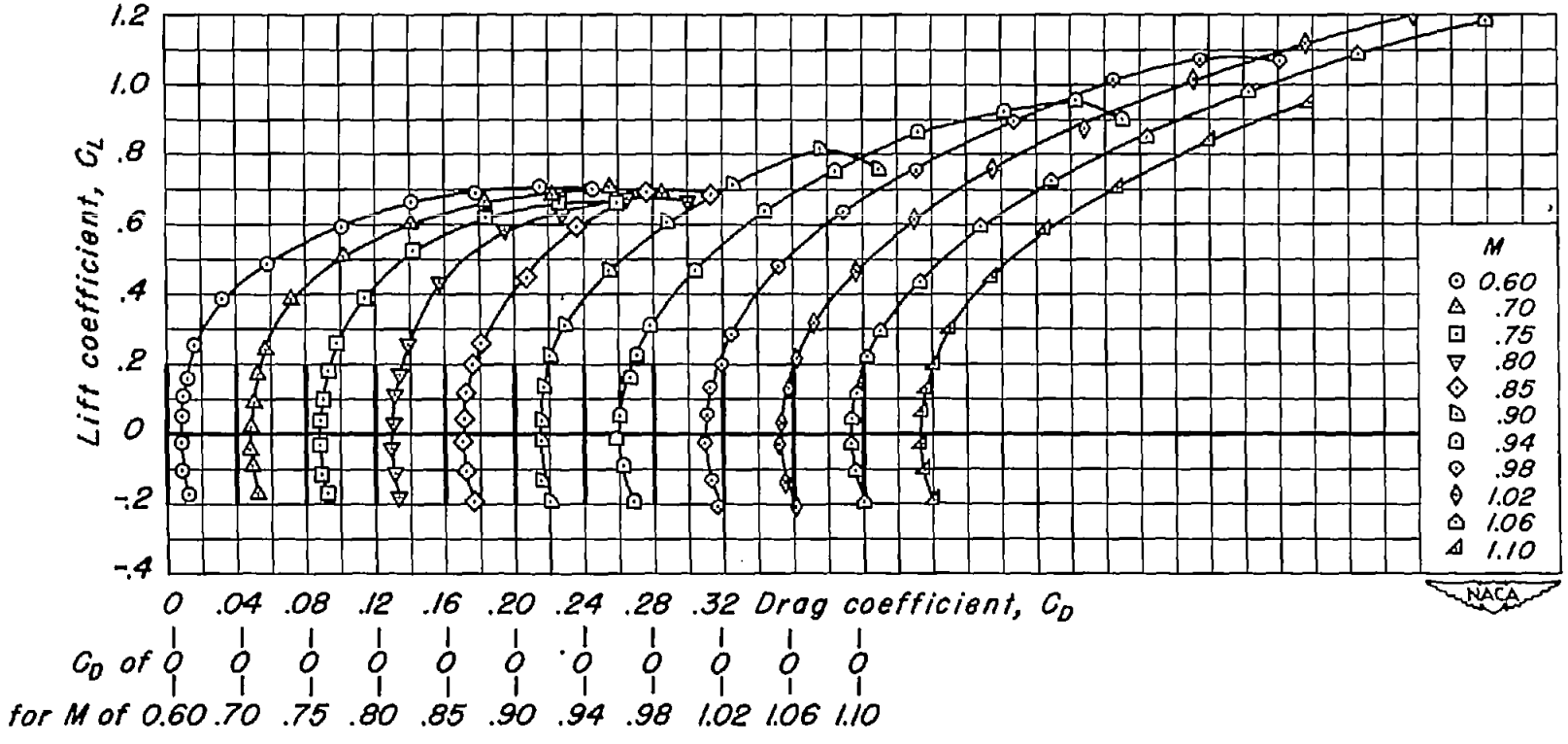

(e) t/c = 0.06; λ = 0.20

Figure 7.- Continued.

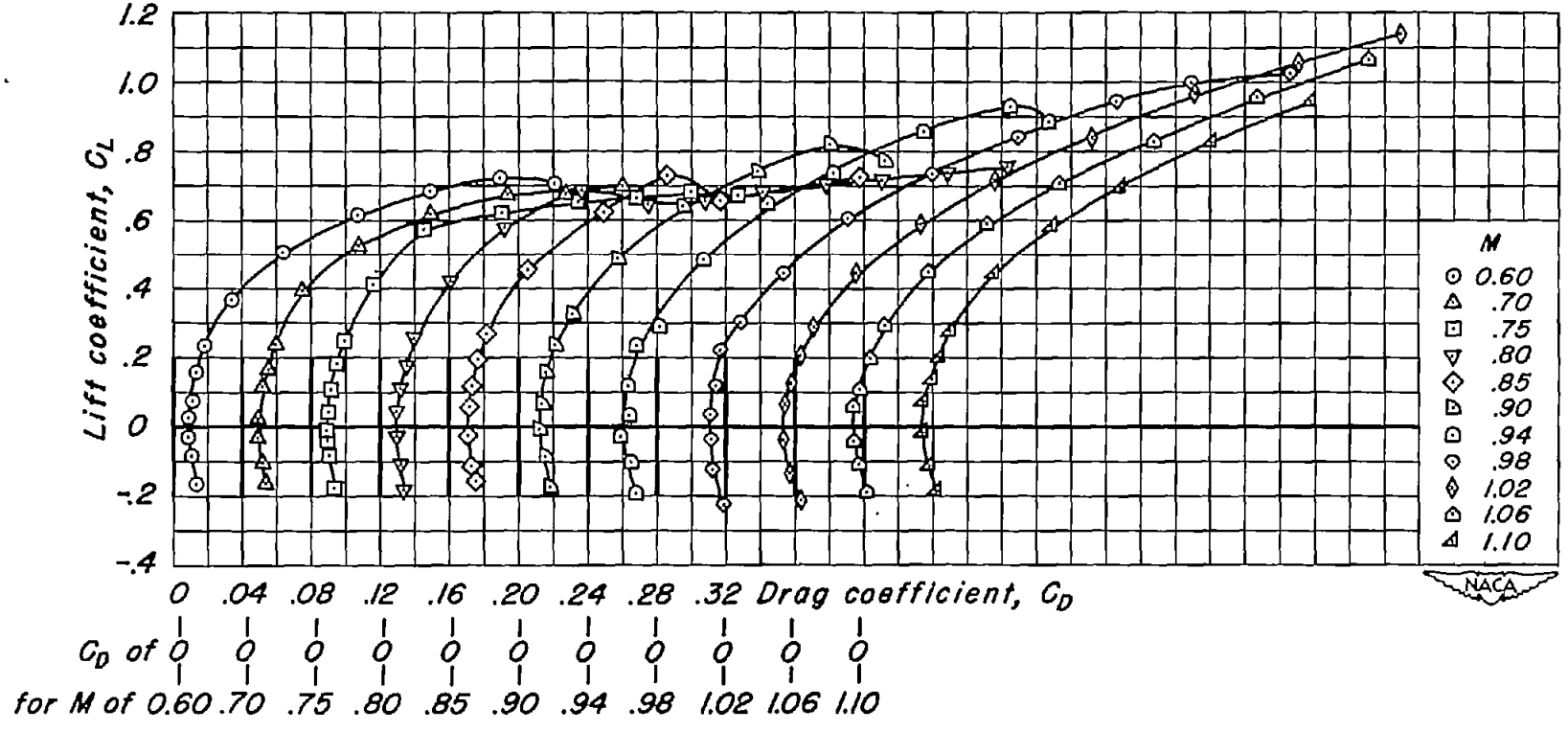

(f) t/c = 0.06; λ = 0.50

Figure 7.- Continued.

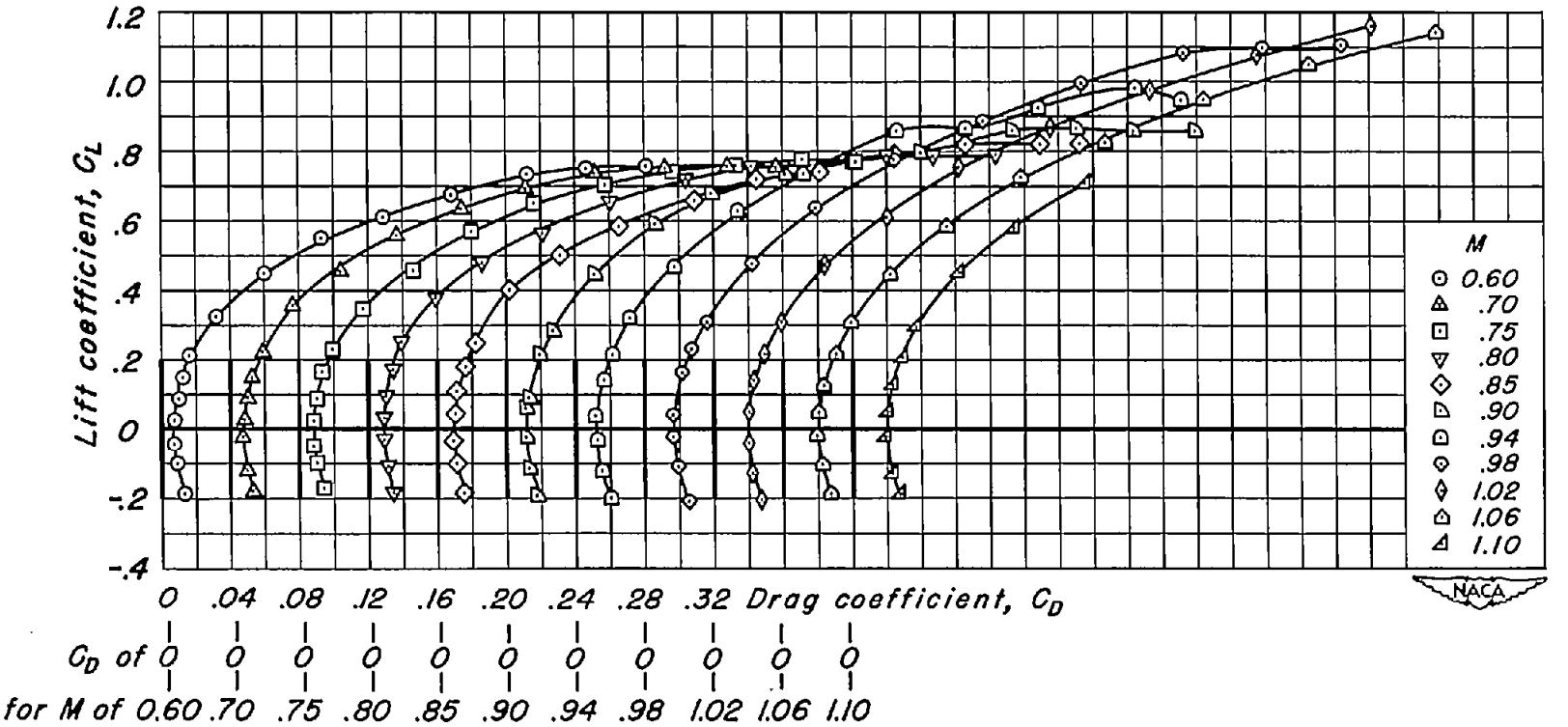

(g) t/c = 0.04; $\lambda = 0$

Figure 7.- Continued.

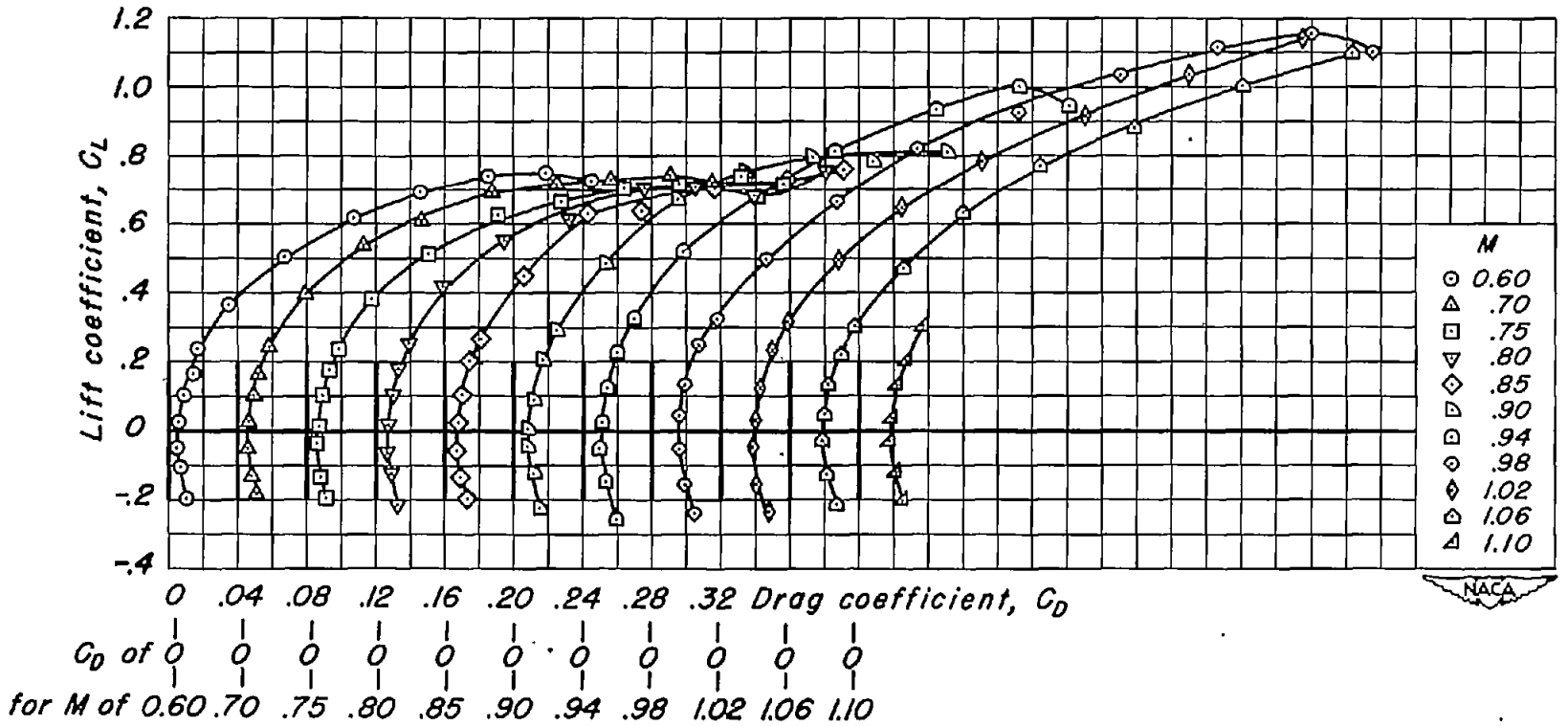

(h) t/c = 0.04; λ = 0.20

Figure 7.- Continued.

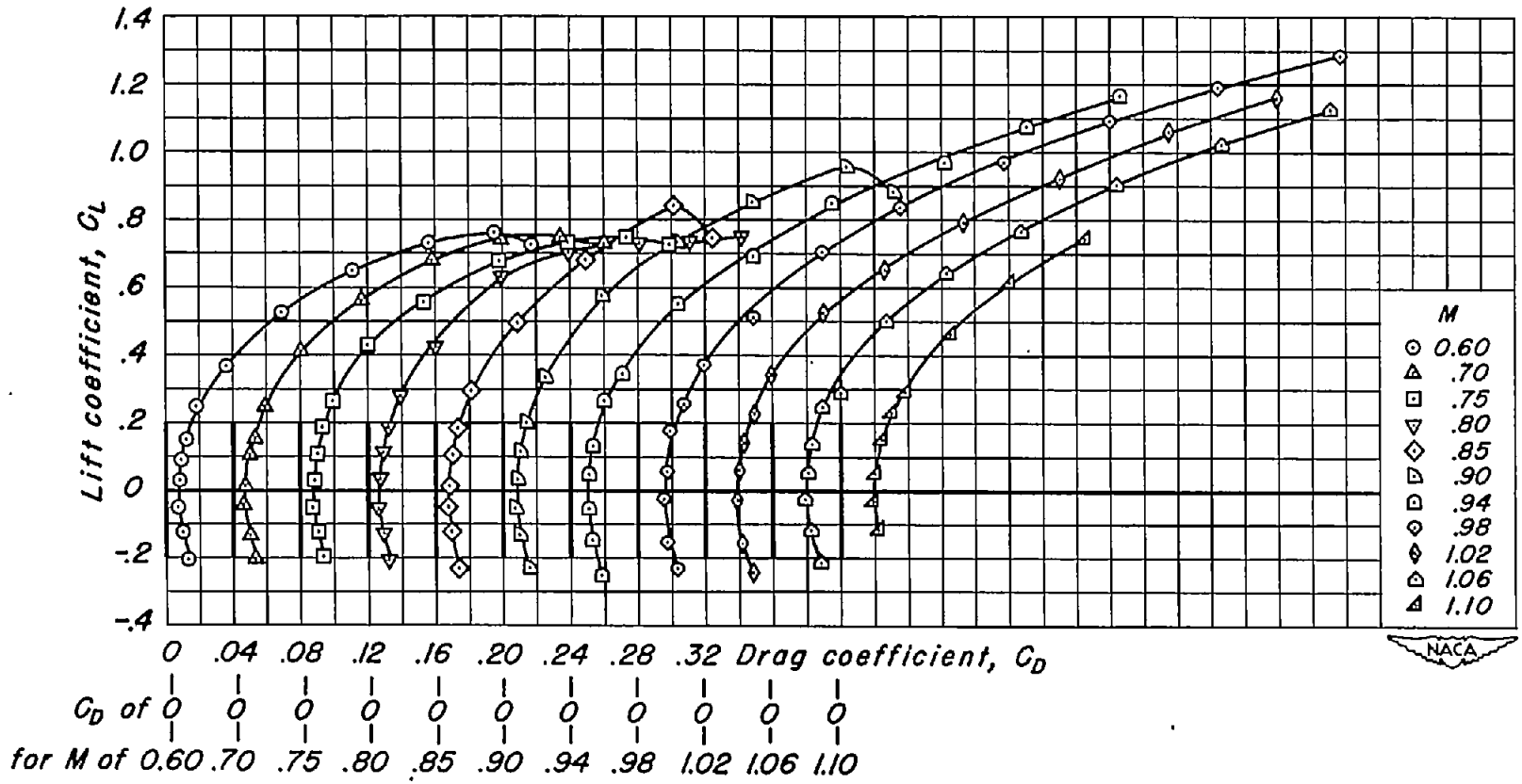

(i) t/c = 0.04; λ = 0.50

Figure 7.- Continued.

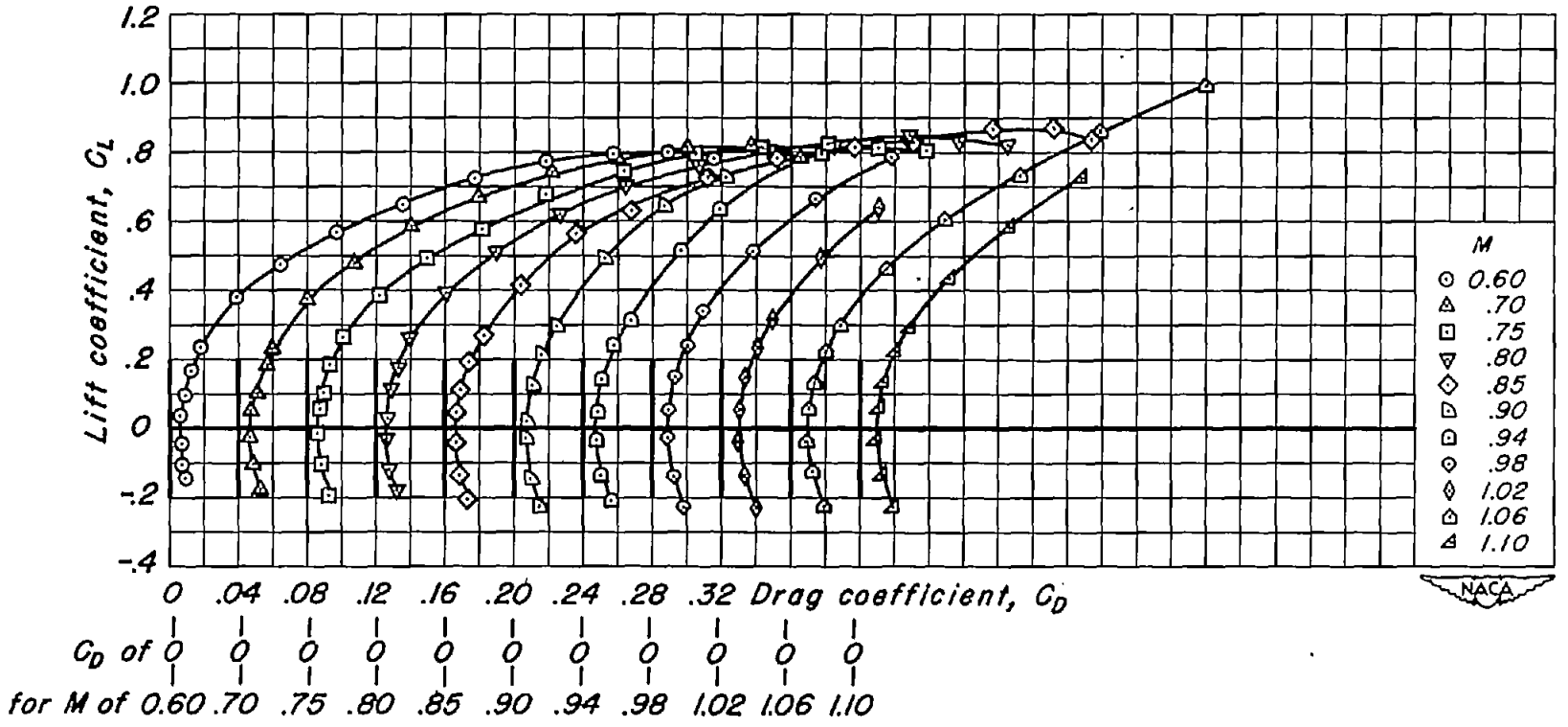

(j) t/c = 0.02; λ = 0

Figure 7.- Continued.

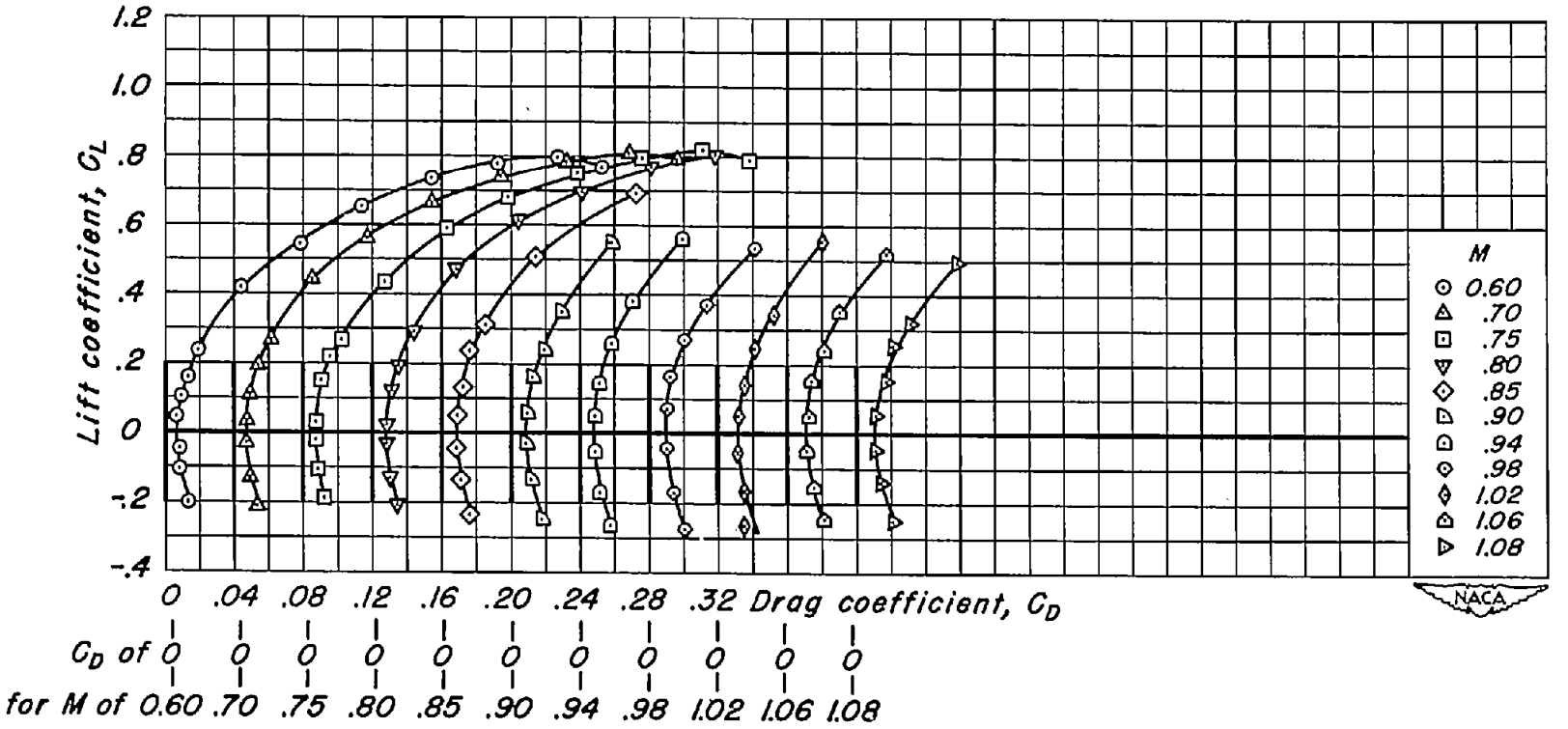

(k) t/c = 0.02; λ = 0.20

Figure 7.- Continued.

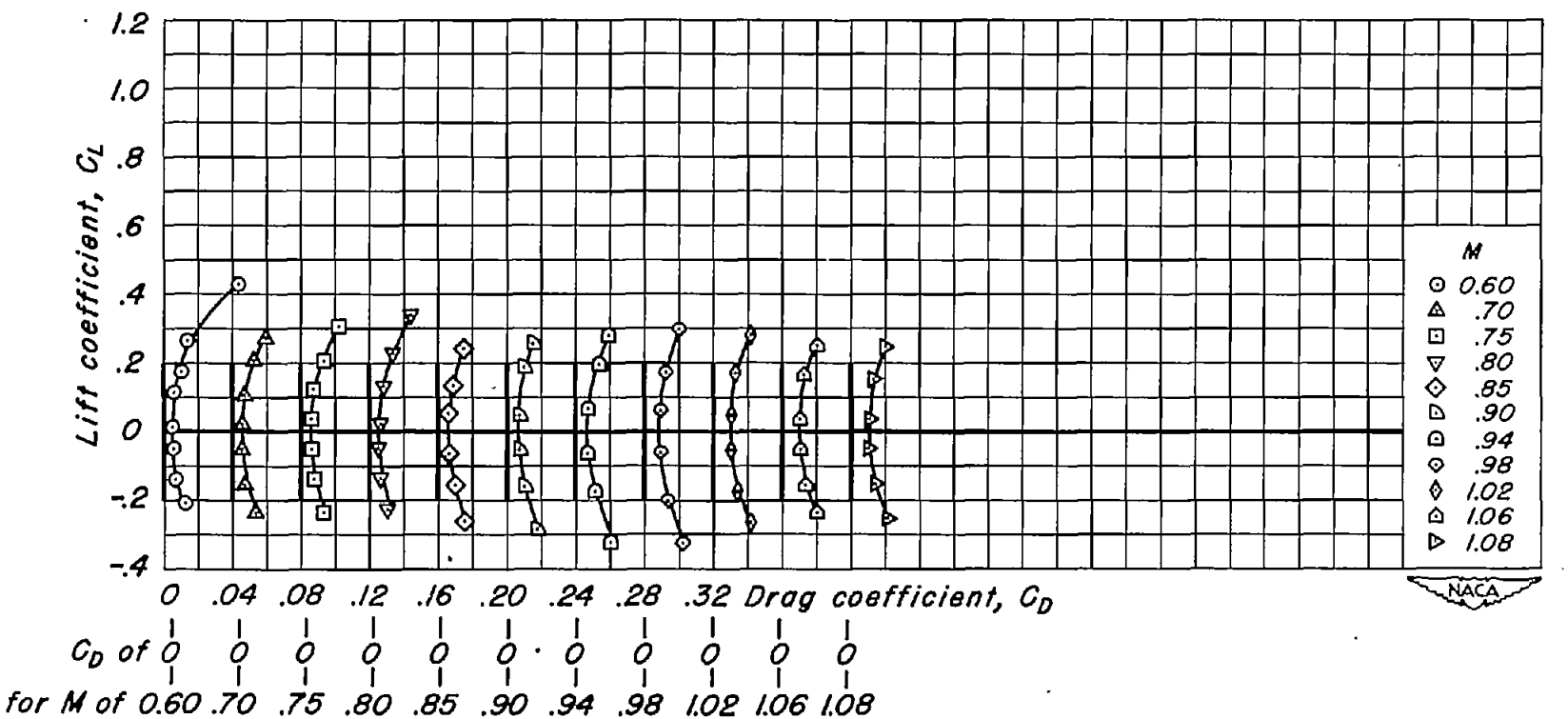

(l) t/c = 0.02; λ = 0.50

Figure 7.- Concluded.

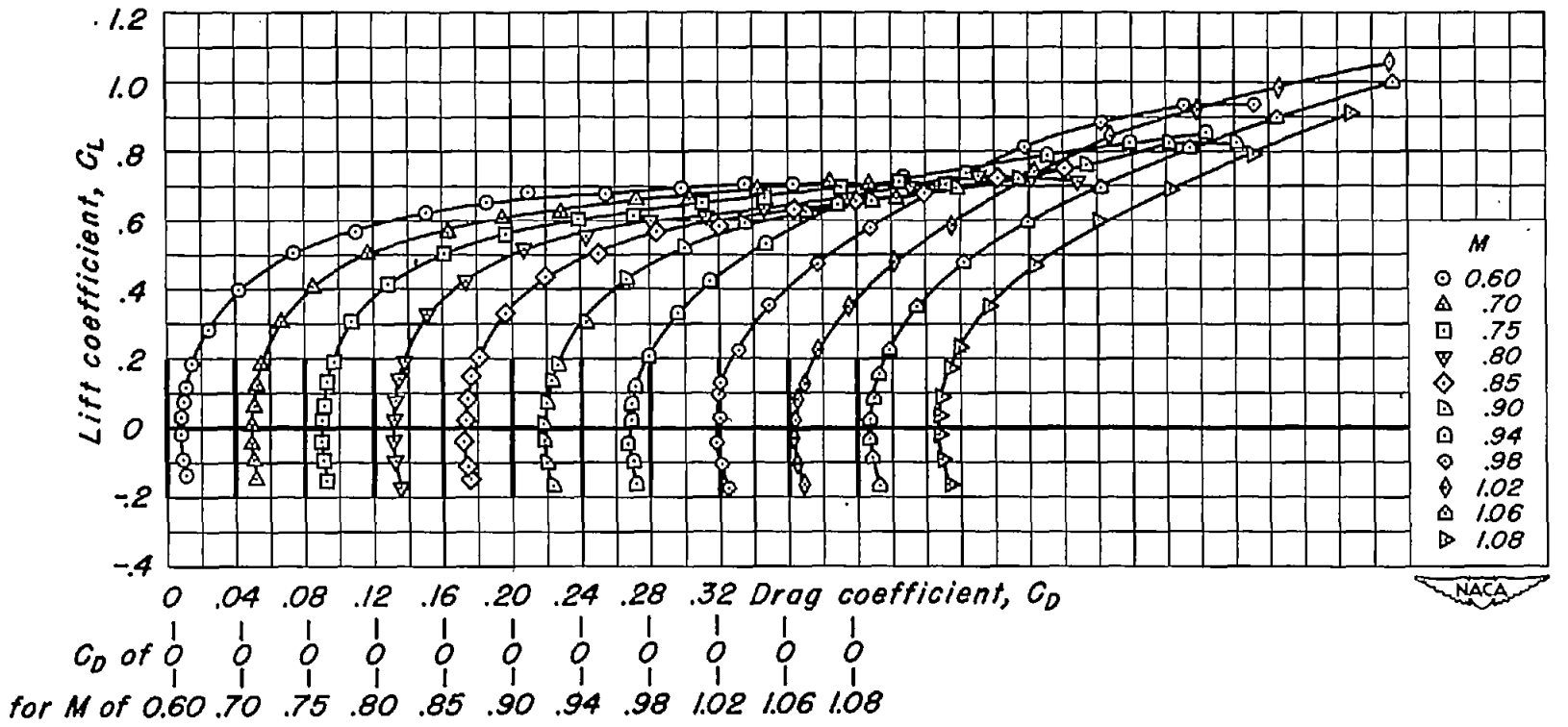

(a) t/c = 0.08; λ = 0.14

Figure 8.- The variation of lift coefficient with drag coefficient for the aspect-ratio-3 wings.

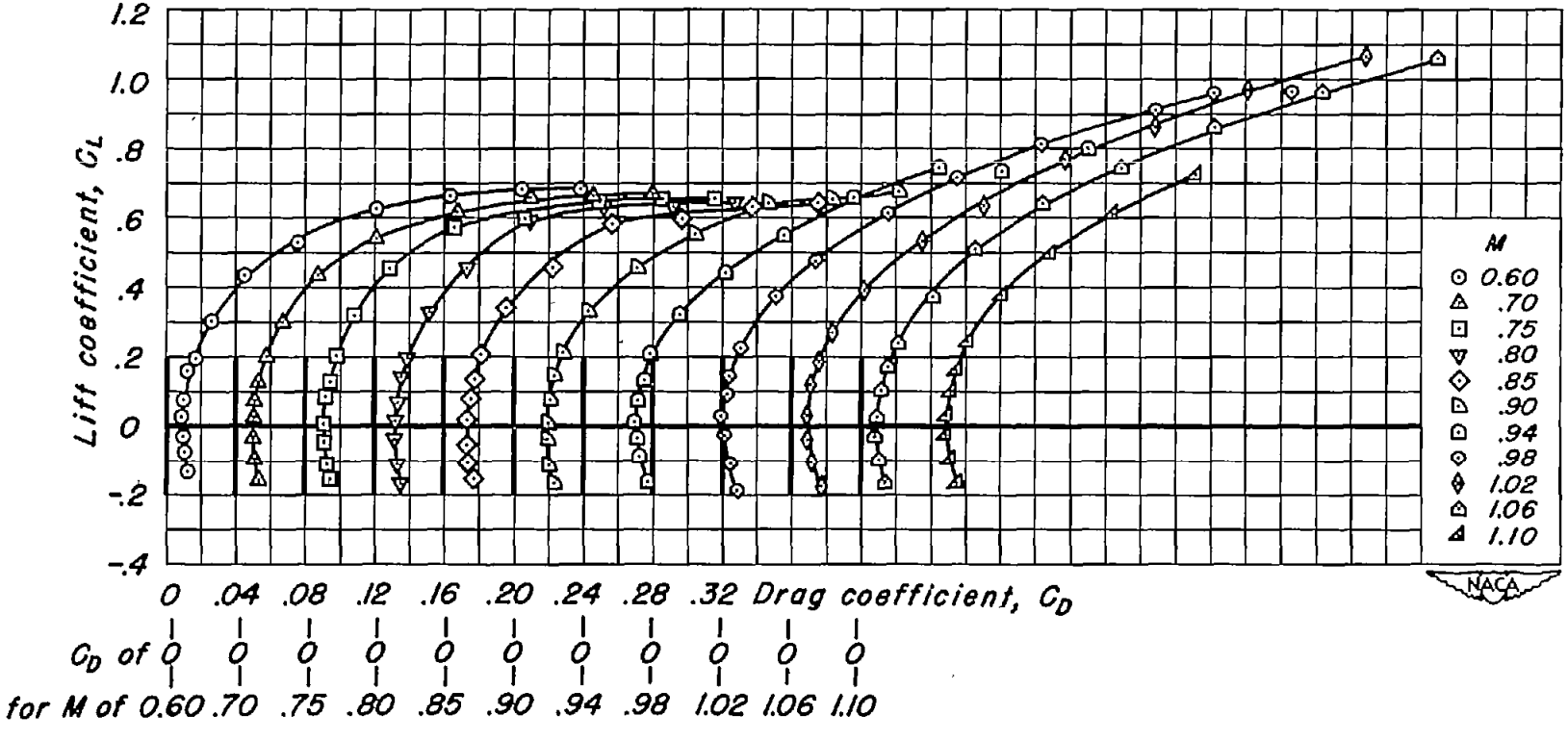

(b) t/c = 0.08; λ = 0.33

Figure 8.- Continued.

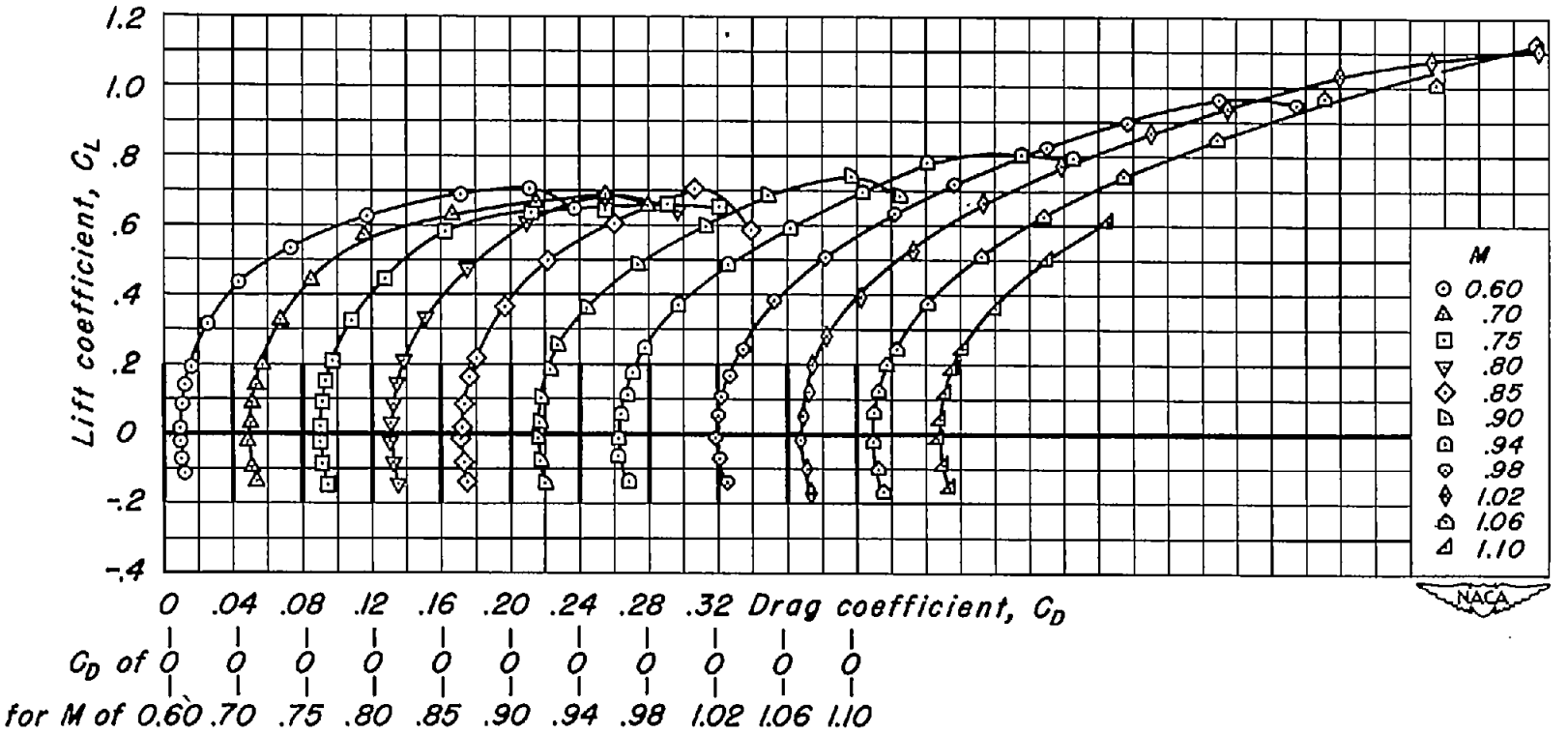

(c) t/c = 0.08; λ = 0.60

Figure 8.- Continued.

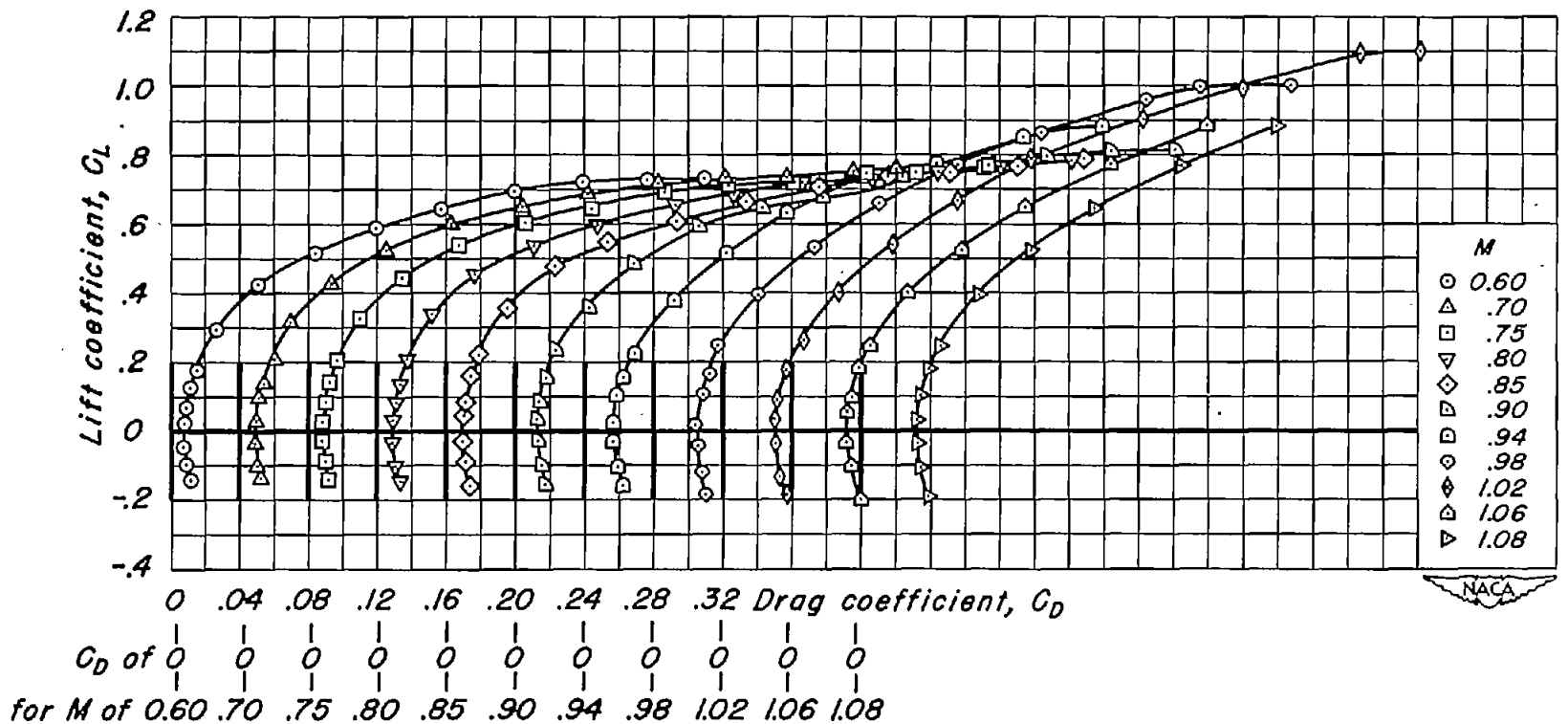

(d) t/c = 0.06; λ = 0.14

Figure 8.- Continued.

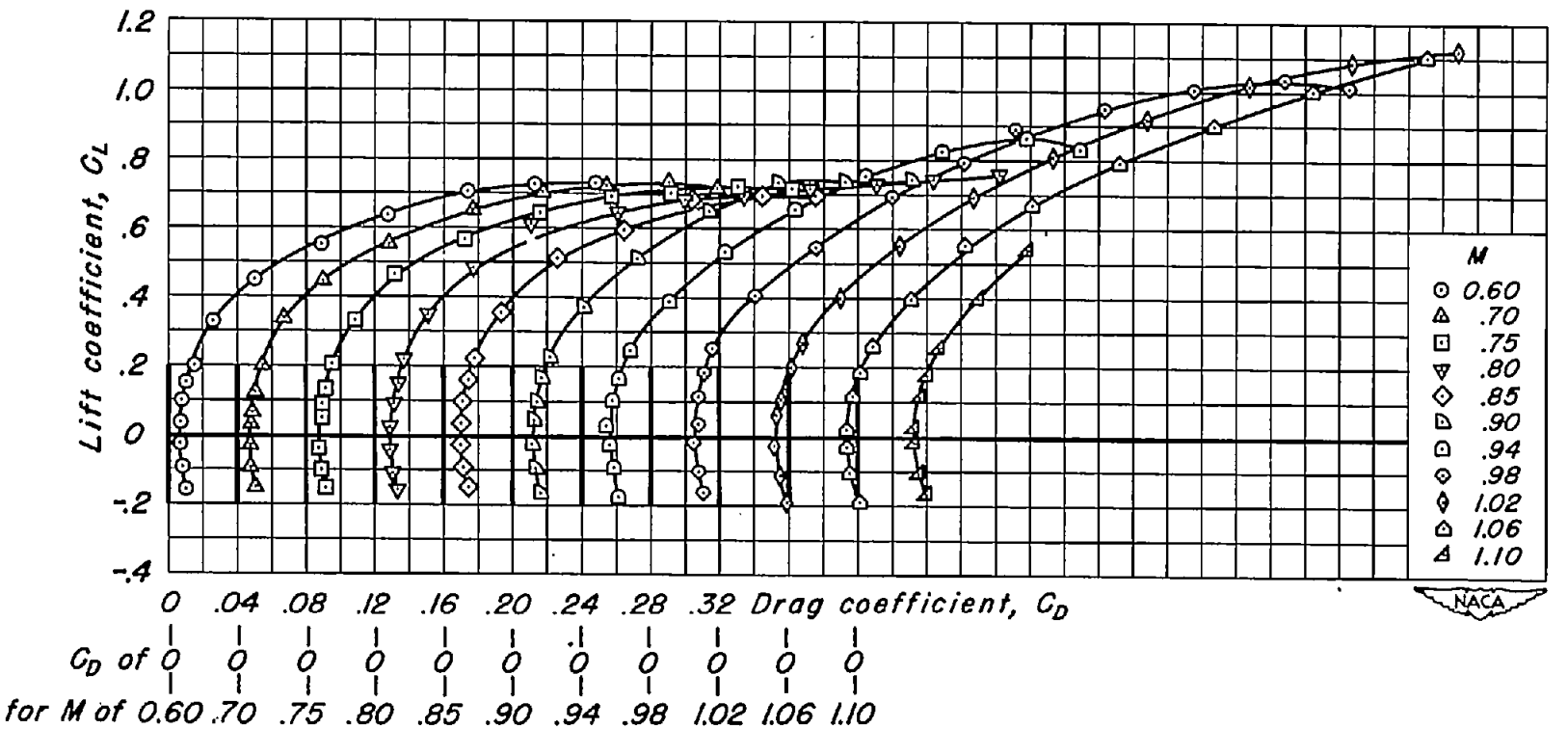

(e) t/c = 0.06; λ = 0.33

Figure 8.- Continued.

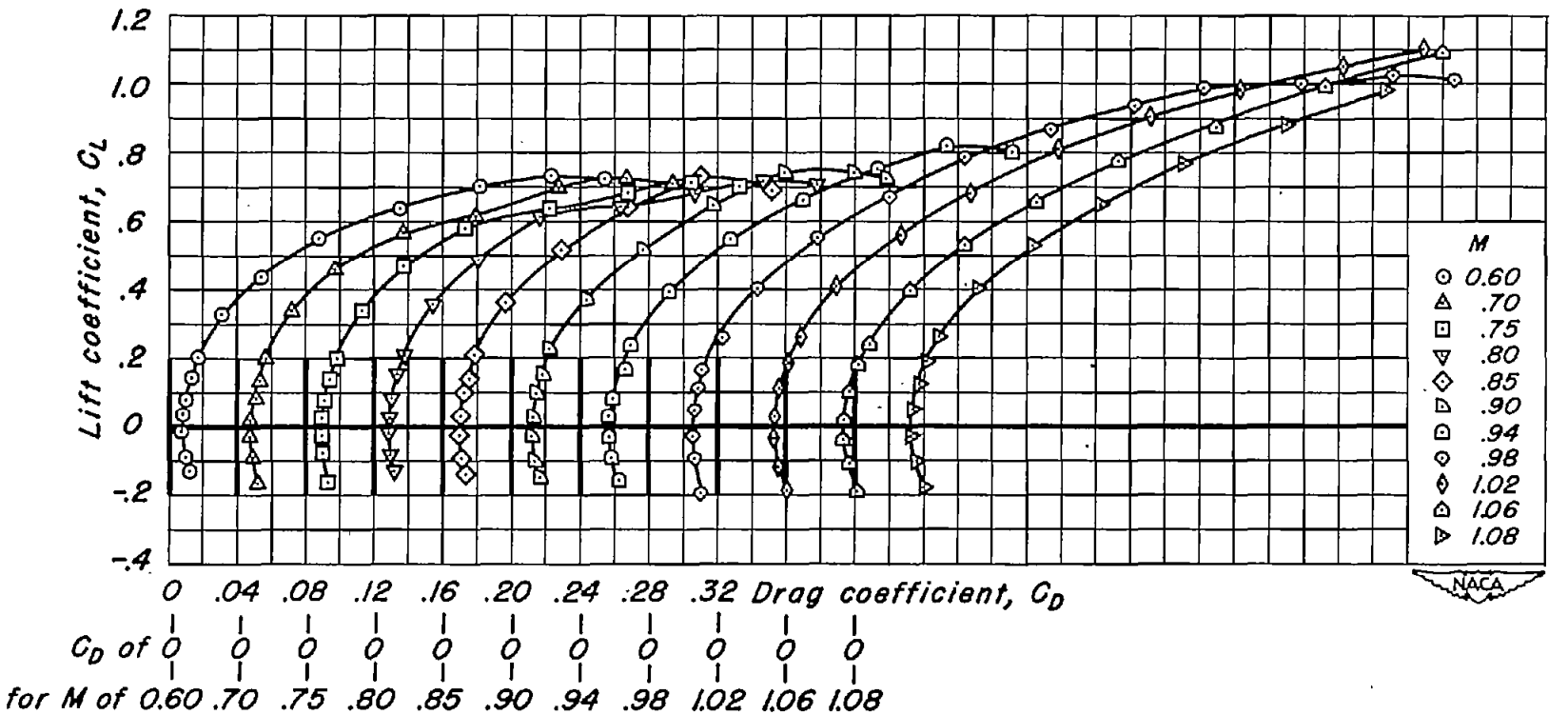

(f) t/c = 0.06; λ = 0.60

Figure 8.- Continued.

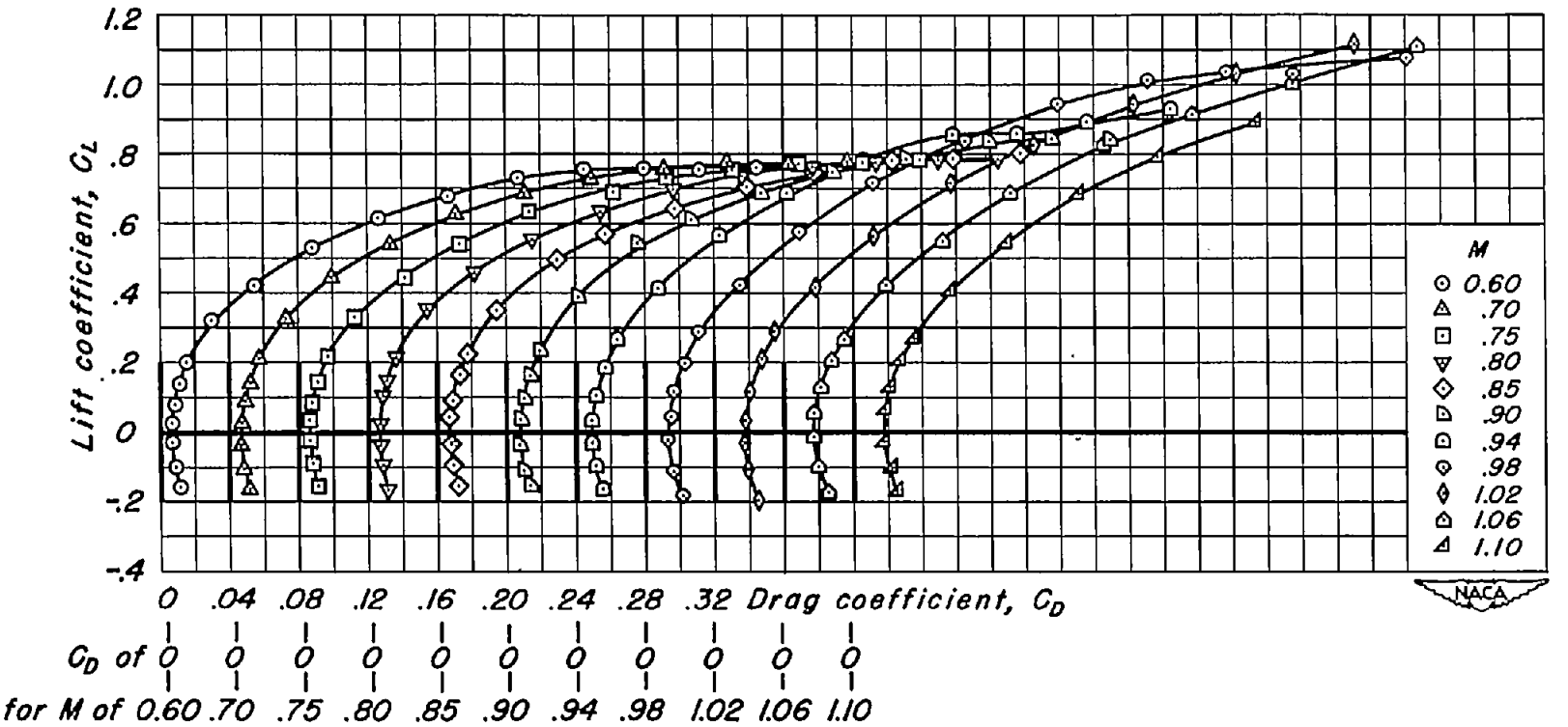

(g) t/c = 0.04; λ = 0.14

Figure 8.- Continued.

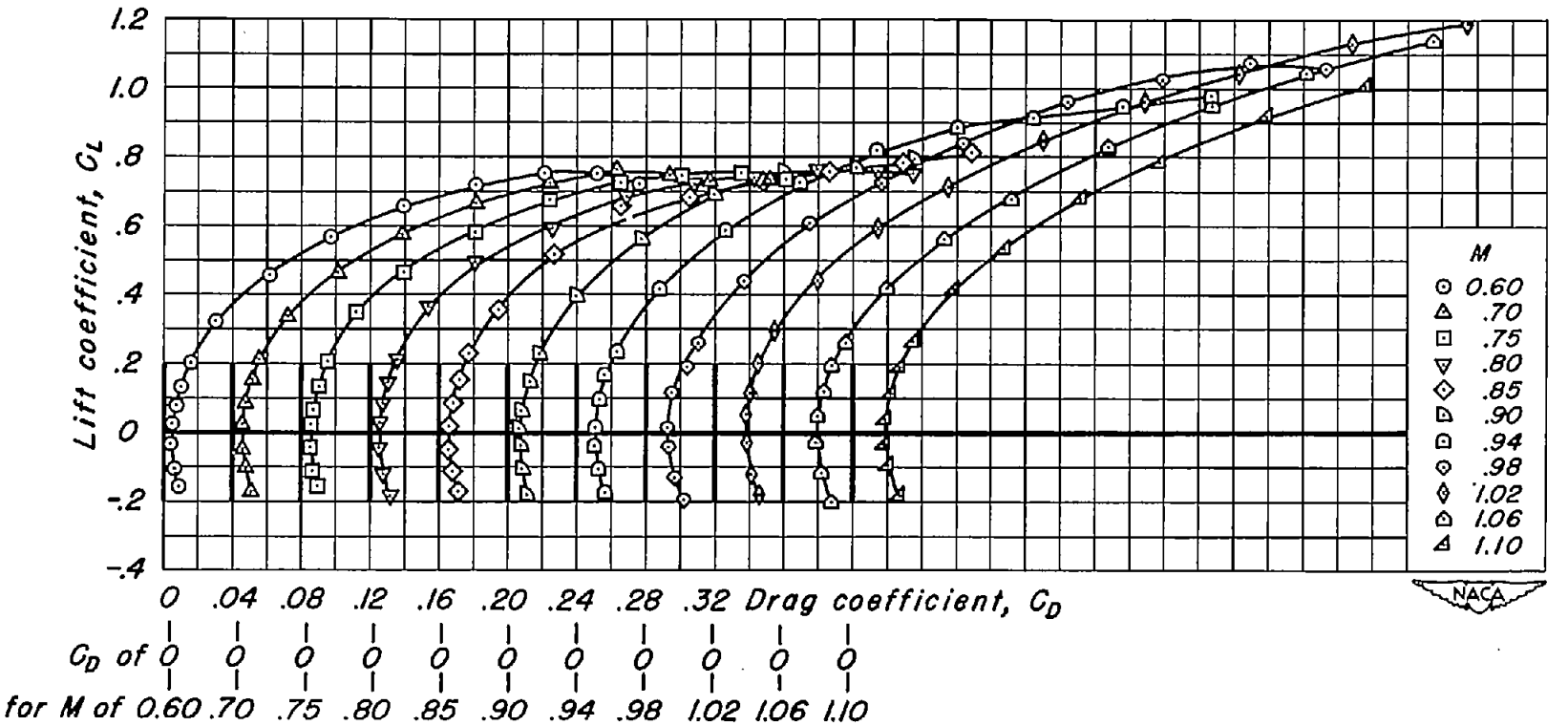

(h) t/c = 0.04; λ = 0.33

Figure 8.- Continued.

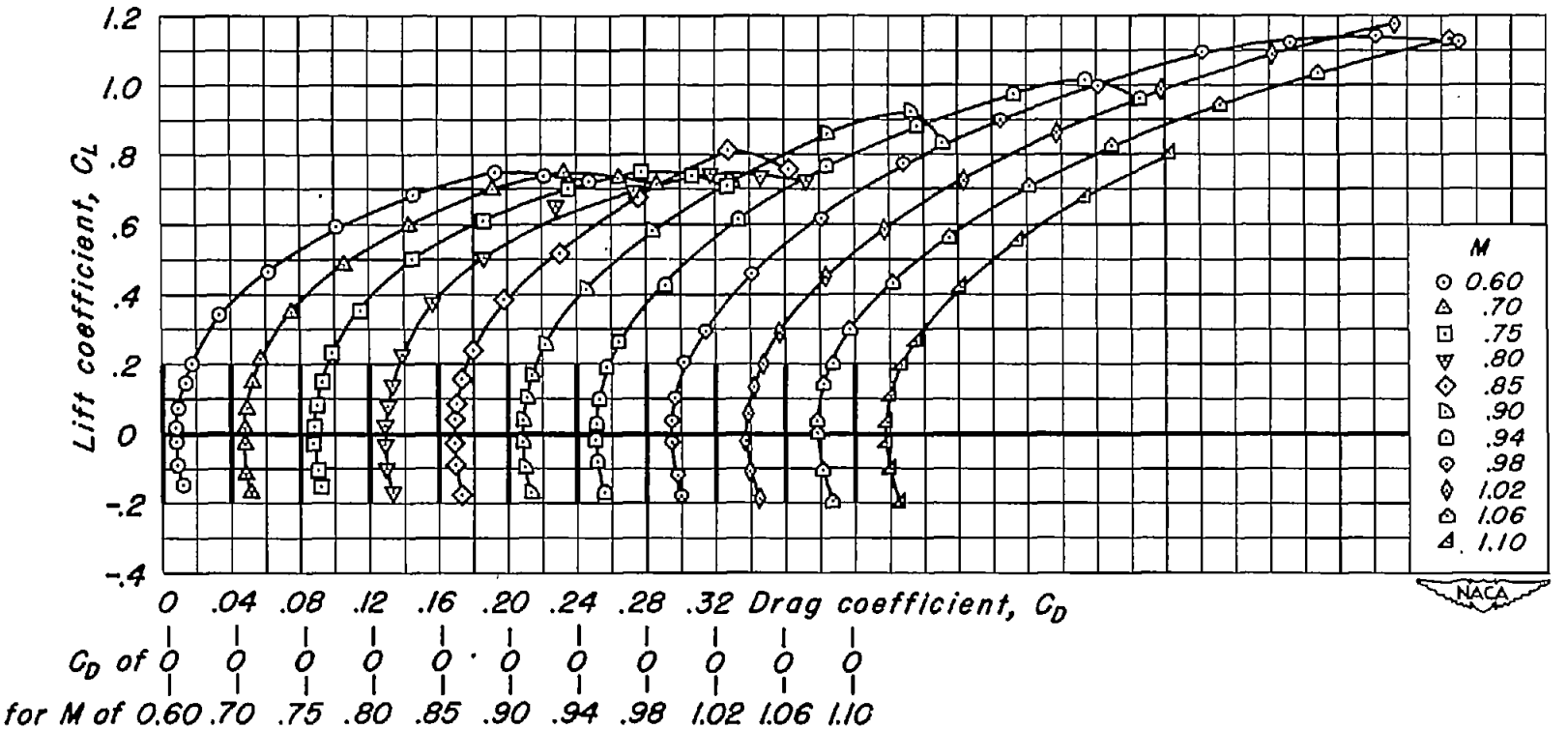

(i) t/c = 0.04; λ = 0.60

Figure 8.- Continued.

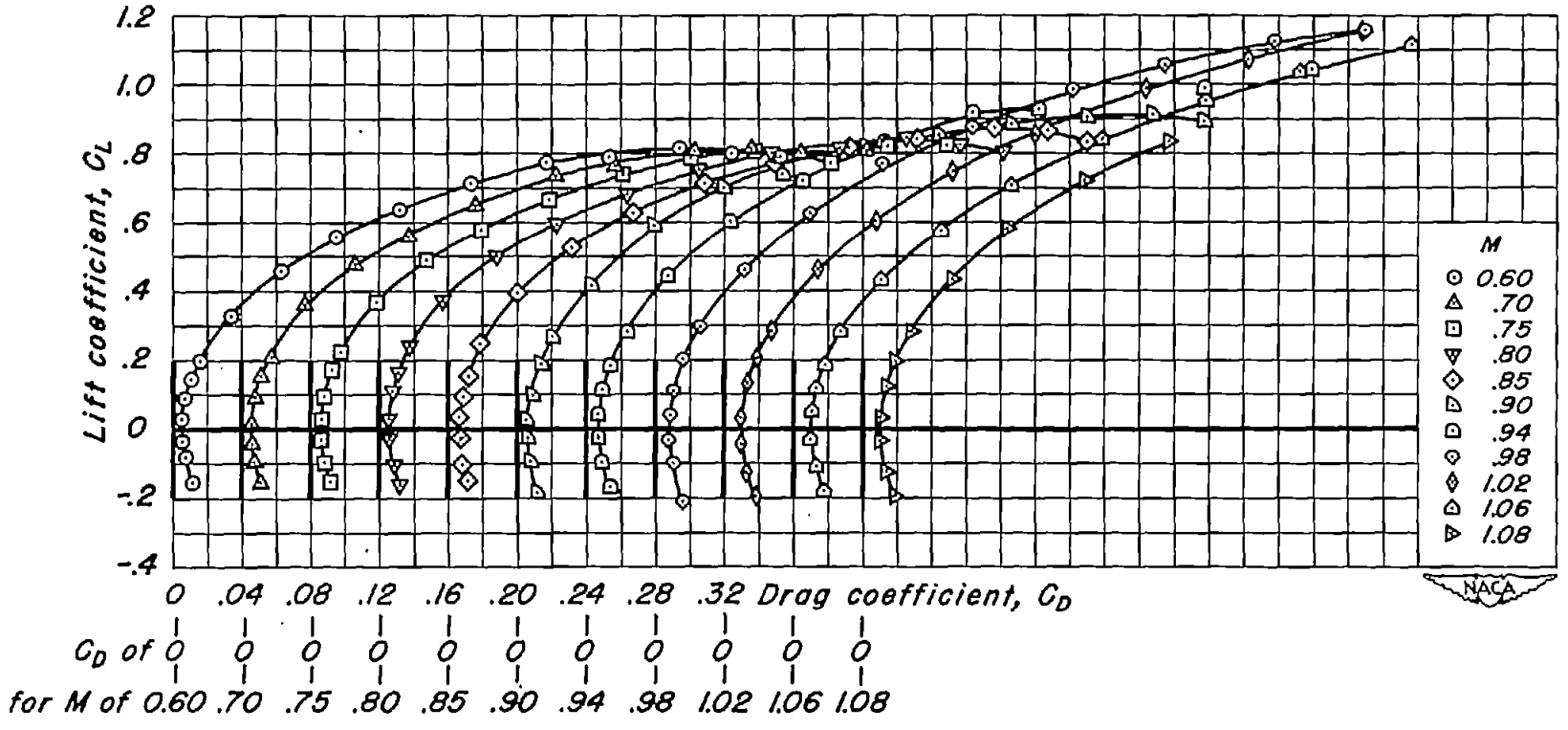

(j) t/c = 0.02; λ = 0.14

Figure 8.- Continued.

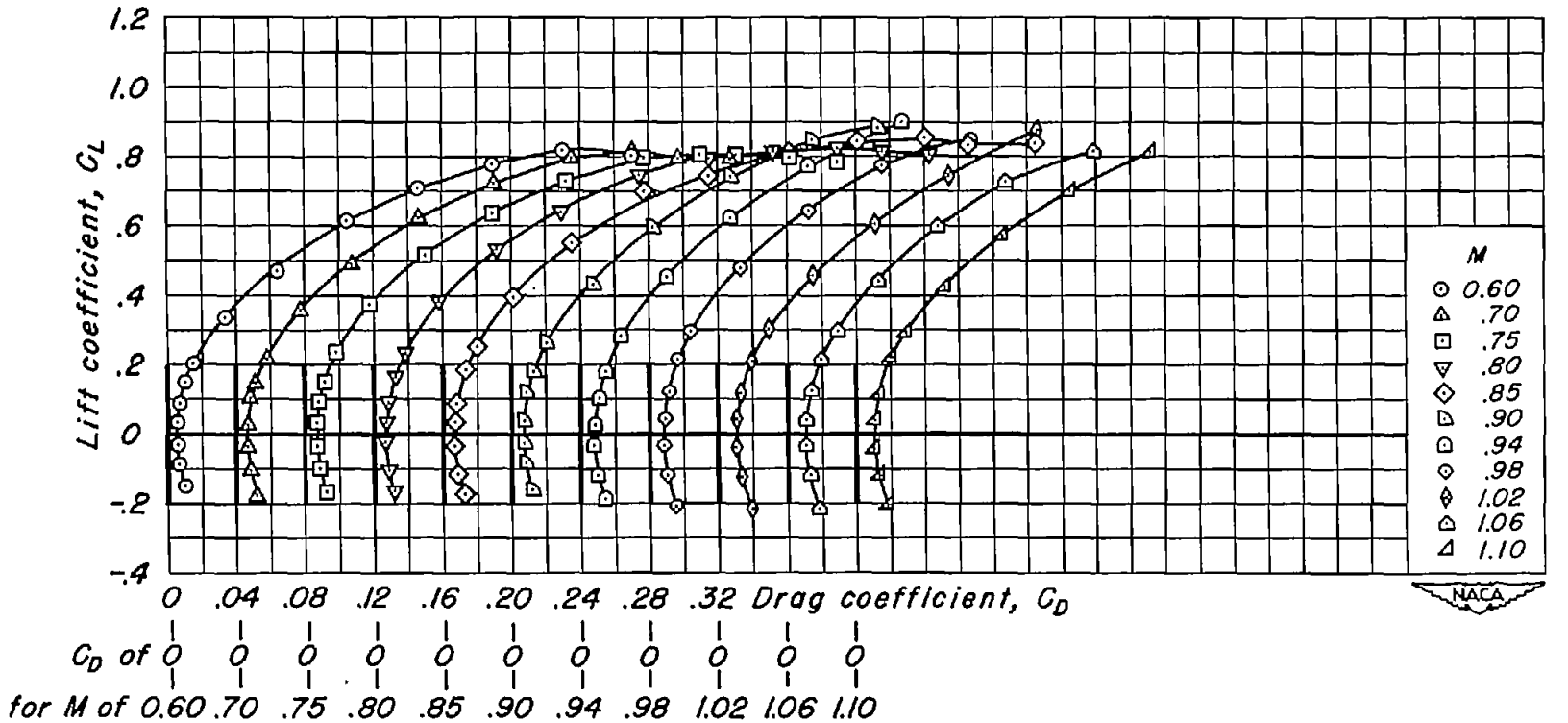

(k) t/c = 0.02; $\lambda = 0.33$

Figure 8.- Continued.

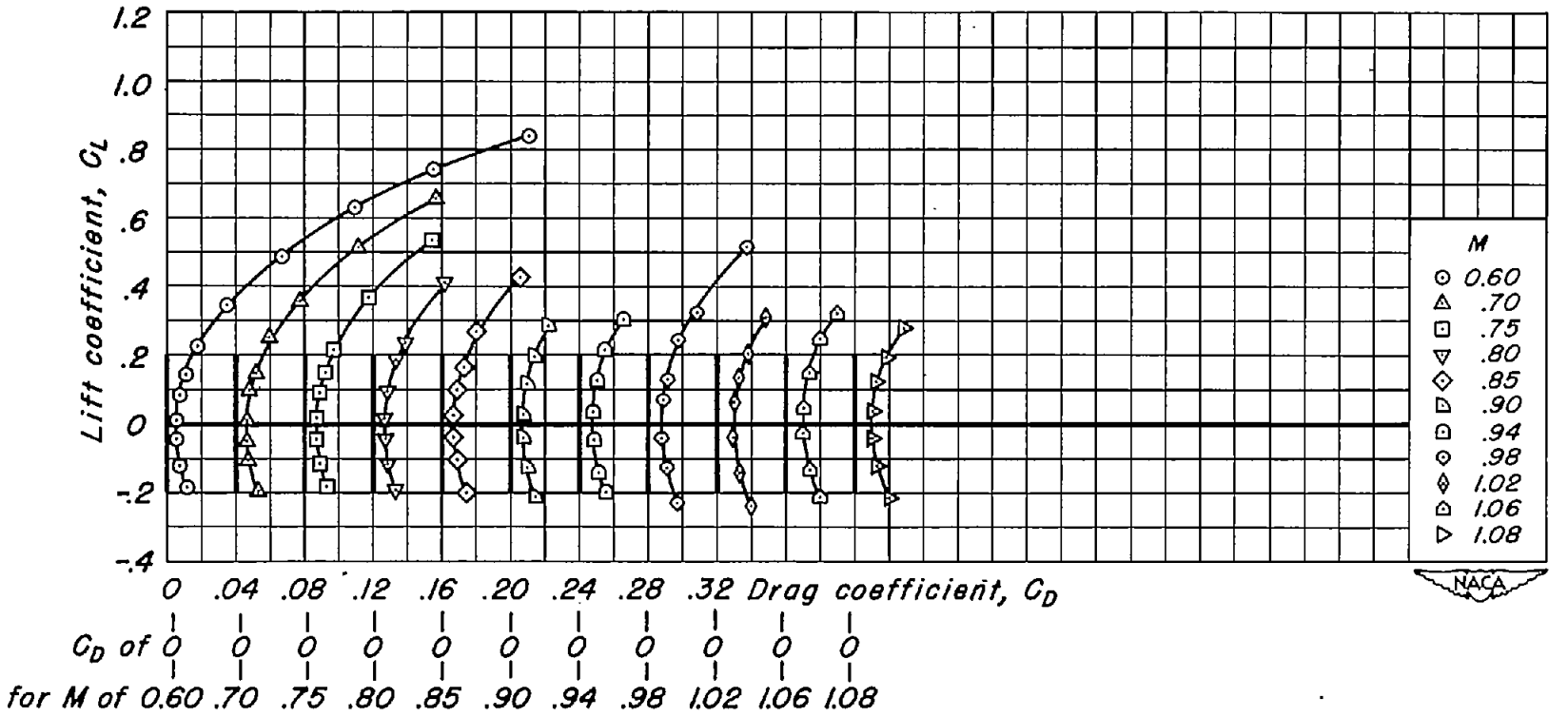

(l) t/c = 0.02; λ = 0.60

Figure 8.- Concluded.

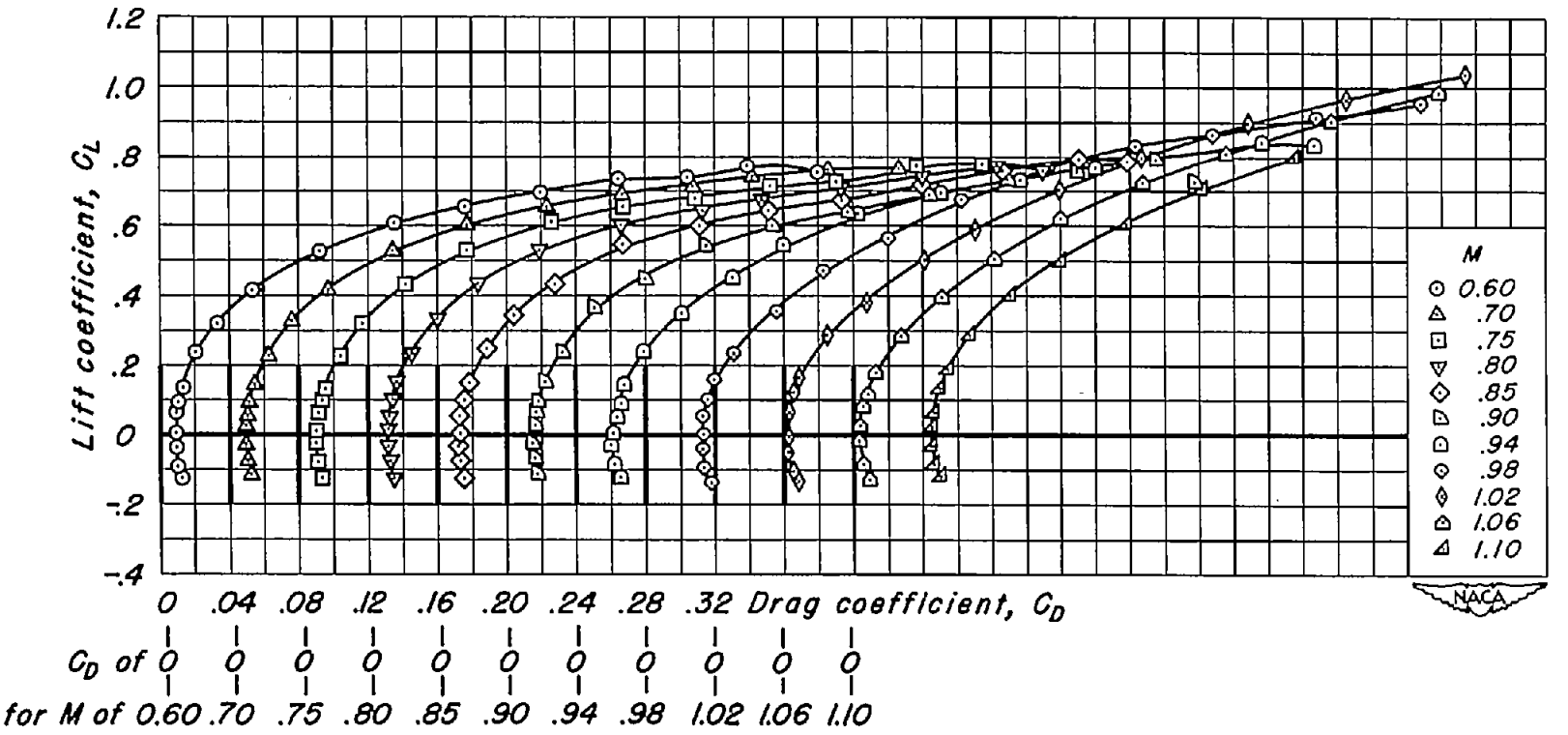

(a) t/c = 0.08; λ = 0.33

Figure 9.- The variation of lift coefficient with drag coefficient for the aspect-ratio-2 wings.

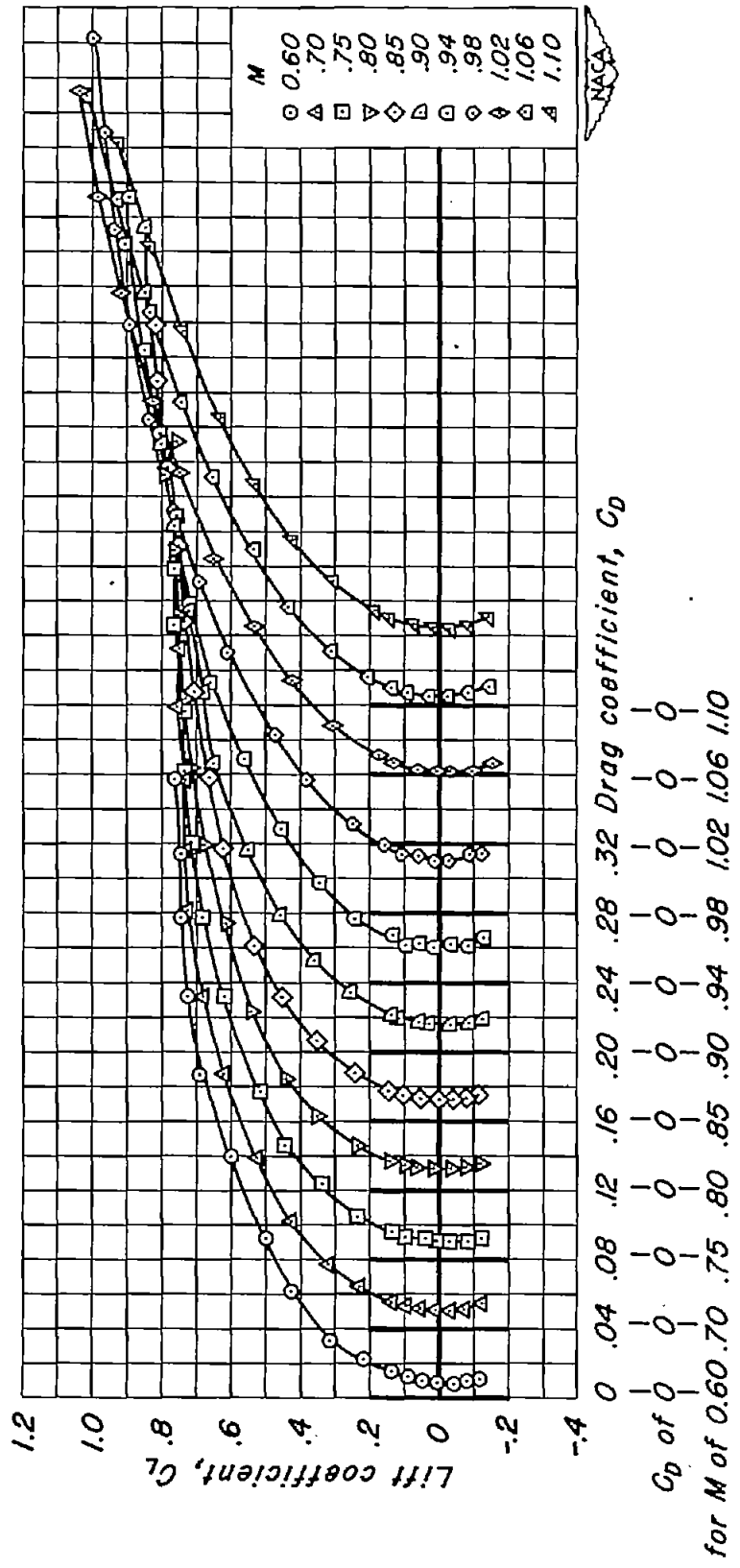

(b) t/c = 0.08; λ = 0.50

Figure 9.- Continued.

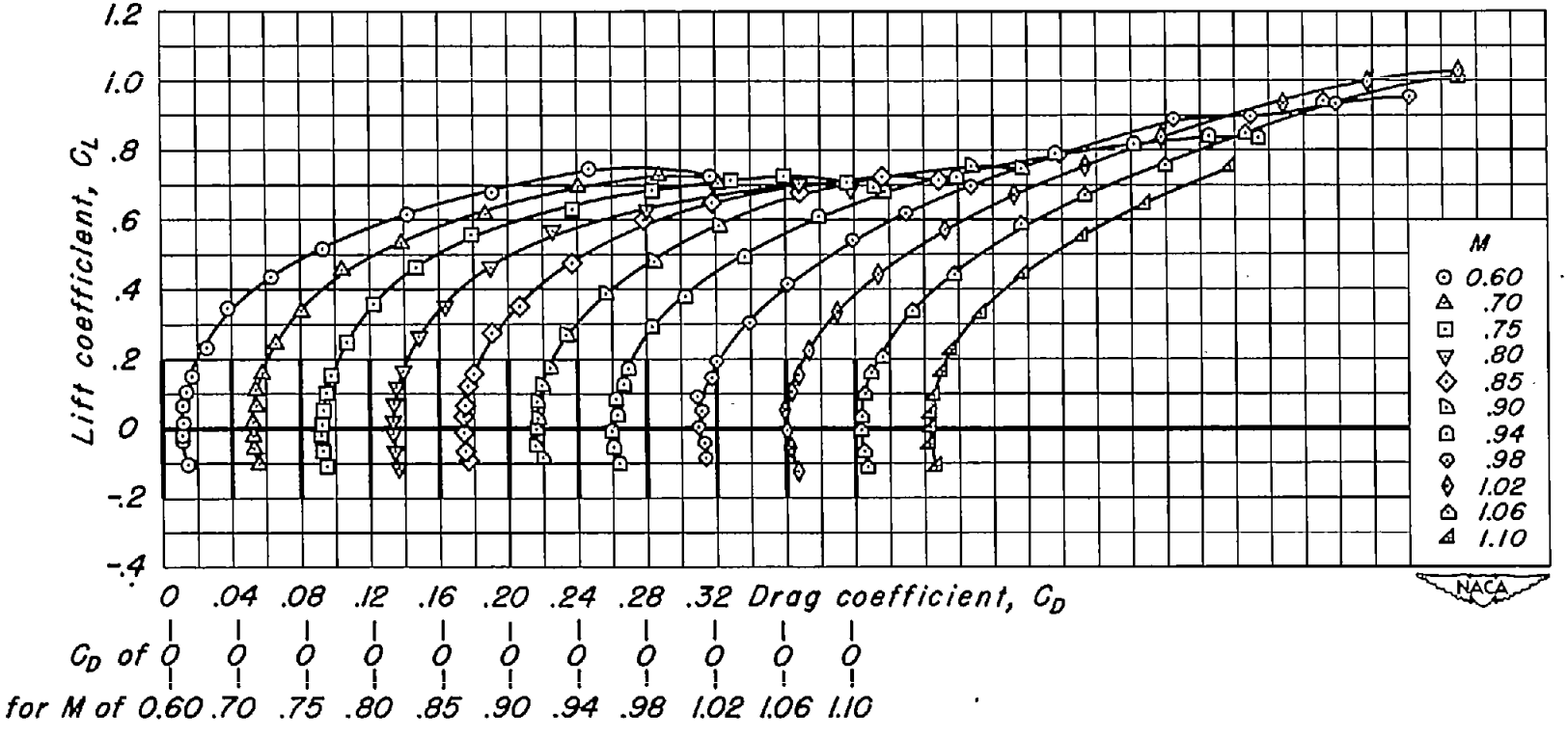

(c) t/c = 0.08; λ = 0.72

Figure 9.- Continued.

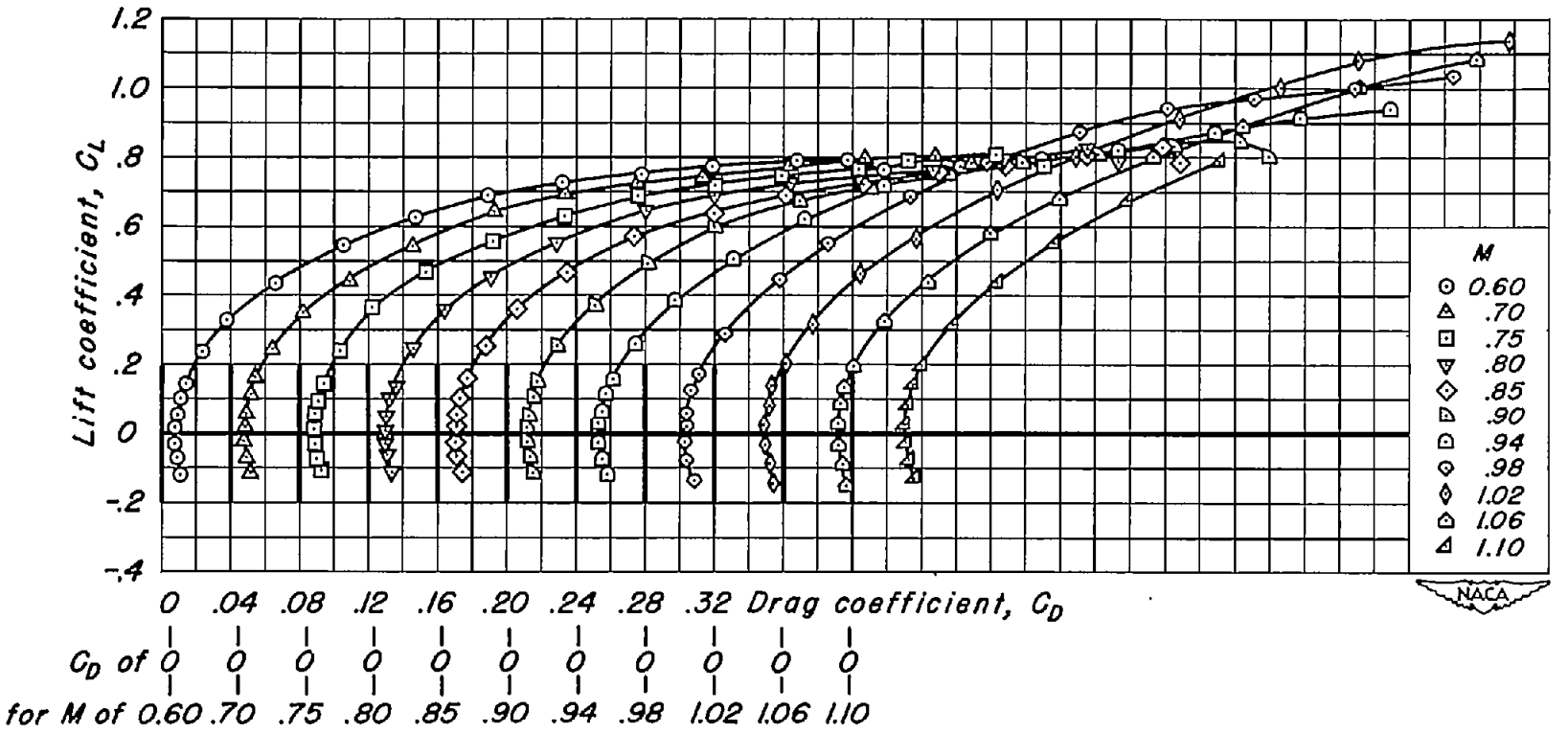

(d) t/c = 0.06; λ = 0.33

Figure 9.- Continued.

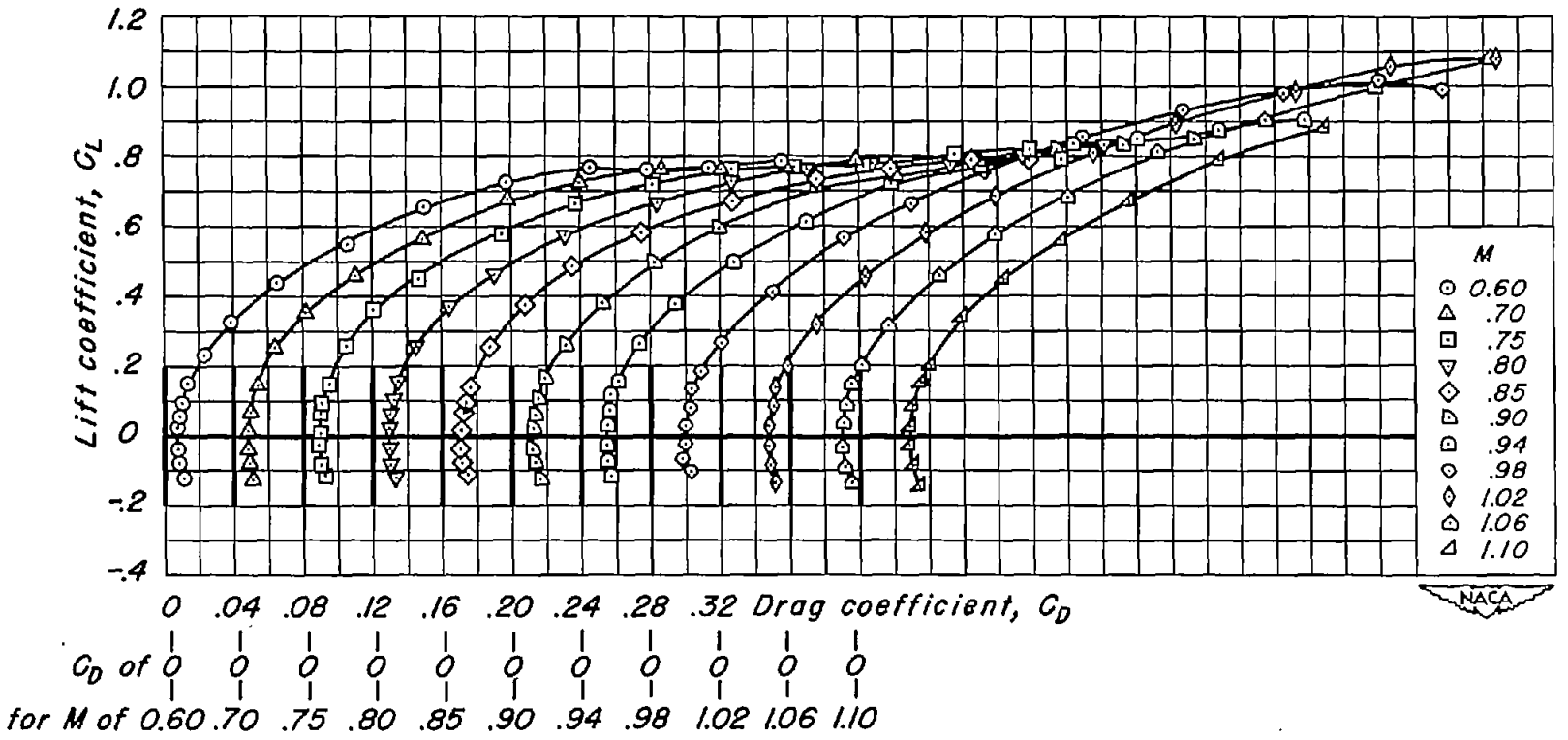

(e) t/c = 0.06; λ = 0.50

Figure 9.- Continued.

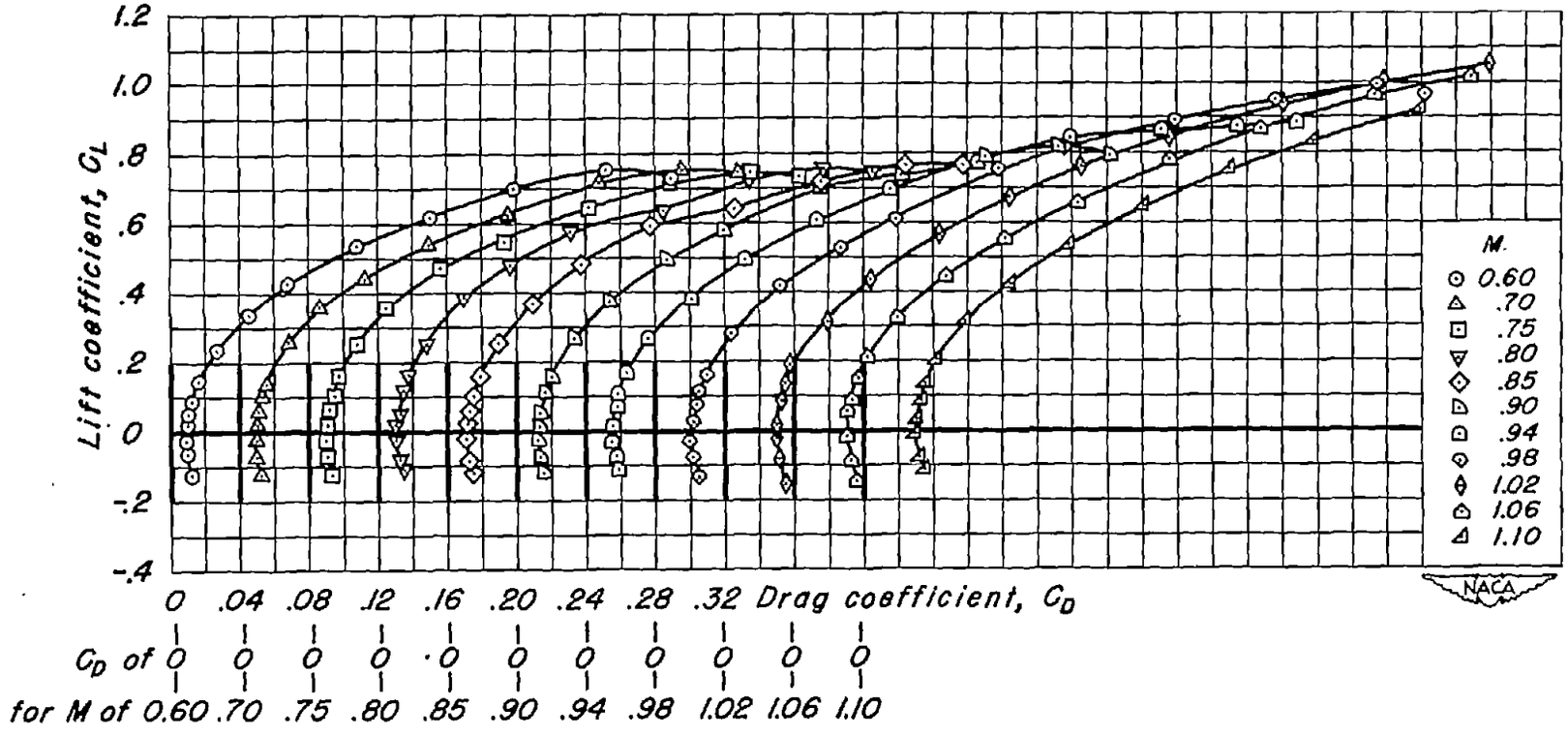

(f) t/c = 0.08; λ = 0.72

Figure 9.- Continued.

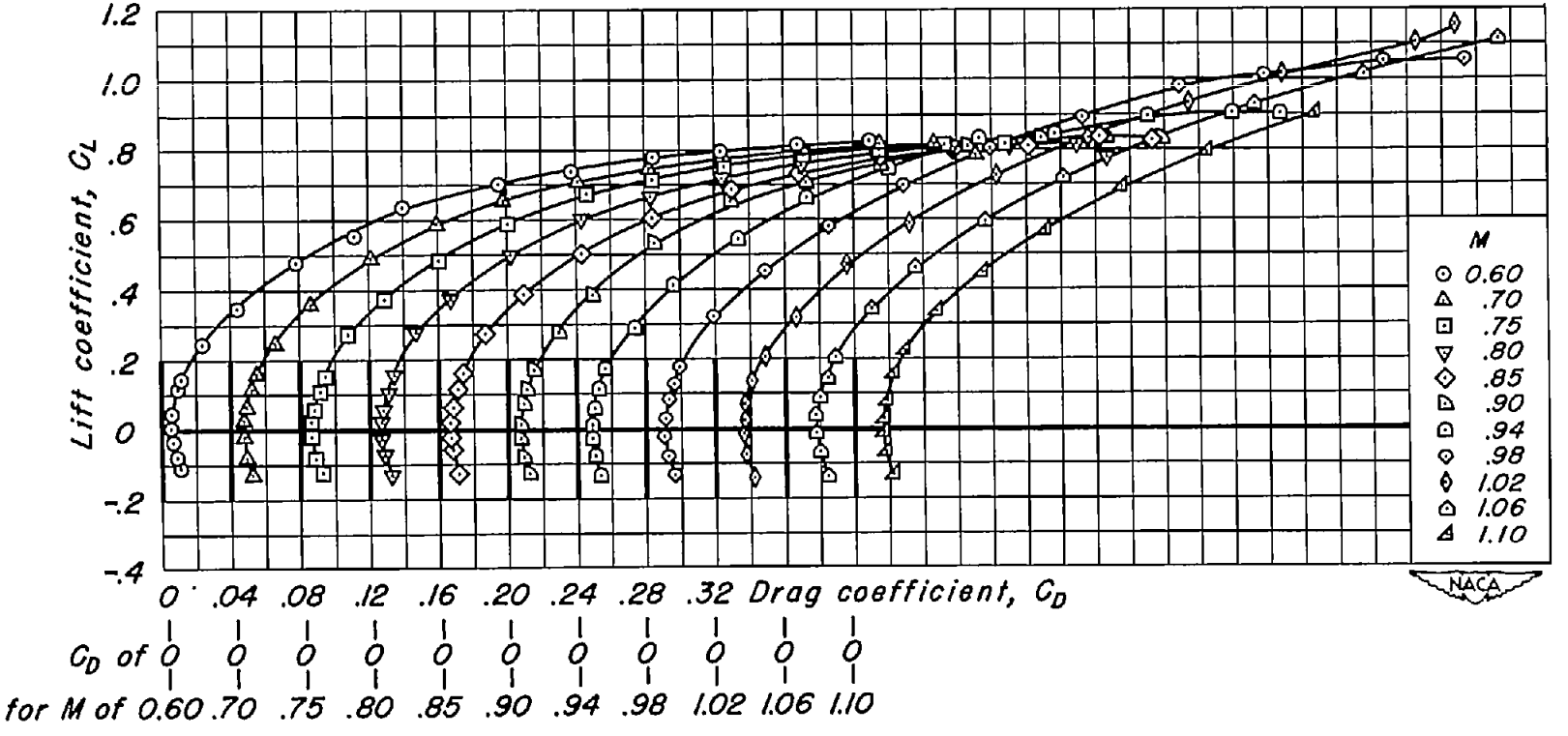

(g) t/c = 0.04; λ = 0.33

Figure 9.- Continued.

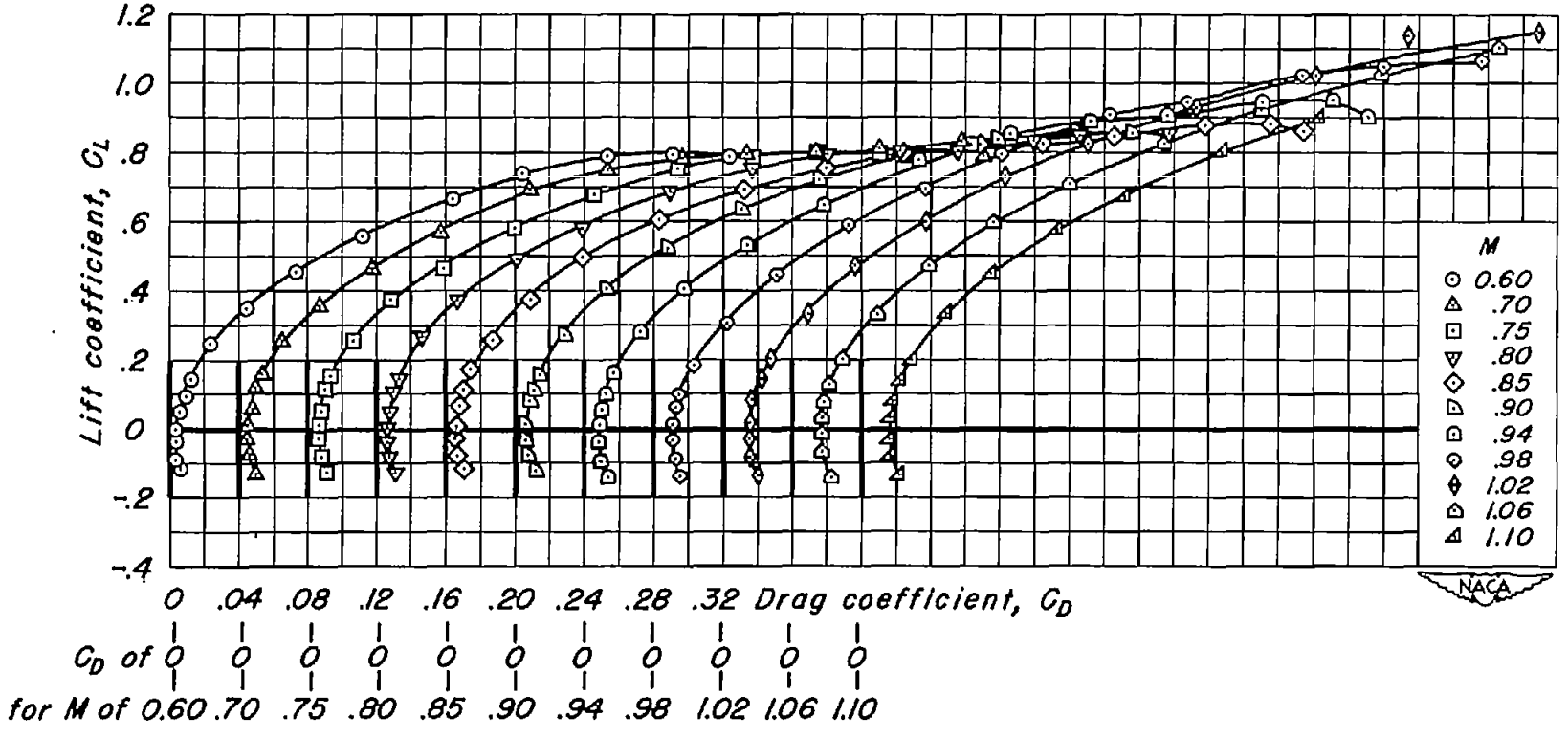

(h) t/c = 0.04; λ = 0.50

Figure 9.- Continued.

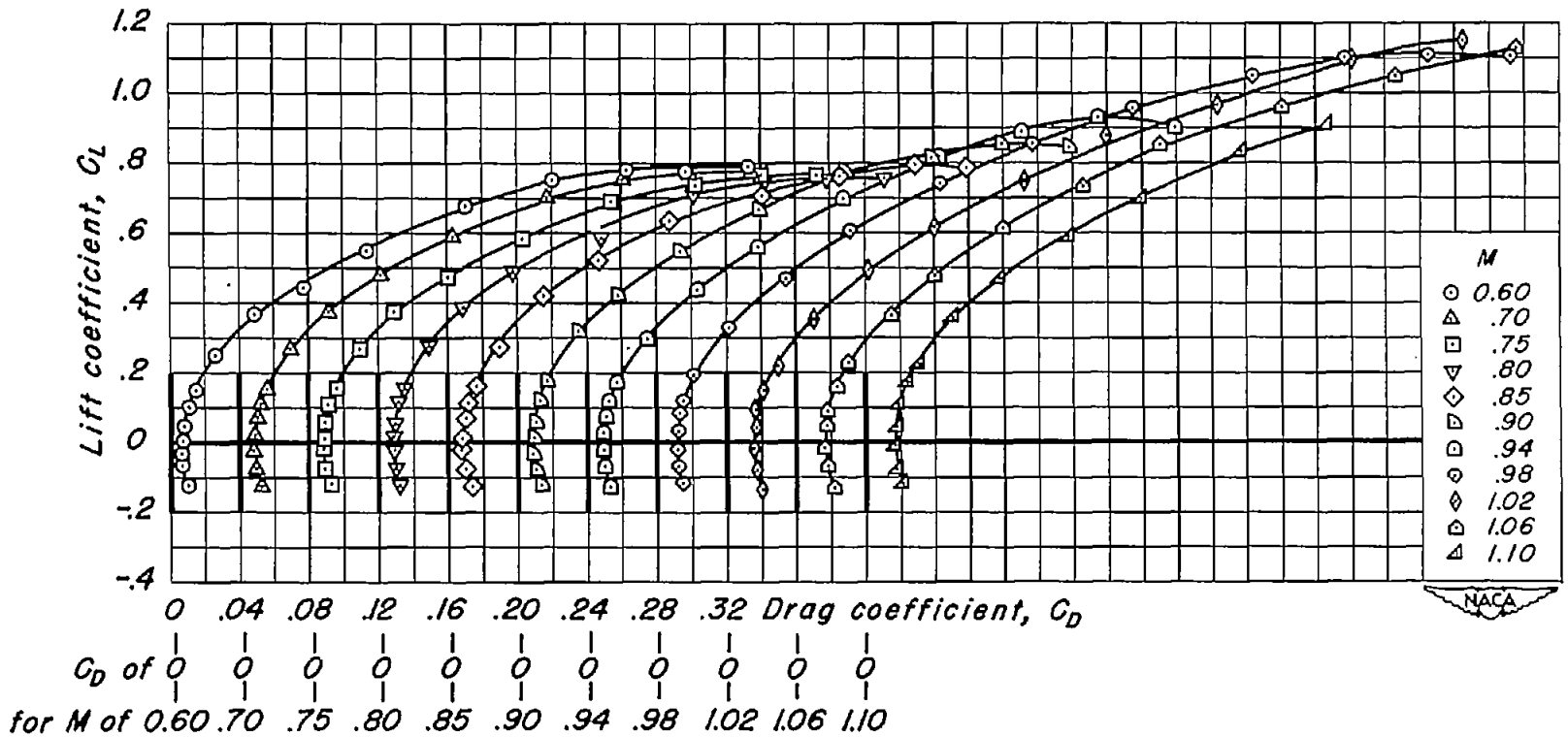

(i) t/c = 0.04; λ = 0.72

Figure 9.- Continued.

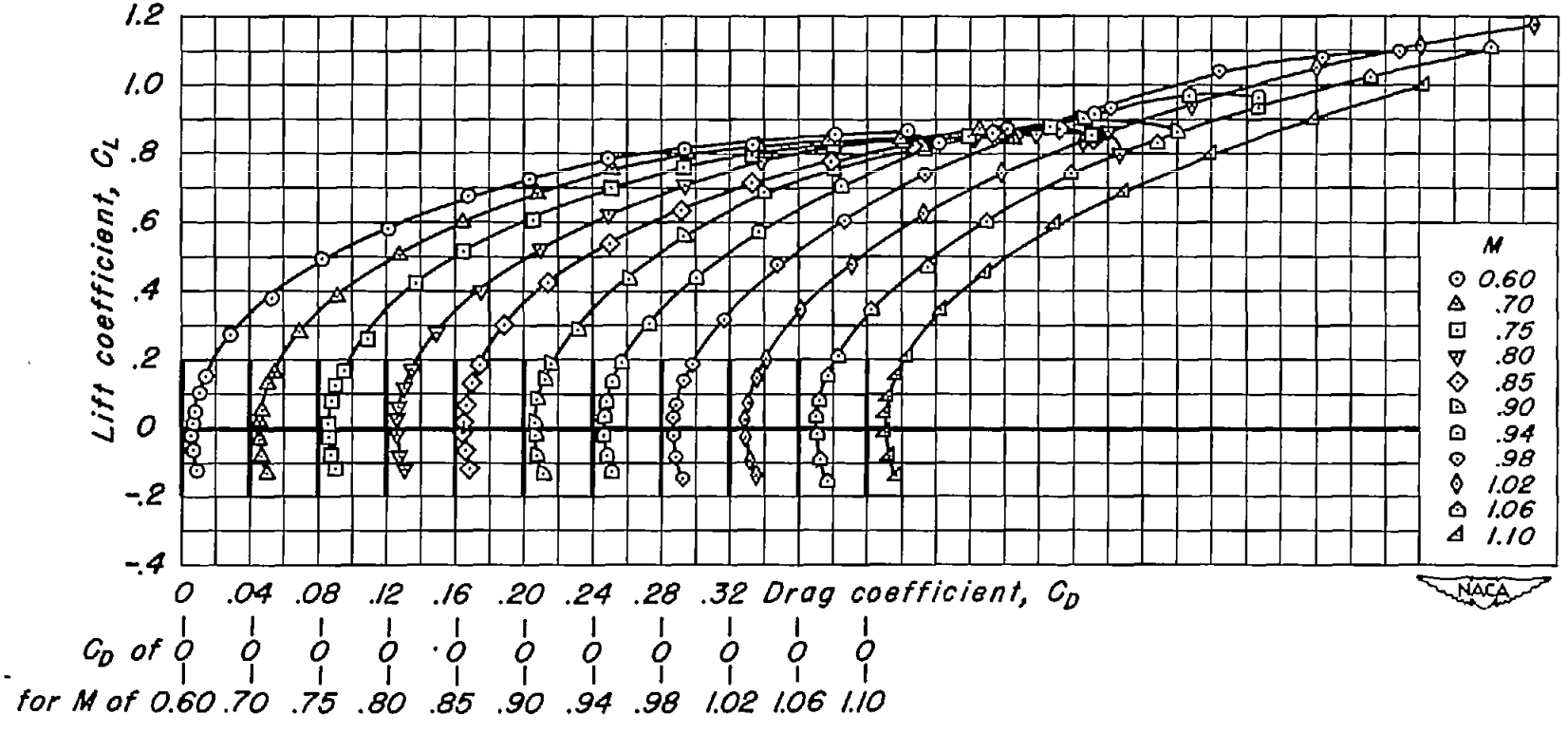

(j) t/c = 0.02; λ = 0.33

Figure 9.- Continued.

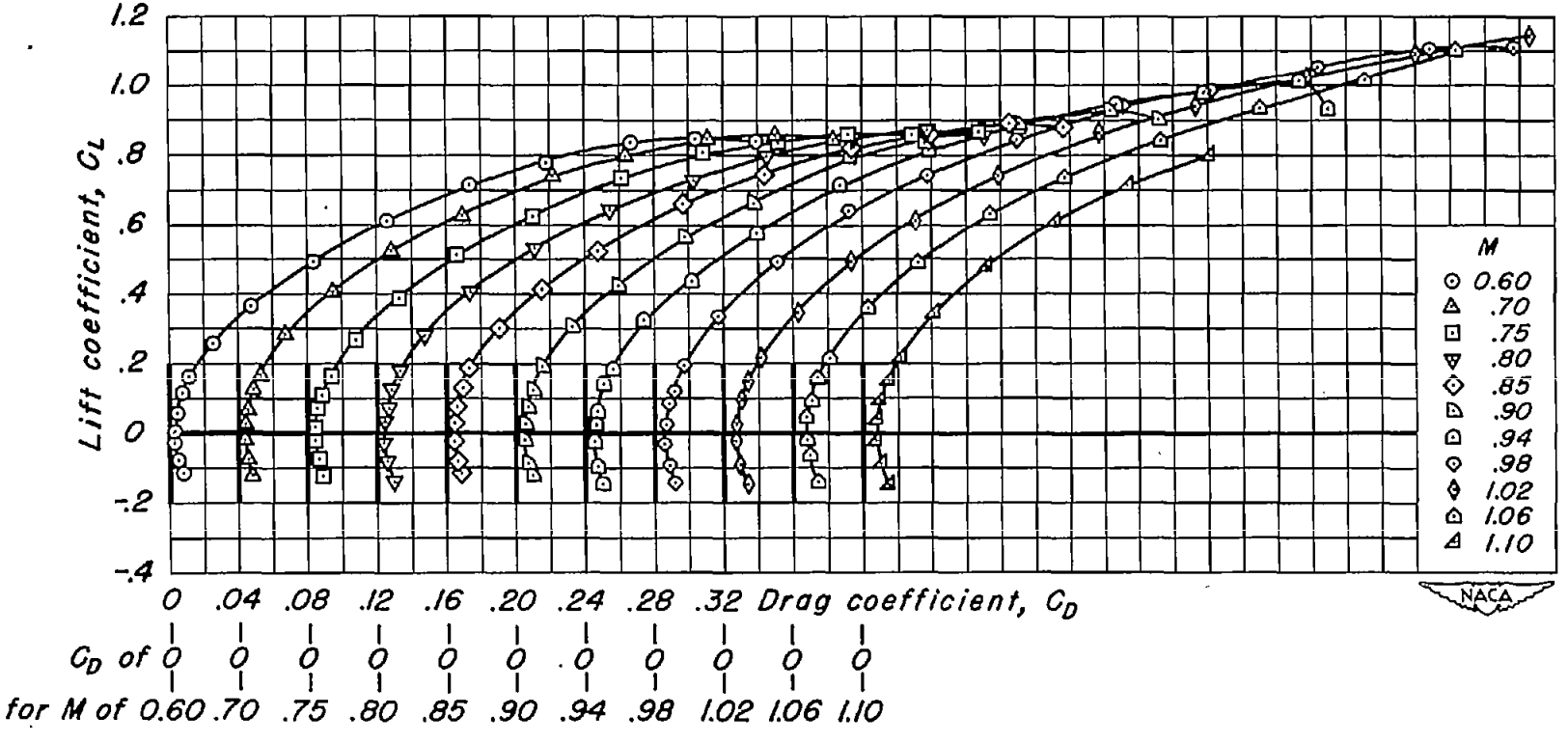

(k) t/c = 0.02; λ = 0.50

Figure 9.- Continued.

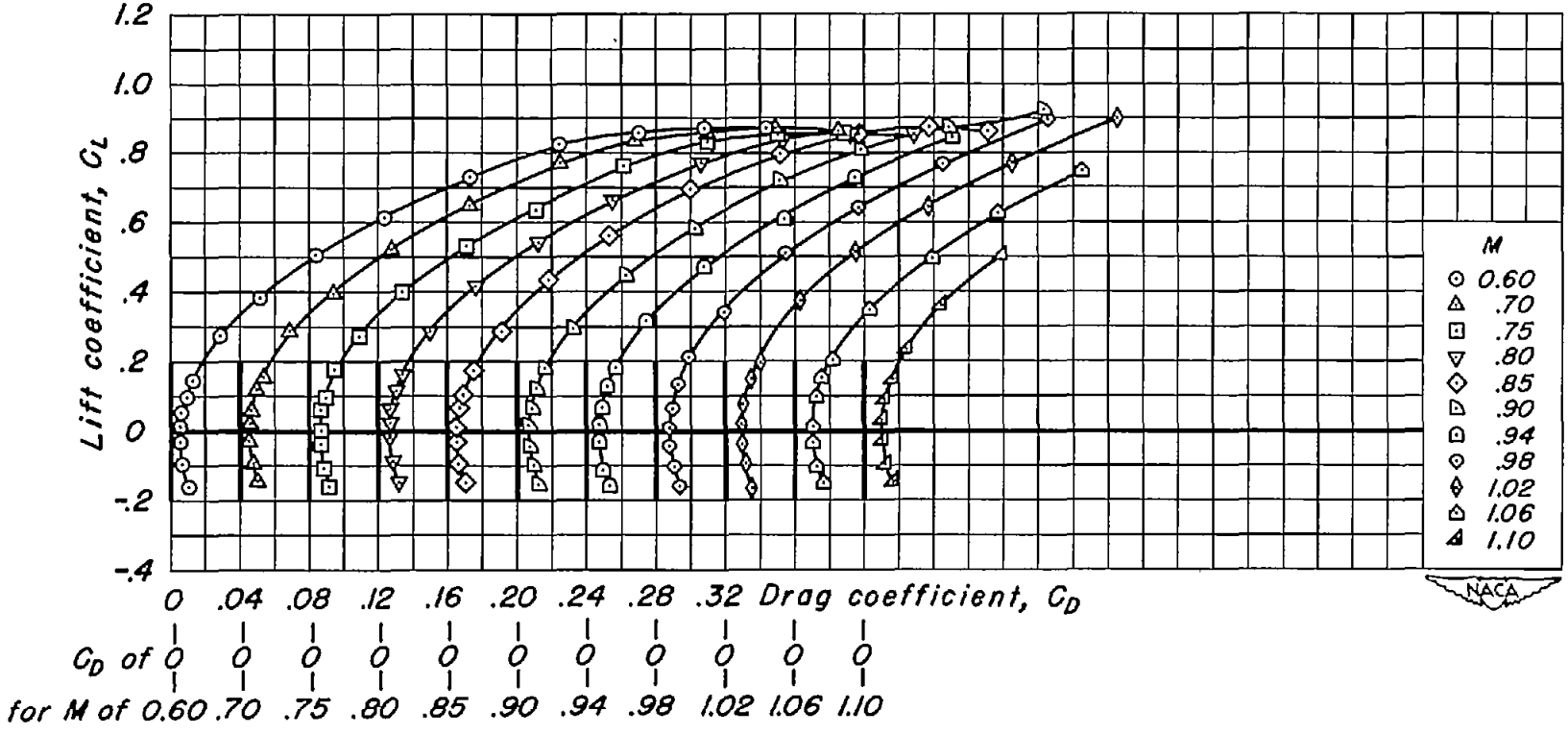

(l) t/c = 0.02; λ = 0.72

Figure 9.- Concluded.

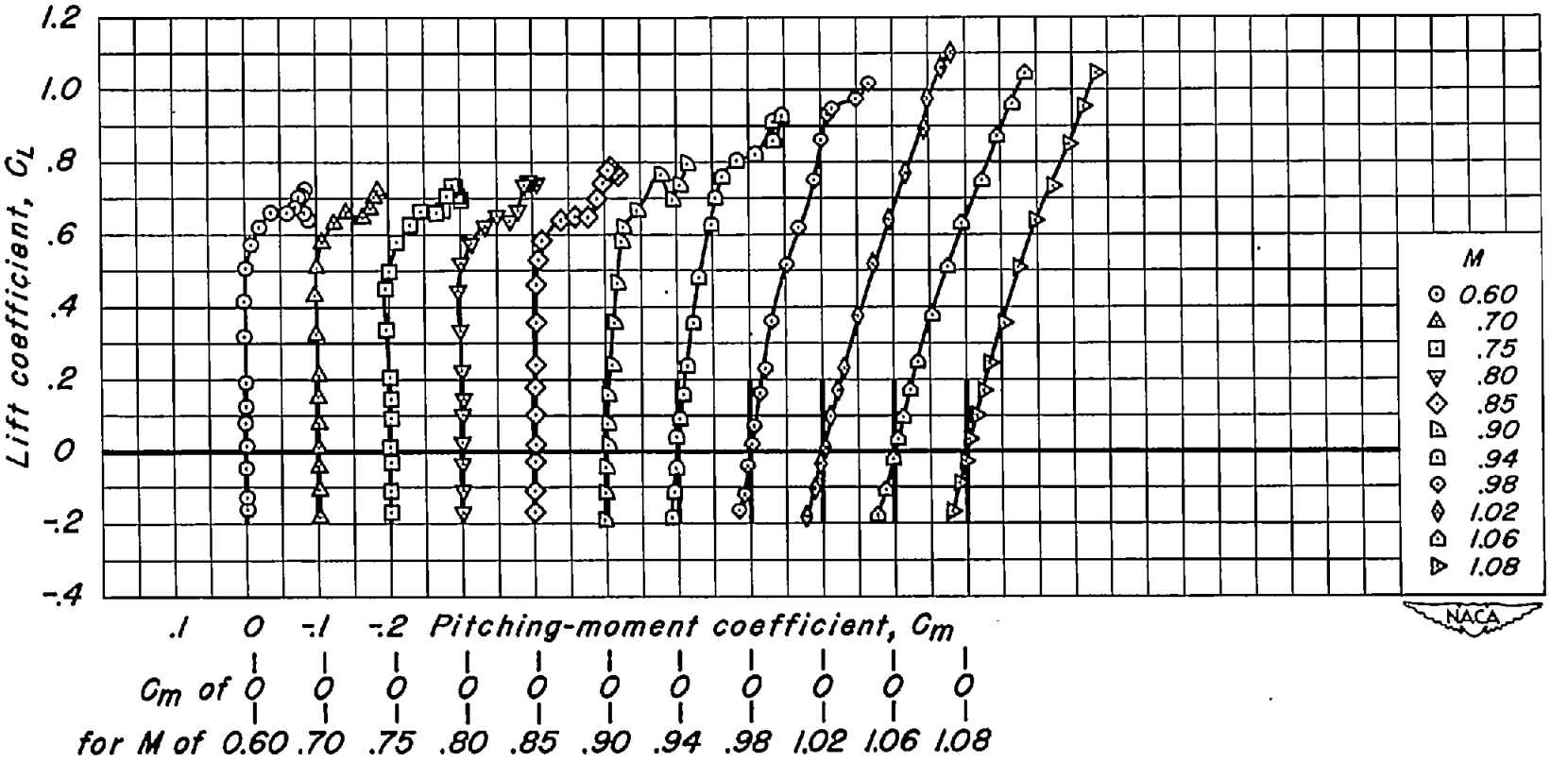

(a) t/c = 0.08; λ = 0

Figure 10.- The variation of lift coefficient with pitching-moment coefficient for the aspect-ratio-4 wings.

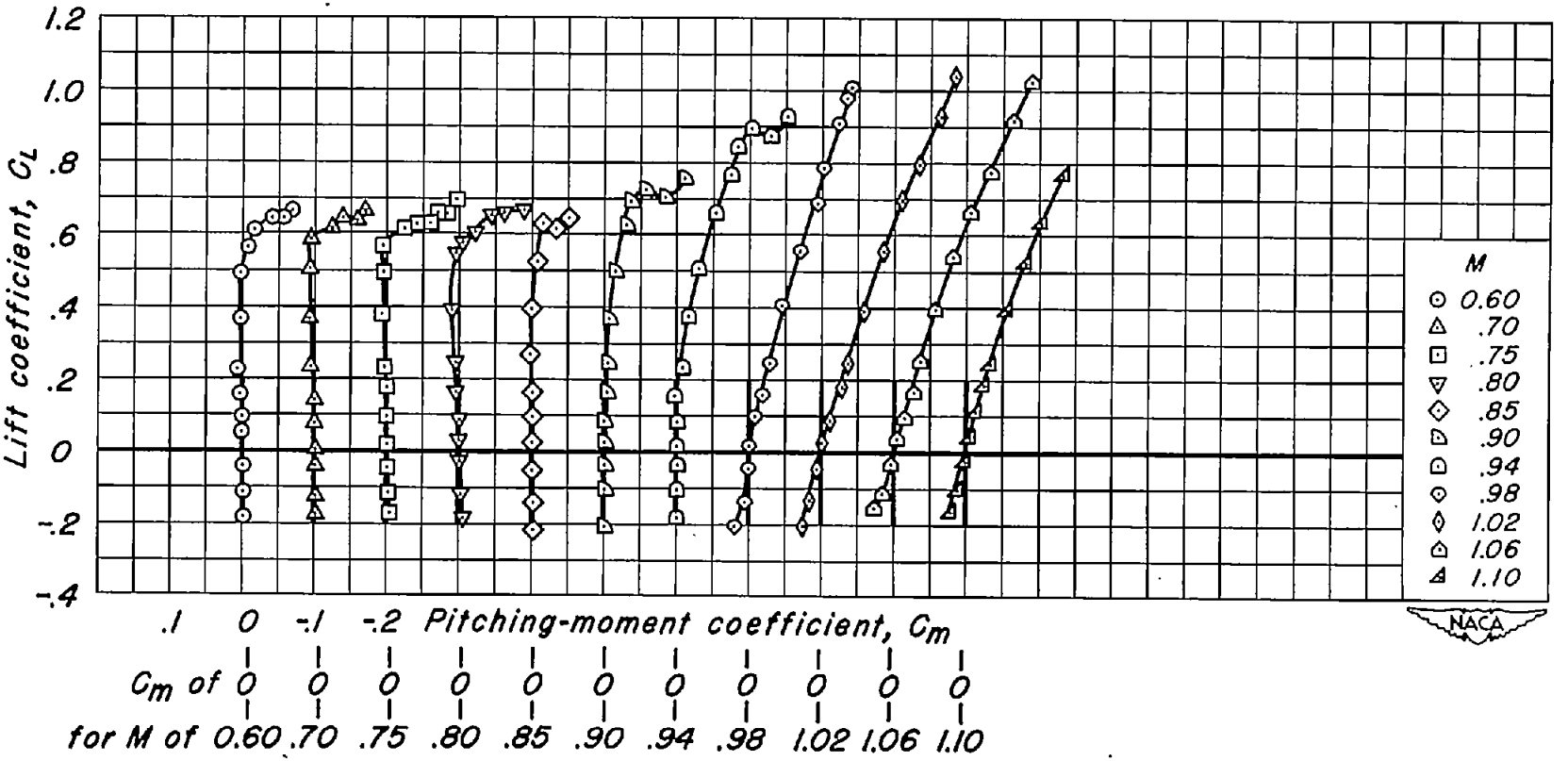

(b) t/c = 0.08; λ = 0.20

Figure 10.- Continued.

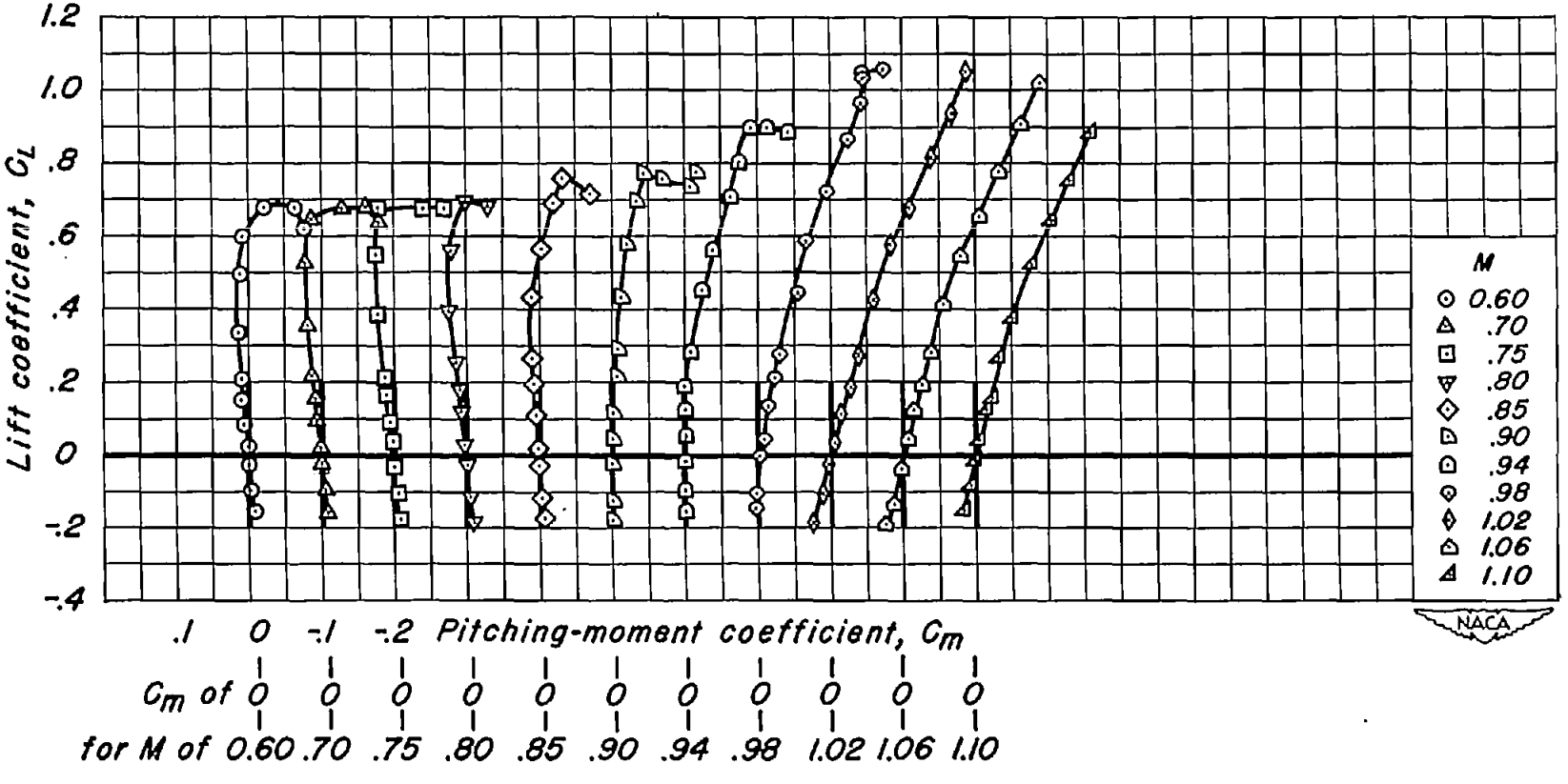

(c) t/c = 0.08; λ = 0.50

Figure 10.- Continued.

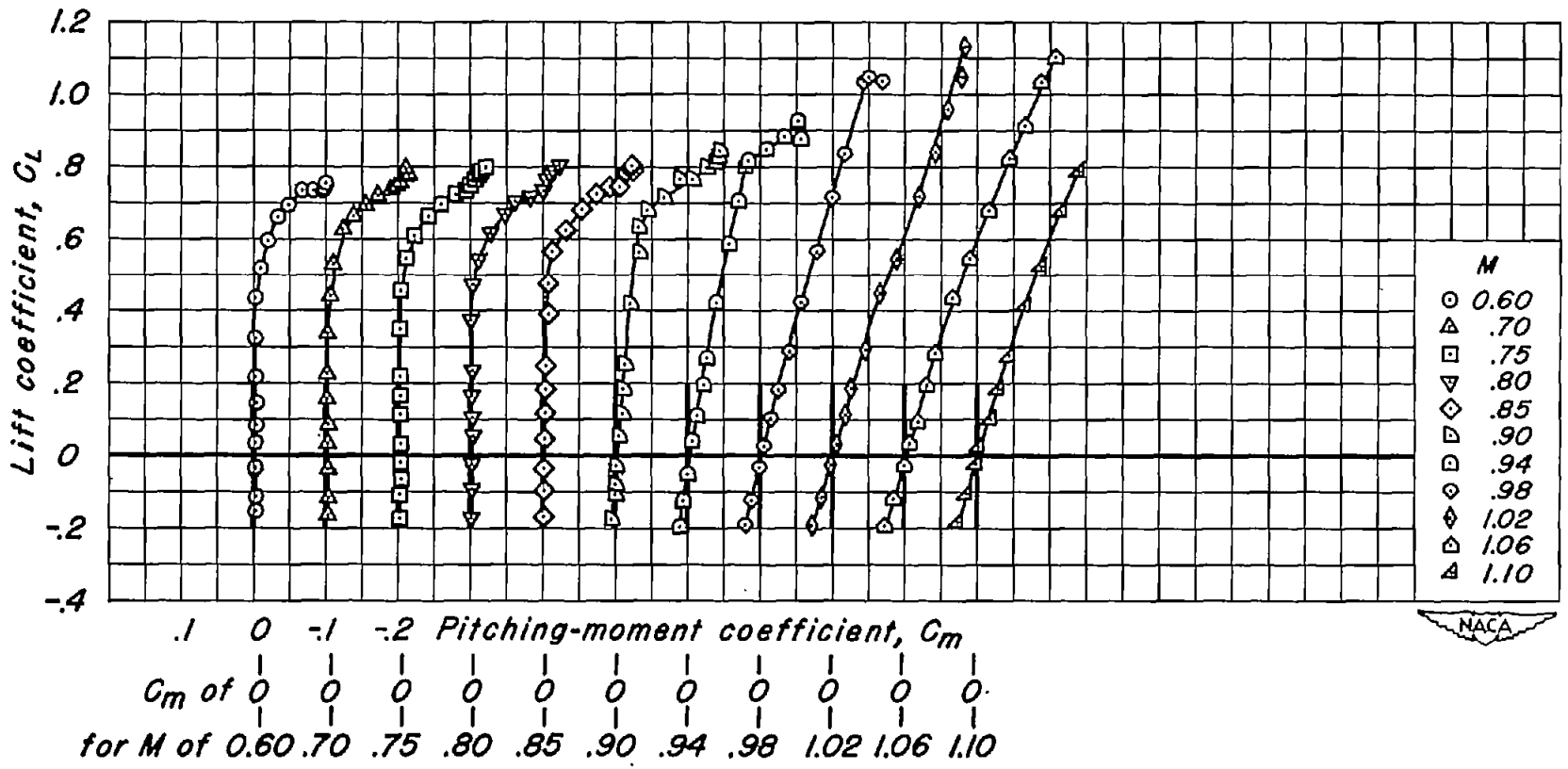

(d) t/c = 0.06; λ = 0

Figure 10.- Continued.

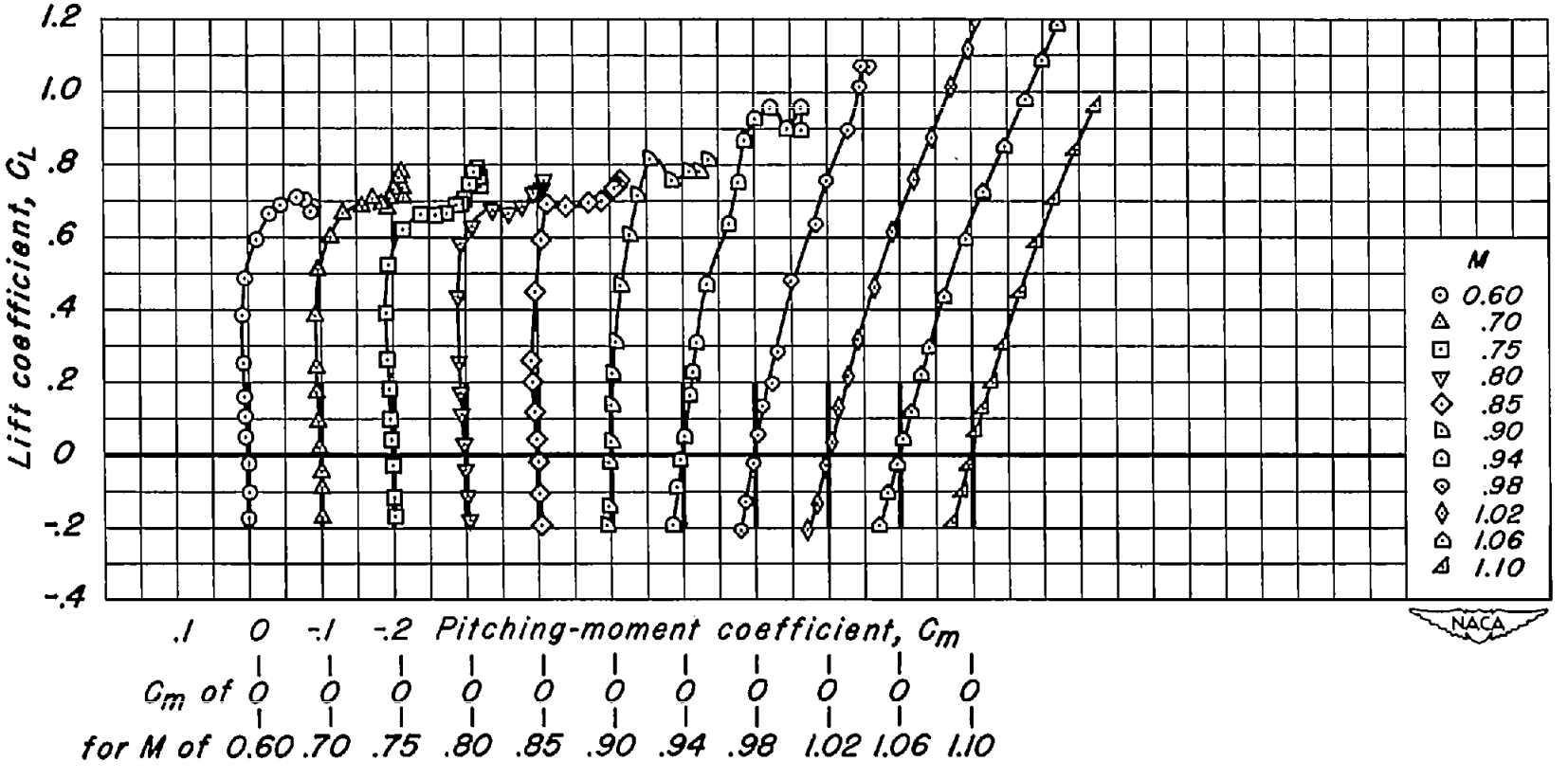

(e) t/c = 0.06; λ = 0.20

Figure 10.- Continued.

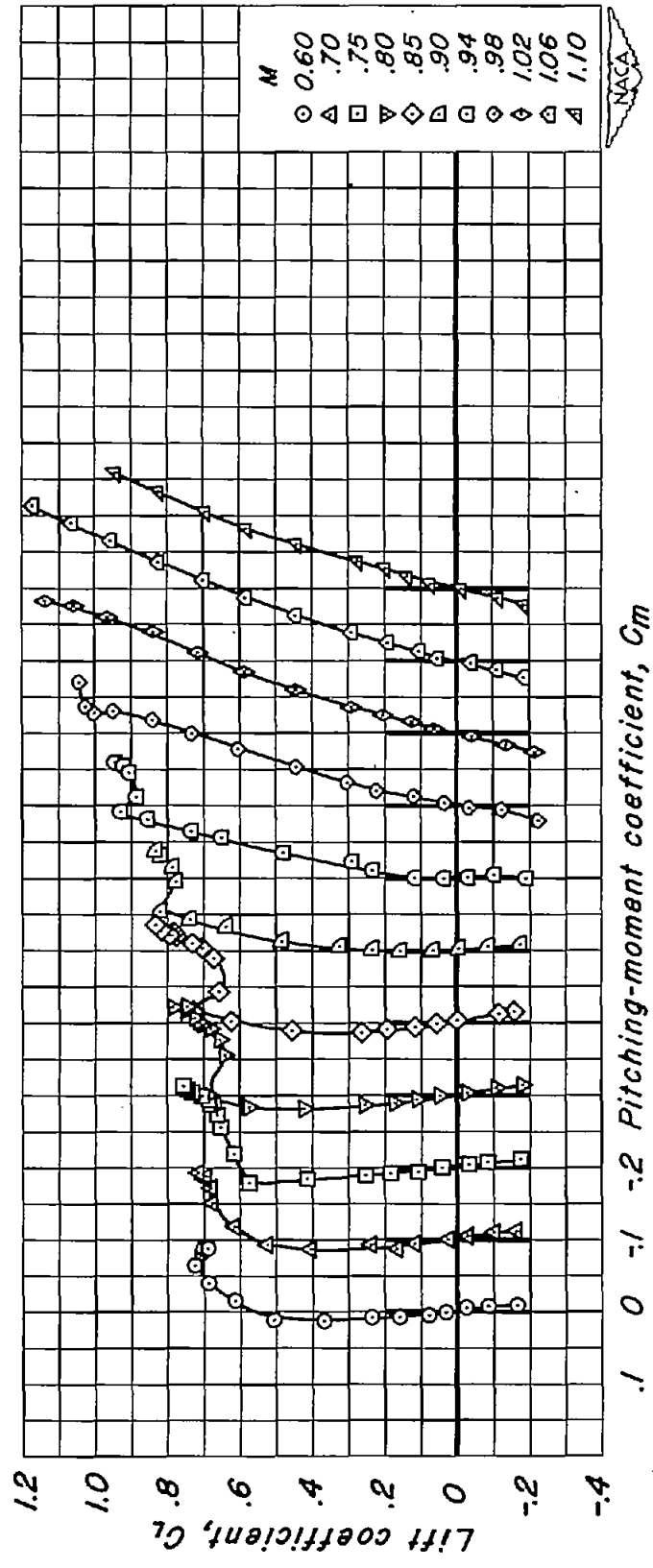

(f) t/c = 0.06; λ = 0.50

Figure 10.- Continued.

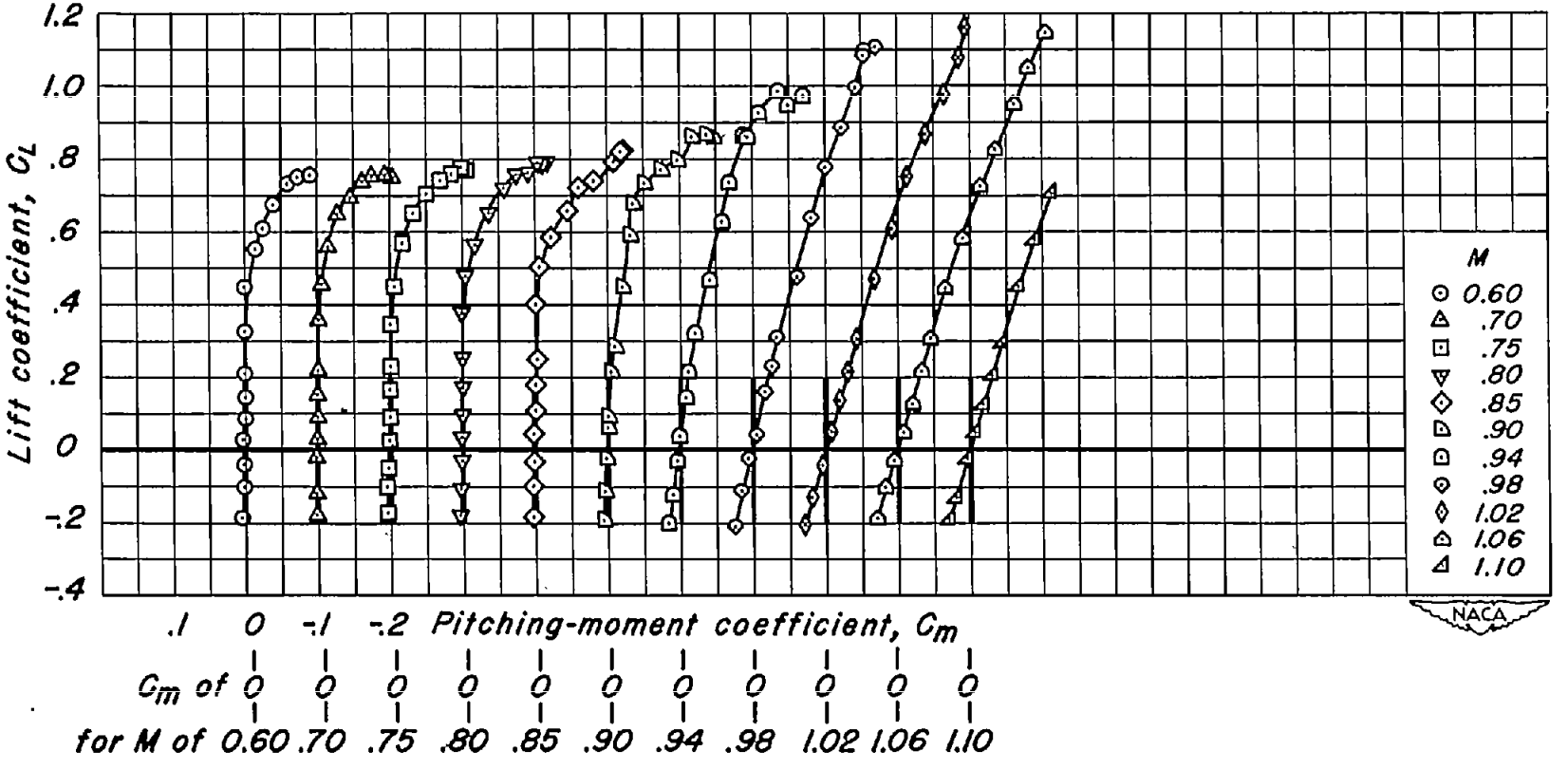

(g) t/c = 0.04; λ = 0

Figure 10.- Continued.

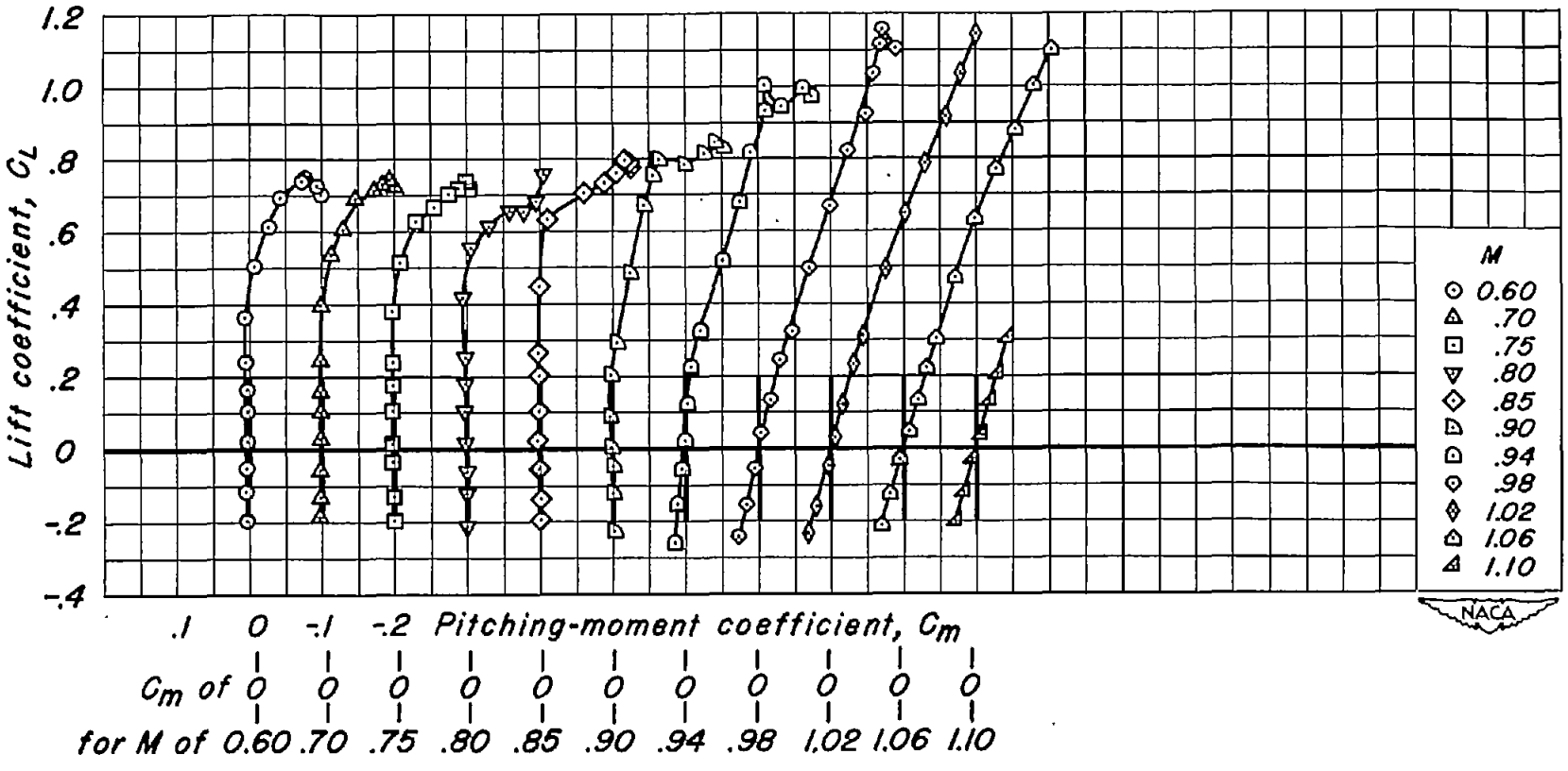

(h) t/c = 0.04; λ = 0.20

Figure 10.- Continued.

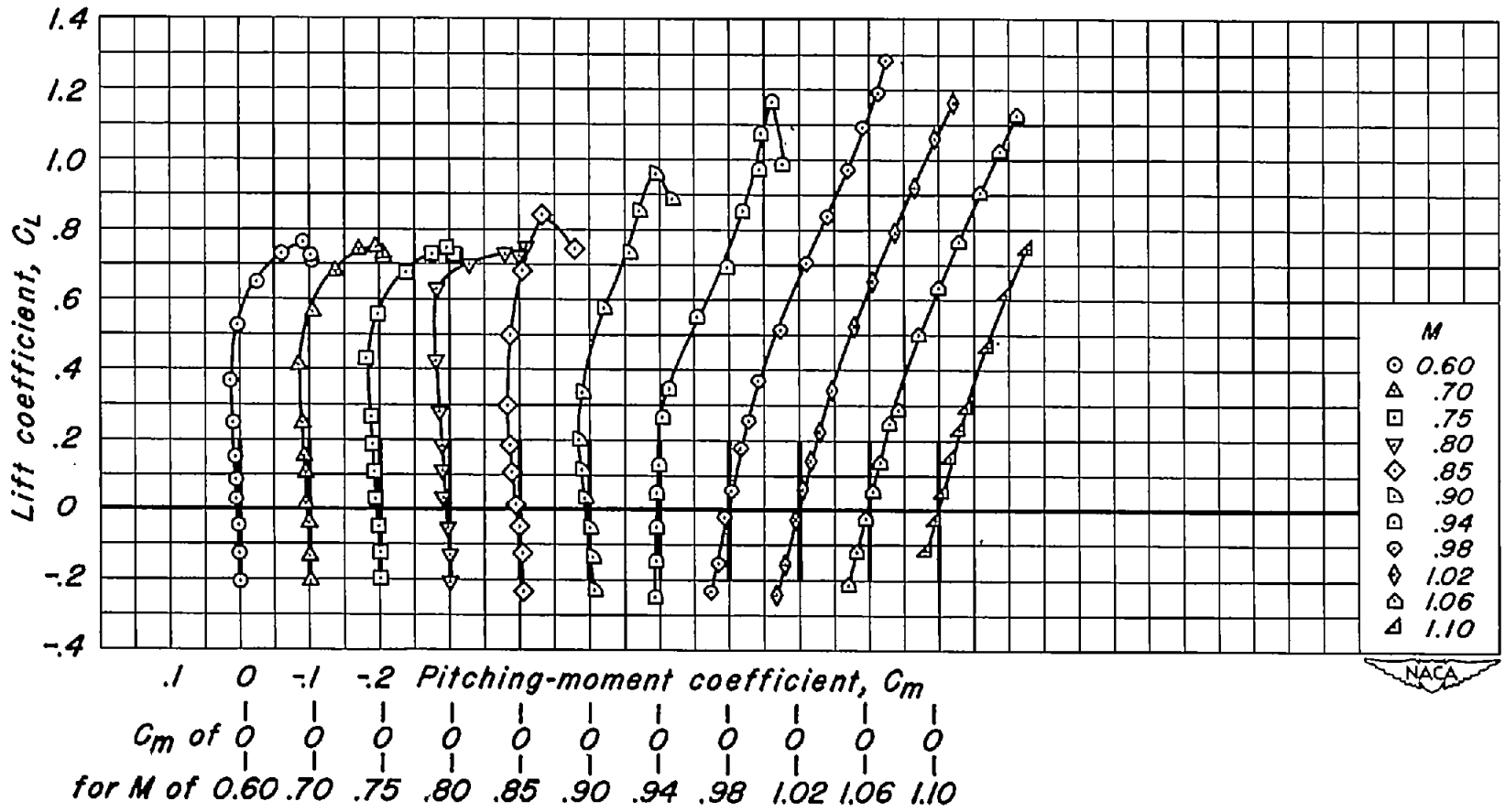

(i) t/c = 0.04; λ = 0.50

Figure 10.- Continued.

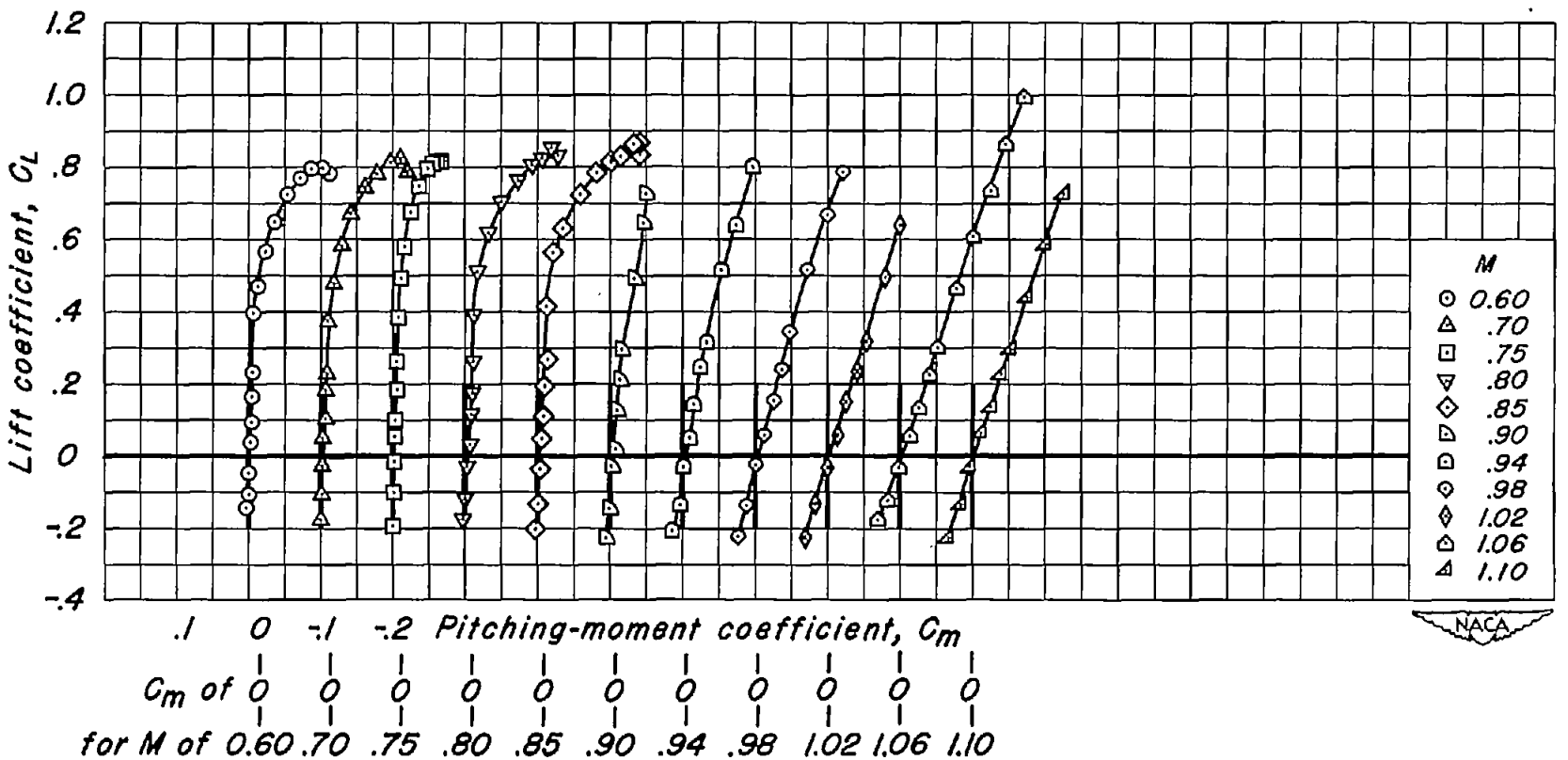

(j) t/c = 0.02; λ = 0

Figure 10.- Continued.

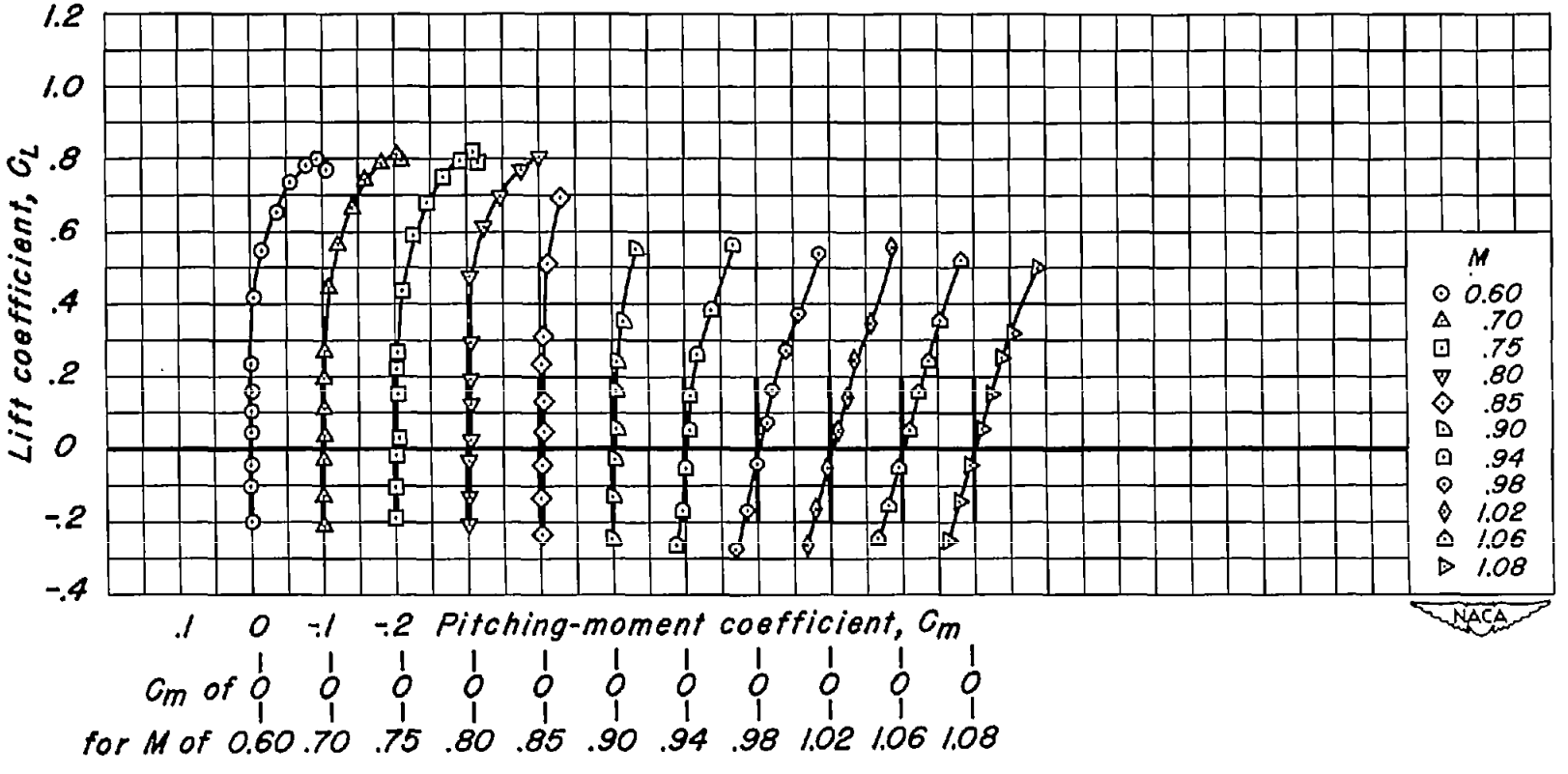

(k) t/c = 0.02; λ = 0.20

Figure 10.- Continued.

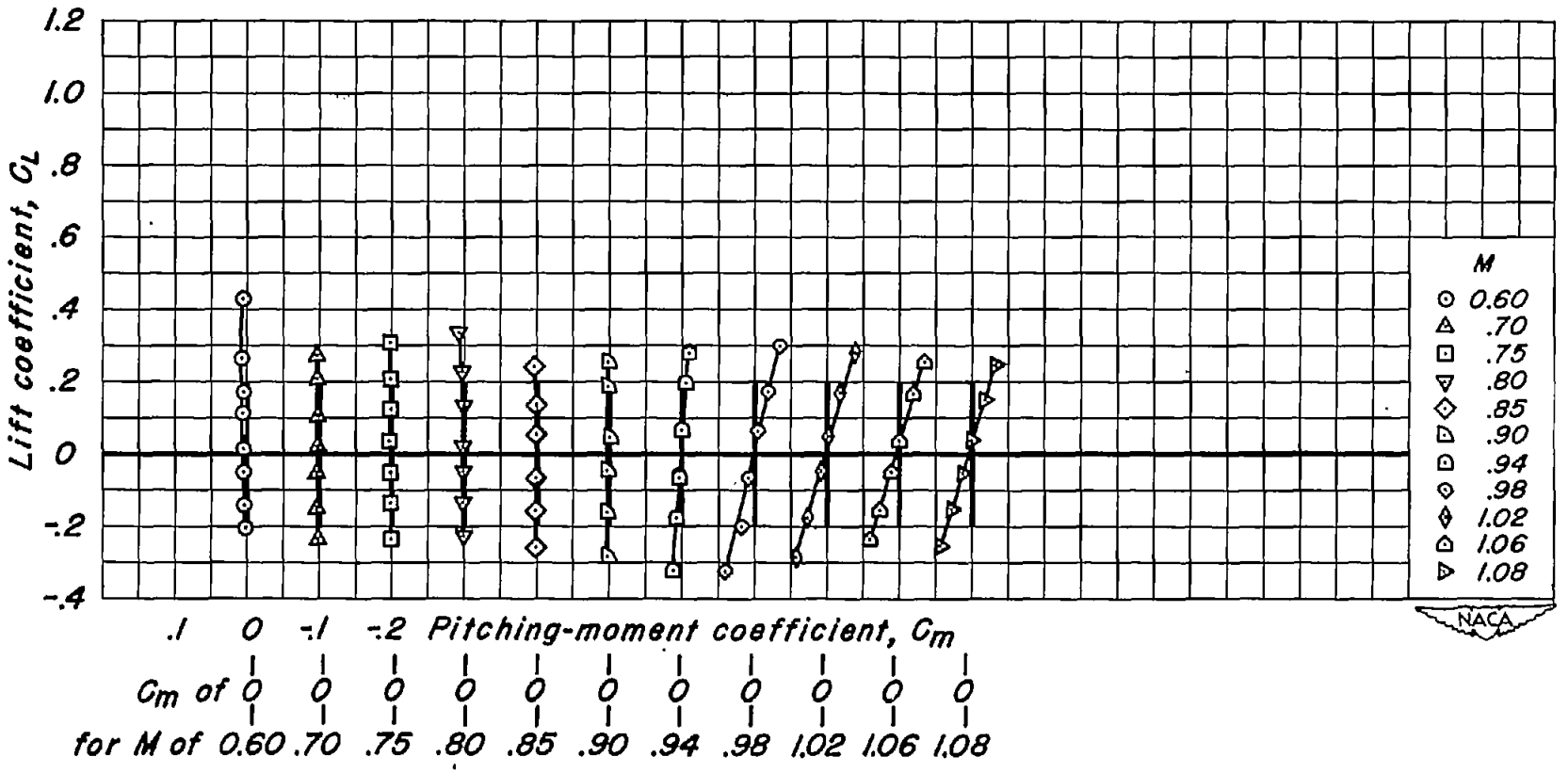

(l) t/c = 0.02; λ = 0.50

Figure 10.- Concluded.

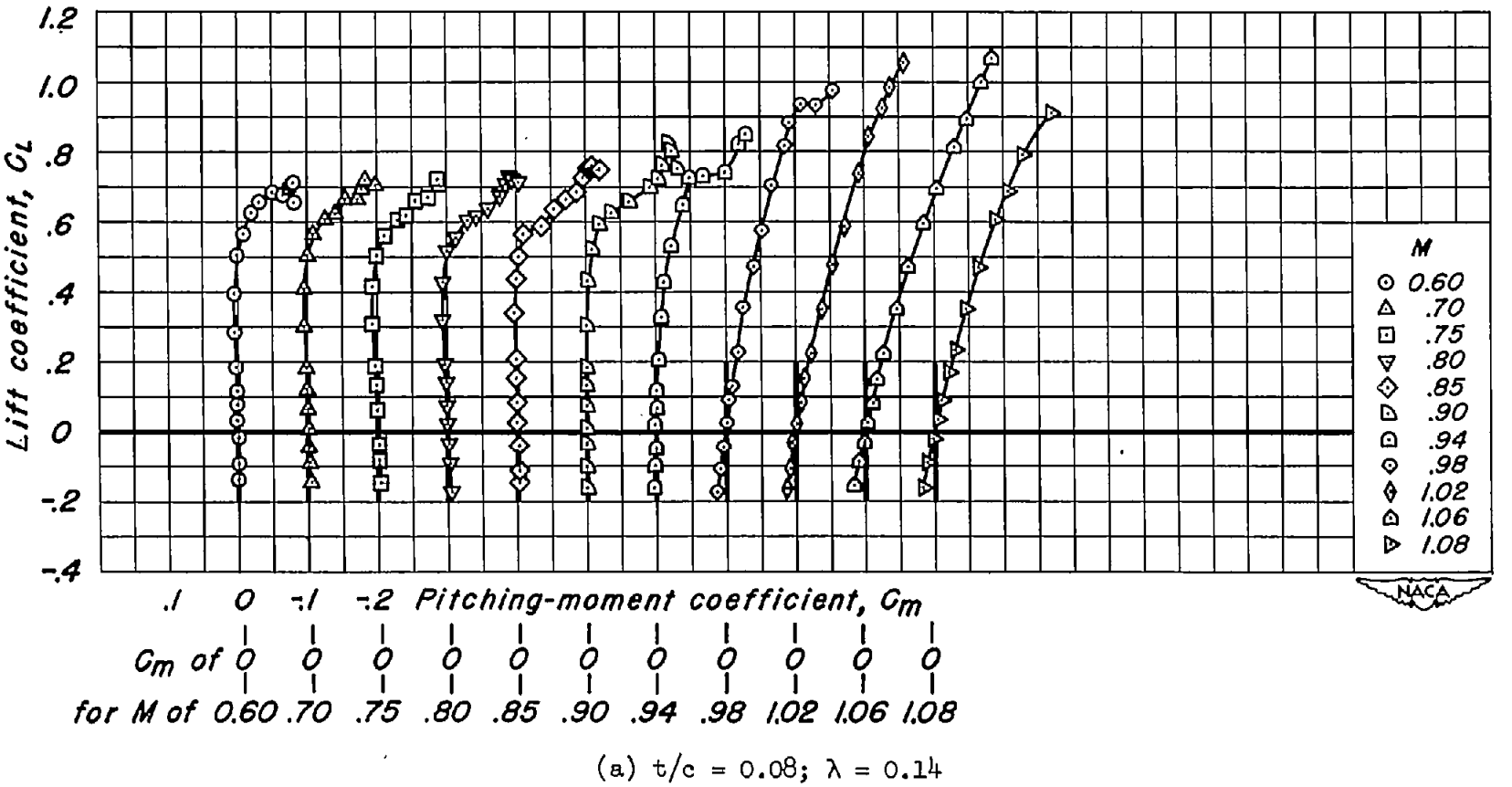

(a) t/c = 0.08; λ = 0.14

Figure 11.- The variation of lift coefficient with pitching-moment coefficient for the aspect-ratio-3 wings.

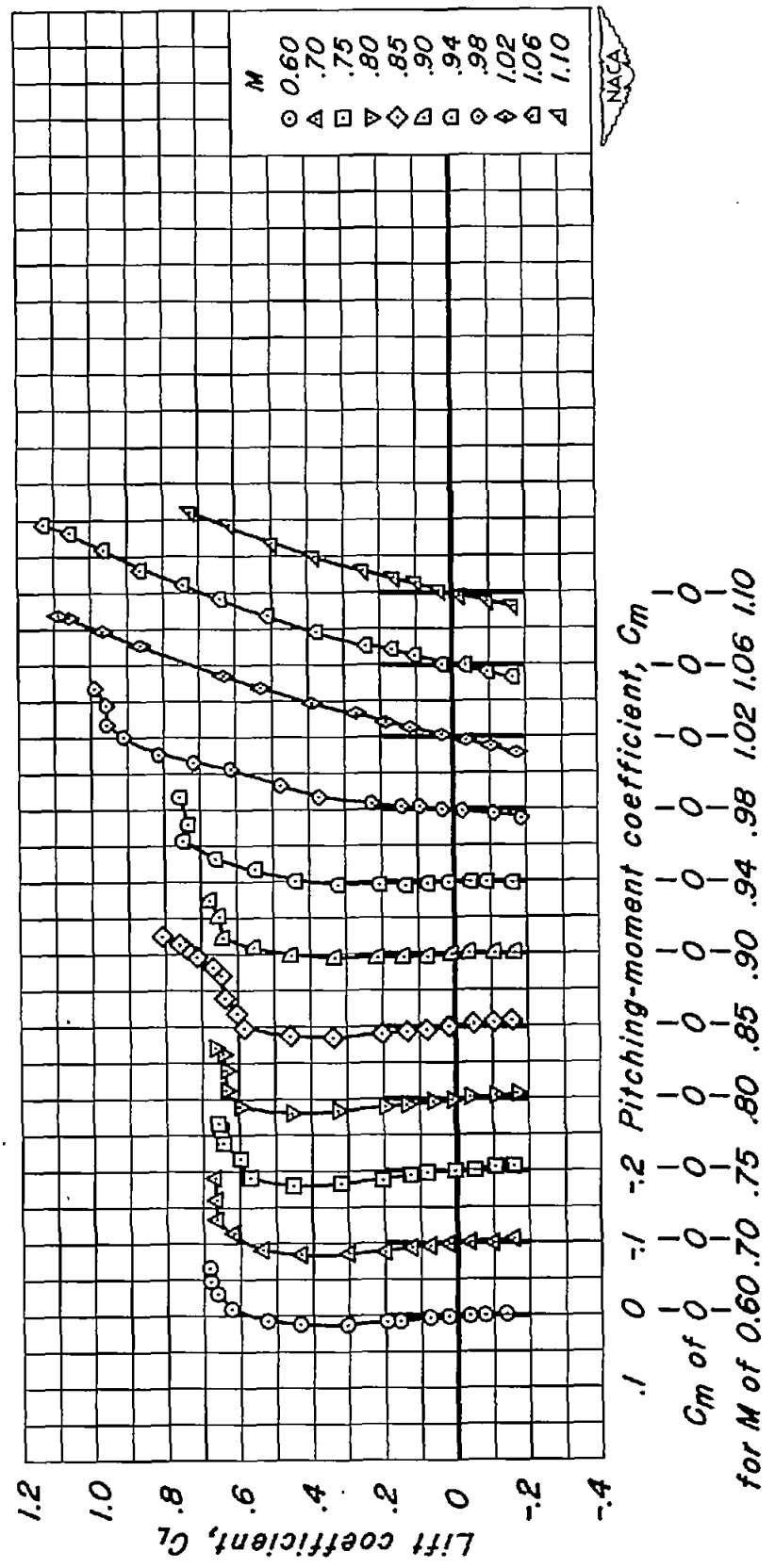

(b) $t/c = 0.08$; $\lambda = 0.33$

Figure 11.- Continued.

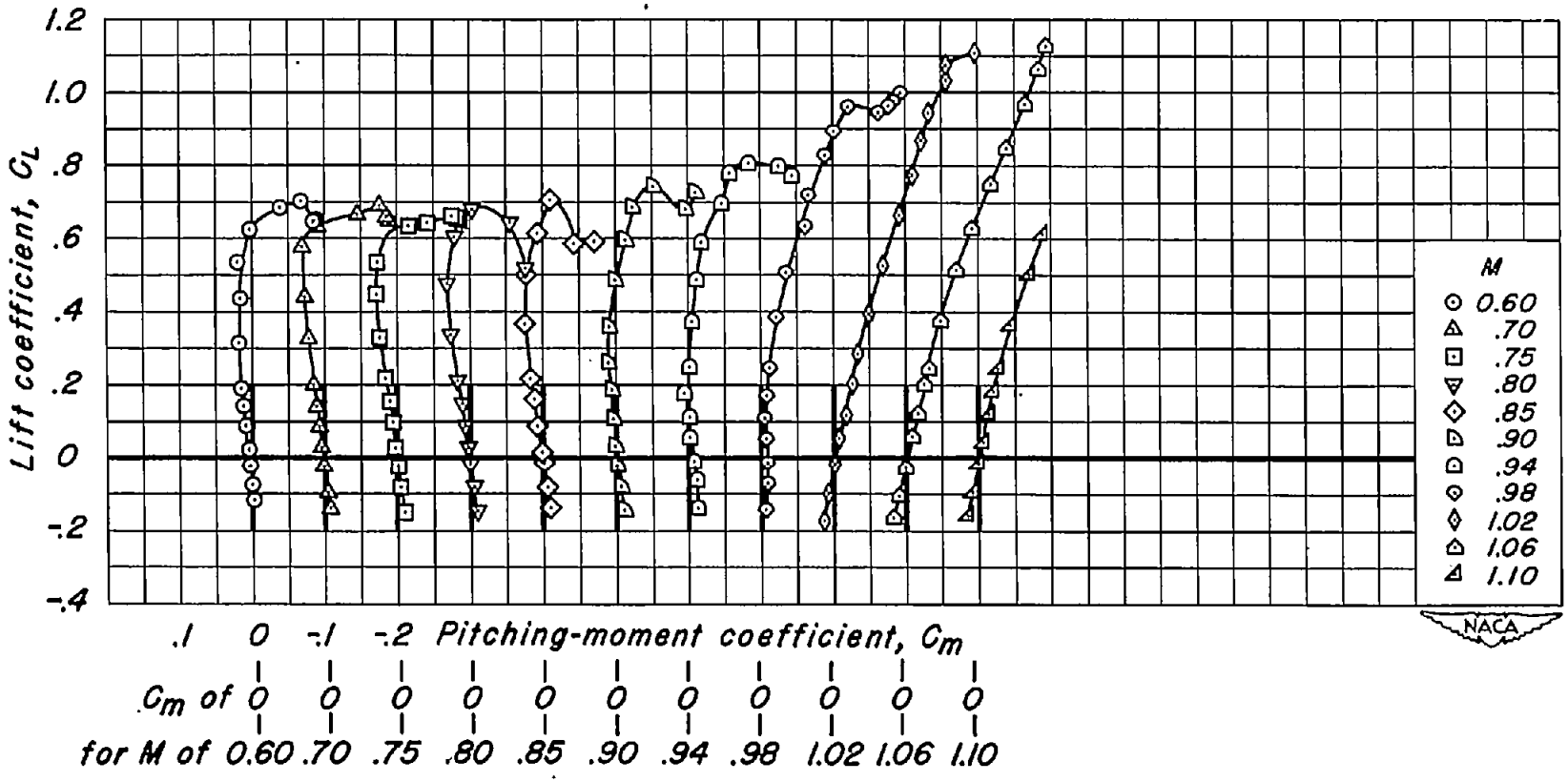

(c) t/c = 0.08; $\lambda = 0.60$

Figure 11.- Continued.

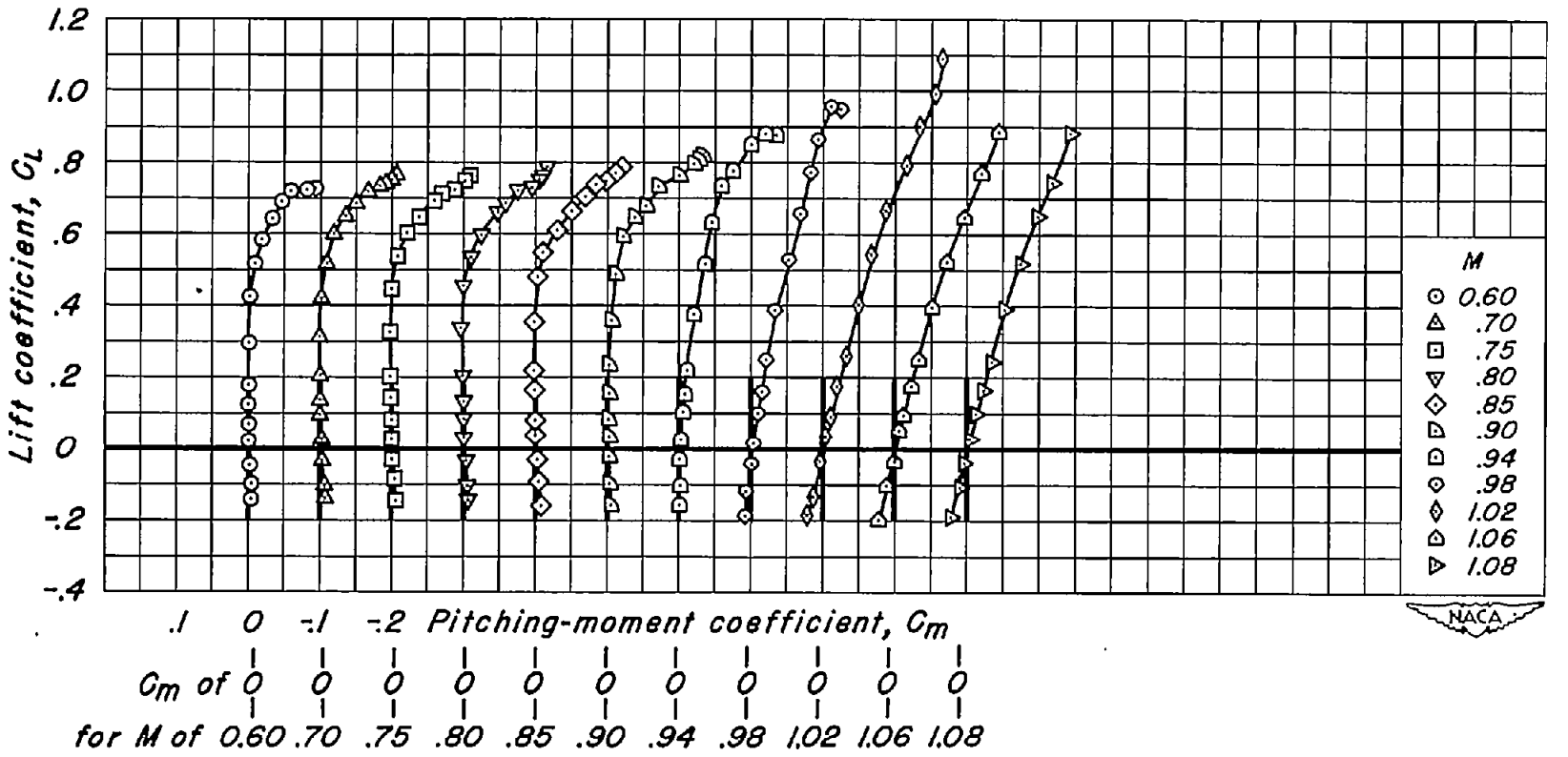

(d) t/c = 0.06; λ = 0.14

Figure 11.- Continued.

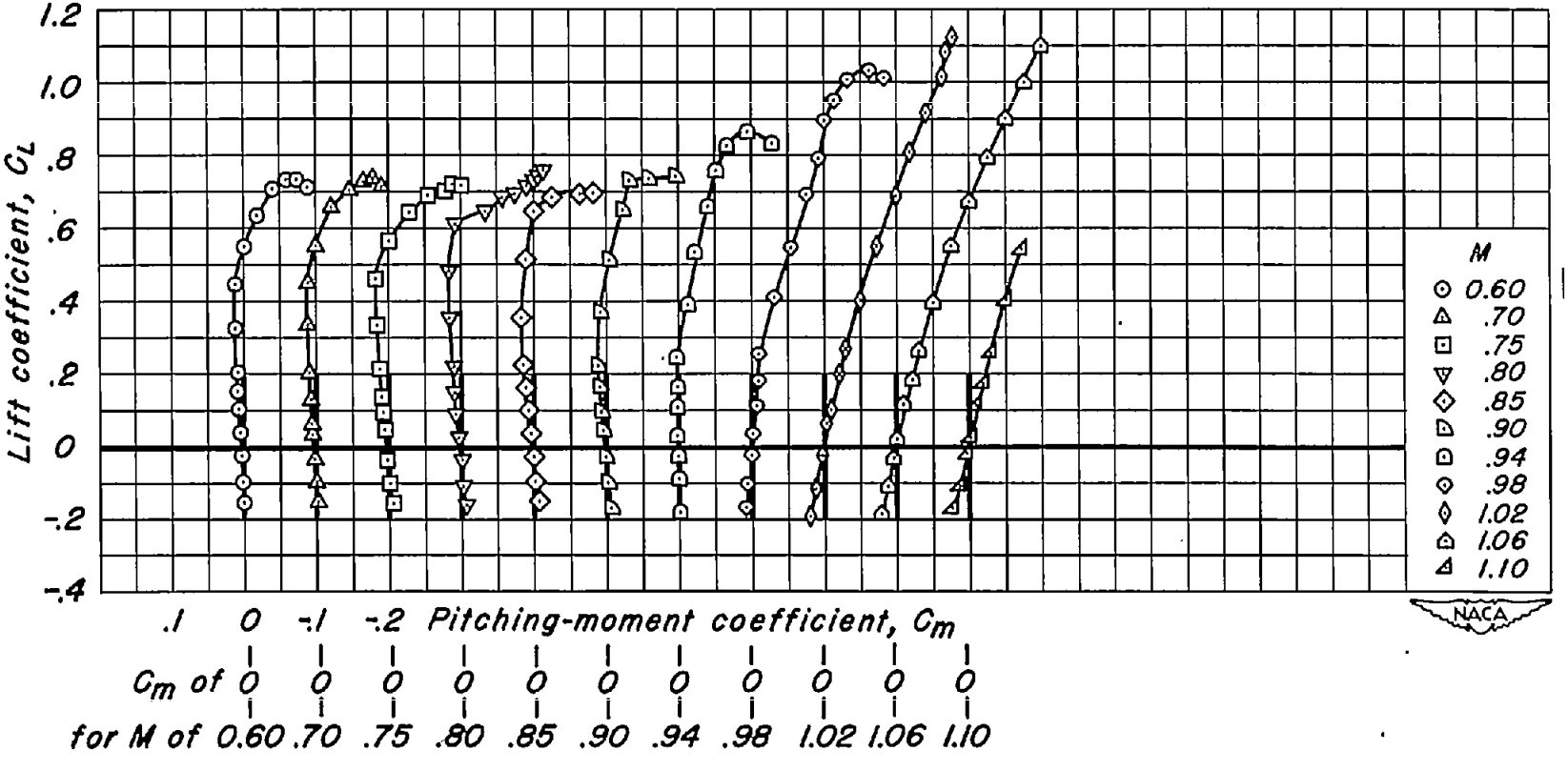

(e) t/c = 0.06; λ = 0.33

Figure 11.- Continued.

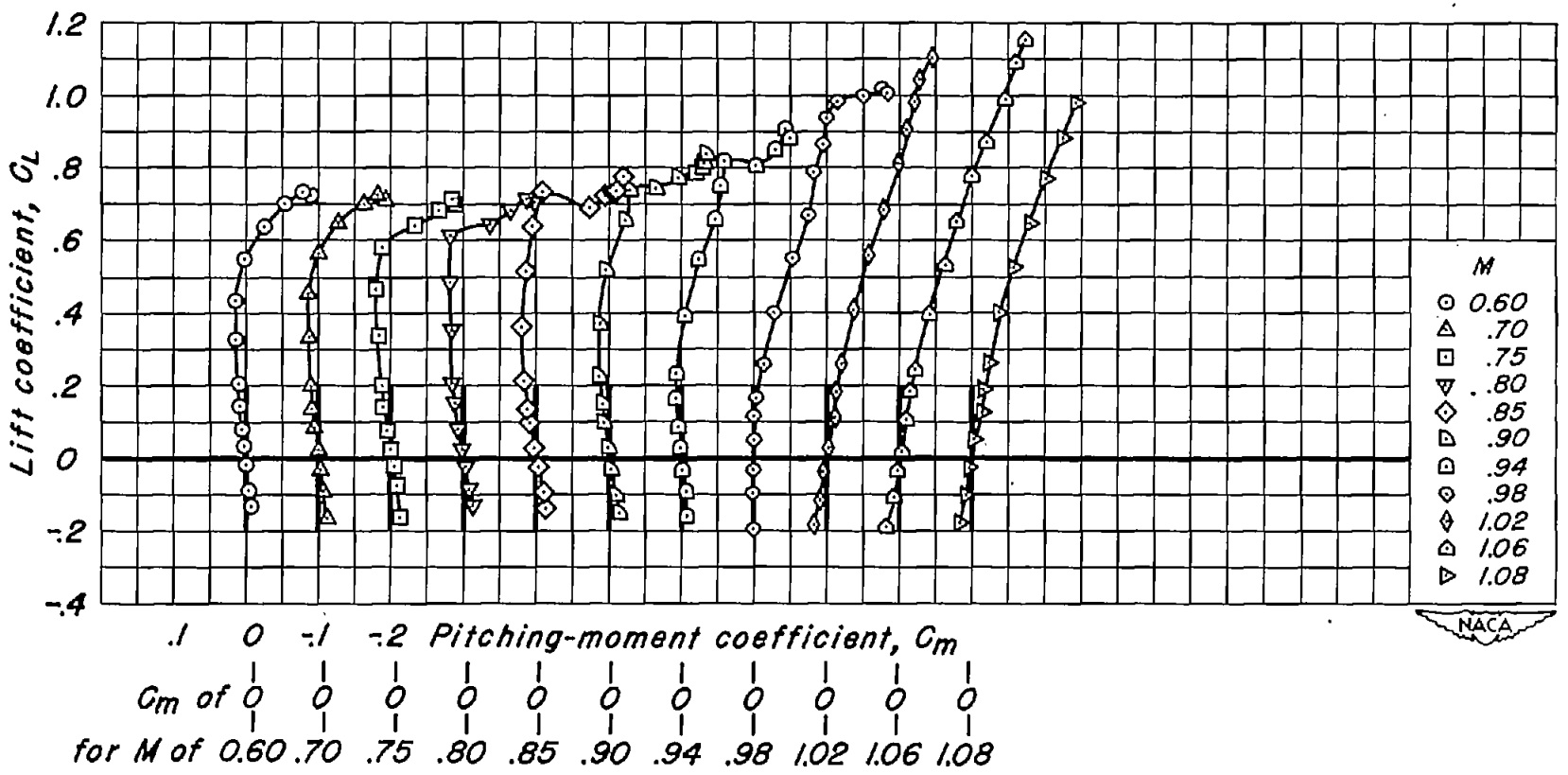

(f) t/c = 0.06; λ = 0.60

Figure 11.- Continued.

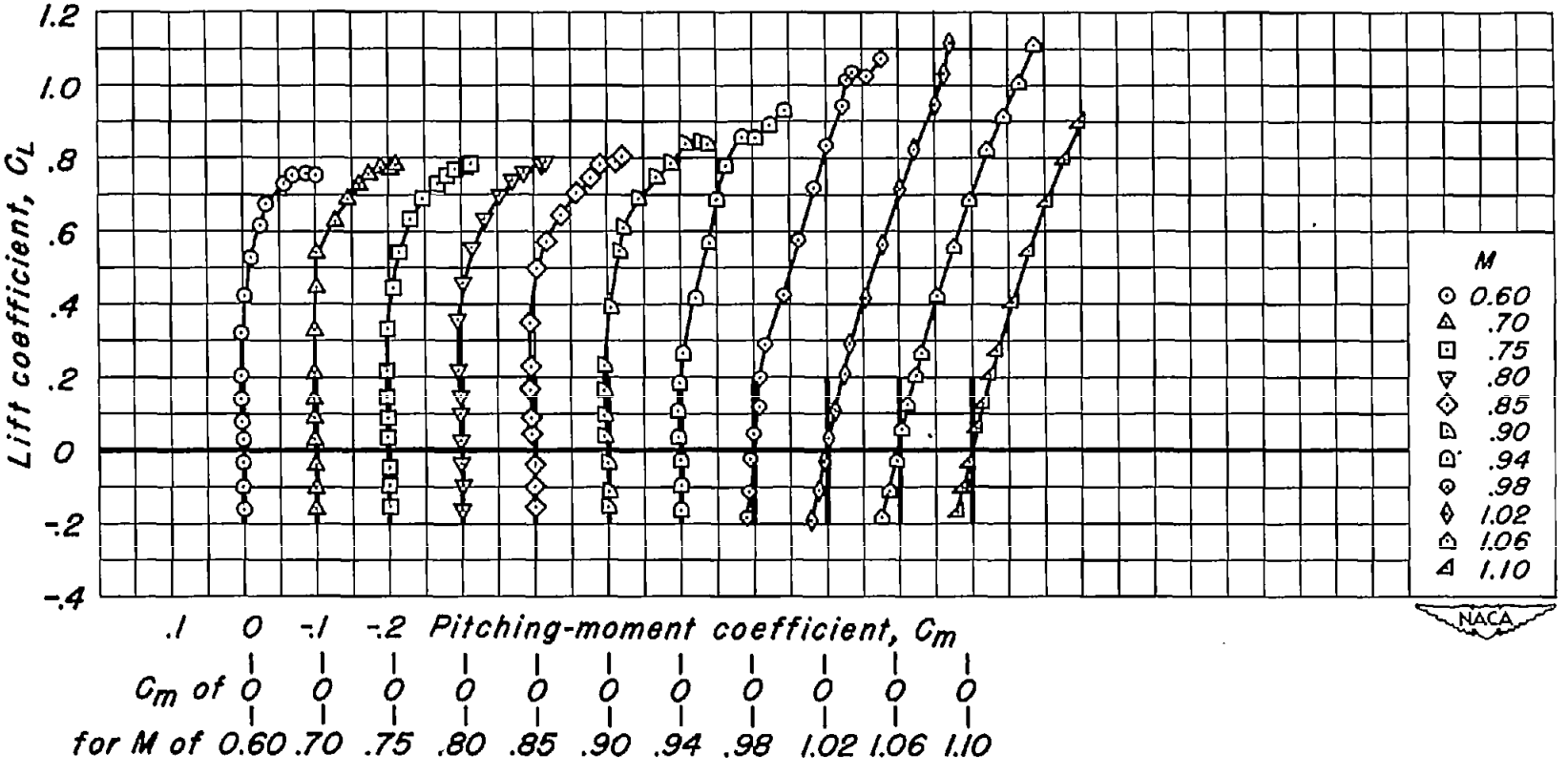

(g) t/c = 0.04; λ = 0.14

Figure 11.- Continued.

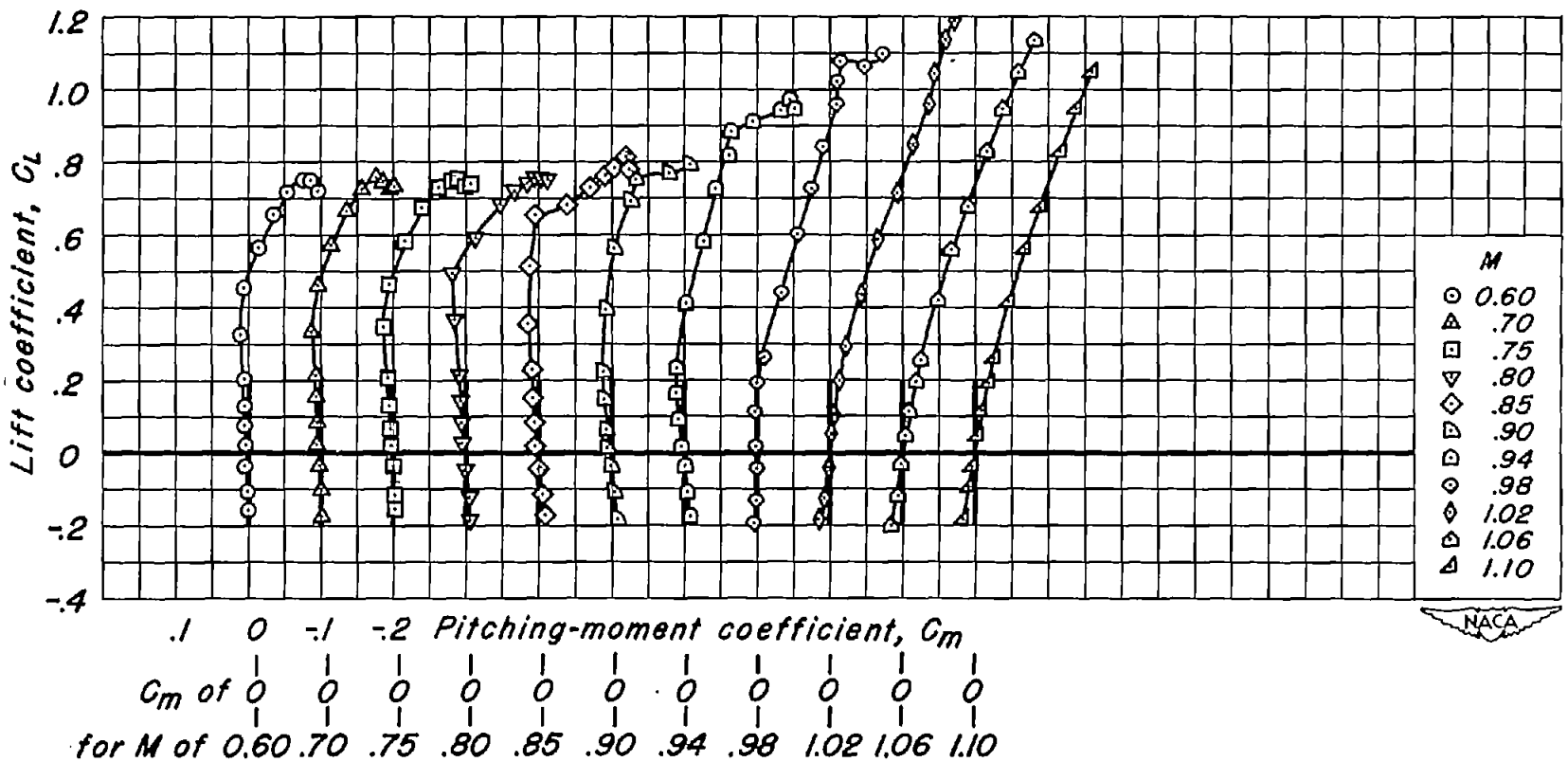

(h) t/c = 0.04; λ = 0.33

Figure 11.- Continued.

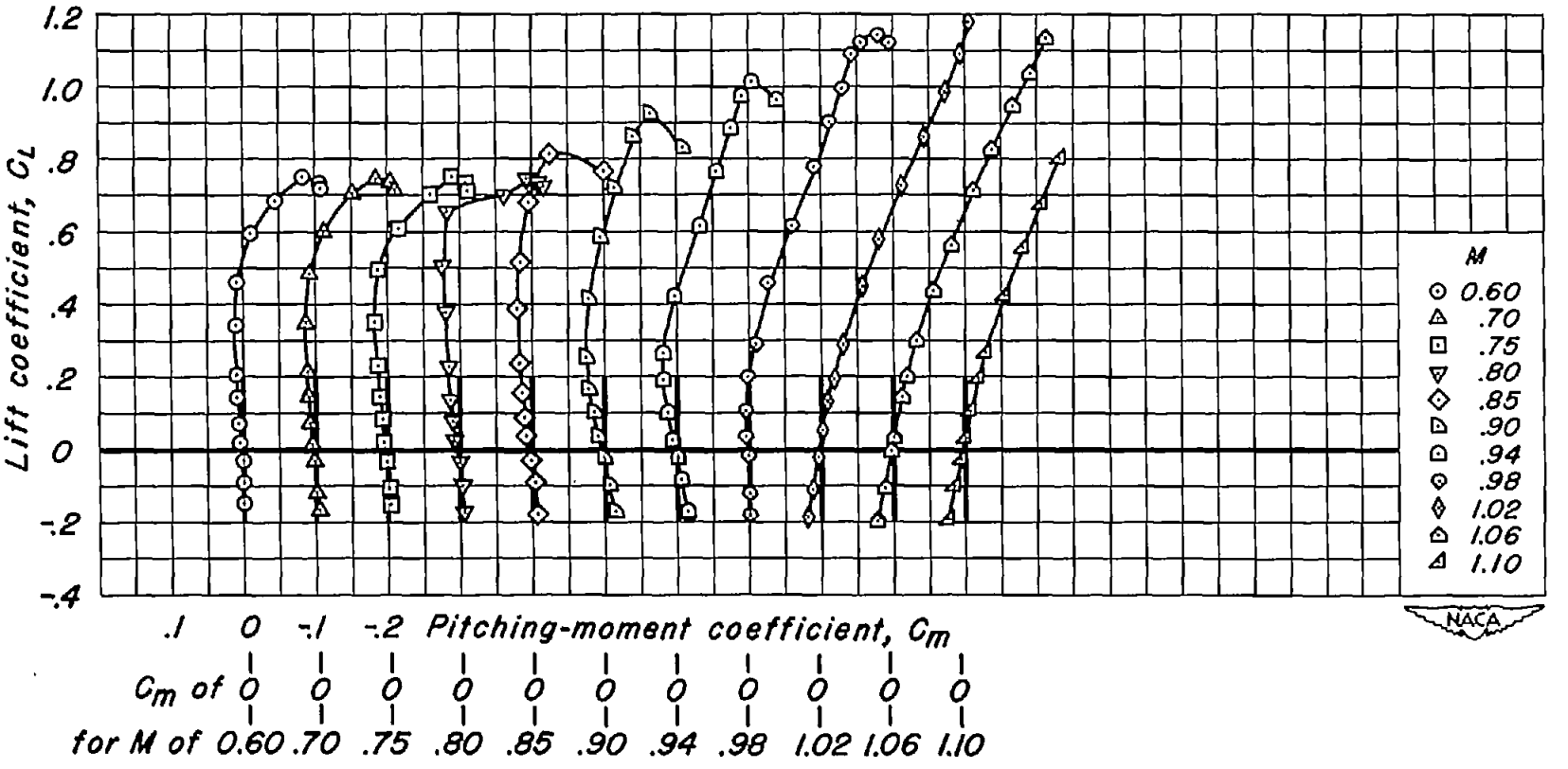

(i) t/c = 0.04; λ = 0.60

Figure 11.- Continued.

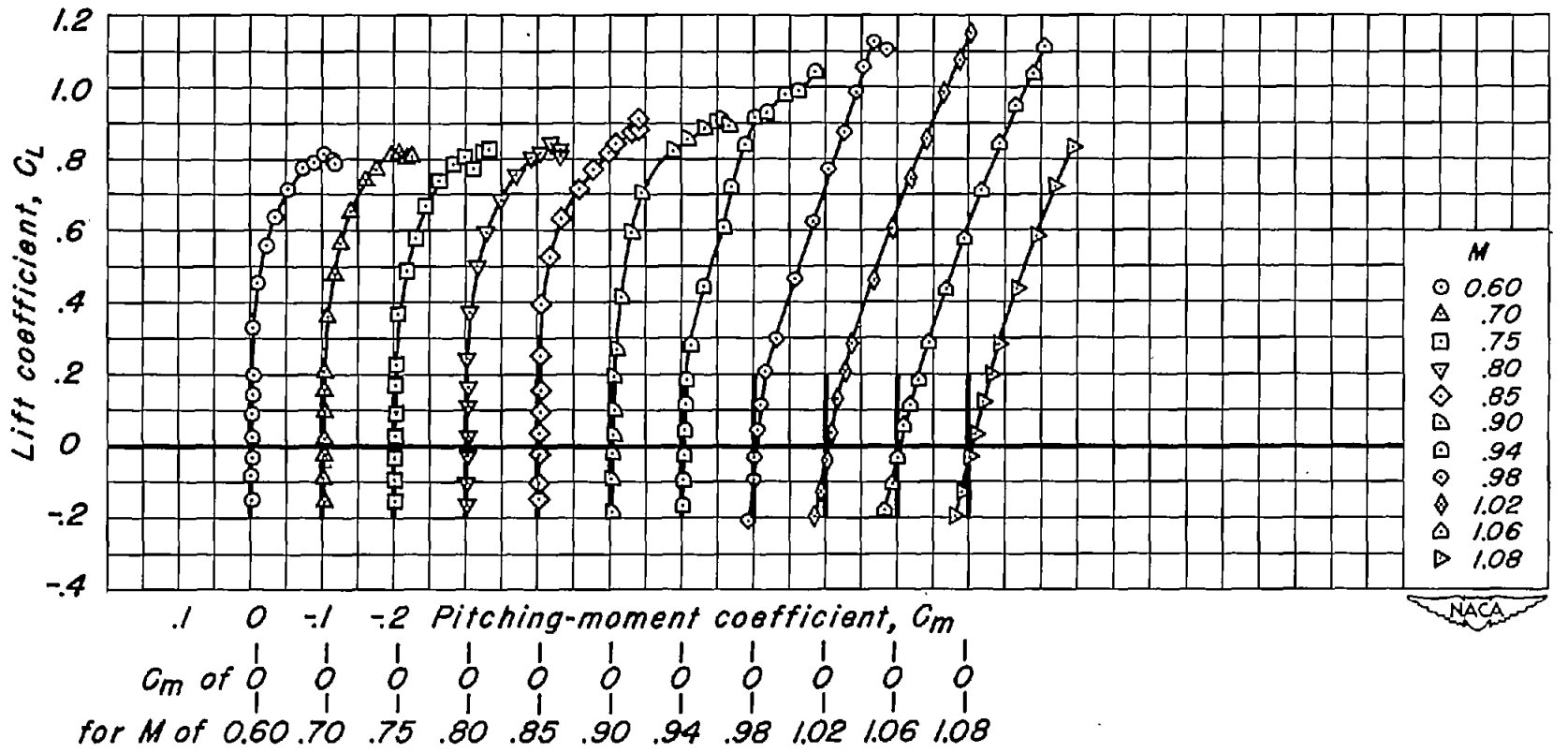

(j) t/c = 0.02; λ = 0.14

Figure 11.- Continued.

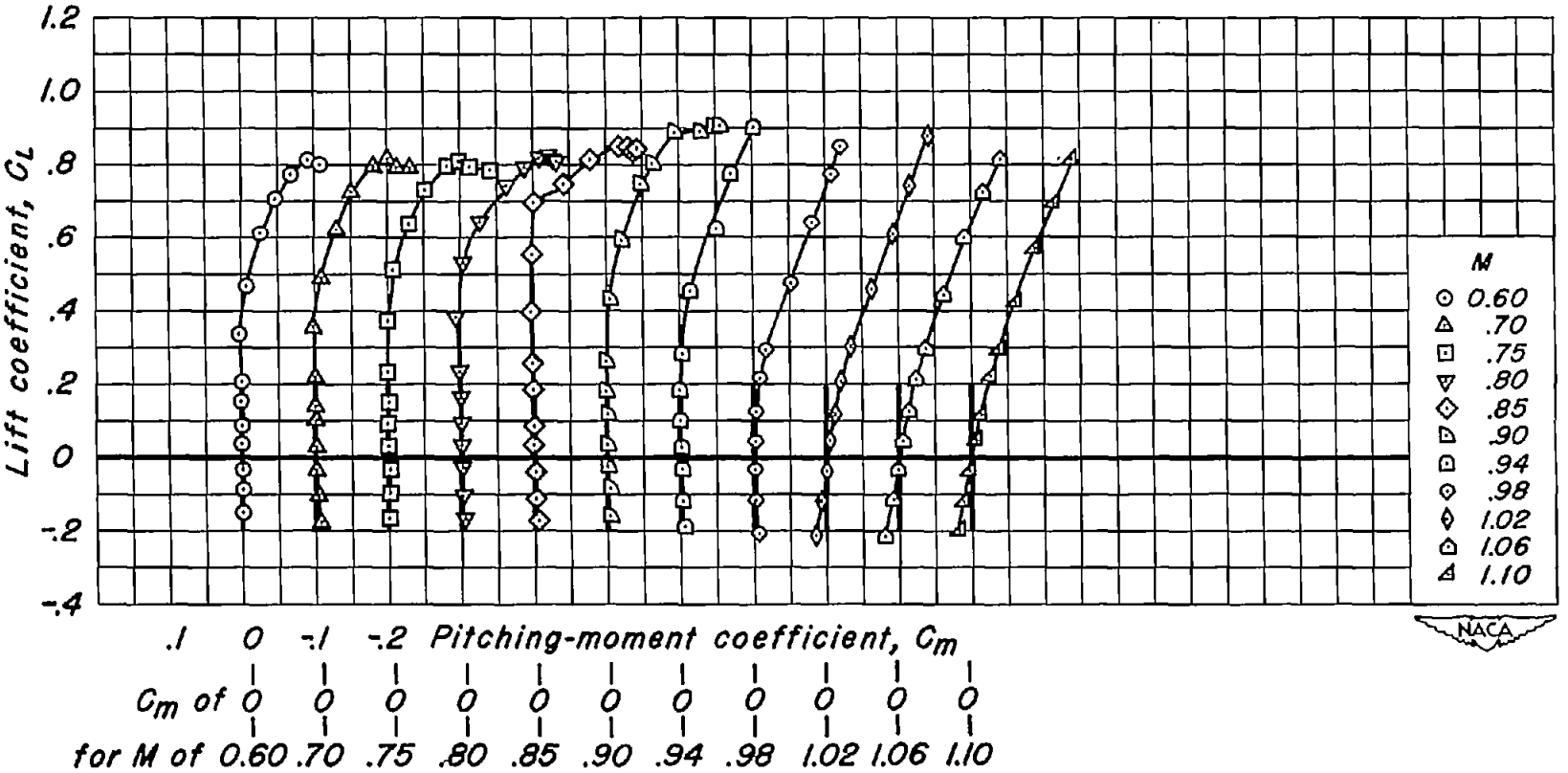

(k) t/c = 0.02; λ = 0.33

Figure 11.- Continued.

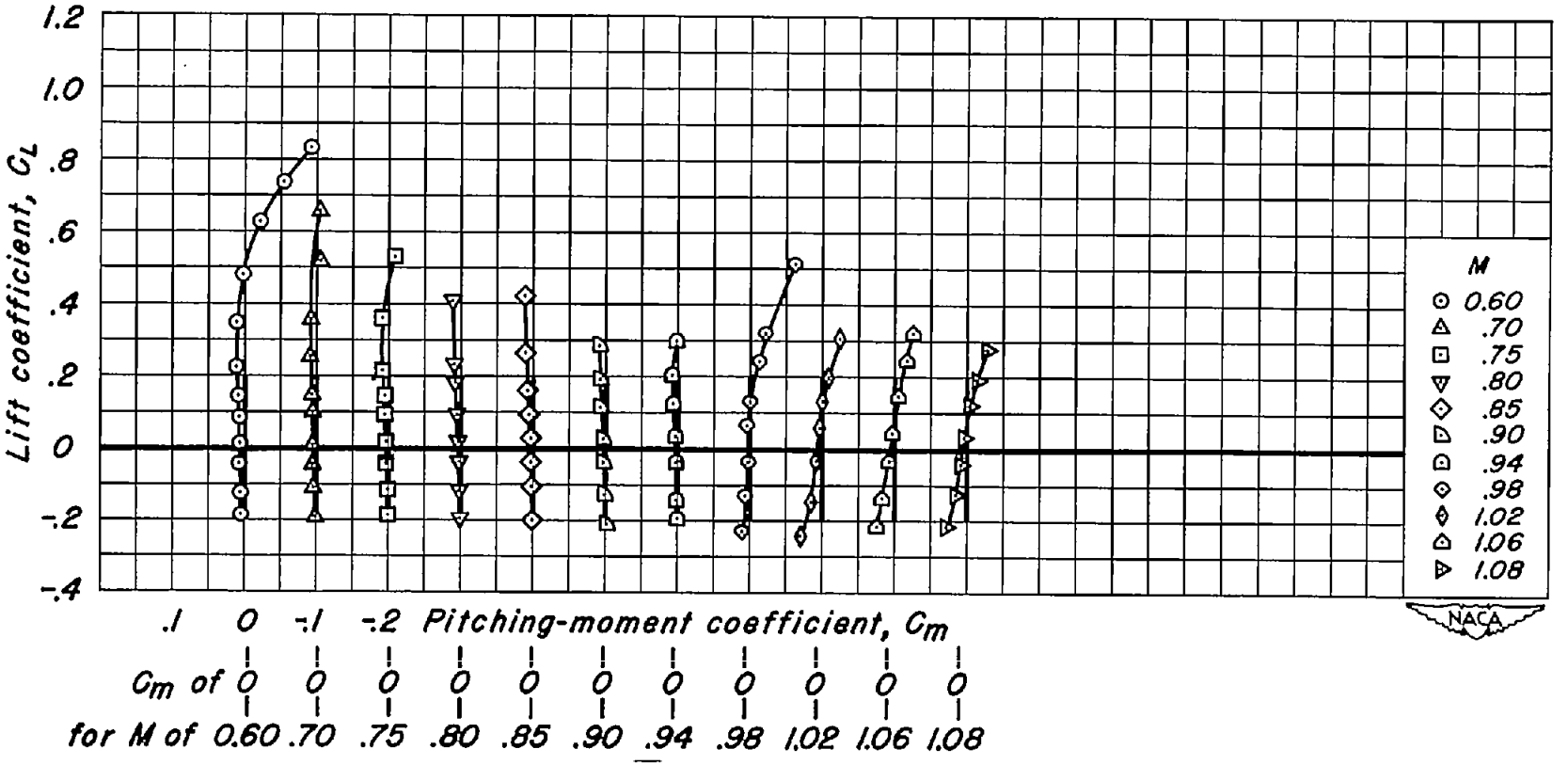

(l) t/c = 0.02; λ = 0.60

Figure 11.- Concluded.

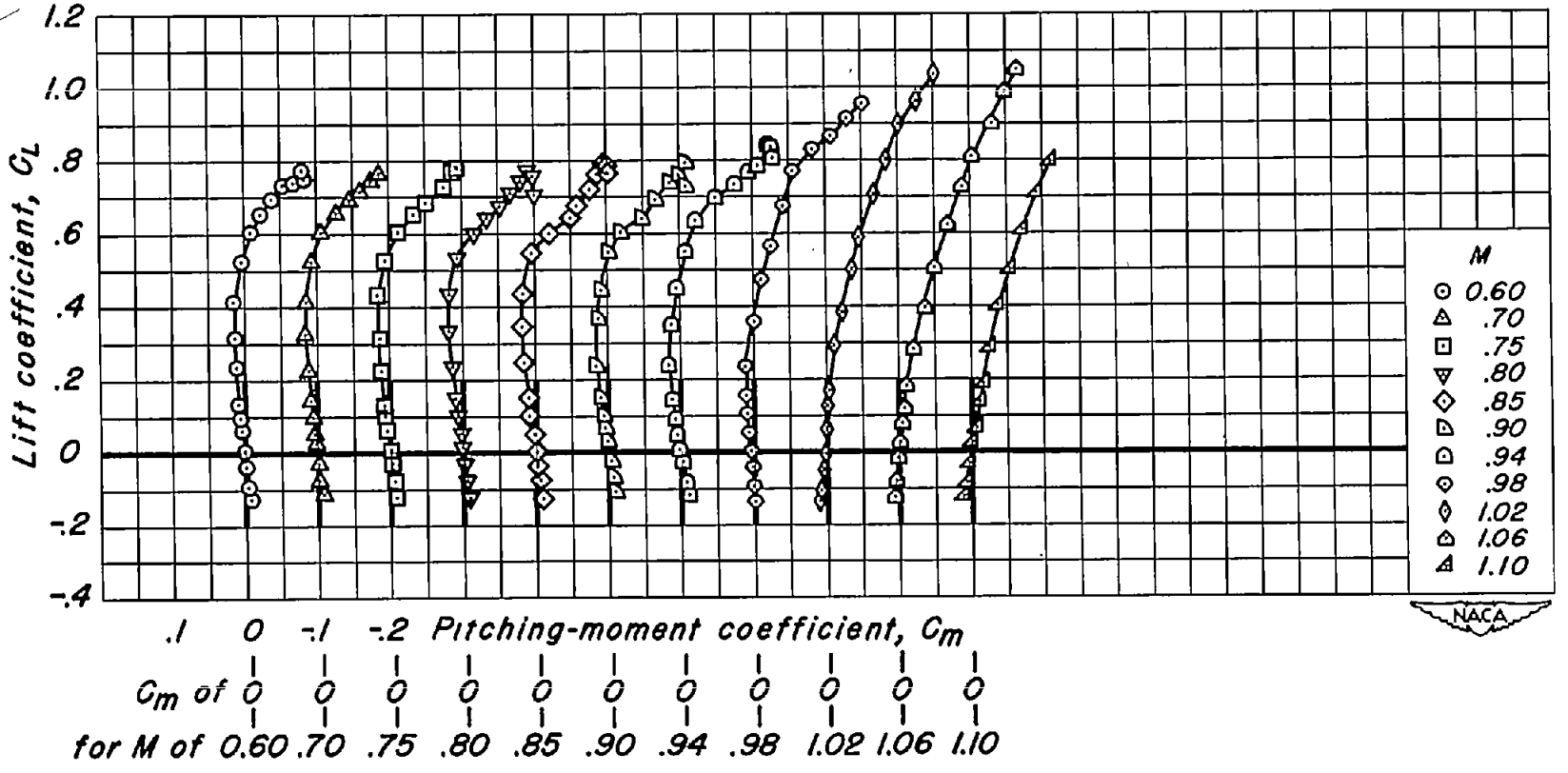

(a) t/c = 0.08; λ = 0.33

Figure 12.- The variation of lift coefficient with pitching-moment coefficient for the aspect-ratio-2 wings.

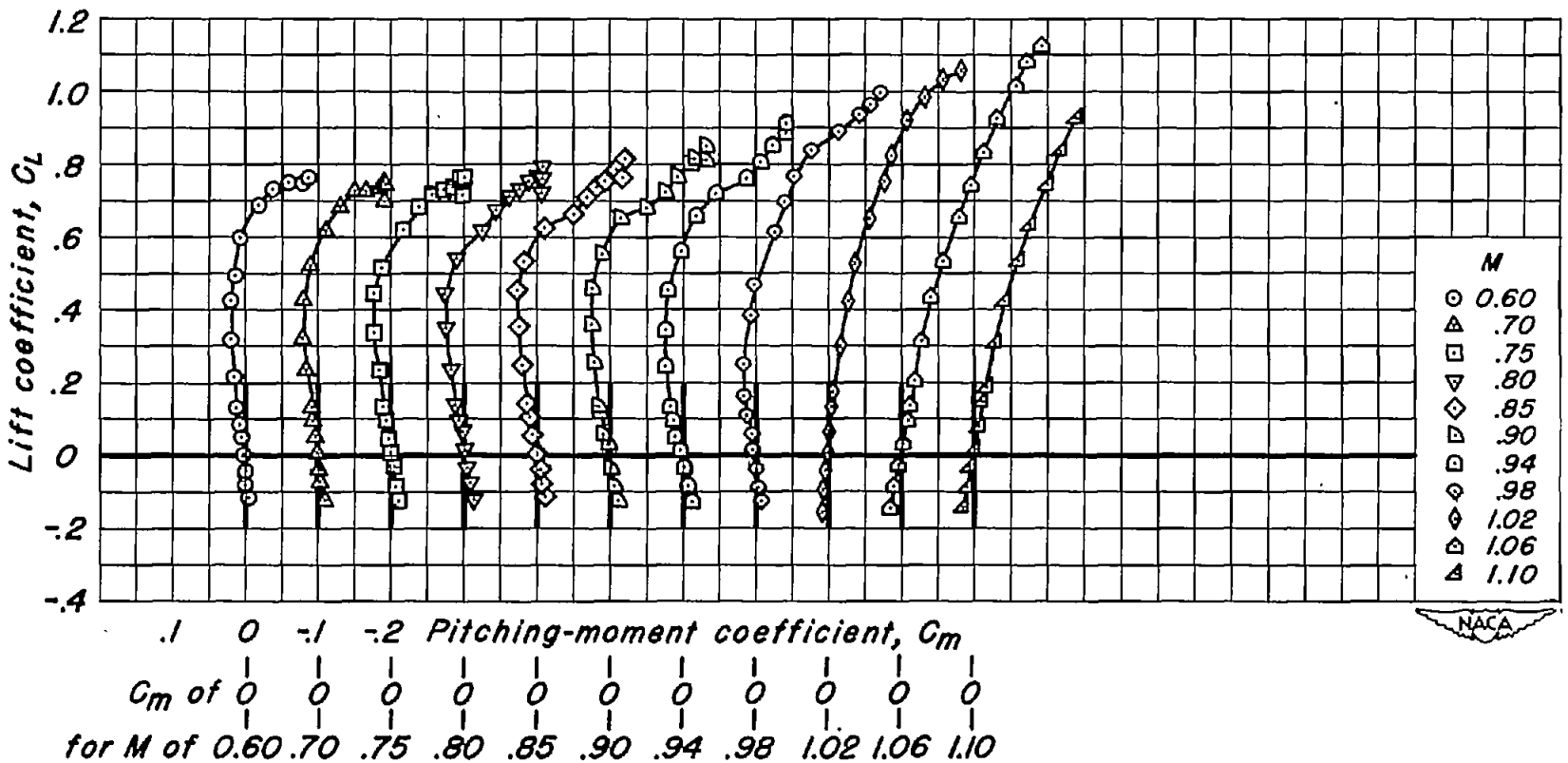

(b) t/c = 0.08; λ = 0.50

Figure 12.- Continued.

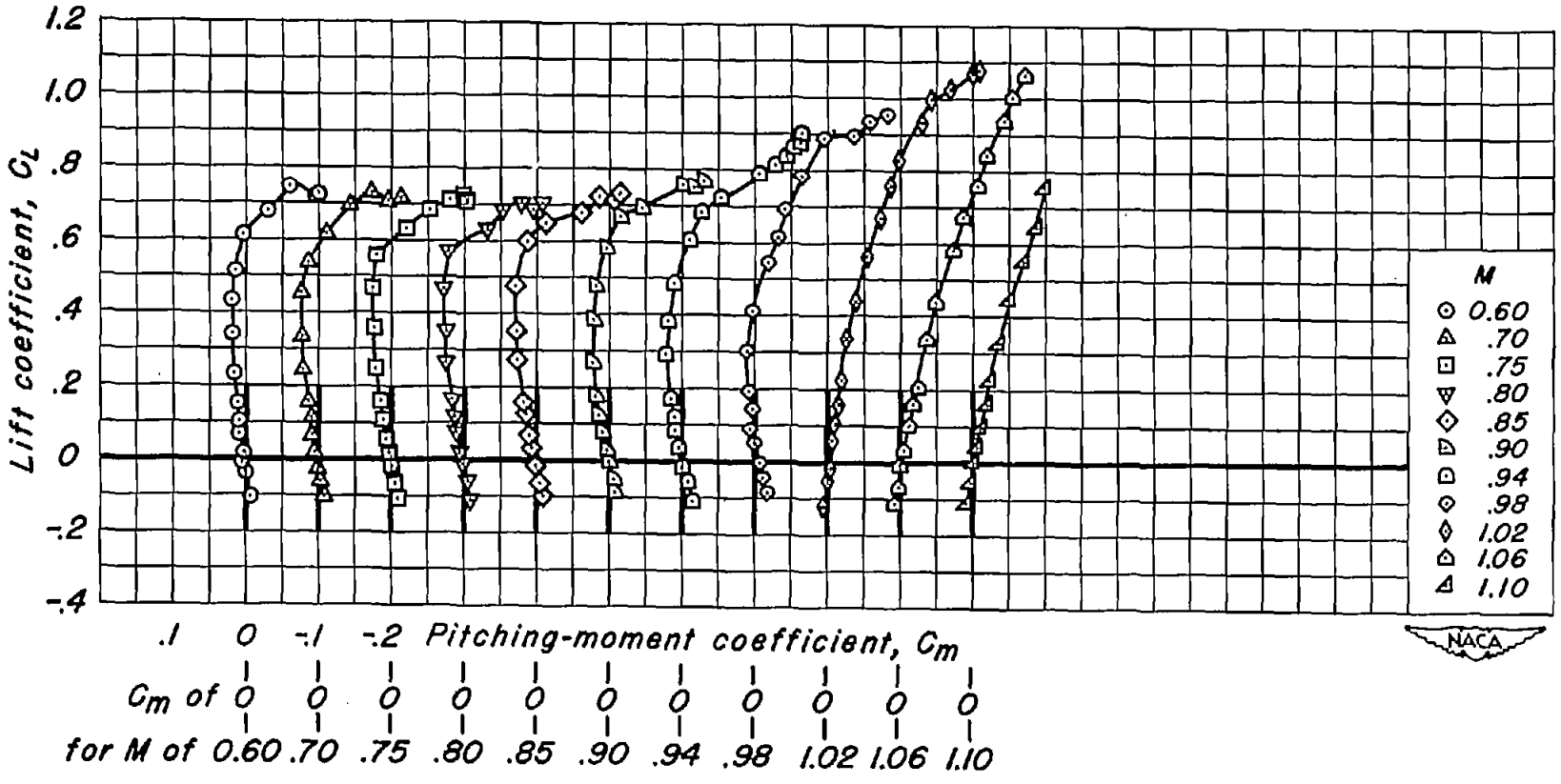

(c) t/c = 0.08; $\lambda = 0.72$

Figure 12.- Continued.

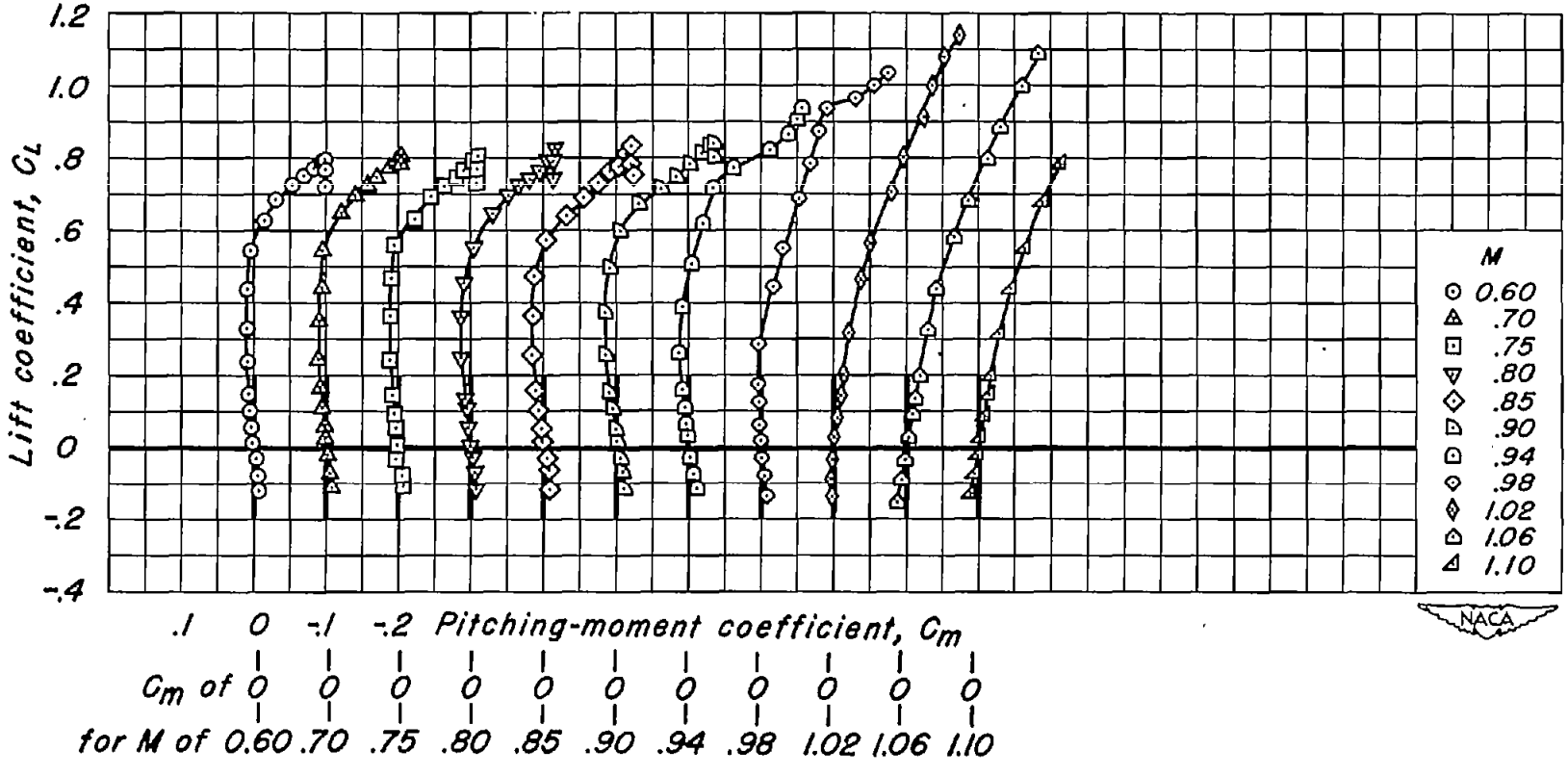

(d) t/c = 0.06; λ = 0.33

Figure 12.- Continued.

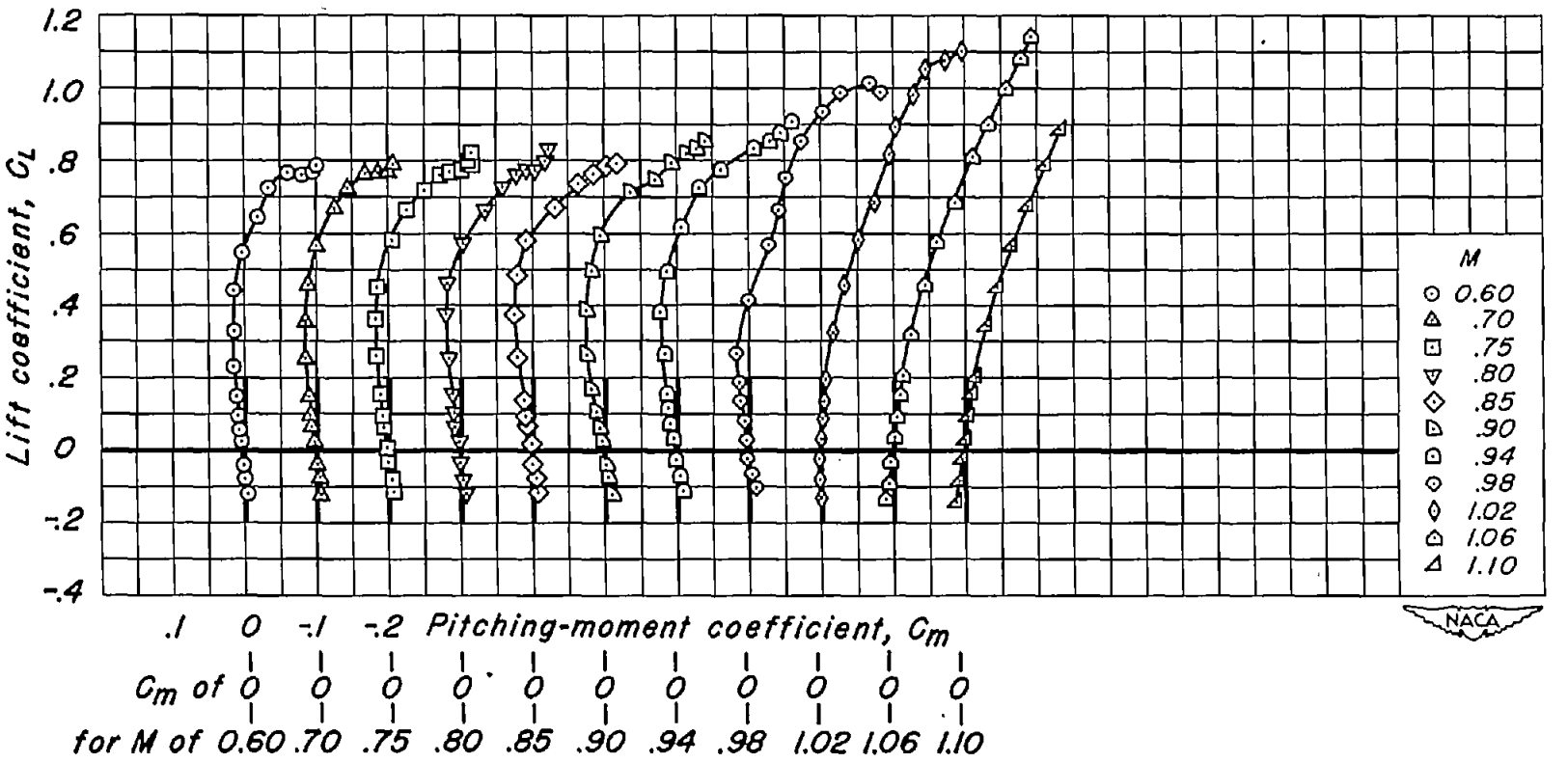

(e) t/c = 0.06; λ = 0.50

Figure 12.- Continued.

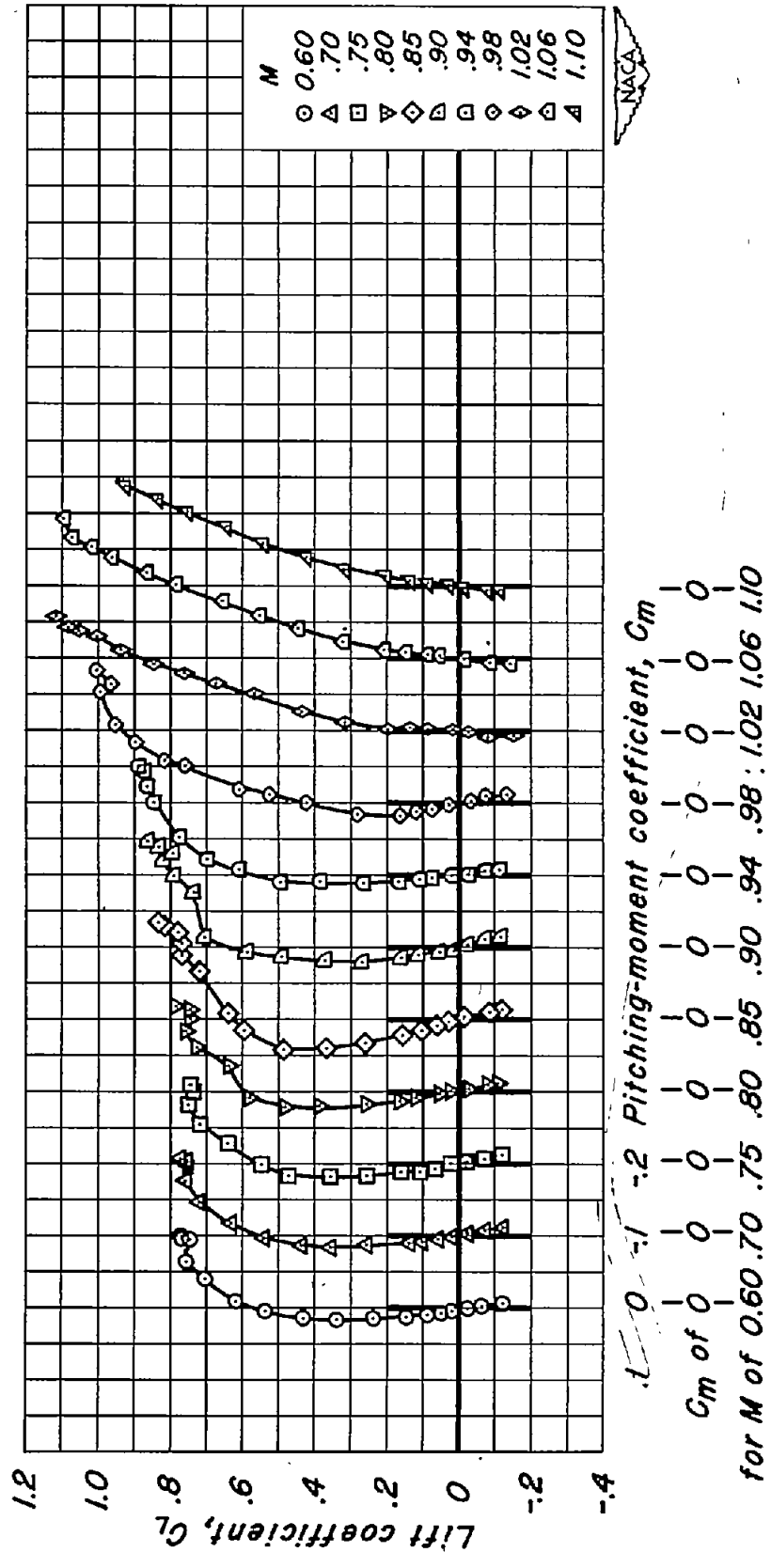

(f) t/c = 0.06; λ = 0.72

Figure 12.- Continued.

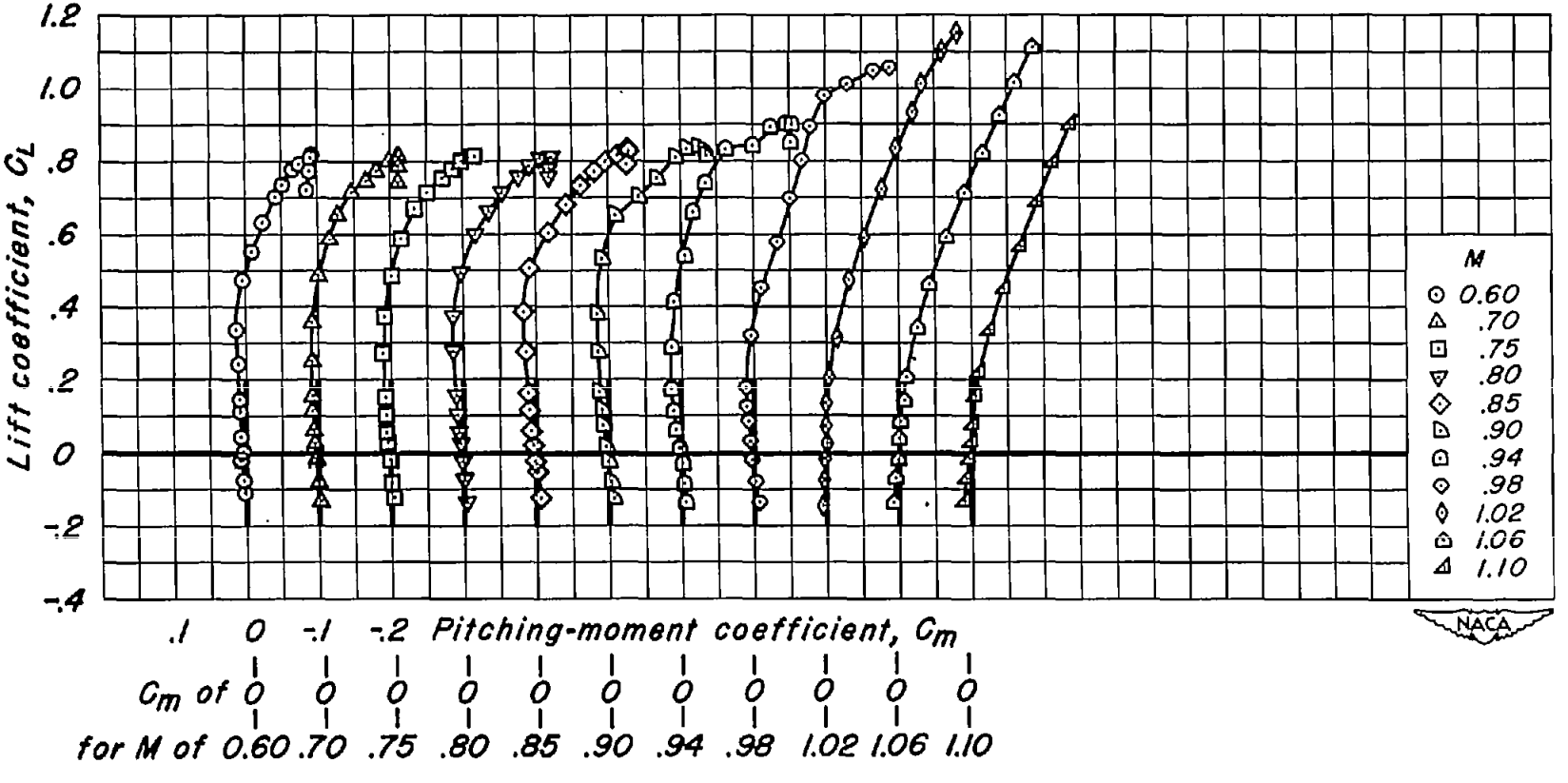

(g) t/c = 0.04; λ = 0.33

Figure 12.- Continued.

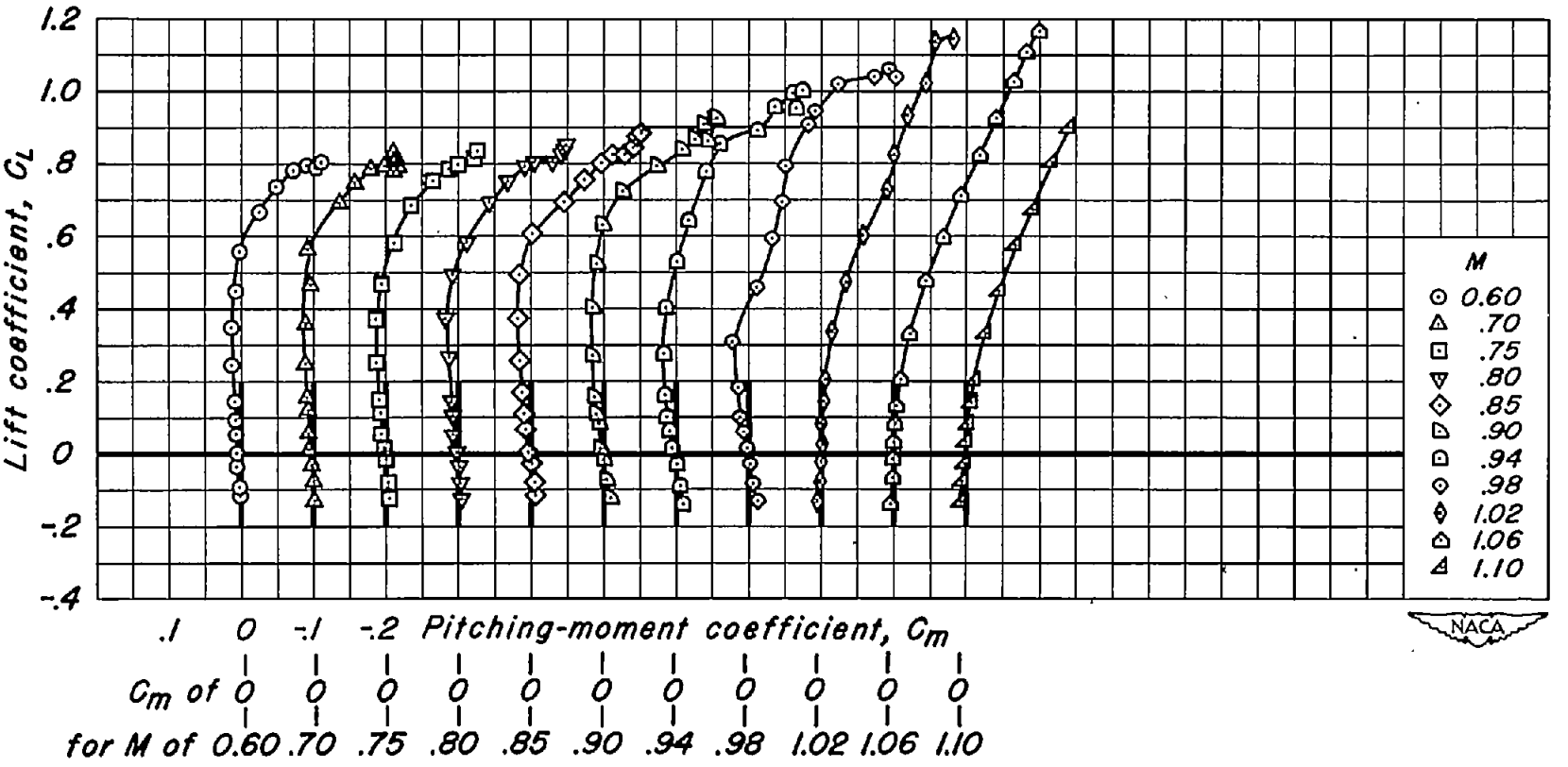

(h) t/c = 0.04; λ = 0.50

Figure 12.- Continued.

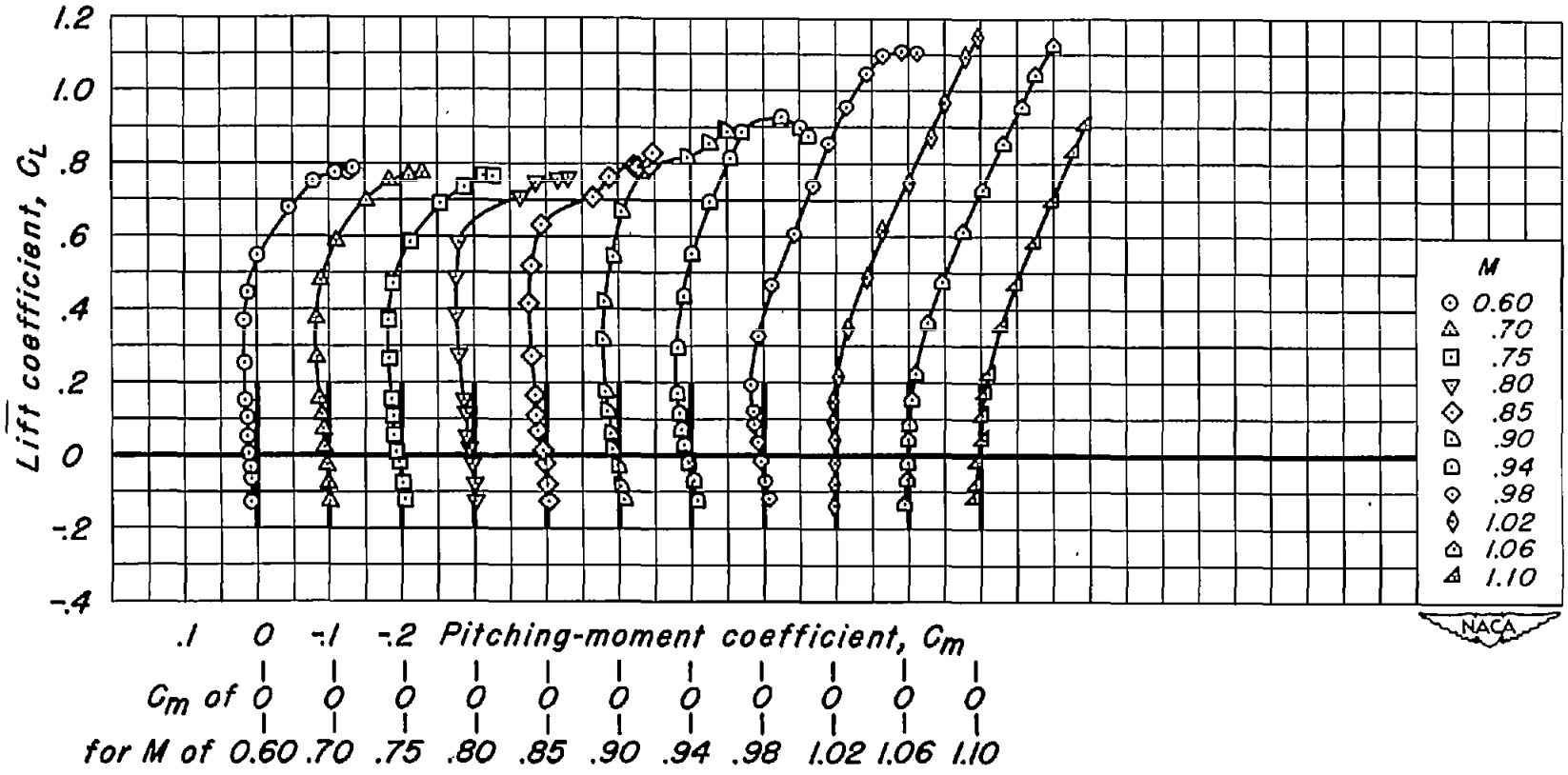

(i) t/c = 0.04; λ = 0.72

Figure 12.- Continued.

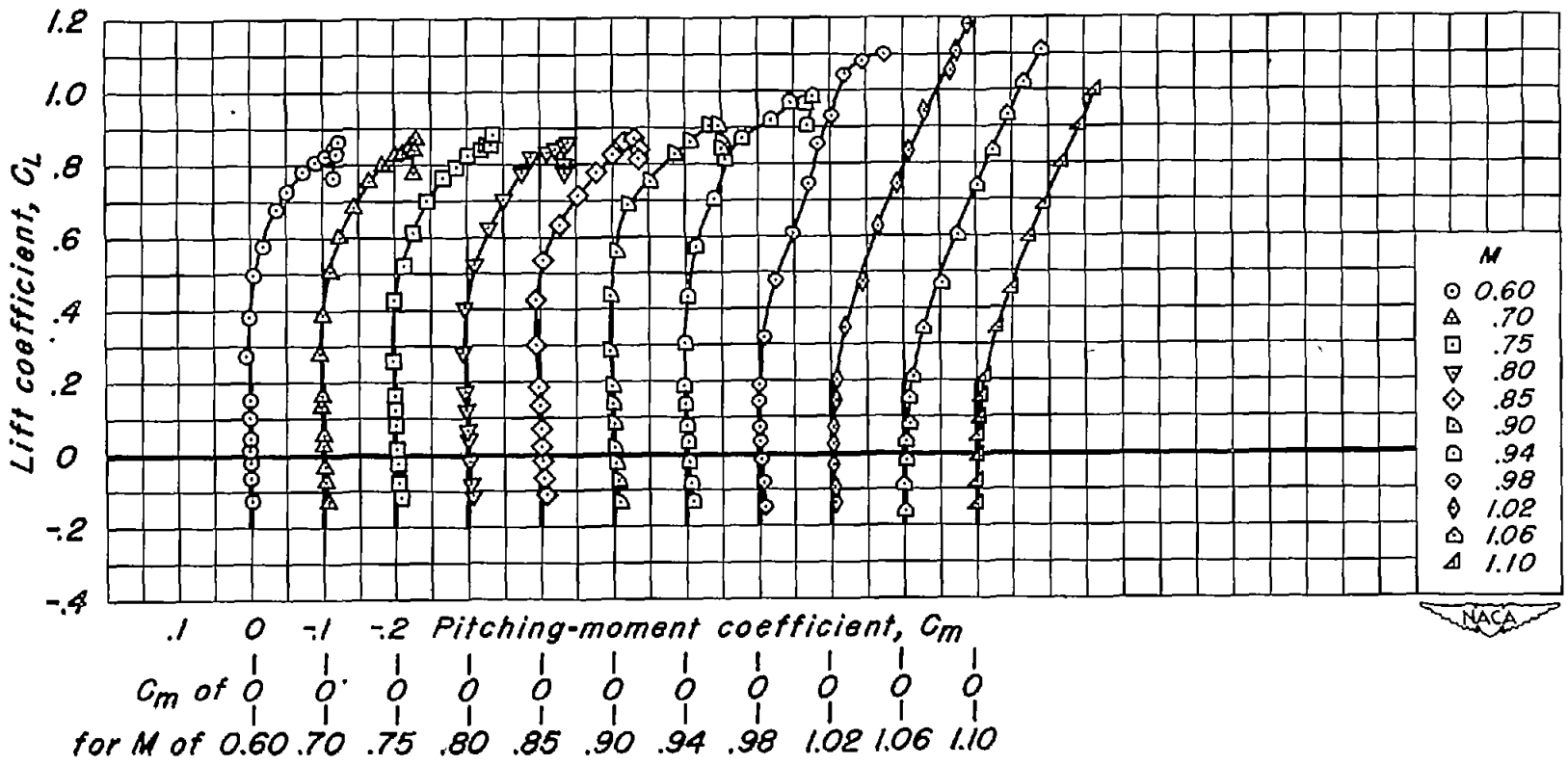

(j) t/c = 0.02; λ = 0.33

Figure 12.- Continued.

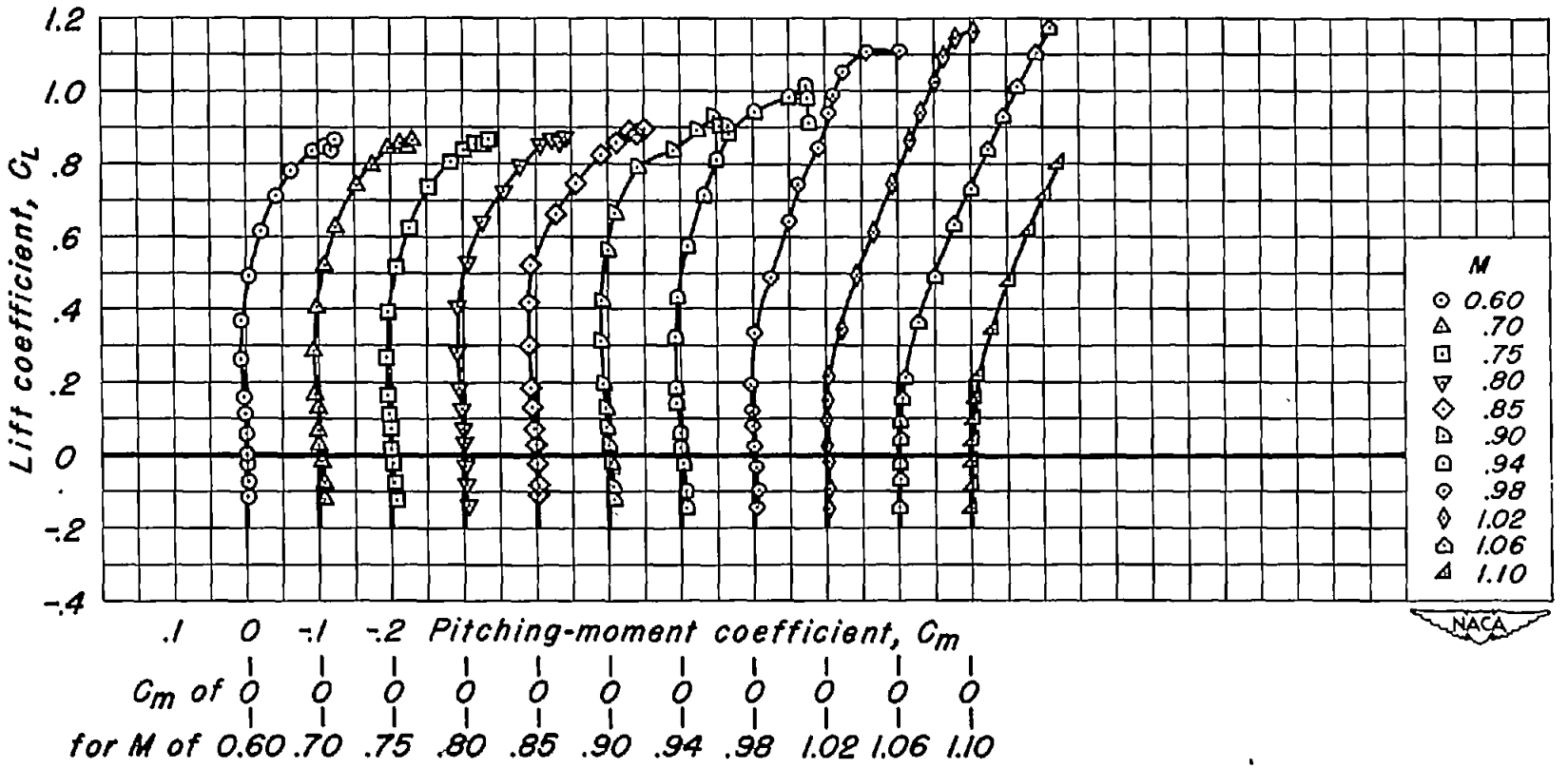

(k) t/c = 0.02; λ = 0.50

Figure 12.- Continued.

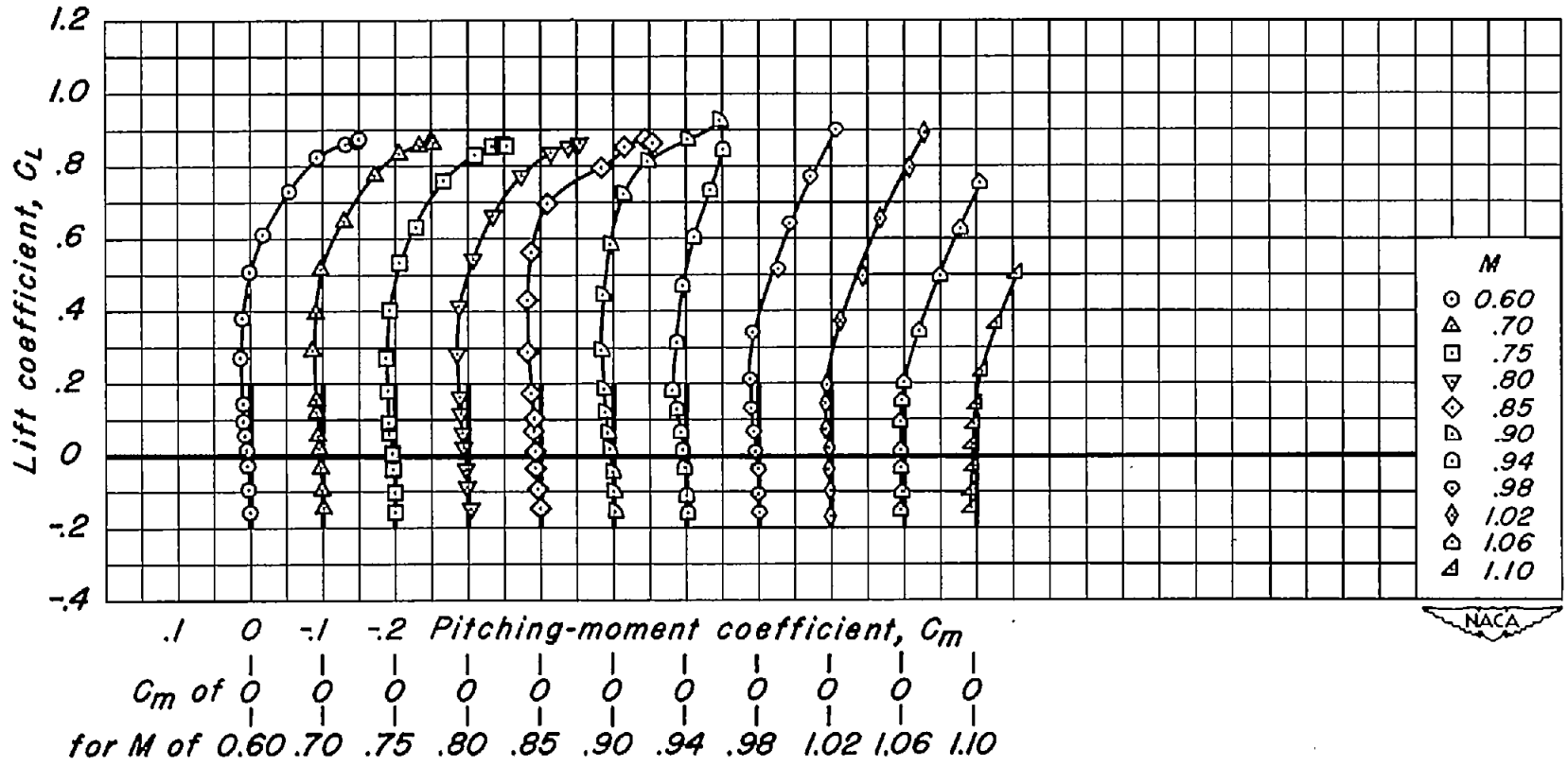

(l) t/c = 0.02; λ = 0.72

Figure 12.- Concluded.

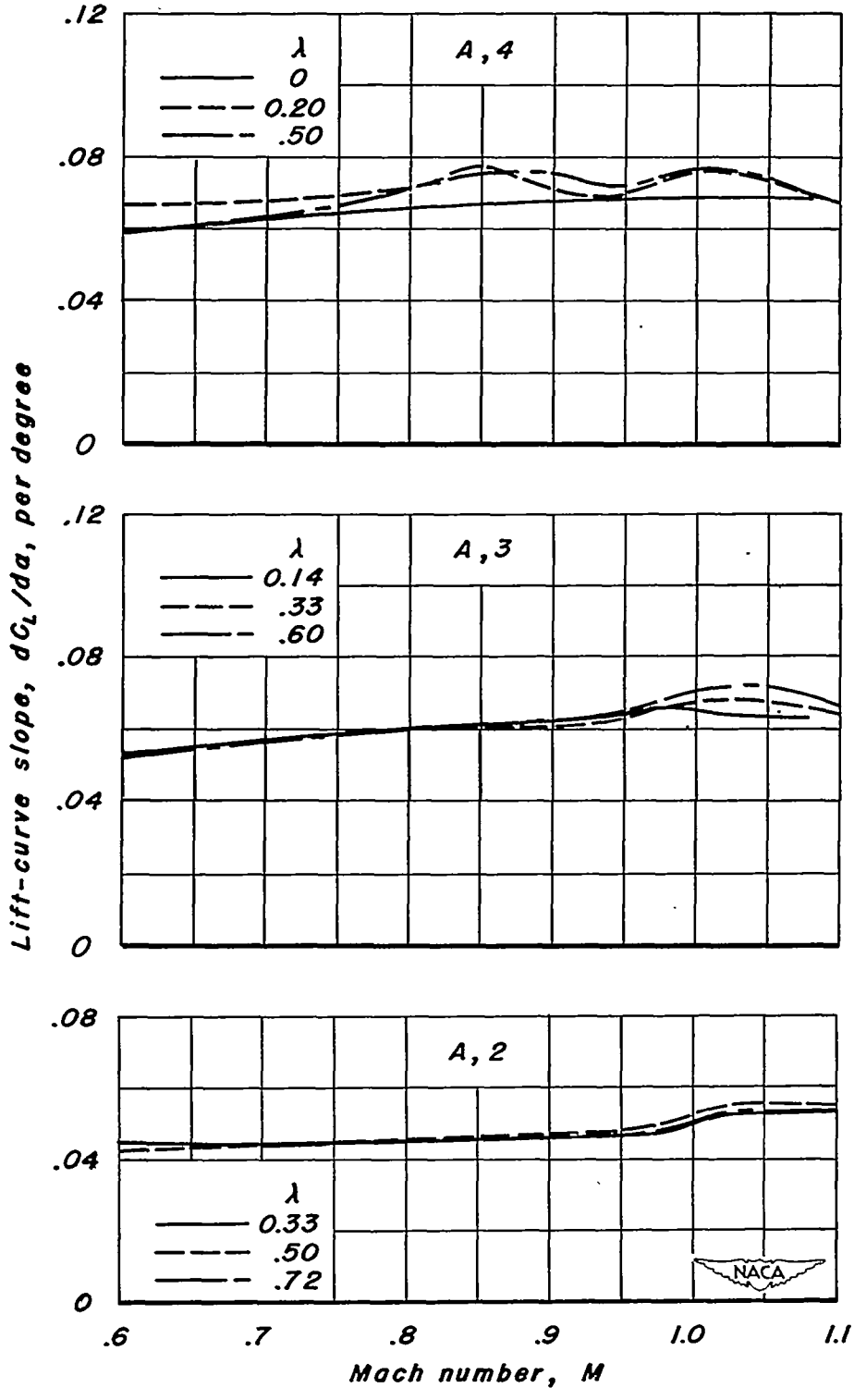

(a) NACA 63A008 sections.

Figure 13.- The variation of lift-curve slope with Mach number.

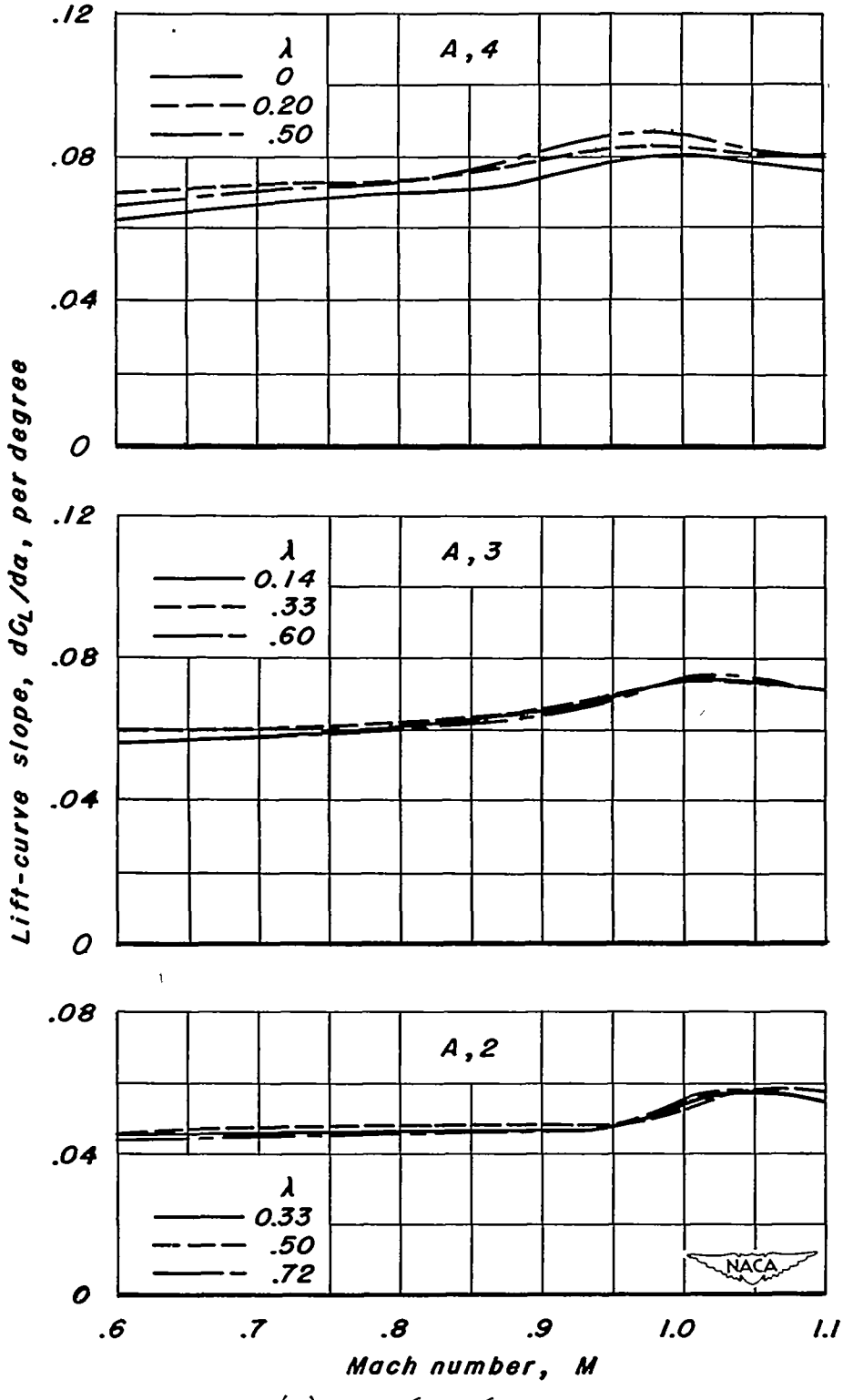

(b) NACA 63A006 sections.

Figure 13.- Continued.

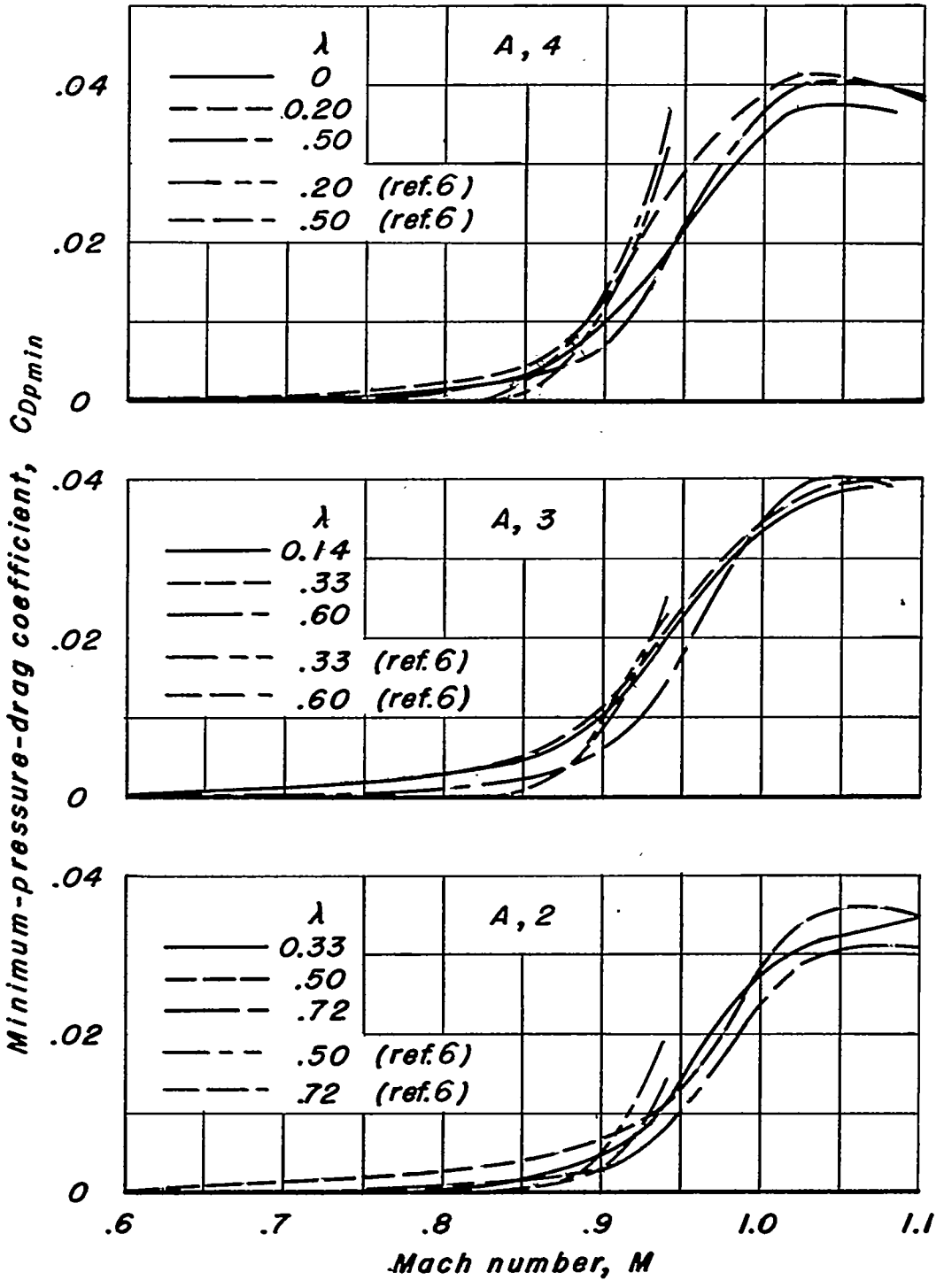

(a) NACA 63A008 sections.

Figure 14.- The variation of minimum-pressure-drag coefficient with Mach number.

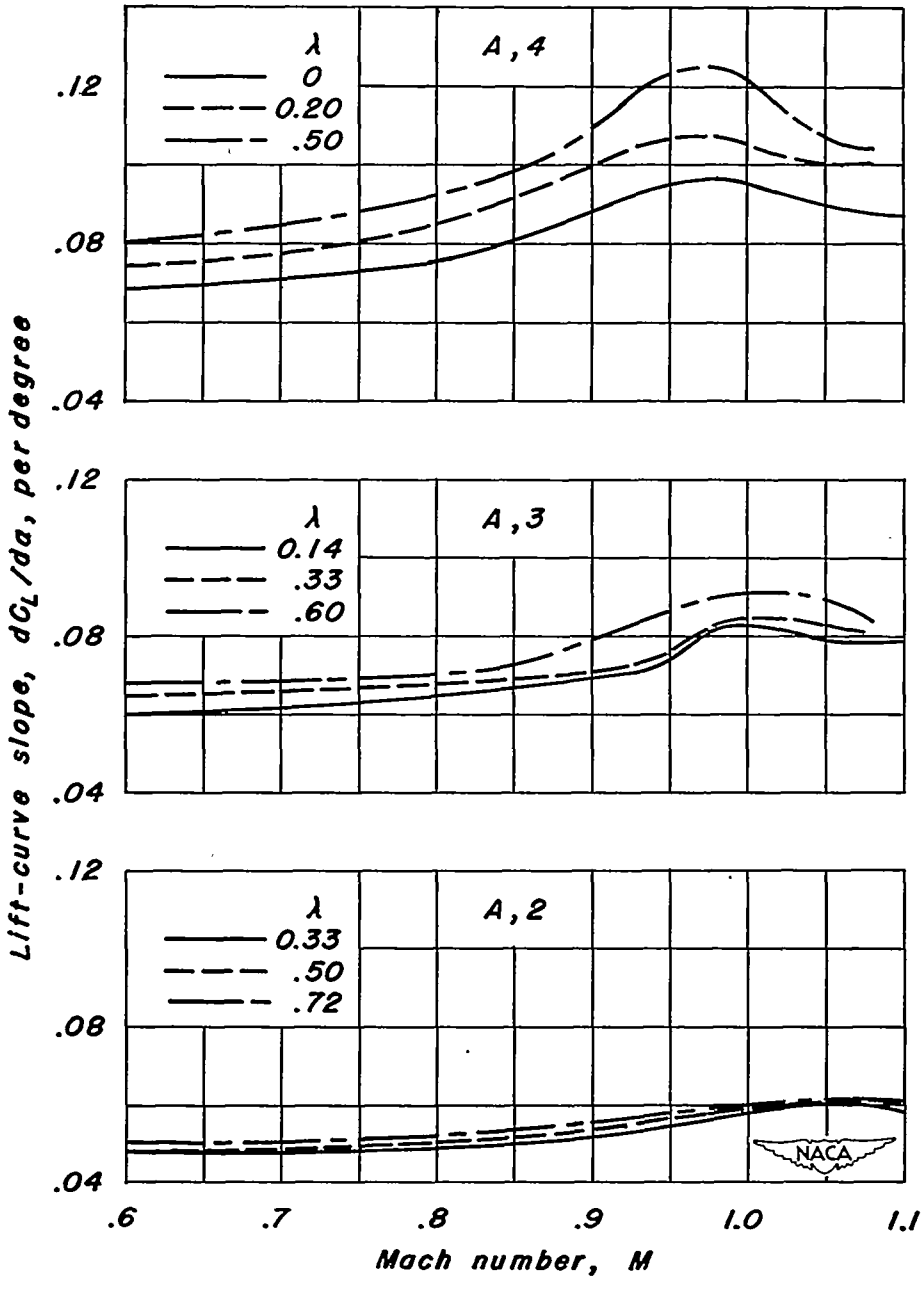

(d) NACA 63A002 sections.

Figure 13.- Concluded.

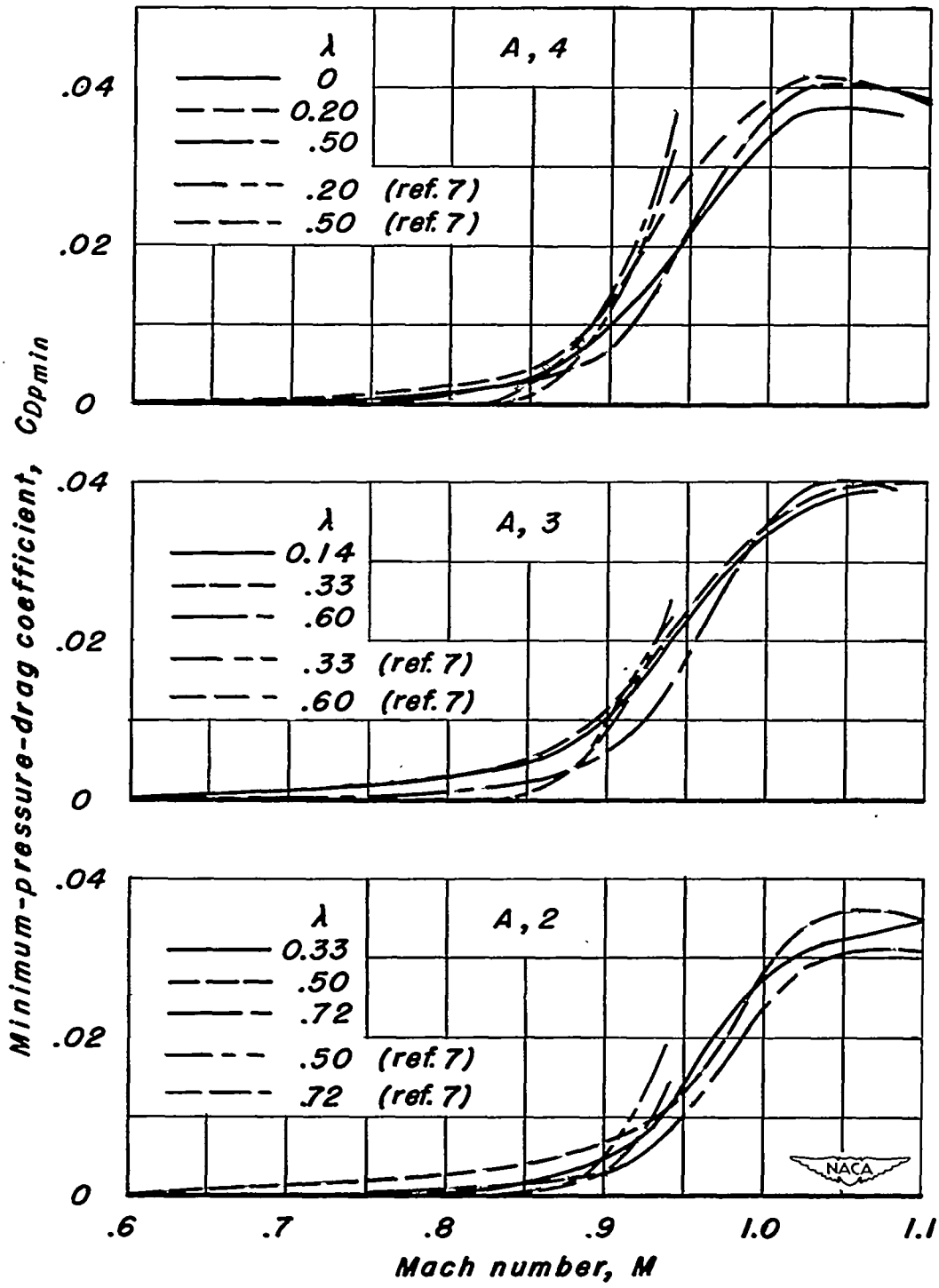

(a) NACA 63A008 sections.

Figure 14.- The variation of minimum-pressure-drag coefficient with Mach number.

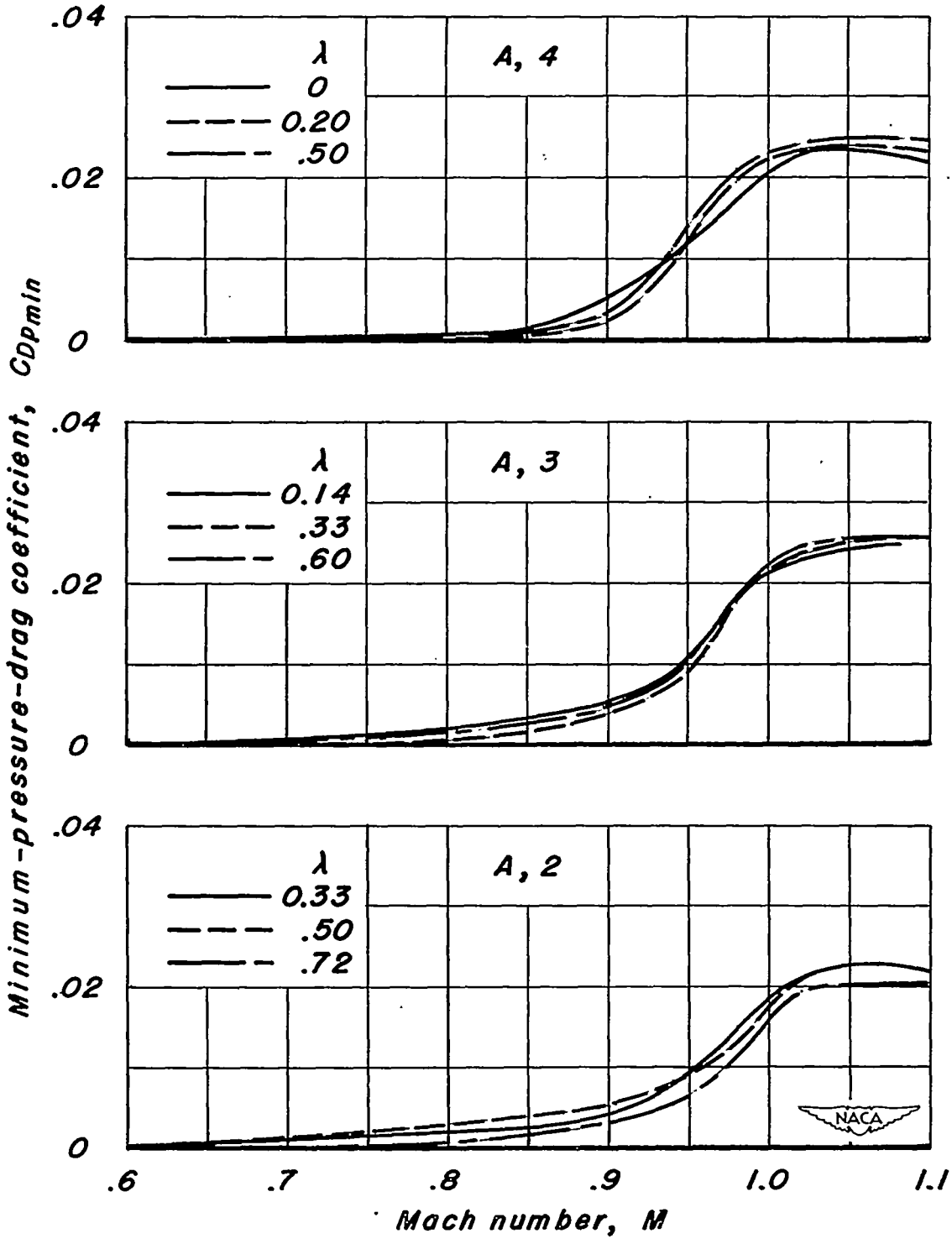

(b) NACA 63A006 sections.

Figure 14.- Continued.

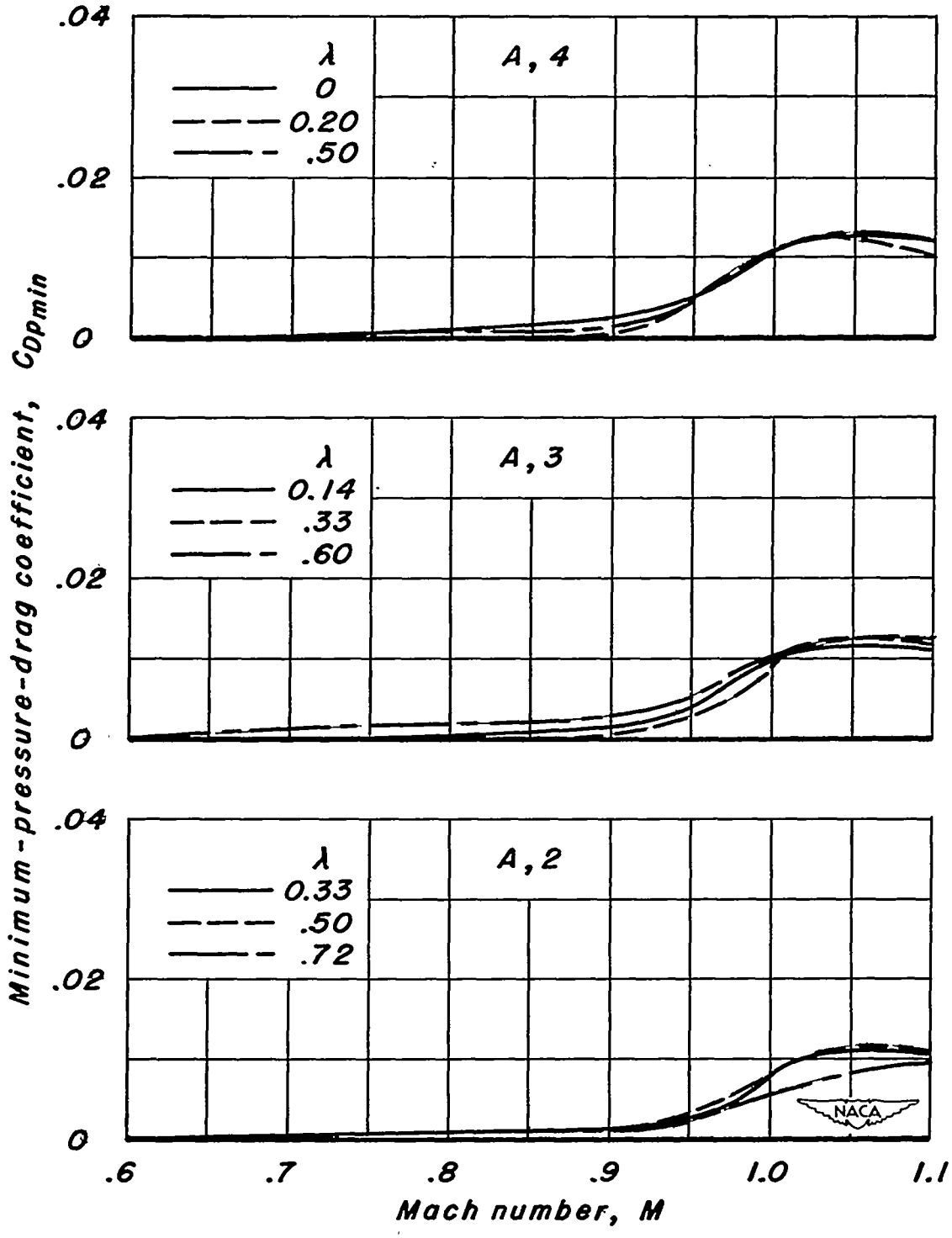

(c) NACA 63A004 sections.

Figure 14.- Continued.

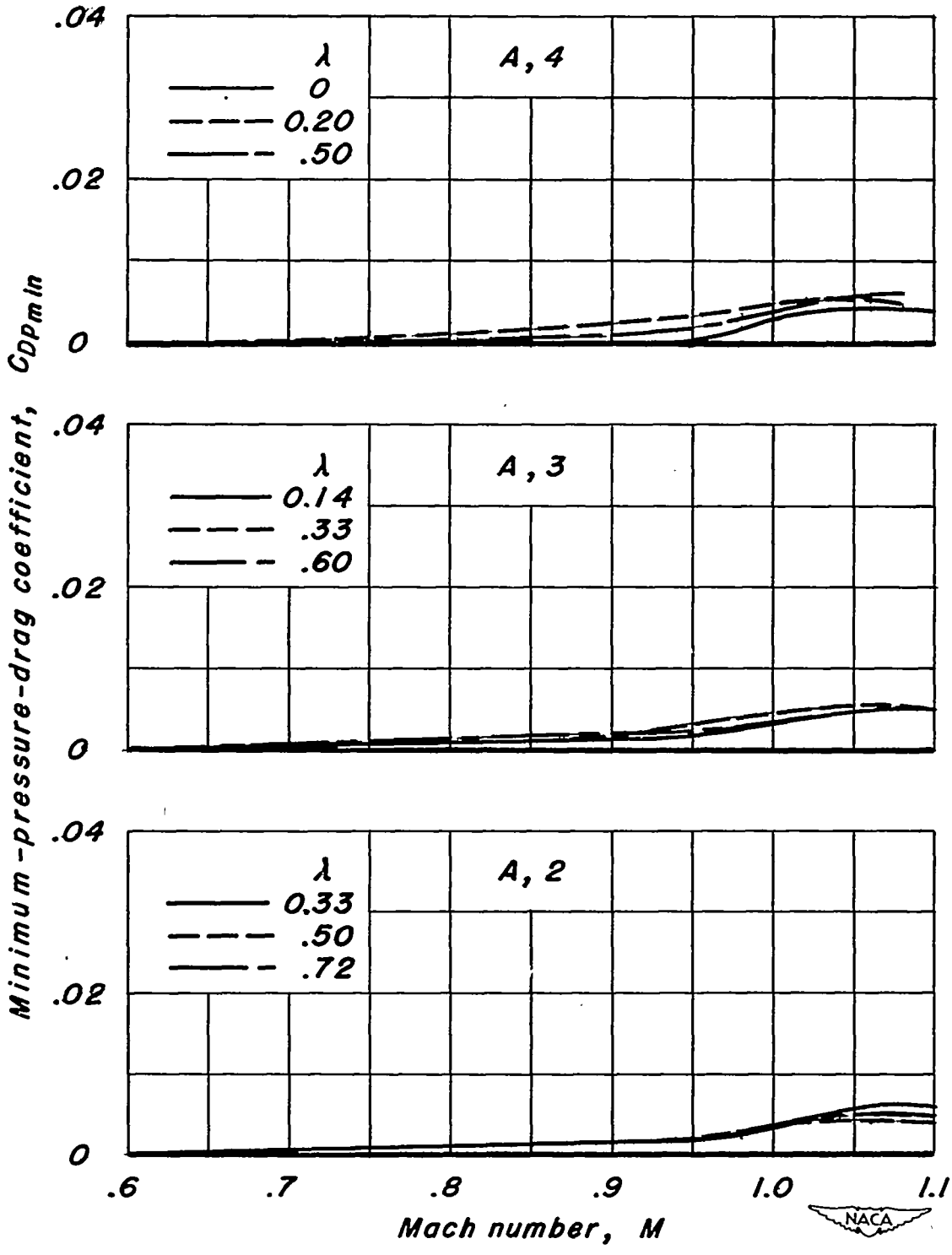

(d) NACA 63A002 sections.

Figure 14.- Concluded.

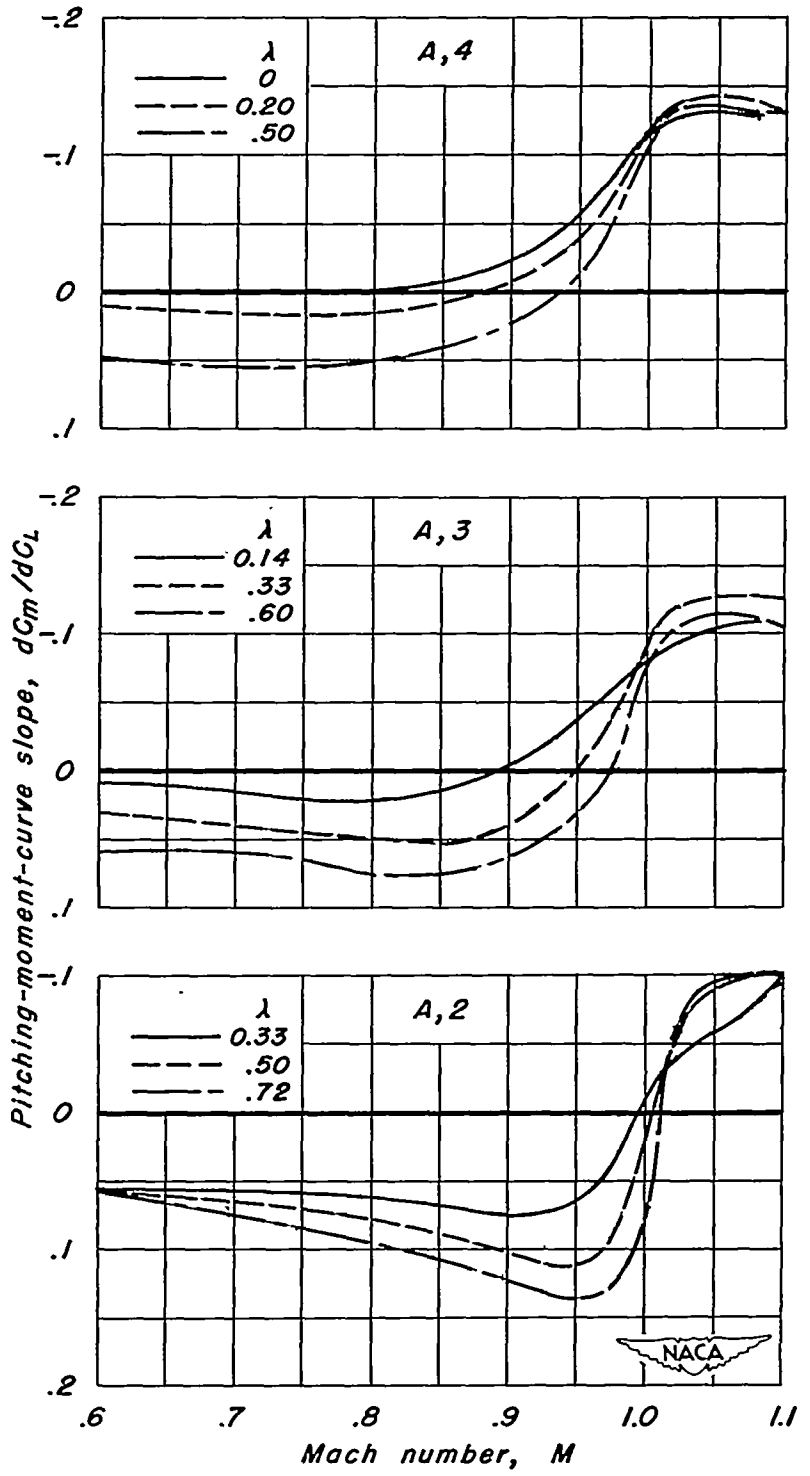

(a) NACA 63A008 sections.

Figure 15.- The variation of pitching-moment-curve slope with Mach number.

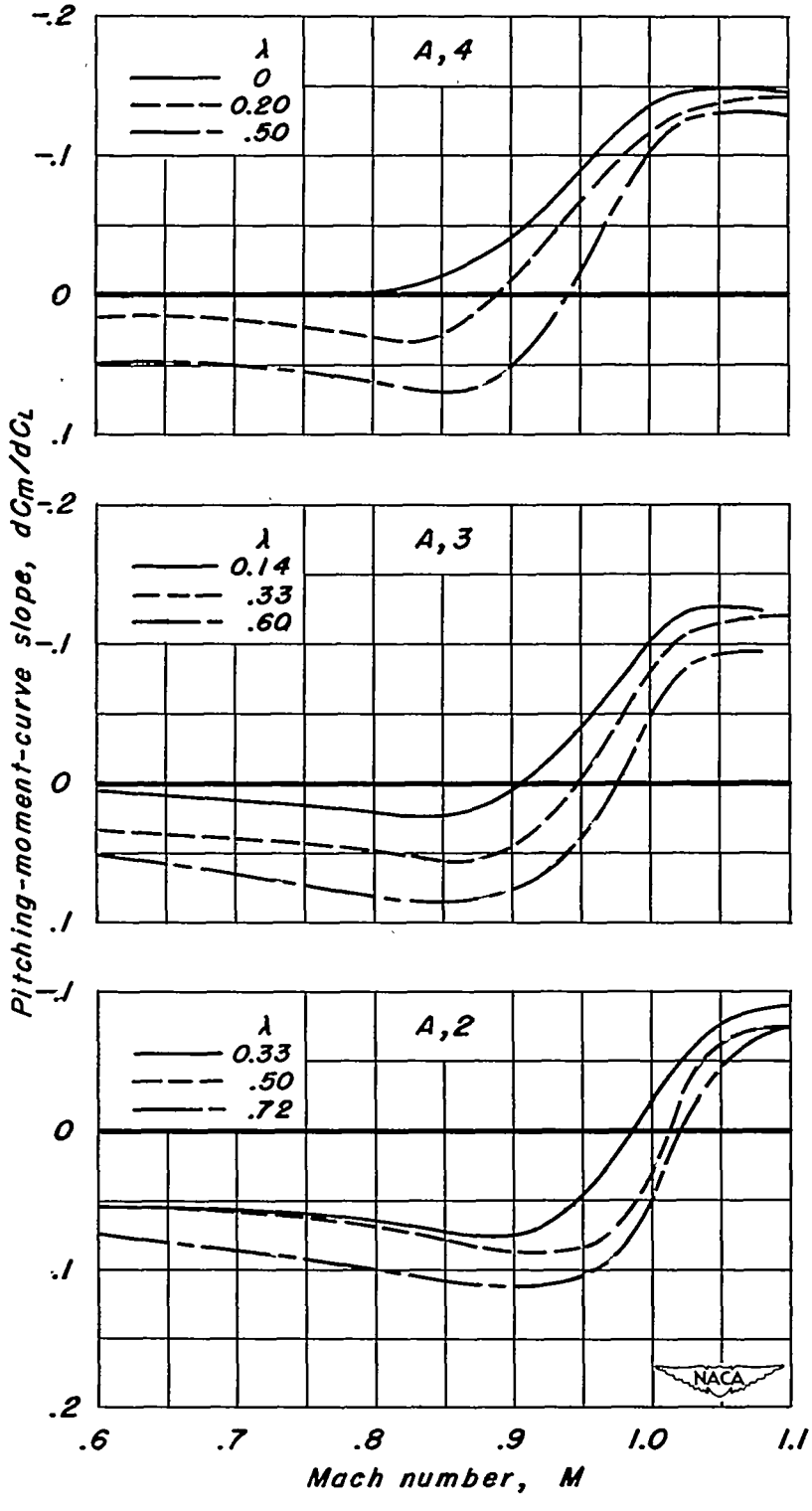

(b) NACA 63A006 sections.

Figure 15.- Continued.

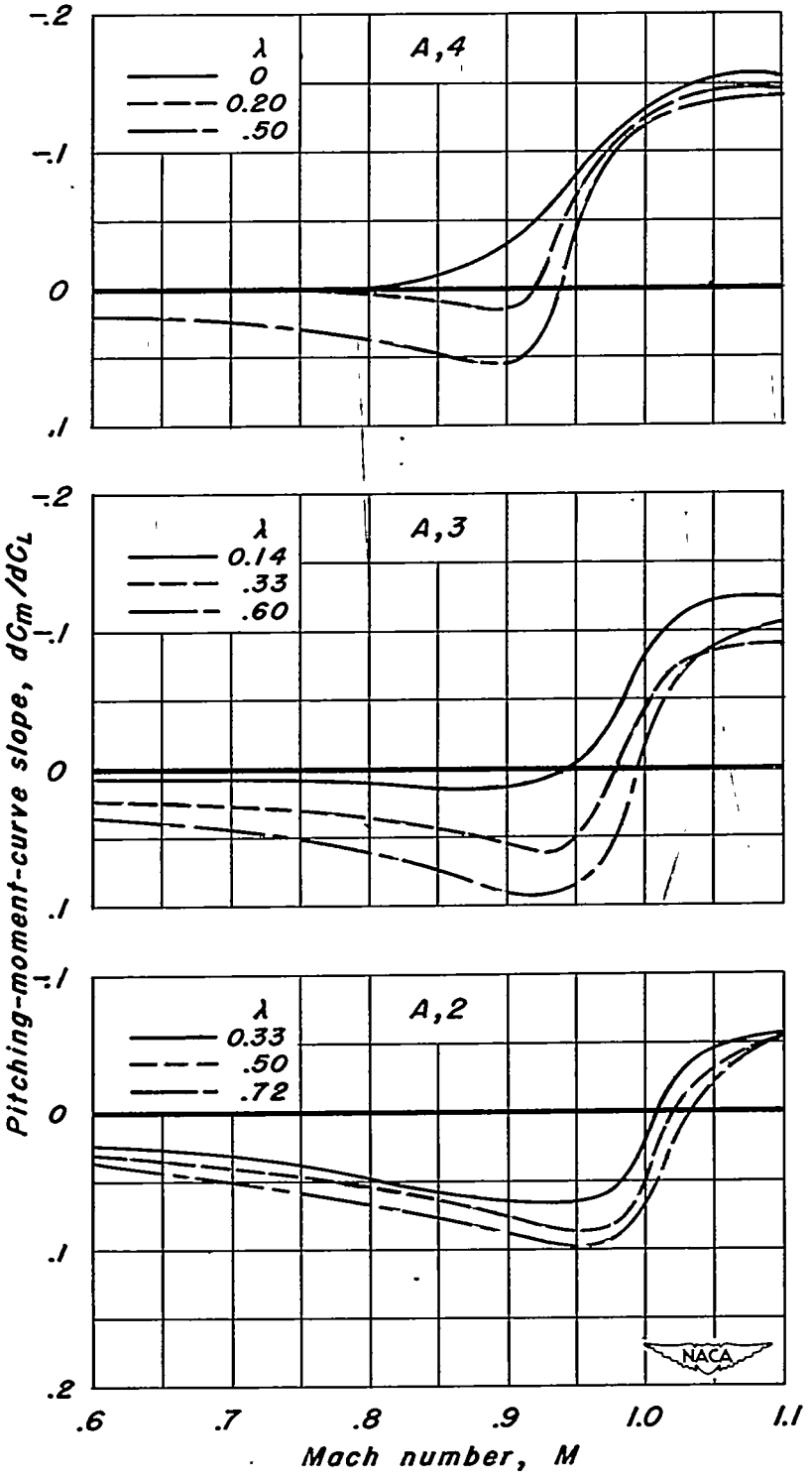

(c) NACA 63A004 sections.

Figure 15.- Continued.

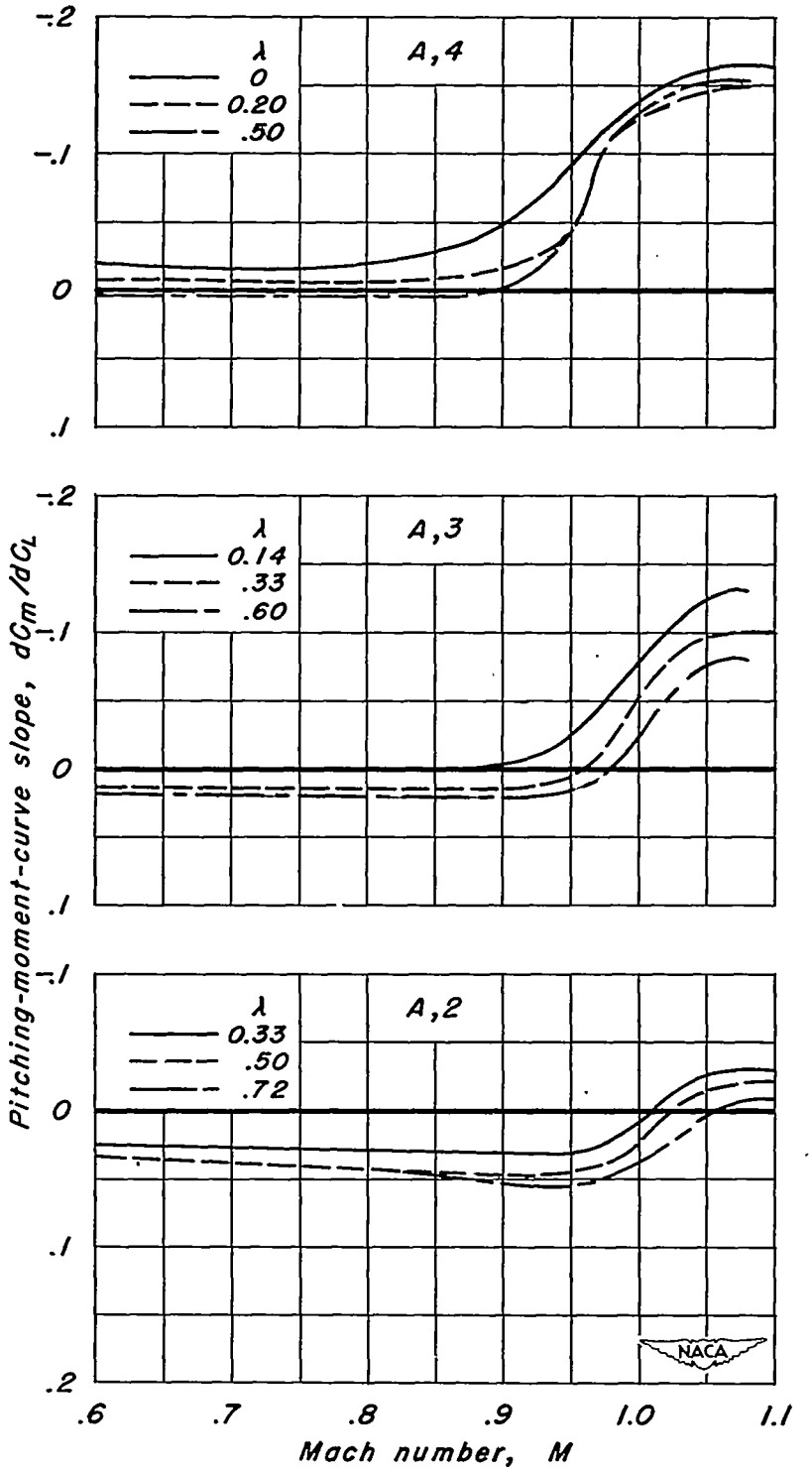

(d) NACA 63A002 sections.

Figure 15.- Concluded.